

book of abstracts

**SCIENTIFIC CONFERENCE
FOR YOUNG RESEARCHERS**

Tuesday

19. 9. 2017

Faculty of
Chemistry and
Chemical Technology,
University of Ljubljana

Organizator in založnik zbornika

Fakulteta za kemijo in kemijsko tehnologijo, Univerza v Ljubljani

Kraj prireditve

Fakulteta za kemijo in kemijsko tehnologijo, Univerza v Ljubljani

Večna pot 113, 1000 Ljubljana

Urednika

Jakob Kljun, Aljaž Gaber

Organizacijski odbor

Sara Drvarič Talian, Aljaž Gaber, Marina Klemenčič, Jakob Kljun, Aleš Ručigaj

Tisk

Jupiter mediji d. o. o.

Naklada

50 izvodov

Publikacija je dostopna na spletu

www.fkkt.uni-lj.si

CIP - Kataložni zapis o publikaciji

Narodna in univerzitetna knjižnica, Ljubljana

54:66(082)

SCIENTIFIC Conference for Young Researchers (2017 ; Ljubljana)

Book of abstracts / Scientific Conference for Young Researchers, 19. 9. 2017 ;
[organizator Fakulteta za kemijo in kemijsko tehnologijo, Univerza v Ljubljani ;
urednika Jakob Kljun, Aljaž Gaber]. - Ljubljana : Fakulteta za kemijo in
kemijsko tehnologijo, 2017

ISBN 978-961-6756-83-9

1. Kljun, Jakob 2. Fakulteta za kemijo in kemijsko tehnologijo (Ljubljana)

291612416



Driven by the enthusiasm and positive feedbacks received after the successful first Cutting Edge conference in September 2015, the second Cutting Edge conference took place on **19. 9. 2017** at the **Faculty of Chemistry and Chemical Technology, UL, in Ljubljana**. In our quest to widen the field of research to undergraduate, graduate and postgraduate students in chemistry, we brought together young researchers for an unforgettable day with our esteemed professors as well as prominent Slovene and foreign scientists. Furthermore, our junior participants were given the opportunity to submit and publish their own scientific article.

We are proud to announce that the Cutting Edge team has joined forces with the Slovenian Chemical Society that has been publishing the journal **Acta Chimica Slovenica (ACSi)** since 1954. Together we are prepared a thematic issue dedicated to the research of students and junior researchers within the fields of chemical and biochemical sciences. Young scientists were invited to submit an article, which underwent a standard reviewing process, and we are more than proud to present 10 of accepted papers in this dedicated **September edition** of ACSi. We are truly grateful to the editor, **prof. dr. Aleksander Pavko**, with his editorial team and **prof. dr. Slavko Kaučič**, president of Slovenian Chemical Society and publisher of ACSi, who kindly supported our initiative.

The conference has been divided into three main sections: *Science behind the living*, *Technologies for the Earth and Environment* and *Materials of the Future*. There were plenary lectures given by renowned experts from foreign countries regarding all three topics.

The conference was attended by more than **120 participants** from Slovenia and also a few other countries with researches from different fields. They include environment preservation, pharmacy, construction, materials, as well as medicine and engineering. Most of them showed their work in a poster exhibition, while selected Masters' and Doctoral students got a chance to present their research in the form of oral presentations.

We would like to thank the members of the scientific committee: **prof. dr. Andreja Žgajnar Gotvajn**, **doc. dr. Boštjan Genorio**, **prof. dr. Janez Plavec**, **prof. dr. Franc Lobnik**, **prof. dr. Boris Rogelj**, **prof. dr. Jurij Lah**, **doc. dr. Gabriela Kalčíkova**, **doc. dr. Matjaž Spreitzer** and **dr. Nejc Hodnik**.

The conference could not have been organized at the level as it was without the help of several students of the Faculty of Chemistry and Chemical Technology. We thank **Maša Arnšek**, **Aleksandar Djurdjević**, **Ana Grom**, **Sara Kotnik**, **Nina Kuzmić**, **Tina Paljk**, **Ervin Rems** and **Nik Rus** for their efforts.

The conference started at **9.00**, with a speech from the next vice dean for 3rd Cycle University Study Programmes and Scientific Research, **prof. dr. Andreja Žgajnar Gotvajn** and the president of the Cutting Edge society, **Sara Drvarič Talian**. The opening was followed by plenary lectures and oral presentations. The one day conference ended with a small ceremony, where best poster and best oral presentation awards were given.

LECTURE HALL 3 (3 rd floor)	
7:30-8:00	Registration
8:00-8:30	
8:30-9:00	
9:00-9:30	Opening (Hall B)
9:30-10:00	Plenary lecture (Hall B) - Science behind the Living
10:00-10:30	
10:30-11:00	Oral presentations - Science behind the Living
11:00-11:30	
11:30-12:00	Coffee break (1 st and 2 nd floor)
12:00-12:30	Plenary lecture (Hall B)-Technolgies for the Earth and Environment
12:30-13:00	
13:00-13:30	Oral presentations - Technolgies for the Earth and Environment
13:30-14:00	
14:00-14:30	Lunch break
14:30-15:00	
15:00-15:30	Poster session (1 st and 2 nd floor)
15:30-16:00	
16:00-16:30	Plenary lecture (Hall B) - Materials of the Future
16:30-17:00	
17:00-17:30	Oral presentations - Materials of the Future
17:30-18:00	
18:00-18:30	Closing ceremony (Hall B)

chair: Janez Plavec	
10:30	Ema Guštin Lipid Droplet Formation in HeLa Cervical Cancer Cells Depends on Cell Density and the Concentration of Exogenous Unsaturated Fatty Acids
10:50	Urška Slapšak Interaction of N-terminus PrP ^C with NCAM Fibronectin Domain
11:10	Boštjan Petrič Development of Caffeine Biosensors based on Anti-Caffeine Nanobodies and Fluorescent Proteins

chair: Gabriela Kalčíkova	
13:00	Ana Bjelič An Effect of Nobel Metals, Support and Operating Conditions of Eugenol Hydrotreatment: A Microkinetic study
13:20	Evelin Cruden Effect of Biochar Application on Pb and As Mobility in Tailings
13:40	Nika Osterman NiO Containing Zeolite as Catalyst for Waste Oils Deoxygenation

chair: Boštjan Genorio	
17:00	Špela Vičič Key parameters Affecting Drug Release from PCL Nanofibres
17:20	Janez Slapnik Synthesis of Biocompatibilizer by Graft Polymerization of Lactic Acid onto a Biopolymer and its Use in Preparation of Biocomposites
17:40	Matic Lozinšek New Development in the Chemistry of Krypton

LECTURE HALL 4 (3 rd floor)	
7:30-8:00	Registration
8:00-8:30	
8:30-9:00	
9:00-9:30	Opening (Hall B)
9:30-10:00	Plenary lecture (Hall B) - Science behind the Living
10:00-10:30	
10:30-11:00	Oral presentations - Technologies for the Earth and Environment
11:00-11:30	
11:30-12:00	Coffee break (1 st and 2 nd floor)
12:00-12:30	Plenary lecture (Hall B) Technolgies for the Earth and Environment
12:30-13:00	
13:00-13:30	Oral presentations - Materials of the Future
13:30-14:00	
14:00-14:30	Lunch break
14:30-15:00	
15:00-15:30	Poster session (1 st and 2 nd floor)
15:30-16:00	
16:00-16:30	Plenary lecture (Hall B) - Materials of the Future
16:30-17:00	
17:00-17:30	Oral presentations - Science Behind the Living
17:30-18:00	
18:00-18:30	Closing ceremony (Hall B)

chair: Franc Lobnik	
10:30	Severina Stavbar Advanced Oxidation Processes for Hospital Wastewater Treatment Containing Antibiotics
10:50	Ida Kraševc Development of Microextraction Methods for Determination of Benzotriazoles
11:10	Arijana Filipić Cold Atmospheric Plasma for Inactivation of Plant Viruses

chair: Matjaž Spreitzer	
13:00	Žiga Štirn Aminomaleimide as a Key Compound for the Preparation of High Performance Benzoxazine Materials
13:20	Leonard Moriau Graphene/TiONx/PtCu ₃ /Ir as Oxygene Reduction and Oxygene Evolution Reactions Catalyst for the Regenerative PEM Fuel Cell
13:40	Matija Gatalo Synthesis of Commercially Viable PtCu ₃ /C ORR Electrocatalyst

chair: Marina Klemenčič, Aljaž Gaber	
17:00	Zorica Latinović Disintegrins from the Venom of Vipera Ammodytes Ammodytes Efficiently Inhibit Migration of Breast Cancer Cells
17:20	Sandi Brudar Use of Differential Scanning Calorimetry and Immunoaffinity Chromatography to Identify Disease Induced Changes in Human Blood Plasma Proteome
17:40	Urban Košak Development of in Vivo Active Non- Covalent Butyrylcholinesterase inhibitors

TABLE OF CONTENTS

SCIENCE BEHIND THE LIVING - PLENARY LECTURE

- 1 ANDRÁS PERCZEL: 3D-structure shields the "achilles heel" of proteins: backbone isomerization at -NG-sites in proteins

TECHNOLOGIES FOR THE EARTH AND ENVIRONMENT - PLENARY LECTURE

- 3 BLAŽ LIKOZAR: Challenges and opportunities of engineering the future (bio)refinery processes

MATERIALS OF THE FUTURE - PLENARY LECTURE

- 5 ANDREJ GRUBIŠIČ: Nanoscale meets gigascale

SCIENCE BEHIND THE LIVING - ORAL PRESENTATIONS

- 7 ZORICA LATINOVIĆ: Disintegrins from the Venom of Vipera Ammodytes Ammodytes Efficiently Inhibit Migration of Breast Cancer Cells
- 8 SANDI BRUDAR: Use of Differential Scanning Calorimetry and Immunoaffinity Chromatography to Identify Disease Induced Changes in Human Blood Plasma Proteome
- 9 EMA GUŠTIN: Lipid Droplet Formation in HeLa Cervical Cancer Cells Depends on Cell Density and the Concentration of Exogenous Unsaturated Fatty Acids
- 10 URBAN KOŠAK: Development of in Vivo Active Non-Covalent Butyrylcholinesterase inhibitors
- 11 URŠKA SLAPŠAK: Interaction of N-terminus PrP^C with NCAM Fibronectin domain
- 12 BOŠTJAN PETRIČ: Development of Caffeine Biosensors based on Anti-Caffeine Nanobodies and Fluorescent Proteins

TECHNOLOGIES FOR THE EARTH AND ENVIRONMENT - ORAL PRESENTATIONS

- 15 SEVERINA STAVBAR: Advanced Oxidation Processes for Hospital Wastewater Treatment Containing Antibiotics
- 16 IDA KRAŠEVEC: Development of Microextraction Methods for Determination of Benzotriazoles
- 17 ARIJANA FILIPIĆ: Cold Atmospheric Plasma for Inactivation of Plant Viruses
- 18 ANA BJELIĆ: An Effect of Noble Metals, Support and Operating Conditions of Eugenol Hydrotreatment: A Microkinetic Study
- 19 EVELIN GRUDEN: Effect of Biochar Application on Pb and As Mobility in Tailings
- 20 NIKA OSTERMAN: NiO Containing Zeolite as Catalyst for Waste Oils Deoxygenation

MATERIALS OF THE FUTURE - ORAL PRESENTATIONS

- 23 ŽIGA ŠTIRN: Aminomaleimide as a Key Compound for the Preparation of High Performance Benzoxazine Materials
- 24 LEONARD MORIAU: Graphene/TiON_x/PtCu₃/Ir as Oxygene Reduction and Oxygene Evolution Reactions Catalyst for the Regenerative PEM Fuel Cell
- 25 MATIJA GATALO: Synthesis of Commercially Viable PtCu₃/C ORR Electrocatalyst
- 26 ŠPELA VIČIČ: Key Parameters Affecting Drug Release from PCL Nanofibres
- 27 JANEZ SLAPNIK: Synthesis of Biocompatibilizer by Graft Polymerization of Lactic Acid onto a Biopolymer and its Use in Preparation of Biocomposites
28. MATIC LOZINŠEK: New Developments in the Chemistry of Krypton

CUTTING EDGE 2017 - POSTERS

- 31 SABINA OTT: Phylogenomic Analysis of RNA Viruses in Invertebrates
- 32 SEBASTIJAN RIČKO: Synthesis and Use of Camphor-derived Organocatalysts in Enantioselective Synthesis
- 33 ANŽEJ HLADNIK: Trans-Activation Response Element RNA is Detectable in the Plasma of Subset of Aviremic HIV-1-Infected Patients
- 34 GORAZD KODERMAN PODBORŠEK: Photocatalytic Activity of Titanium Dioxide Thin Films Doped with Silicon or Iron
- 35 EVA ŽUNEC: Application of German Self-Assessment Method about Management Effectiveness in Protected Areas on Slovenian Nature Parks
- 36 NEJC PETEK: Synthesis and Bioactivity of Novel 7-(1-aminoalkyl)pyrazolo[1.5-a]pyrimidines
- 37 VITA HUDI: Mathematical Modeling of the 2014 West African Ebola Epidemic
- 38 TOMAŽ PIRMAN: Microkinetics of Photocatalytic Partial Oxidation of Glicerol over CuO/MWCNT to Value-added Platform Chemical Building Blocks
- 39 HARINARAYANAN PULIYALIL: Hybrid Plasma Reactors for the Efficient Conversion of Methane to Liquid Chemicals
- 40 DAŠA ROBIČ: Studies on Biological Activity of Nystatin in Lipid Membranes
- 41 BOJANA BRADIĆ: Modeling of Heterogeneous N-deacetylation of Chitin in Alkaline Solution
- 42 EVA JARC: Apidose Triglyceride Lipaze-mediated Lipid Droplet Breakdown is not Essential for Cell Survival During Nutrient Stress, but is Involved in Eicosanoid Production in Breast Cancer Cells
- 43 NIKA STRAŠEK: Synthesis and Testing of Potential Inhibitors of the Plasmodium Falciparum Dihydroorotate Dehydrogenase
- 44 ANJA AJDOVEC: Preparation of N-HALO Substituted Derivatives of Bicyclo[2.2.2]octenes Obtained from Cycloadditions of Maleimides on 2H-pyran-2-ones
- 45 ANDRAŽ ŠULIGOJ: TiO₂-mesoporous SiO₂ Films for Removal od VOCs from Indoor Air
- 46 JAN PERUTKA: Basic Haematology and Citochemical Characteristics of Blood Cells from two Freshwater Turtle Species: Mauremys rivulata (valenciennes in Bory de Saint-Vincent 1833) and Emys orbicularis (linnaeus 1758) in Croatia
- 47 EVA PLUT: The Chiral Thiourea Organocatalyst for the Enantioselective Carbon-Carbon Bond Formation

- 48 **MIHA VIRANT:** The Evolution of Pyridine-Tethered Mesoionic Ligands and their Palladium Complexes as Catalysts in Sustainable Cross-Coupling Reactions
- 49 **BRUNO ALEKSANDER MARTEK:** Arylation of Selected Pyrrole-Containing Heterocycles via C-H Bond Activation
- 50 **KATERINA TOMSIČ:** Oxidative Stress During Sevoflurane or Propofol Anesthesia in Dogs with Early-Stage Myxomatous Mitral Valve Degeneration
- 51 **JAN PETROVČIČ:** Evaluation of Imidazolium Fluoride Based Reagents for Nucleophilic Fluorination of Organic Compounds
- 52 **PATRICIJA HRIBERŠEK:** Self-Assembly of Isotactic and Atactic Poly(Methacrylic Acid) Chains in Aqueous Solutions: Effect of Temperature
- 53 **TJAŠA GOLTNIK:** Synthesis of Flower-like TiO₂ Particles
- 54 **JERNEJ EKAR:** Oxidation of Guanine Nucleos(t)ides with Peroxynitrite
- 55 **MARKO RADAK:** Wildfire Propagation Modeling
- 56 **LEV MATOH:** Hydrothermal Synthesis of Nanostructured TiO₂ Particles with High Surface Area
- 57 **MAKSIMILJAN ADAMEK:** Phytotoxicity of Guaiacol and its Nitrated Derivatives
- 58 **DAŠA PAVC:** G-quadruplex Structure of DNA Oligonucleotides with GC Ends
- 59 **MARJAN LUKEŽIČ:** Impact of the Vent-Shape on the Efficiency of the Natural Smoke Ventilation and Heat Transfer from a Small Compartment
- 60 **BARBARA DEBEVEC:** Removal of Artificial Sweeteners from Aquatic Solutions by Ozonation
- 61 **IGOR BOSEVSKI:** Comparison of Oxidation Techniques for Removal of Antibiotic Tiamulin
- 62 **KLEMEN STROJAN:** In vitro Assessment of Potential Papillary Urothelial Neoplasm Treatment with Functionalized Polyethyleneimine Coated Magnetic Nanoparticles
- 63 **MIHA DREV:** Microwave Assisted C-H Bond Functionalization of Phenylpyrimidines in Water
- 64 **ANA OBERLINTNER, TJAŠA RIJAVEC:** Electric Conductivity of Gel Electrolytes
- 65 **MATJAZ DLOUHY:** Theoretical Study of 'Graphene-Like' Monomer Structures
- 66 **TINA PALJK:** Impact of the Electrolytes in the Li-S Battery System on the Process of Electrocrystallization of Lithium Sulfide
- 67 **MILKA BORIČ:** Non-thermal Plasma Assisted Removal of Proteins from Shrimp Shell Waste Material
- 68 **URŠA TOMAŽIN:** Additional Applications of Enaminones
- 69 **KATJA TRAVEN:** Ruthenium (II) Coordination Compounds as Inhibitors of 15-lipoxygenase-1
- 70 **TJAŠA GORIČAN:** Characterization of Allosteric Mechanism of Cathepsin K Using a Novel Allosteric Effector
- 71 **JURE CERAR:** Modelling of Liquid Glycols: Molecular Dynamics and SWAXS Studies
- 72 **ANŽE IVANČIČ:** Stereoselective Organocatalyzed Michael Addition of Hydroxy-Pyrroles to trans-β-Nitrostyrenes
- 73 **SABINA KOLŠEK:** The Impact of Copper Nanoparticles on the Compositing Process
- 74 **MILENA IVANOVIČ:** Chemometric Characterization of Slovenian Red Wines
- 75 **URBAN GARTNER:** Evaluation of Trametes Versicolor's Capability for Nanoparticle Synthesis and Bioremediation
- 76 **LUKA ŽNIDERŠIČ:** Development of a SPME-GC-MS/MS Method for the Determination of Some Contaminants from Food Contact Material

- 77 **MARKO TRAMPUŽ:** Fesoterodine Fumarate Batch Crystallization Modelling: Mass Transfer Resistances, Kinetics, Equilibrium and Particle-size Distribution Prediction
- 78 **BOŠTJAN ŽENER:** Highly Efficient Titania Thin Films, Co-doped with Nitrogen and Platinum
- 79 **ULA ROZMAN:** Toxicity of Veterinary Antibiotic Tiamulin to Freshwater Organisms
- 80 **MATIJA URŠIČ:** Structural Investigation of Novel Ruthenium-Diketonate Complexes
- 81 **GRIŠA GRIGORIJ PRINČIČ:** Non-symetric Phenyl Substituted 1, 2, 4, 5-tetraoxanes: Synthesis and Optimization
- 82 **MONIKA HORVAT:** Oxidation of Trifluoromethyltolated Aromatic Compounds with Hydrogen Peroxide
- 83 **EVA PUŠAVEC KIRAR:** Copper Catalyzed Synthesis of 6,7-dihydri-1H,5H-pyrazolo[1,2-a]pyrazolones, Followed by Ring Opening
- 84 **MOJCA JUTERŠEK:** Development of DNA Barcoding Approach Based on rRNA Genomic Sequences for Detection of Cyanobacteria in Environmental Samples
- 85 **JURE ZABRET:** Protein Expression and Characterization of Three *M. aeruginosa* NIES843 orthocapases
- 86 **ANDREJA BRATOVŠ:** Targeting Cathepsins B, S and L with DARPIn/stefinA-conjugated Liposomes in Cancer
- 87 **ANA KRIŠELJ:** Timelapse-Microscopy Analysis of Stochastic Cell Fate Decisions in Nematode *Caenorhabditis Elegans*
- 88 **DOMINIK NABERGOJ:** Effect of Bacterial Growth Rate on Phage Growth Parameters and Bacteriophage Fitness
- 89 **DOMINIK NABERGOJ:** Effect of Dillution Rate on Productivity of Continuous Production of Bacteriophages
- 90 **PREDRAG KORICA:** Influence of Waste Prevention on Greenhouse Gases Emissions of Waste Management in Croatia
- 91 **SANJA POPOVIČ:** Impact of Antibiotic Tiamulin Fumarate on Extracellular Ligninolytic Enzymes of Fungus *Dichmitus Squalens*
- 92 **INES KULAŠIČ:** Synthesis of Bimetal Fenton-like Catalyst for Wastewater Treatment
- 93 **MARJAN LUKEŽIČ:** Numerical Simulation of Ethene Molecular Motion in a Small Chamber
- 94 **DOMEN ŽALEC, MATIC MOŽE:** Correlation Between Surface Roughness and Wetting Properties of Stainless Steel Surfaces
- 95 **EVA ŽOS:** Reactions of Ethoxymethylene Hydrazones with Anilines
- 96 **ANŽE PAVLIN:** The Synthesis of Selected Hydrazonoformamides
- 97 **JAKOB KLJUN:** Organoruthenium-Clioquinol Complex Impairs Tumour Cell Invasion by Inhibiting Cathepsin B Activity
- 98 **ANA KUMP:** Lipid Droplets Protect Cancer Cells Drom Lipotoxicity and Oxidative Stress
- 99 **KLEMEN BERLEC:** Corrosion Monitoring by Utilizing Electrochemical Impedance Spectroscopy and Visual Inspection Evaluation
- 100 **LUKA KAVČIČ:** Structural Features of α -hydrazino Peptidomimetics as Potential Modulators of p53-MDM2 Interaction
- 101 **ROK MIKLAVČIČ:** Use of Carbohydrate-binding Proteins for Affinty Separation of Glycoproteins
- 102 **ROK NAROBÉ:** Exploiting Hydrogen Peroxide's Potential in Oxidative Iodination of Arenes
- 103 **MOJCA ZALOKAR:** Problems Related to Laboratory Breeding of Water Flea *Daphnia Magna*

- 104EVA SREČNIK:** Novel HPLC-UV Method for Simultaneous Determination of Fat-soluble Vitamins and Coenzyme Q10 in Medicines and Supplements
- 105UROŠ ZAVRTANIK:** Correlation between Binding Surfaces and the Thermodynamics of Camelid Antibody Fragments Binding to Antigens
- 106GAJA ŠPES, JAKA ZUPANIČ:** The Effect of Clinical Escherichia coli Strains on Recipient Ability in Conjugative Transfer
- 107BLAŽ KOZJAN:** Separation of Amino Acids by Various Chromatography Columns
- 108JAKOB RUPERT:** Structural Studies of ALS-associated Proteins
- 109BOŽIDAR ČOBELJIČ:** Synthesis and Characterization of Cd(II) Complexes with the Condensation Product of 2-quinolinecarboxaldehyde and Girard's T Reagent
- 110ANDRAŽ OŠTREK:** Fluoridooxidovanadates(V) with Small Nitrogen-Containing Cations
- 111GREGOR ŠILC:** Compost Water Extract (Compost Tea) as an Alternative Nutrient Solution for Vegetables Grown on Hydroponic System
- 112HELENA BRODNIK ŽUGELJ:** Synthesis of 8-Heteroarylquinolines via Sequential One-Pot Palladium-catalyzed Reaction
- 113AGNIESZKA HAMERA:** Density and Viscosity of Aqueous Solutions of Functionalized Quaternary Ammonium Surfactants
- 114NIK RUS:** Syntheses of Substituted 2H-pyran-2-ones with a Special Emphasis on Attempted Synthesis of Derivatives That Contain 2-fluoro-4-methoxyphenyl Group



PLENARY LECTURE



Science
behind
the
living

3D-Structure Shields the ‘Achilles Heel’ of Proteins: Backbone Isomerization at –NG– Sites in Proteins

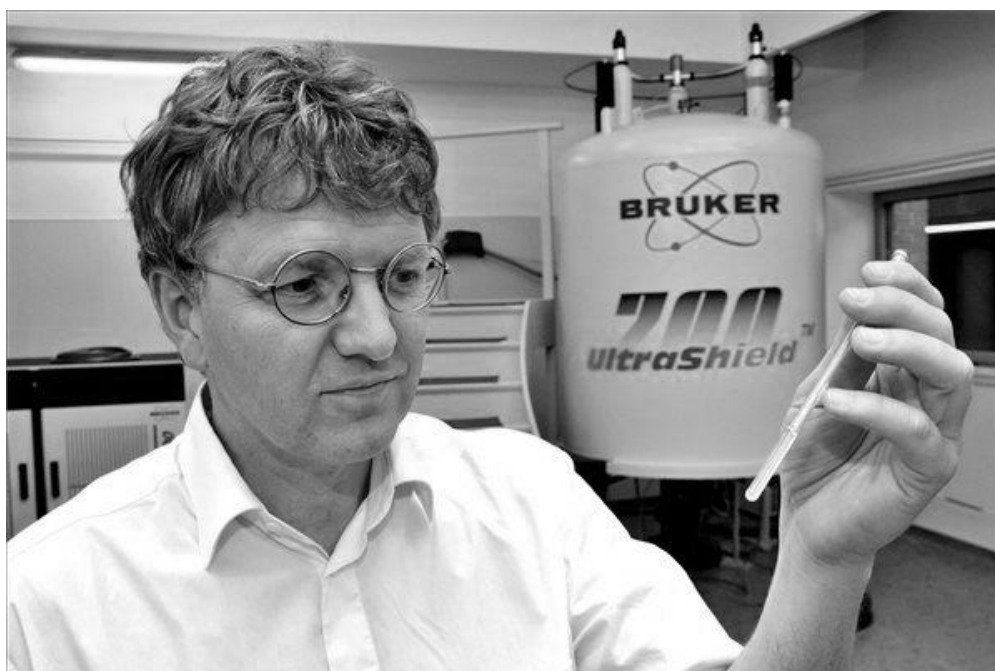
prof. dr. András Perczel

Eötvös Loránd University, Institute of Chemistry, Budapest

Deamidation of Asn was described over a century ago however, while kinetic parameters of the spontaneous isomerization of -Asn-Gly- is yet unknown. The most fragile amide bond connecting Asn/Asp to Gly isomerizes easily at physiological conditions (pH=7.4, 37°C) and thus forms the “Achilles heel” of polypeptides and proteins. Introducing suitable model systems and measuring key kinetic and thermodynamic parameters by NMR, atomic details of this isomerization/deamidation are to be revealed. Small “tricks”, NMR-data fed kinetic simulations, MD computations assisted structural details, analysis of homology-filtered large data set will be shown to give yet unknown details of this reaction. We found that backbone flexibility surrounding -Asn-Gly- sites increases, while 3D-fold compactness and reduced

internal dynamics decreases and/or hinders the above isomerization.

Dr. András Perczel attended the Faculty of Sciences of the Eötvös Loránd University, from where he graduated as a chemistry major (1985) and continued with his studies by finishing a Ph.D titled “Synthesis and conformational analysis of peptides and glycopeptides” in 1989. He is a full professor of chemistry from the year 2001 and a full member of the Hungarian Academy of Sciences since 2016. Her work includes synthetic experience on peptide and glycopeptide chemistry as well as protein expression and purification, biospectroscopy including CD, IR and NMR, structure elucidation of peptides, foldamers, miniproteins, proteins; dynamic characterization of peptides and proteins and molecular modeling.





PLENARY LECTURE

Technologies
for the
earth
and
environment



Challenges and Opportunities of Engineering the Future (Bio)refinery Processes

prof. dr. Blaž Likozar

National Institute of Chemistry, Ljubljana, Slovenia

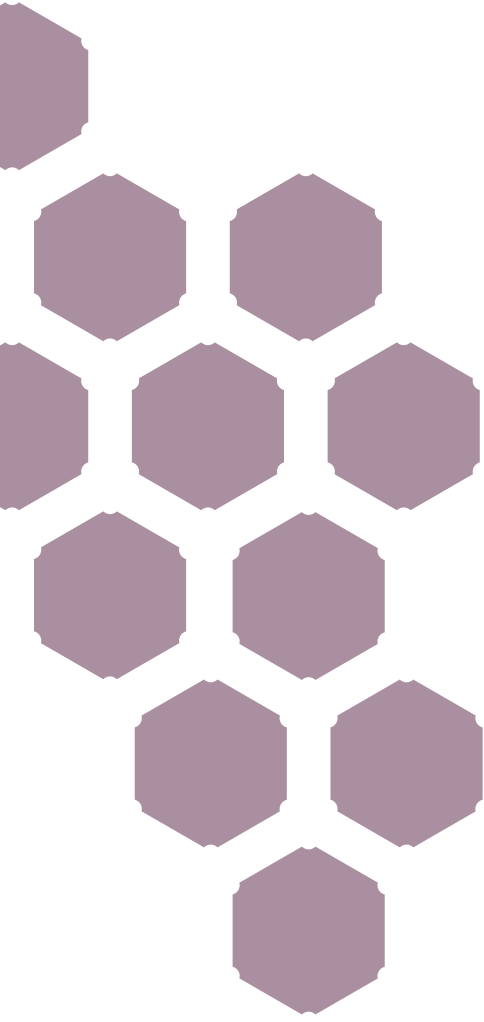
Increased refining capacities, particularly in Asia and the Middle East, alongside with uncertain crude oil and natural gas supply are mirroring the reduced operation of oil refineries in Europe. The latter are challenged to modify their business models by adjusting their value chains to be more sustainable and reliable, by adjusting the process in terms of material and energy integration and by adjusting the portfolio of targeted products. Numerous research groups are evaluating biomass as a possible complementary feedstock for the gasoline, diesel and kerosene production by its gasification in fluidised-bed reactor, subsequent Fischer–Tropsch (FT) synthesis, and by co-feeding the products in hydrocracker. Alternatively, biopolymers such as (hemi)cellulose and lignin can be utilised in existing or modified units or converted to value-added chemicals. Furthermore, methane activation by the oxidative or non-oxidative CH₄ coupling into liquid fuels using renewable energy sources (e.g. by plasma) is becoming of interest. An attempt of catalysis and the energy integration in the periods of surplus electricity (H₂ production) by the direct methanol synthesis from CO₂ (captured from flue gases) is also being investigated. Reactor design and modification, process parameters optimisation, alongside with catalyst design (activity, stability and selectivity improvement) remain an evergreen topic on the rise, also in traditional oil and gas-related processes like steam (methane or methanol) reforming, (reverse) water–gas shift, hydro-treatment, etc. Researchers are thus also involved in those research activities within various industrial and scientific projects. In this fashion, the existing and emerging (catalytic) (bio)refining processes are being rendered greener.



Prof. Dr. Blaž Likozar earned his PhD in Chemical Engineering in 2008 at the University of Ljubljana, Faculty of Chemistry and Chemical Technology. He has been a member of NIC since 2011, working senior research fellow, assistant professor and department head in the field of chemical engineering (Department of Catalysis and Chemical Reaction Engineering); leading the programme “Chemical Reaction Engineering” as well as several research projects. His expertise lies (among others) in heterogeneous catalyst materials, modelling, simulation and optimization of process fluid mechanics, transport phenomena and chemical kinetics. He worked in 2014–2015 at the University of Delaware (Catalysis Center for Energy Innovation, Newark, Delaware, USA), as a Fulbright Program researcher in the field of chemical engineering. Prof. Likozar has published over 60 original peer-reviewed scientific research papers and has the *h*-index of 15.



PLENARY LECTURE



Materials
of the
future



Nanoscale Meets Gigascale

dr. Andrej Grubišič

Sciences and exploration Directorate, NASA, US

Materials research is the bedrock underlying the advancement of the human civilization. From Stone Age to the Silicon Age, we continue to be indebted to the perseverance (and often fortuity) of those who discover new materials. In this talk, I will attempt to convey the tortuous path from fundamental materials research to materials application by focusing on a subset of cutting edge materials that I have been extensively working on over the course of my scientific career. This will include materials of interest in solar energy conversion, such as plasmonic nanoparticles and quantum dots, as well as designer materials of the not-so-distant future, such as cluster-assembled materials. In the end, I will showcase how one such designer material met a very specialized need in the Mars Organic Molecule Analyzer instrument bound for Mars onboard ESA's ExoMars Rover to search for signs of past and/or present life on the Red Planet.

Andrej Grubisic attained his B.A. degree in the Department of Chemistry at the University of Ljubljana and received his Ph.D. degrees in Chemistry at the Johns Hopkins University under mentorship of Prof. Kit H. Bowen, where he studied electronic, geometric and reactive properties of mass-selected, gas-phase cluster ions of interest as building blocks of cluster-assembled materials. He was an NRC/NIST Postdoctoral fellow at JILA/NIST University of Colorado, where he worked with Prof. David J Nesbitt on developing a novel technique for studying ultrafast electron dynamics in individual, supported plasmonic and quantum confined systems.



His strong affinity for experimental chemistry, physics, and materials research (plus non-negligible interest in the final frontier) prompted him to join the Center for Research and Exploration in Space Science and Technology (CRESST) at the University of Maryland, where he is intimately involved in the development of space-bound instrumentation as an affiliate of the Planetary Environments Laboratory at NASA Goddard Space Flight Center.



ORAL PRESENTATIONS

Science
behind
the
living



Disintegrins from the Venom of *Vipera Ammodytes Ammodytes* Efficiently Inhibit Migration of Breast Cancer Cells

Zorica Latinović^{1,2}, Adrijana Leonardi¹, Toni Petan¹, Margareta Žlajpah¹ and Igor Križaj^{*,1}

¹ Department of Molecular and Biomedical Sciences, Jožef Stefan Institute, Jamova cesta 39, SI-1000 Ljubljana, Slovenia

² Jožef Stefan International Postgraduate School, Jamova cesta 39, SI-1000 Ljubljana, Slovenia

Cancer, one of the deadliest diseases worldwide, is caused by inherited or acquired mutations of the genetic material. The main characteristics of cancer include sustaining proliferative signalling, evading growth suppressors, resisting cell death, enabling replicative immortality, inducing angiogenesis, and activating invasion and metastasis. Prevention of metastatic growth is an efficient therapy in cancer control. The key roles in the process of migration and cell viability are played by transmembrane proteins called integrins^{1,2}.

Integrins are cell adhesion receptors on the cells' surface that bind components of the extracellular matrix, various biological ligands and receptors on adjacent cells. Recent studies have exposed integrins as important factors in tumour cell survival, tumour growth and metastasis by establishing and breaking bonds between malignant cells and molecules in their surroundings. For this reason, integrins have become important targets of anti-tumour therapy².

Snake venom (SV) proteins are broadly investigated as substances that can be used in diagnosis and treatment of human diseases. Among them, disintegrins (Dis) have been found to inhibit various cell functions by their interaction with different integrins, for example platelet aggregation, angiogenesis, tumour growth and metastasis.³ In attempts to discover new molecules for treatment of breast cancer, the major type of cancer in women, we isolated from the venom of the nose-horned viper dimeric Dis (*Vaa-Dis*).

We investigated their influence on cell viability and *in vitro* migration in a model of highly invasive triple-negative breast cancer and found that *Vaa-Dis* potently inhibited the migration of cancer cells. By cell viability testing we demonstrated that 50 nM and higher concentrations of *Vaa-Dis* were toxic to highly invasive human breast adenocarcinoma cell line MDA-MB-231. Wound-healing assay revealed that already at one order of magnitude lower concentrations *Vaa-Dis* efficiently inhibited MDA-MB-231 cell migration. This exposed a promising anti-metastatic potential of *Vaa-Dis* and a good perspective of these natural snake

venom proteins for further research and development towards the application in breast cancer treatment.

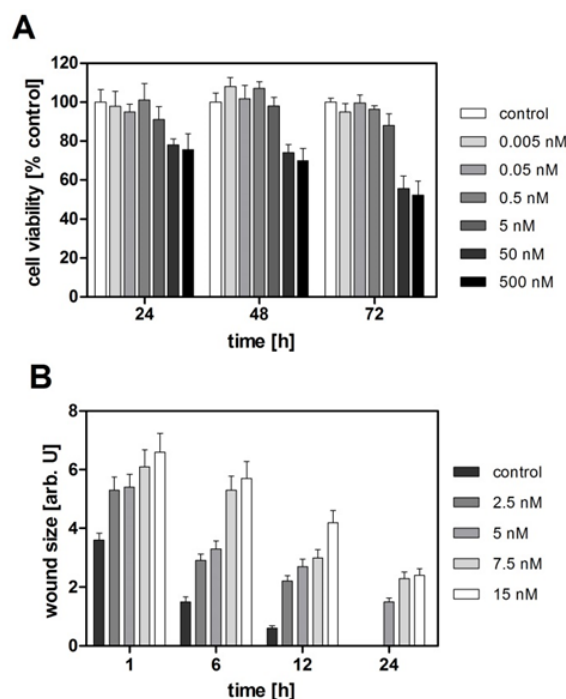


Figure 1: Effects of *Vaa-Dis* on breast cancer cells.

(A) As established by PrestoBlue™ cell viability testing, the cytotoxicity of *Vaa-Dis* for MDA-MB-231 cells is evident at 50 nM and higher concentrations. (B) The wound-healing assay on MDA-MB-231 cells was performed in the presence of *Vaa-Dis* at concentrations, which did not affect cell viability.

References:

1. D. Hanahan, R. A. Weinberg, *Cell*. **2011**, *144*, 646–674.
2. L. Seguin, J. S. Desgrosellier, S. M. Weis, D. A. Cheresh, *Trends Cell Biol.* **2015**, *25*, 234–40.
3. J. K. Arruda Macêdo, J. W. Fox, M. de Souza Castro, *Curr. Protein Pept. Sci.* **2015**, *16*, 532–548.

Use of Differential Scanning Calorimetry and Immunoaffinity Chromatography to Identify Disease Induced Changes in Human Blood Plasma Proteome

Sandi Brudar¹, Urh Černigoj², Helena Podgornik³, Mojca Kržan⁴, Iztok Prislan^{*,5}

¹ Faculty of Chemistry and Chemical Technology, University of Ljubljana, Večna pot 113, SI-1000 Ljubljana, Slovenia

² BIA Separations, Mirce 21, 5270 Ajdovščina, Slovenia

³ University Medical Centre Ljubljana, Department of Haematology, Zaloška cesta 7, 1000 Ljubljana, Slovenia

⁴ Faculty of Medicine, University of Ljubljana, Korytkova ulica 2, 1000 Ljubljana, Slovenia

⁵ Biotechnical Faculty, University of Ljubljana, Jamnikarjeva ulica 101, 1000 Ljubljana, Slovenia

Despite of rapid development of medicine and other sciences, timely and reliable diagnosis of diseases is sometimes still a pretentious task. A solution to such difficulties could lie in new methods for human plasma analysis. Human plasma serves as an important source of information about human health. Various diseases are often associated with biomarkers. The human plasma proteome consists of more than 3000 proteins and peptides, therefore the search for potential disease biomarkers, and their identification in the plasma proteome is a very complicated procedure¹. Only ten proteins make up 90% of the mass of plasma proteins and albumin (HSA) and immunoglobulins (Ig) represent 75% out of these ten proteins. Majority of biomarkers in blood plasma are often scarce and small in size. Consequently, their detection can be limited by the presence of more abundant and larger proteins such as HSA or IgG¹. Because of the complexity of plasma no single technique can fully exploit the information plasma has to offer. Chaires et al. have discovered the potential use of differential scanning calorimetry (DSC) for plasma analysis¹. Using a DSC to analyze plasma yields a thermogram that is sensitive to differences in thermodynamic properties of the most abundant plasma proteins. Chaires et al. have shown that thermograms of plasma from diseased individuals differ significantly from thermograms of plasma from healthy individuals^{1,2}. Another tool to facilitate the search for biomarkers is liquid chromatography, in particular affinity chromatography and ion-exchange chromatography³.

In our research plasma samples from individuals suffering from chronic lymphocytic leukemia, multiple myeloma and acute myeloid leukemia were measured with DSC. To obtain additional information about thermal behavior of plasma proteins an immunoextraction of HSA using a chromatographic column with immobilized anti-HSA was carried out. Obtained thermograms from diseased individuals differ

significantly from one another and from the thermogram of healthy blood plasma samples (Figure 1). With the immunoextraction of HSA we managed to enrich less abundant plasma proteins, which could provide a further insight into disease development. Efficiency of HSA depletion and protein composition of fractionated plasma was validated by SDS-PAGE.

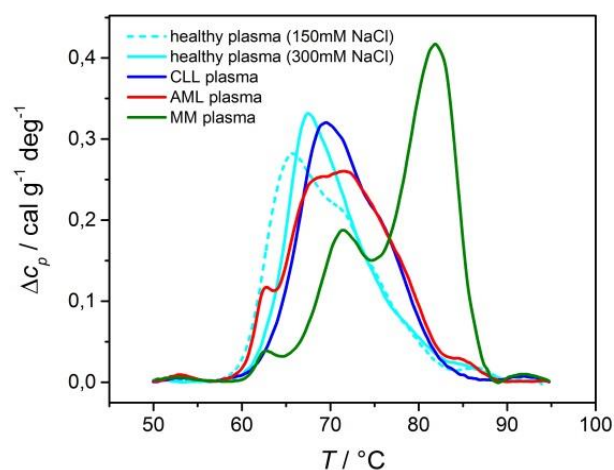


Figure 1: Comparison of thermograms of blood plasma from diseased individuals dissolved in 20 mM phosphate buffer and 300 mM NaCl and with a thermogram of blood plasma from healthy individual dissolved in 10 mM phosphate buffer and 150 mM NaCl (dashed cyan line) and 20 mM phosphate buffer and 300 mM NaCl (full cyan line).

References:

1. N. C. Garbett, J. J. Miller, A. B. Jensen, J. B. Chaires, *Biophys. J.*, **2008**, 94, 1377-1383.
2. N. C. Garbett, M. L. Merchant, C. W. Helm, A. B. Jensen, J. B. Klein, J. B. Chaires, *PLoS One*, **2014**, 9, e84710, 1-12.
3. T. Čerk Petrič, P. Brne, B. Gabor, L. Govednik, M. Barut, A. Štrancar, L. Zupančič Kralj, *J. Pharm. Biomed. Anal.*, **2007**, 43, 243-249.

Lipid Droplet Formation in HeLa Cervical Cancer Cells Depends on Cell Density and the Concentration of Exogenous Unsaturated Fatty Acids

Ema Guštin^{1, #}, Eva Jarc^{1, 2, #}, Ana Kump^{1, 2}, Toni Petan^{*, 1}

¹ Department of Molecular and Biomedical Sciences, Jožef Stefan Institute, Jamova cesta 39, SI-1000 Ljubljana, Slovenia

² Jožef Stefan International Postgraduate School, Jamova cesta 39, SI-1000 Ljubljana, Slovenia

[#] These authors contributed equally to the work.

Lipid droplets (LDs) are cytosolic structures composed of a core of neutral lipids surrounded by a phospholipid monolayer embedded with proteins. They were traditionally viewed as inert lipid storage depots. However, as it became clear in the past several years, they are highly organized multi-functional dynamic organelles. Besides providing energy and building blocks for biosyntheses, they have important roles in protein quality management, viral replication and immune response. Importantly, they act as platforms integrating cell signaling and metabolism with implications for metabolic diseases and cancer¹.

One of the most important roles of LDs in most cells is storing excess exogenous and endogenous fatty acids (FAs), thus preventing lipotoxicity and starvation-induced cell death. However, the role of different unsaturated fatty acids (FAs) in supporting LD accumulation and cell survival in different cancer cell types under different environmental conditions is not clear^{2,3}.

Here we studied the ability of mono- and polyunsaturated FAs to affect LD formation and cell death in HeLa cervical cancer cells. We found that while in most cells LD content decreases with cell culture density (e.g. in MDA-MB-231 breast cancer cells), high culture density of HeLa cells is associated with elevated accumulation of LDs (Figure 1). Exogenously added unsaturated FAs (oleic, linoleic, arachidonic, eicosapentaenoic and docosahexaenoic acids) displayed a similar ability to alter LD formation in HeLa cells. There was a dual, concentration-dependent effect on LD accumulation: all FAs induced LD formation at higher concentrations, while some of them, surprisingly, reduced LD content at low micromolar concentrations. In serum-starved HeLa cells, oleic acid stimulated LD formation, but, contrary to expectations, it promoted, rather than reduced cell death⁴.

Our results reveal a link between cell population density and LD formation in HeLa cells and show that unsaturated FAs may both suppress or stimulate LD formation. This dynamic regulation of LD content must

be accounted for when studying the effects of lipids and lipid metabolism-targeting drugs on LD metabolism in HeLa cells.

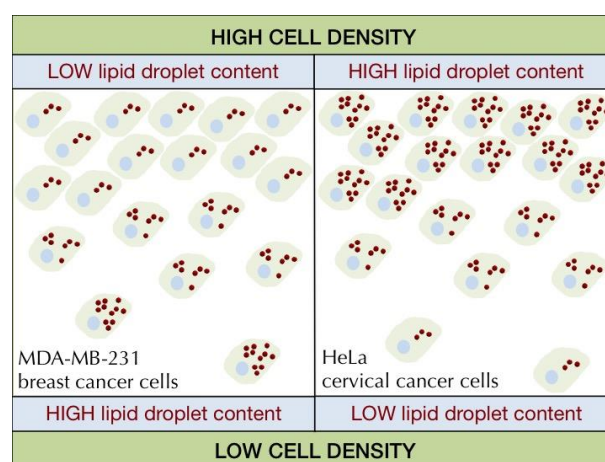


Figure 1: Lipid droplet content increases with cell density in HeLa cervical cancer cells, but it decreases in breast cancer cells.

References:

1. Farese, R. V.; Walther, T. C., Lipid Droplets Finally Get a Little R-E-S-P-E-C-T. *Cell*. **2009**, 139, 855-60.
2. Cabodevilla, A. G.; Caballero-Sánchez, L.; Nintou, E. et al, Cell Survival during Complete Nutrient Deprivation Depends on Lipid Droplet-fueled β -Oxidation of Fatty Acids. *J. Biol. Chem.* **2013**, 288, 27777-88.
3. Pucer, A.; Brglez, V.; Payré, C.; Pungerčar, J.; Lambeau, G.; Petan, T., Group X secreted phospholipase A₂ induces lipid droplet formation and prolongs breast cancer cell survival. *Mol. Cancer*. **2013**, 12, 111.
4. Guštin, E.; Jarc, E.; Kump, A.; Petan, T., Lipid Droplet Formation in HeLa Cervical Cancer Cells Depends on Cell Density and the Concentration of Exogenous Unsaturated Fatty Acids. *Acta Chim. Slov.* **2017**, 64, in press.

Development of *in Vivo* Active Non-Covalent Butyrylcholinesterase Inhibitors

Urban Košak¹, Damijan Knez¹, Boris Brus¹, Anja Pišlar¹, Simon Žakelj¹, Jurij Trontelj¹, Jure Stojan², Marko Živin³, Adrian Podkowa⁴, Kinga Sałat⁴, Nicolas Coquelle⁵, Jacques-Philippe Colletier⁵, and Stanislav Gobec^{*,1}

¹ Faculty of Pharmacy, University of Ljubljana, Aškerčeva 7, 1000 Ljubljana, Slovenia

² Institute of Biochemistry, Faculty of Medicine, University of Ljubljana, Vrazov trg 2, 1000 Ljubljana, Slovenia

³ Institute of Pathological Physiology, Faculty of Medicine, University of Ljubljana, Vrazov trg 2, 1000 Ljubljana, Slovenia

⁴ Faculty of Pharmacy, Jagiellonian University, Medyczna 9 St., 30-688 Krakow, Poland

⁵ University Grenoble Alpes, and CNRS and CEA, IBS, F-38044 Grenoble, France

Memory and cognitive deficits, characteristic for patients with Alzheimer's disease (AD), are the result of a decrease in the levels of neurotransmitter acetylcholine (ACh). Acetylcholinesterase and butyrylcholinesterase (BChE) are cholinesterases (ChEs), which terminate cholinergic neurotransmission by catalyzing the hydrolysis of ACh. Enzymatic activity of BChE increases with the disease progression, thus classifying BChE as a viable therapeutic target in advanced AD.

We recently discovered carboxamide **1** (Figure 1), a potent ($IC_{50} = 21.3$ nM) and selective inhibitor of human (h)BChE.¹ Based on the chemical structure of this compound or crystal structure of its complex with human BChE we designed several distinctive types of selective hBChE inhibitors. We synthesized 121 compounds and evaluated their *in vitro* inhibitory potencies against both ChEs. The solved crystal structures of complexes of 6 inhibitors with hBChE revealed their binding modes and represent an excellent basis for their further structure-based optimization.²⁻⁶ Two compounds, sulfonamide **2**³ (Figure 1) and carboxamide **3**⁵ (Figure 1) are particularly interesting as the most potent (**2**: $IC_{50} = 4.92$ nM; **3**: $IC_{50} \leq 1$ nM) and selective hBChE inhibitors of the series and were therefore biologically evaluated further. Both compounds inhibit BChE *ex vivo* in rat brain slices, are not cytotoxic and have neuroprotective properties. *In vitro* pharmacokinetic experiments showed that compounds **2** and **3** are highly protein bound, highly permeable and metabolically stable. Finally, they cross the blood-brain barrier and improve memory, learning abilities and cognitive functions of mice in a model of the cholinergic deficit that characterizes AD, without producing acute cholinergic adverse effects. Our research thus provides two advanced lead compounds for developing drugs for alleviating symptoms caused by cholinergic hypofunction in advanced AD.

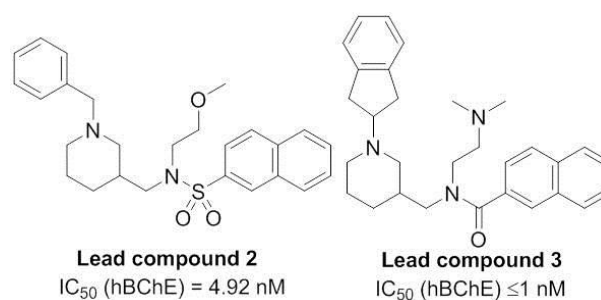


Figure 1: Structures and inhibitory potencies of *in vivo* active non-covalent BChE inhibitors.

References:

1. Brus, B.; *et al* Discovery, Biological Evaluation, and Crystal Structure of a Novel Nanomolar Selective Butyrylcholinesterase Inhibitor. *J. Med. Chem.* **2014**, *57*, 8167-8179.
2. Knez, D.; *et al* Structure-Based Development of Nitroxoline Derivatives as Potential Multifunctional Anti-Alzheimer Agents. *Bioorg. Med. Chem.* **2015**, *23*, 4442-4452.
3. Košak, U.; *et al* Development of an *In-Vivo* Active Reversible Butyrylcholinesterase Inhibitor. *Sci. Rep.* **2016**, *6*, 39495.
4. Košak, U.; *et al* *N*-Propargylpiperidines with Naphthalene-2-Carboxamide or Naphthalene-2-Sulfonamide Moieties: Potential Multifunctional Anti-Alzheimer's Agents. *Bioorg. Med. Chem.* **2017**, *25*, 633-645.
5. Košak, U.; *et al* The Magic of the Cation- π Interaction: a Picomolar *In-Vivo*-Active Butyrylcholinesterase Inhibitor. *Submitted for publication*.
6. Knez, D.; *et al* Butyrylcholinesterase inhibitors as multi-target directed ligands with antioxidant and neuroprotective activity. *Submitted for publication*.

Interaction of N-terminus PrP^C with NCAM Fibronectin Domain

Urška Slapšak^{1, 2}, Giulia Salzano², Ladan Anim², Romany N. N. Abskharon³, Gregor Ilc^{1, 4}, Blaž Zupančič¹, Ivana Biljan⁵, Gabriele Giachin^{2, 6}, Giuseppe Legname^{*, 2}, Janez Plavec^{*, 1, 7}

¹ Slovenian NMR Centre, National Institute of Chemistry, Hajdrihova 19, SI-1001 Ljubljana, Slovenia

² Laboratory of Prion Disease, Department of Neuroscience, Scuola Internazionale Superiore di Studi Avanzati, 265-34136 Trieste, Italy

³ Vrije Universiteit Brussel, Structural Biology Research Center, Pleinlaan 2, 1050 Brussels, Belgium

⁴ EN-FIST Centre of Excellence, Trg Osvobodilne fronte 13, SI-1000 Ljubljana, Slovenia

⁵ Department of Chemistry, Faculty of Science, University of Zagreb, Horvatovac 102A, HR-10 000 Zagreb, Croatia

⁶ Structural Biology Group, European Synchrotron Radiation Facility, avenue des Martyrs, CS 40220, 38043 Grenoble, France

⁷ Faculty of Chemistry and Chemical Technology, University of Ljubljana, Večna pot 113, SI-1000 Ljubljana, Slovenia

The cellular form of the prion protein (PrP^C) is a highly conserved glycoprotein mostly expressed in the central and peripheral nervous systems by different cell types in mammals. A misfolded, pathogenic isoform, denoted as prion (PrP^{Sc}), is related to a class of fatal human and animal neurodegenerative diseases known as transmissible spongiform encephalopathy¹. Despite the fact that PrP^C is highly conserved among different species, its function has not been unequivocally clarified and it is rather defined as a pleiotropic protein likely acting as a dynamic cell surface scaffolding protein for the assembly of different signalling modules². Among the variety of PrP^C protein interactors, the neuronal cell adhesion molecule (NCAM) has been studied *in vivo*, but the structural basis of this functional interaction is still a matter of debate³.

In this study we focused on the structural determinants responsible for human PrP^C (HuPrP) and NCAM interaction using STED nanoscopy, SPR and NMR spectroscopy approaches. PrP^C co-localizes with NCAM in mouse hippocampal neurons and this interaction is mainly mediated by the intrinsically disordered PrP^C N-terminal domain, which binds with high affinity the NCAM fibronectin type-3 domain (FNIII1,2) (Fig. 1). Detailed NMR structural investigations revealed surface interacting epitopes governing the interaction between different peptides originated from HuPrP N-terminus and the second module of NCAM fibronectin type-3 domain (FNIII2). Our data provided molecular details about the interaction between HuPrP and NCAM fibronectin domain, and revealed a new role of PrP^C N-terminus as a dynamic and functional element responsible for protein-protein interaction⁴.

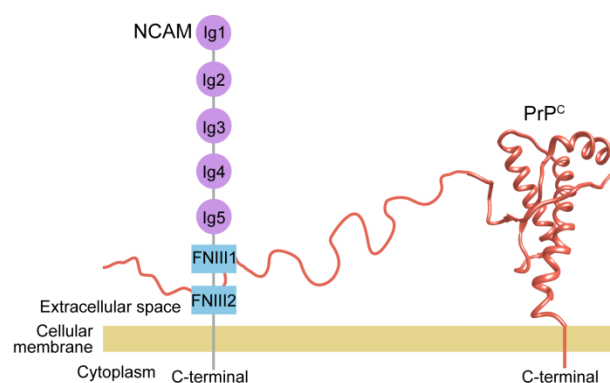


Figure 1: Schematic representation of interaction model of complex between NCAM domain and PrP^C.

References:

1. Colby, D. W.; Prusiner, S. B., Prions. *Cold Spring Harbor Perspectives in Biology* **2011**, 3, a006833.
2. Westergaard, L.; Christensen, H. M.; Harris, D. A., The cellular prion protein (PrP^C): Its physiological function and role in disease. *Biochimica et Biophysica Acta (BBA) - Molecular Basis of Disease* **2007**, 1772, 629-644.
3. Crossin, K. L.; Krushel, L. A., Cellular signaling by neural cell adhesion molecules of the immunoglobulin superfamily. *Developmental Dynamics: An Official Publication of the American Association of Anatomists* **2000**, 218, 260-279.
4. Slapšak, U.; Salzano, G.; Amin, L.; Abskharon, R. N.; Ilc, G.; Zupančič, B.; Biljan, I.; Plavec, J.; Giachin, G.; Legname, G., The N terminus of the prion protein mediates functional interactions with the neuronal cell adhesion molecule (NCAM) fibronectin domain. *Journal of Biological Chemistry* **2016**, 291 (42), 21857-21868.

Development of Caffeine Biosensors Based on Anti-Caffeine Nanobodies and Fluorescent Proteins

Boštjan Petrič¹, Katja Hrovat Arnež¹, Gregor Gunčar^{*, 1}

¹ Faculty of Chemistry and Chemical Technology, University of Ljubljana, Večna pot 113, SI-1000 Ljubljana, Slovenia

The use of antibodies as parts of fusion-protein-based biosensors has a long history, both *in vitro* and *in vivo*. Split marker proteins, such as fluorescent proteins, have been used in this context as fusion partners of antibodies, but their use has been limited since we could seldom use them to detect a single molecule present in a system. The discovery of anti-caffeine nanobodies which form dimers upon binding to caffeine promised to change this and allow the construction of biosensors made of anti-caffeine nanobodies and split biomarker proteins. We have tried out two different fusion protein designs.

In the first design, based on the splitting of enhanced green fluorescent protein (EGFP) by Magliery and Regan (2006)¹, we fused one nanobody with the N-terminal part of EGFP including amino acid residues 1-157 and the other nanobody with the C-terminal part including amino acid residues 158-238. The parts of split EGFP were both on the N-terminus of the fusion proteins. We prepared both fusion proteins and performed fluorimetric measurements in the presence and absence of caffeine. The results demonstrated increased fluorescence with increasing caffeine concentration, but only to a certain point – this could be explained by reduced dimerization when most nanobodies are bound to their own caffeine molecule instead of sharing one. However, the increase in fluorescence was small, and the system showed itself to be difficult to optimize.

In the second design, we utilized components of the FPX system which was originally designed by Ding et al. (2015) to detect calcium *in vivo*². The system consists of three modified dimerization-dependent fluorescent proteins, ddGFP A, ddFP B and ddRFP A. None of them fluoresce on their own, but when ddGFP A and ddFP B, or ddRFP A and ddFP B, form a dimer, they acquire green or red fluorescence, respectively. When these are bound to fusion partners that can bind to one another, the interactions between fusion partners can alter the ratio between red and green fluorescence, thus making FPX a useful reporting system. We designed two systems, both of them for *in vivo* use in mammalian cells as well as *in vitro* use. The first system consists of 1) ddGFP A, 2) a fusion protein combining ddFP B and a nanobody, and 3) a fusion protein combining ddRFP A and a nanobody. Upon

binding of caffeine, proteins 2 and 3 will bind to one another because of nanobody dimerization, thus shifting emitted light from green to red. In the second system, we have a single protein consisting of, respectively, a nanobody, ddGFP A, ddFP B, another nanobody and ddRFP A. Upon binding of caffeine, binding of ddGFP A to ddFP B will be substantially increased due to their increased proximity, and fluorescence will shift from red to green. Both systems have been modelled *in silico* and are in the process of development. Upon completion, we expect their *in vitro* application to be one of the easiest methods for caffeine detection available, and their application *in vivo* to open the possibility of using caffeine as an inducer molecule in living systems.



Figure 1: Model of the structure of a single fusion protein composed of ddGFP A (green), ddFP B (gray), ddRFP A (red) and two anti-caffeine nanobodies (brown). Due to nanobody dimerization, ddGFP A and ddFP B have been brought close together. The model was created by the RaptorX online tool.

References:

1. Magliery, T. J.; Regan, L, Reassembled GFP: detecting protein-protein interactions and protein expression patterns. *Methods of biochemical analysis* **2006**, 47, 391-405.
2. Ding, Y.; et al., Ratiometric biosensors based on dimerization-dependent fluorescent protein exchange. *Nature communications* **2015**, 12, 195–198.



ORAL PRESENTATIONS

Technologies
for the
earth
and
environment



Advanced Oxidation Processes for Hospital Wastewater Treatment Containing Antibiotics

Severina Stavbar*,¹ Maša Knez,¹ Gabriela Kalčíková,² Andreja Žgajnar Gotvajn,² Mitja Kolar,² Sonja Šostar Turk,³

¹ Faculty of Chemistry and Chemical Technology, University of Maribor, Smetanova ulica 17, 2000 Maribor, Slovenia

² Faculty of Chemistry and Chemical Technology, University of Ljubljana, Večna pot 113, 1000 Ljubljana, Slovenia

³ Faculty of Health Sciences, University of Maribor, Žitna ulica 15, 2000 Maribor, Slovenia

The use of antibiotics in modern society is an important source of environmental pollution, especially in the case of environmentally resistant molecules. The residues of antibiotics can enter the environment directly or indirectly from a variety of sources. Various studies showed that antibiotic residues are present in waste waters, surface waters, groundwater, in various organisms, in soil and drinking water.¹ It is known that individual antibiotics adverse effects on non-target organisms even at low concentrations and they can accumulate in the aquatic environment and the organisms and can also pass into the food chain.² Preliminary studies have shown that the highest concentrations of antibiotics are found in hospital wastewater. To remove such pollutants, existing treatment plants are not suitable, and new cleaning technologies have not yet been tested.

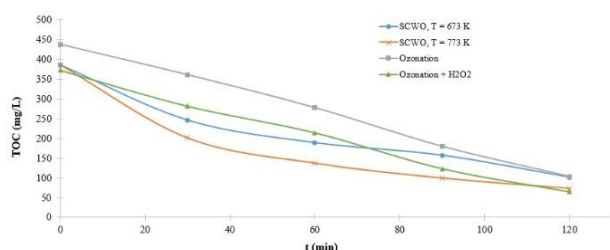


Figure 1: Changes of TOC of model wastewater sample with reaction time at different processes.

The aim of our study was to evaluate and compare two advanced oxidation techniques, for the removal of amoxicillin and ciprofloxacin from model wastewater. First technique was the supercritical water oxidation (SCWO). Experiments were carried out at a temperature of 673 K and 773 K and pressure of 29 MPa and 30 MPa. The second technique was ozonation with and without addition of hydrogen peroxide. Working pressure was 0.5 bar, gas flow 50 m³/h and the system capacity was 100 g/Nm³. The removal efficiency was monitored with TOC (Total Organic Carbon) (Figure 1). We were also interested in reducing the toxicity to microorganisms of active sludge (Figure 2).

As expected with SWCO, TOC removal increased with increasing the reaction temperature. We can also see the impact of H₂O₂, as the removal of TOC was faster.

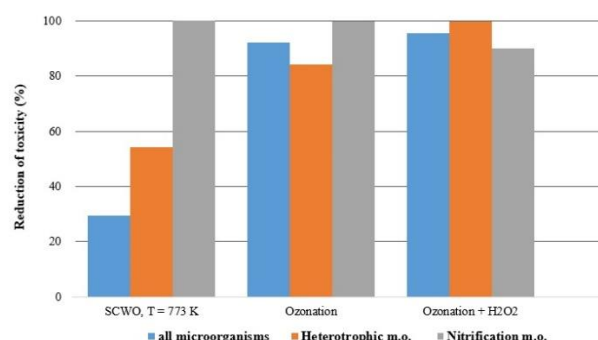


Figure 2: Reduction in toxicity to activated sludge.

The results show that the toxicity to heterotrophic microorganisms is completely removed by ozonation with addition of hydrogen peroxide. A comparable reduction in toxicity to nitrification microorganisms is achieved by ozonation and SCWO.

Ozonation and SCWO are both promising techniques to reduce toxicity of wastewater containing low biodegradable, persistent antibiotic agents and could be used in the pre-treatment system, prior to the conventional biological treatment plant.

References:

1. Kümmerer, K., The presence of pharmaceuticals in the environment due to human use-present knowledge and future challenges. *Journal of Environmental Management* **2009**, 90, 2354-2366.
2. Narvaez, V.J.F., Jimenez, C.C., Pharmaceutical products in the environment: sources, effects and risks. *VITAE* **2012**, 19(1), 93-108.

Development of Microextraction Methods for Determination of Benzotriazoles

Ida Kraševac*, Helena Prosen

Faculty of Chemistry and Chemical Technology, University of Ljubljana, Večna pot 113, SI-1000 Ljubljana, Slovenia

Benzotriazoles are heterocyclic compounds, used as corrosion inhibitors in different industrial processes and as UV stabilizers in plastics. They are classified as emerging pollutants due to their harmful effects on plants and toxicity to some aquatic organisms, can be only partially removed from water in wastewater treatment plants and are therefore found in various environmental samples in concentrations ranges of $\mu\text{g/L}$. Their determination demands the use of preconcentration techniques, combined with sensitive analytical techniques, such as LC-MS/MS.¹

Solvent microextraction methods are techniques that use microliter amounts of solvents, and are therefore regarded as more environmentally friendly than classical extraction techniques. Among others, this group includes techniques known as dispersive liquid-liquid microextraction (DLLME) and hollow fibre microextraction (HFME), which were in this work optimized for extraction of 6 polar benzotriazoles from water based samples.

DLLME is a technique, where the fast injection of a mixture of a water-immiscible extraction solvent and a miscible dispersive solvent into an aqueous sample forms a stable emulsion, which is later separated to obtain a single drop of extract. Such an extraction is almost instantaneous and does not demand any special equipment.² For optimal enrichment factors the following parameters were optimized in addition to the selection of the correct extraction and dispersive solvents: sample volume, pH and salt content, volumes of solvents chloroform and acetonitrile, centrifugation speed and time. At optimal conditions, the enrichment factors for the analysed benzotriazoles ranged from 14 to 104, according to their polarity.

For HFME, small amounts of organic solvent are immobilized into the pores of a hollow polypropylene fibre. The analytes from aqueous sample are extracted into this organic solvent, and further concentrated in the acceptor solution placed into the lumen of the fibre (Figure 1). This results in high enrichment factors and good clean-up of the matrix components.³ The optimization of this method in this work included the selection of the membrane solvent and acceptor solution, and experimental optimization of the sample volume, pH and salt content, fibre length, acceptor

solution pH, speed of stirring and extraction time. At optimal conditions, the enrichment factors for the analysed compounds ranged from 30 to 165, with correlation to their polarity.

Finally, the developed methods were compared to a solid phase extraction (SPE) method, considered as a more standard practice, in terms of enrichment factors, repeatability, solvent volume usage, extraction time and ease of handling. For this step, different suitable literature methods were tested, of which the extraction with Oasis MAX cartridges gave the best results.⁴ The extracts were analysed with HPLC with UV detection and LC-MS/MS.

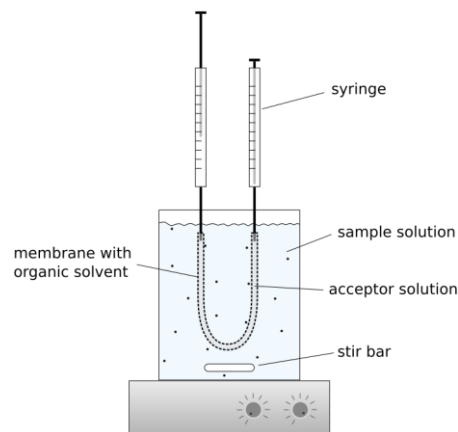


Figure 1: Scheme of HFME extraction setup.

References:

1. Alotaibi M. D., McKinley A. J., Patterson B. M., Reeder A. Y., Benzotriazoles in the Aquatic Environment: a Review of Their Occurrence, Toxicity, Degradation and Analysis. *Water Air Soil Pollut.* **2015**, 226(7), 1-20.
2. Zgoła-Grzeskowiak A., Grzeskowiak T., Dispersive liquid-liquid microextraction. *Trends Anal. Chem.* **2011**, 30(9), 1382-1399.
3. Ghambarian M., Yamini Y., Esrafil A., Developments in hollow fiber based liquid-phase microextraction: principles and applications. *Microchim. Acta* **2002**, 177, 271-294.
4. Salas D., Borrull F., Marcé R.M., Fontanals N., Study of the retention of benzotriazoles, benzothiazoles and benzenesulfonamides in mixed-mode solid-phase extraction in environmental samples. *J. Chromatogr. A* **2016**, 1444, 21-31.

Cold Atmospheric Plasma for Inactivation of Plant Viruses

Arijana Filipić^{*,1}, David Dobnik¹, Nataša Mehle¹, Gregor Primc², Ita Junkar², Miran Mozetič², Maja Ravnikar¹, Jana Žel¹

¹ National Institute of Biology, Večna pot 111, 1000 Ljubljana, Slovenia

² Jožef Stefan Institute, Jamova 39, 1000 Ljubljana, Slovenia

The possibility of food shortage is getting higher and higher due to different factors that are affecting crop yield and food safety. One of those factors are plant viruses, which can destroy entire crops or lower the germination rate, consequently lowering the yield.¹ *Potato Virus Y* (PVY) is a plant virus that can infect different plants and cause different symptoms depending on the virus strain and plant species. Isolates from the recombinant PVY^{NTN} group are the most aggressive, resulting in symptoms that include mosaic, chlorotic and necrotic lesion on leaves as well as necrotic ringspot on tubers (Figure 1). PVY is economically the most important potato virus, which can cause up to 80% annual losses in potato crop production.² PVY is transmitted with infected “seed” material, mechanically by contact, artificially in the laboratory or even with water. Many other plant viruses can be transmitted with water and all of them have unpleasant properties like great stability, direct infection of the plants and a wide host range. Water transmission poses a big problem in closed irrigation systems as once the plant viruses get in there they will likely infect all of the crops.³ That is why it is very important to find a new method for plant virus inactivation in waters and nutrient solutions. One of possible solutions is cold atmospheric plasma, which was already proven to be very successful for sterilization in different fields like medicine and food processing. Plasma is the fourth state of matter. It is a complex mixture of charged particles, reactive species, UV photons and neutral particles⁴. Plasma has many advantages over classical sterilization methods as it has strong antimicrobial properties (like ROS and RNS, UV photons, charged particle), is easy to set up and maintain, and is environmentally friendly as well as inexpensive.^{4,5}

In our research cold atmospheric plasma (CAP) was used for inactivation of PVY. Samples of 10 ml solution containing nutrient elements and the virus were treated with CAP different amounts of time. Viral RNA was undetectable after the longest treatment (3 hours) whilst shorter treatment times did not completely destroy viral RNA. Regardless, viral presence in the test plants that were mechanically inoculated with mentioned samples was undetectable even at shorter treatment times down to only 15 min.

With that, we showed that with our plasma source we can effectively inactivate PVY in liquids.



Figure 1: All test plants inoculated with untreated samples have developed typical symptoms. Viral presence was confirmed with molecular methods.

References:

1. Sivachandiran, L.; Khacef, A., Enhanced seed germination and plant growth by atmospheric pressure cold air plasma: combined effect of seed and water treatment. *RSC Adv.* **2017**, *7*, 1822-1832.
2. Kogovšek, P.; Pompe-Novak M.; Petek, M.; Fragner, L.; Weckwert, W.; Gruden, K., Primary Metabolism, Phenylpropanoids and Antioxidant Pathways Are Regulated in Potato as a Response to Potato virus Y Infection. *PLoS ONE* **2016**, *11*, 1-20.
3. Mehle, N.; Ravnikar, M., Plant viruses in aqueous environment - Survival, water mediated transmission and detection. *Water Res.* **2012**, *46*, 4902-4917.
4. Hoffmann, C.; Berganza, C.; Zhang, J., Cold Atmospheric Plasma: methods of production and application in dentistry and oncology. *Med gas res.* **2013**, *3*, 1-21.
5. Pradeep, P.; Chulkyoon, M., Non-thermal plasmas (NTPs) for inactivation of viruses in abiotic environment. *Res. J. BioTechnol.* **2016**, *11*, 91-96.

An Effect of Noble Metals, Supports and Operating Conditions on Eugenol Hydrotreatment: A Microkinetic Study

Ana Bjelić¹, Miha Grilc^{*,1}, Matej Huš¹, Blaž Likozar¹

¹ Department of Catalysis and Chemical Reaction Engineering, National Institute of Chemistry, Hajdrihova 19, Ljubljana, Slovenia

Lignin, a natural amorphous polymer, with its unique structure and chemical properties offers a great potential to be used as a feedstock for the production of aromatic compounds and therefore significantly improve biorefinery operation. Hydrotreatment at elevated temperatures and pressures has been considered as an effective route for lignin valorization. Numerous catalysts based on transition metals and lately more and more on noble metals have been tested in this process¹. Mechanistic and kinetic studies referred to lignin processing have mostly been based on model compounds hydrotreatment. In our work we have chosen eugenol as a representative lignin monomer model compound since it consists three typical functional groups present in the native lignin.

We have tested activity and selectivity of noble metals Ru, Pd, Pt, Rh supported on C, Al₂O₃, TiO₂, SiO₂, SiO₂-Al₂O₃ and HZSM-5 in the eugenol hydrotreatment process. Experiments have been performed in a 300 mL autoclave. Three temperatures 225, 275 and 325 °C, two pressures 5 and 7 MPa and two catalyst loadings of 0.180 and 0.315 g were tested. Microkinetic model developed in our previous study has been applied in this work to estimate relevant kinetic parameters over each employed noble metal catalysts. The advantage of our model versus other conventional ones is that it takes into account thermodynamic and transport phenomena, adsorption and desorption of components on the catalyst surface and finally reactions without assuming any of them as a rate limiting step. In this way the effect of each elementary step on the total kinetic can be considered enabling deeper understanding and consequently enhanced intensification of the process. .

Figure 1 shows product distribution over Ru/C at different temperatures. Most dominant products were 2-methoxy-4-propylphenol (HMPB) (olive), 2-methoxy-4-propylcyclohexanol (HMPC) (orange), 4-propylcyclohexanol (HPC) (violet), and propylcyclohexane (PC) (magenta). It can be observed that the temperature increase favors more energy demanding reactions being thus in accordance with the Arrhenius law. All tested noble metal catalysts have shown tendency towards benzene ring hydrogenation, Rh the highest (HMPC predominant product), while Ru

showed also significant deoxygenation ability. Beside the metal effect on the reaction course, support has shown significant influence on product distribution. Namely, more neutral supports promoted hydrogenation reactions, while more acidic such as HZSM-5 and Al₂O₃ favored oxygen removal reactions in a great extent. Pressure has not shown significant influence on the product distribution, although slightly higher yields of hydrogenated compounds can be observed at higher pressure. Catalyst loading affected the reaction as expected; by a catalyst mass increase all reactions were proportionally enhanced. Lines in Figure 1 correspond to model results matching the components in color. A good agreement between modeled and experimentally observed concentrations has been achieved.

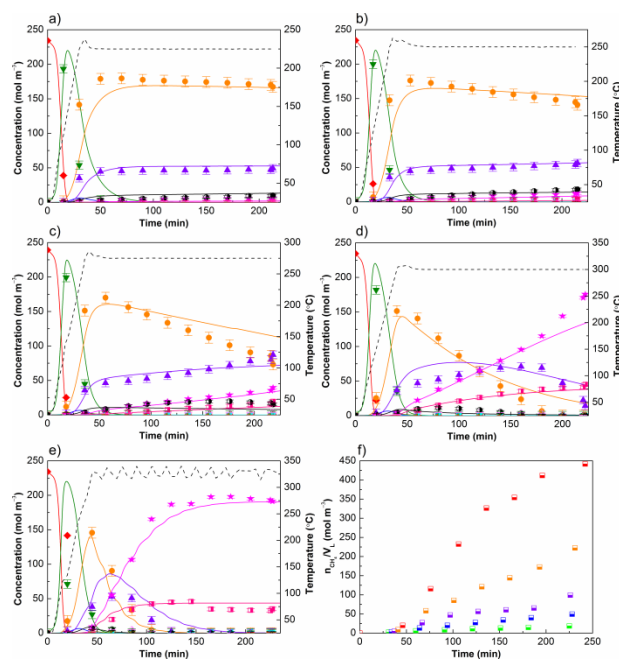


Figure 1: Temperature influence on the product distribution over Ru/C catalyst a) 225 °C, b) 250 °C, c) 275 °C, d) 300 °C, e) 325 °C, f) methane yield

References:

1. Galkin, M. V.; Samec, J. S. M., Lignin Valorization through Catalytic Lignocellulose Fractionation: A Fundamental Platform for the Future Biorefinery. *ChemSusChem* **2016**, 9 (13), 1544-1558.

Effect of Biochar Application on Pb and As Mobility in Tailings

Evelin Gruden^{*,1}, Marija Zupančič¹

¹ Faculty of Chemistry and Chemical Technology, University of Ljubljana, Večna pot 113, 1000 Ljubljana, Slovenia

Mine tailings are characterized by high toxic inorganic element concentrations and subsequently pose a risk to the environment and to human health.¹ In situ chemical stabilization is a promising remediation technique used to reduce the mobility of metals in contaminated soil by adding amendments.² Biochar and phosphate additions have already been shown to be highly effective in reducing metal availability.¹⁻³

In this study the mine tailings from Sasa zinc and lead mine in Macedonia were used as an example of mine area soil. To evaluate the effect of biochar addition on Pb and As mobility in tailings, 16 mixtures were prepared at different application rates using animal bone char (ABC, source of soluble phosphate), commercially available biochar Carbon Gold (CG, prepared from wooden biomass), or biochar from pyrolysed cherry twigs (CB). The mobility of As and Pb in tailings and mixtures was then determined by Toxicity Characteristic Leaching Procedure (TCLP). Furthermore, the mobility of P in mixtures and tailings was evaluated according to SIST ISO 11263:1996.

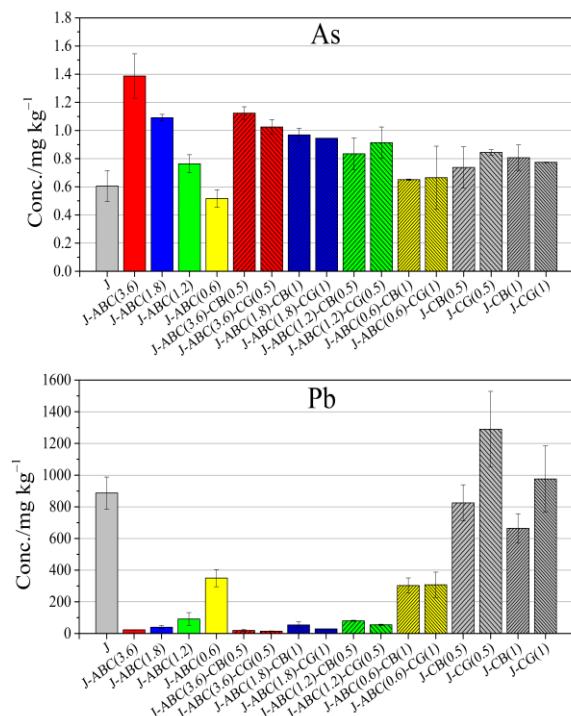


Figure 1: TCLP concentrations of As and Pb (in mg kg⁻¹) of the tailings and mixtures.

Results have shown that the addition of soluble P mainly influenced the decrease of Pb mobility. ABC addition resulted in the highest Pb stabilization among

all three types of biochar. Besides that, the addition of biochar prepared from wooden biomass additionally improved Pb stabilization. In almost all mixtures the solubility of Pb decreased to values lower than the TCLP regulatory level of 5 mg L⁻¹. On the other hand, As mobility in mixtures increased with biochar addition due to the competitive adsorption of arsenate and phosphate on the same adsorption sites. Despite that As TCLP concentrations remained well below the regulatory value of 5 mg L⁻¹.

We concluded, that ABC could be successfully used as Pb stabilizing agent. However, attention should be paid at soils highly contaminated with As.

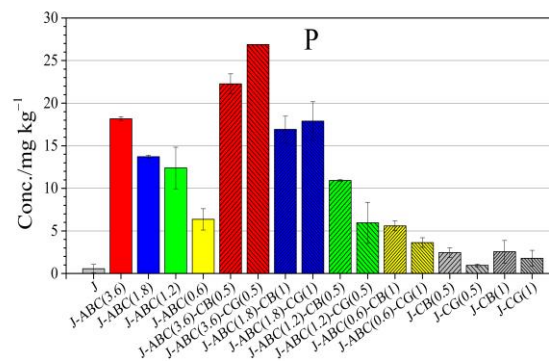


Figure 2: Mobile concentrations of P (in mg kg⁻¹) in tailings and mixtures.

References:

1. Beesley, L.; Inneh, O. S.; Norton, G. J.; Moreno-Jimenez, E.; Pardo, T.; Clemente, R.; Dawson, J. J. C. Assessing the influence of compost and biochar amendments on the mobility and toxicity of metals and arsenic in a naturally contaminated mine soil. *Environ. Pollut.* **2014**, *186*, 195-202.
2. Xiao-Wei, H.; Yi-Zong, H.; Yan-Shan, C., Effect of bone char addition on the fractionation and bio-accessibility of Pb and Zn in combined contaminated soil. *Acta Ecol. Sin.* **2010**, *30*, 118-122.
3. Morshedizad, M.; Zimmer, D.; Leinweber, P. Effect of bone chars on phosphorus-cadmium-interactions as evaluated by three extraction procedures. *J. Plant Nutr. Soil Sci.* **2016**, *179*, 388-398.

NiO Containing Zeolite as Catalyst for Waste Oils Deoxygenation

Nika Osterman^{1,2}, Manuel Ojeda Rodriguez³, Anton Meden², Blaž Likozar¹, Nataša Novak Tušar^{*,1,4}

¹ National Institute of Chemistry, Hajdrihova 19, SI-1000 Ljubljana, Slovenia, e-mail: natasa.novak.tusar@ki.si

² Faculty for Chemistry and Chemical Technology, University of Ljubljana, Večna pot 113, SI-1000 Ljubljana, Slovenia

³ University of Cordoba, Campus de Rabanales, Edificio Marie Curie (C-3), Ctra Nnal IV, Córdoba, E-14014, Spain

⁴ University of Nova Gorica, Vipavska 13, SI-5000 Nova Gorica, Slovenia

The use of biomass for production of biofuels, which have the chemical composition and properties similar than fuel derived from oil is one of the areas of sustainable development. Cheaper types of biomass as a raw material play an important role here. The cost of biodiesel produced from refined vegetable oil for example is higher than the cost of biodiesel produced from waste oils. However, waste oils containing large amounts of unsaturated fatty acids and water which cause problems in the process of normal production of bio-diesel. Solution of the problem is possible with the procedure of a catalytic deoxygenation¹. Catalysts that operate in the before mentioned reaction are metals such as Pd, Ni, Ru, Ir, Os, Rh immobilized on porous carriers such as silica, alumina, zeolites and active charcoal. Transition metals such as nickel on the zeolite carrier (type BEA) are cheaper and are efficient at lower temperatures (between 250 to 300 °C), but their performance usually does not reach the efficiency of noble metals^{2,3}.

The results presented herein demonstrate the development of a Ni-functionalized H-ZSM-5 catalyst (type zeolite MFI) for palmitic acid deoxygenation, the latter being a model compound, representing one of the intermediates in triglyceride scission and deoxygenation. The aim of this study was thus to optimize the catalytic material (through its composition) to intensify deoxygenation process.

H-ZSM-5 zeolites with the different Al contents were synthesized using a template-free procedure, developed at the local zeolite producer (Silkem, Kidričevo, Slovenia). The Ni/H-ZSM-5 catalysts with the different Ni contents were prepared using incipient wetness impregnation method. The prepared catalysts were characterized using SEM with EDX, XRD, TEM with SEAD, TPD and XPS. Catalytic tests were performed using palmitic acid as a model oil compound to screen prepared Ni/H-ZSM-5 performance. Catalysts were loaded in 600 mL Parr pressurised reactor and reduced at 300 °C *in-situ* using continuous supply of hydrogen gas at 20 atm for 1 h. The fatty acid conversion of hydrogenated/cracked mixture was determined by gas chromatography (GC).

The results of the characterization techniques mentioned above combined with the findings of the

catalytic tests enabled us to define the NiZSM-5 with molar ratio Ni/Al= 0,5 as the most promising catalyst due to its good crystallinity and catalytic activity. Nickel is present in Ni/H-ZSM-5 in the form of NiO.⁴

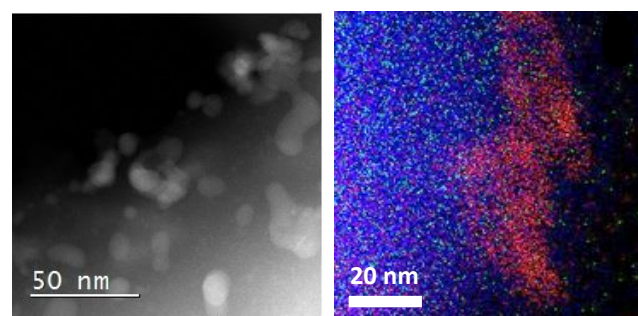


Figure 1: HAAD/STEM micro-clip of NiO nanoparticles (left) and elemental distribution of Ni, Si and Al (right) in the Ni/H-ZSM-5 sample with Ni/Al molar ratio 0,5.

Acknowledgments

The authors gratefully acknowledge the financial support of the Slovenian Research Agency (ARRS) Programs P1-0021, P2-0152 and EU Framework Programme FA COST Action TD1203 Food waste valorisation for sustainable chemicals, materials & fuels (EUBis).

References :

1. Botas, J. A.; Serrano, D. P.; García, A.; De Vicente, J.; Ramos, R., Catalytic Conversion of Rapeseed Oil into Raw Chemicals and Fuels over Ni- and Mo-Modified Nanocrystalline ZSM-5 Zeolite. *Catal. Today* **2012**, *195* (1), 59–70.
2. Ko, C. H.; Park, S. H.; Jeon, J. K.; Suh, D. J.; Jeong, K. E.; Park, Y. K., Upgrading of Biofuel by the Catalytic Deoxygenation of Biomass. *Korean Journal of Chemical Engineering*, **2012**, pp 1657–1665.
3. McArdle, S.; Girish, S.; Leahy, J. J.; Curtin, T., Selective Hydrogenation of Sunflower Oil over Noble Metal Catalysts. *J. Mol. Catal. A Chem.* **2011**, *351*, 179–187.
4. Osterman, N., Razvoj nikljevega katalizatorja na zeolitnem nosilcu za deoksigenacijo odpadnih olj, *Fakulteta za kemijo in kemijsko tehnologijo Ljubljana*, **2016**.



ORAL PRESENTATIONS



Materials
of the
future



Aminomaleimide as a Key Compound for the Preparation of High Performance Benzoxazine Materials

Žiga Štirn, Aleš Ručigaj, Matjaž Krajnc*

Faculty of Chemistry and Chemical Technology, University of Ljubljana, Večna pot 113, SI-1000 Ljubljana, Slovenia

In the past decade high performance materials continue to receive considerable attention.^{1,2} Polybenzoxazines as materials exhibit many attractive properties, including high glass transition temperatures, low moisture absorption, good thermal stability, mechanical and electrical properties, excellent properties in chemical resistance and flame retardancy. Additionally many of benzoxazine monomers could be obtained from various low-cost materials. All these extraordinary properties contribute towards growing trend of benzoxazine resin modification for the purpose of even further broadening of high performance material universe.

One of such modifications is incorporation of maleimide moiety into benzoxazine structure, furnishing maleimidobenzoxazine compounds. These materials are usually prepared from 4-hydroxyphenylmaleimide (HPMI) accompanied with formaldehyde and various amines as reactants. The mentioned is reflected in the lack of chemical versatility as in the synthesis of the benzoxazine monomer only the amine part contributes to the diversity of the molecule. Therefore there is huge lack of phenol diversity for currently known maleimidobenzoxazines. Already known maleimidobenzoxazines have shown excellent thermal stability, increased car yield and glass-transition temperature. On the other hand, synthesis of maleimidobenzoxazines results in lower yields compared to normal benzoxazines (with no maleimide functional group) in the range from 30–80%. The mentioned could be assigned to the lower reactivity of the HPMI comparing to the typical phenols used in benzoxazine synthesis, and the competitive side reactions.³

For this reason a new innovative synthetic approach for the preparation of maleimidobenzoxazines was developed. Phenolic diversity in maleimidobenzoxazine compounds was enabled, opening a vast possibility for tailoring properties of maleimidobenzoxazines through phenolic diversity. The key in a successful implementation of a novel synthetic approach was utilization of aminomaleimide compound prepared by modified synthetic path, void of the need for chromatographic

purification. Yields of reaction between aminomaleimide and phenolic derivative, which resulted in maleimidobenzoxazines reached up to 95%, being is a significant improvement prior previous studies dealing with the maleimidobenzoxazine studies. Aminomaleimide and all novel maleimidobenzoxazine substances were characterized by ¹H NMR, ¹³C NMR and FTIR spectroscopies. The curing behaviour of prepared maleimidobenzoxazines was investigated by DSC analysis and mechanical properties by DMA analysis. Novel maleimidobenzoxazines showed similar properties comparing to the already presented in the literature showing high glass transition temperature values over 240 °C. Thermogravimetric analysis proved improved thermal stability of maleimidobenzoxazines compared to anilino benzoxazines. Finally, the use of prepared maleimidobenzoxazines was investigated by the means of Diels-Alder reaction as a possible benzoxazine bearing maleimide group precursor for self-healing purposes.

References:

1. Ghosh, N. N.; Kiskan, B.; Yagci, Y. Polybenzoxazines - New High Performance Thermosetting Resins: Synthesis and Properties. *Prog. Polym. Sci.* **2007**, *32* (11), 1344–1391.
2. Iredale, R. J.; Ward, C.; Hamerton, I. Modern Advances in Bismaleimide Resin Technology: A 21st Century Perspective on the Chemistry of Addition Polyimides. *Prog. Polym. Sci.* **2016**.
3. Agag, T.; Takeichi, T. Preparation, Characterization, and Polymerization of Maleimidobenzoxazine Monomers as a Novel Class of Thermosetting Resins. *J. Polym. Sci. Part A Polym. Chem.* **2006**, *44* (4), 1424–1435.

Graphene/TiON_x/PtCu₃/Ir as Oxygen Reduction and Oxygen Evolution Reactions Catalyst for the Regenerative PEM Fuel Cell.

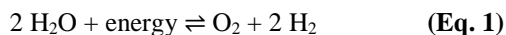
Leonard Moriau¹, Marjan Bele², Francisco Ruiz Zepeda², Matija Gatalo², Urša Petek², Alen Vižintin²,
Miran Gaberšček², Nejc Hodnik^{1,*}

¹ Department of Catalysis and Chemical Reaction Engineering and

² Department for Materials Chemistry, National Institute of Chemistry, Hajdrihova 19, 1000 Ljubljana, Slovenia

Global warming and the reliance on non-renewable fossil fuels is arguably the most urgent challenge of our time. Furthermore, increases in energy demand along with environmental changes force us to make use of sustainable energy sources like solar and wind power. Unfortunately, these renewable sources provide energy intermittently, which doesn't commonly fit the demand. Thereby, challenges for energy conversion and storage devices appear. Ones of the most promising electrochemical devices are batteries, electrolyzers, and proton exchange membrane (PEM) fuel cells.

The hydrogen cycle is seen as the most suitable choice for energy conversion and storage.¹ One interesting and well-developed approach is to couple water electrolyzer, which splits water into hydrogen and oxygen when there is a surplus of energy (left to right in equation 1) with a fuel cell, which on demand converts back chemically stored energy to electricity (Equation 1 backward).



It is well known that the best catalyst for hydrogen evolution and oxidation reactions is platinum. For both oxygen involved reactions already relatively good catalysts are in use e.g. Pt-alloys for the oxygen reduction (ORR) and Ir-based for the oxygen oxidation (OER).¹ However, adding the water splitting device to a fuel cell increase the already high cost of the entire system. Thus, to avoid this problem, it is highly desirable to make one device that could work in both electrolyzer and fuel cell mode; regenerative PEM fuel cell. For this purpose, a bifunctional catalyst with the same level of activity for OER and ORR than the current catalysts needs to be developed.²

The activity of a PtCu₃/Ir bifunctional catalyst was electrochemically investigated for both ORR and OER and compared to the activity of only Pt- and Ir-containing catalyst respectively (see Figure 1).

Using a graphene/TiON_x-support composite presents a promising solution to overcome the problem of severe carbon corrosion at high potentials. HR-TEM and EDX analysis of the catalyst was performed to

understand the morphology and structure of Pt, Cu, and Ir in our catalyst. It is showed in Figure 2 that Pt and Ir are segregated forming Janus-type nanoparticles that are deposited on TiON_x.

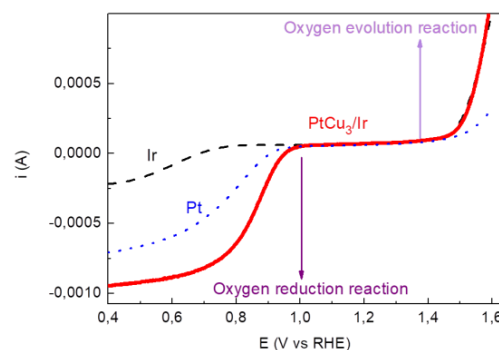


Figure 1: Voltammograms for the ORR and the OER for Pt, Ir and PtCu₃/Ir catalysts, recorded in O₂ saturated 0,1M HClO₄ solution.

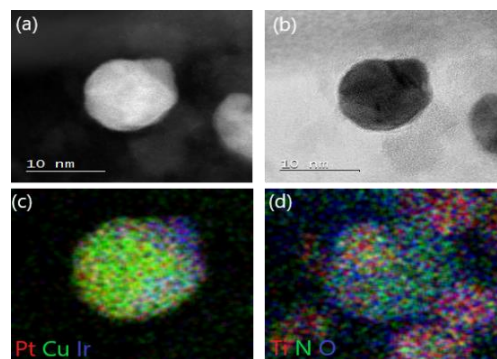


Figure 2: Bright (a) and dark (b) field STEM images of Graphene/TiON_x/PtCu₃/Ir. Energy-dispersive X-ray analysis of Janus behavior of our nanoparticles (c) and its deposition on TiON_x (d).

References :

1. Katsounaros I., Koper M.T.M., Electrocatalysis for the Hydrogen Economy. In *Electrochemical Science for a Sustainable Society*; Uosaki K., Ed., Springer, **2017**, pp 23-50.
2. Biddyut, P.; Andrews, J., PEM unitized reversible/regenerative hydrogen fuel cell systems: State of the art and technical challenges. *Renewable and Sustainable Energy reviews*, **2017**, 79, 584-599.

Synthesis of Commercially Viable PtCu₃/C ORR Electrocatalyst

Matija Gatalo¹, Francisco Ruiz-Zepeda¹, Primož Jovanovič², Nejc Hodnik³, Goran Dražič¹, Marjan Bele¹, Miran Gaberšček^{1,*}

¹ Department of Materials Chemistry, National Institute of Chemistry, Hajdrihova Ulica 19, 1000 Ljubljana, Slovenia

² Department of Analytical Chemistry, National Institute of Chemistry, Hajdrihova Ulica 19, 1000 Ljubljana, Slovenia

³ Department of Catalysis and Reaction Engineering, National Institute of Chemistry, Hajdrihova Ulica 19, 1000 Ljubljana, Slovenia

While vehicles with proton exchange membrane fuel cells (PEMFC) are already commercially available, its most vital part – the electrocatalyst – still contains too high quantities of the very precious platinum. In order to make the electrocatalyst cheaper, one has to further enhance the kinetics of the slow oxygen reduction reaction (ORR), for example by alloying Pt with other transition metals; a principle known for a long time.¹

In addition to improving the kinetics of the electrocatalyst, one also has to consider the scalability of the electrocatalyst synthesis process. In this work, we reveal insight into the synthesis development of already patented² in-house made and incredibly reproducible and highly uniform gram-scale synthesis of a PtCu₃/C electrocatalyst (Fig. 1a). Briefly, the process involves preparation of copper nanoparticles dispersed on a high-surface area carbon (Cu/C precursor) via a modified sol-gel synthesis process and a partial galvanic displacement of Cu/C with a platinum precursor salt (K₂PtCl₄). Obtained composite is then further annealed in order to form PtCu₃ alloy nanoparticles with an ordered pm3m structure (Fig. 1b and c).³

Both the process of the electrocatalyst preparation, as well as the electrocatalyst itself shows promise for future implementation as the cathode (ORR electrocatalyst) material for the PEMFC. On the laboratory and semi-industrial scales it exceeds the Pt₃Co/C electrocatalyst used in first commercial fuel cell vehicle from Toyota – Mirai by 380% in terms of mass activity (measured current per gram of platinum at 0.9 V vs. reversible hydrogen electrode).

References:

1. Stoneheart, P. *J. Appl. Electrochem.* **1992**, 22 (11), 995–1001.
2. Bele M., Gaberšček M., Kapun G., Hodnik N., Hočevar S., others, Electrocatalytic composite (s), associated composition (s), and associated process (es), **2015**.
3. Hodnik, N.; Jeyabharathi, C.; Meier, J. C.; Kostka, A.; Phani, K. L.; Rečnik, A.; Bele, M.; Hočevar, S.; Gaberšček, M.; Mayrhofer, K. J. *J. Phys. Chem. Chem. Phys.* **2014**, 16 (27), 13610–13615.

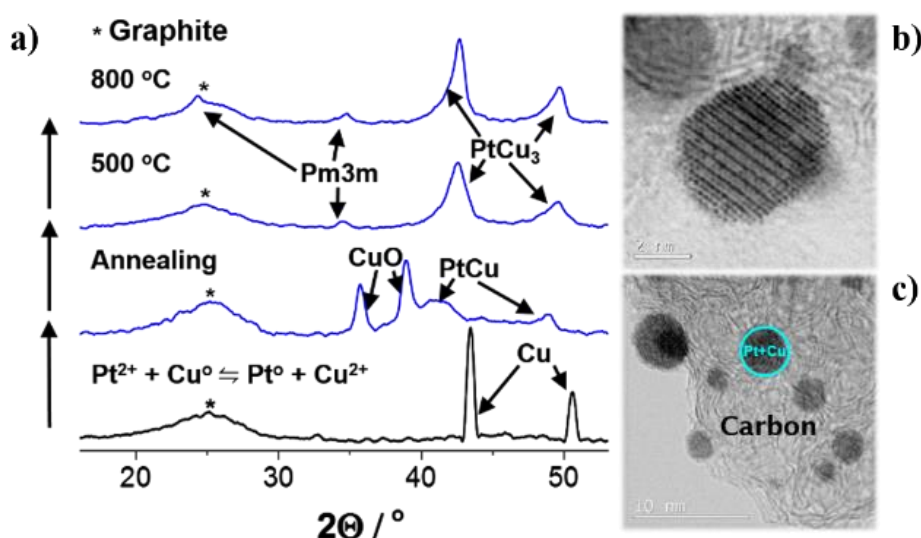


Figure 1: (a) XRD spectra of PtCu₃/C ORR electrocatalyst synthesis development during all main stages of the synthesis, (b) TEM image a single Pt-skin and ordered PtCu₃ core nanoparticle and (c) of the PtCu₃/C composite.

Key Parameters Affecting Drug Release from PCL Nanofibers

Špela Vičič, Špela Zupančič¹, Julijana Kristl^{*,1}

¹ Faculty of Pharmacy, University of Ljubljana, Aškerčeva cesta 7, SI-1000 Ljubljana, Slovenia

Periodontal disease is chronic inflammation of gums and periodontal tissue. The patient first notices red and painful gums, which is a sign of inflammation. In the case of irregular oral hygiene and without treatment, inflammation can spread to the surrounding tooth and progress to periodontal disease. This is accompanied by symptoms such as gum withdrawal, destruction of periodontal ligament and alveolar bone, the formation of periodontal pockets, and eventually tooth loss.¹ One of the ways to treat the periodontal disease is antimicrobial drugs in the form of tablets or capsules. The disadvantage of such treatment is a low concentration of an active substance at the targeted tissue. Therefore, low effectiveness of therapy can lead to bacterial resistance.² The goal of local drug delivery system with the controlled release is to deliver an active substance to the target tissue in the span of treatment and to avoid before mentioned disadvantages.³ Polymeric nanofibers are relatively new nanostructured material, they can be used as a local drug delivery system and are usually made with electrospinning method.⁴ However, the incorporation of a larger amount of hydrophilic drug into the hydrophobic polymer and achieving a sustained drug release for more than seven days still present a challenging task.

In our research polycaprolactone (PCL, 10-15%), hydrophobic polymer, had a role of the reservoir for a hydrophilic drug, metronidazole (MNZ) and they were both dissolved in different solvent mixtures. Polymer solutions were electrospun with Bioinicia Fluidnatek LE100 machine. We investigated different process parameters affect the morphology of nanofibers, thickness of mats and release profiles of MNZ. Scanning electron microscope (SEM) was used to characterize the morphology of nanofibers. To determine the release of MNZ from nanofiber mats, *in vitro* test was used (buffer solution with pH of 7.4 and quantified MNZ with UV-VIS in time period).

One of the key parameters affecting production and drug release was solvent mixtures used for polymer solution preparation. Electrospinning of 15 % (w/w) PCL solution in formic and acetic acid resulted in beadless nanofibers (Figure 1) with sustained release of MNZ for 7 days. The process was shown to be repeatable. When the drug loading was increased from 5 to 10 %, the sustained release was not accomplished. By regulation of nanofiber mat thickness, the

prolonged release was obtained up to 14 days. This was probably due to the higher ratio between surface and volume of nanofibers.

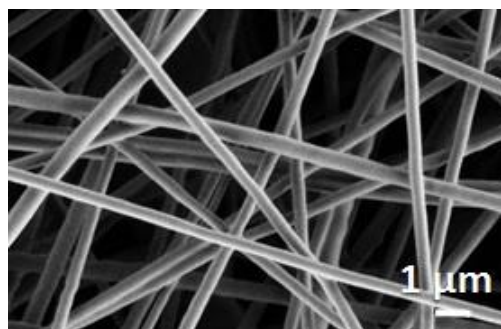


Figure 1: SEM picture of nanofibers with 15% PCL in solvent mixture of formic and acetic acid with mass ratio 1:3

Uniform nanofibers were successfully produced and repeatability of electrospinning process was confirmed. Sustained release of MNZ was obtained for 7 days. Thickness of nanofiber mats turned out to be important for prolonged MNZ release up to 14 days.

References:

1. Genco, R. J., Evans, R. T., & Ellison, S. A., Dental research in microbiology with emphasis on periodontal disease. *The Journal of the American Dental Association* **1969**, 78(5), 1016-1036.
2. Hau, H., Rohanizadeh, R., Ghadiri, M., & Chrzanowski, W., A mini-review on novel intraperiodontal pocket drug delivery materials for the treatment of periodontal diseases. *Drug delivery and translational research* **2014**, 4(3), 295-301.
3. Khansari, S., Duzyer, S., Sinha-Ray, S., Hockenberger, A., Yarin, A. L., & Pourdeyhimi, B., Two-stage desorption-controlled release of fluorescent dye and vitamin from solution-blown and electrospun nanofiber mats containing porogens. *Molecular pharmaceutics* **2013**, 10(12), 4509-4026.
4. Zupancic, S., Kocbek, P., Baumgartner, S., & Kristl, J., Contribution of nanotechnology to improved treatment of periodontal disease. *Current pharmaceutical design* **2015**, 21(22), 3257-3271

Synthesis of Biocompatibilizer by Graft Polymerization of Lactic Acid onto a Biopolymer and its Use in Preparation of Biocomposites

Janez Slapnik¹, Janja Zule², Silvester Bolka¹, Thomas Wilhelm¹, Irena Pulko^{1,*}

¹ Faculty for Polymer Technology, Ozare 19, SI-2380 Slovenj Gradec, Slovenia

² Pulp and Paper Institute, Bogisiceva 8, SI-1000 Ljubljana, Slovenia

Natural fibers are often incorporated into polymers to achieve specific properties desired in the final product.¹ They offer advantages over synthetic fibers in terms of lower density, lower cost, less damage to processing equipment, biodegradability and reduction in carbon dioxide emission. However, they have disadvantages such as poor fiber-matrix compatibility, high moisture uptake and poor thermal stability.² Many strategies to improve interfacial adhesion have been developed such as physical modification of fibers, chemical modification of fibers and addition of various compatibilizers, but they often compromise biodegradability or decrease biobased content of the material.^{2,3} Lignin is the second most abundant renewable biopolymer in nature and an inexpensive waste product.⁴ Since lignin contains both polar hydroxyl groups and non-polar hydrocarbon and benzene groups it can improve compatibility between fiber and matrix.⁵ Two basic approaches to use lignin as a compatibilizer have been developed – deposition of lignin on the surface of the fibers and incorporation of unmodified and chemically modified lignin into the polymer/natural fiber composite.⁶ Chung et. al. reported successful grafting of poly(lactide) (PLA) onto unmodified lignin by ring-opening polymerization with an organic catalyst. Addition of lignin-g-PLA copolymers into PLA increased tensile strength and strain and increased dispersion compared to addition of pure lignin.⁴ In the present study lignin was extracted from beech wood using Acetosolv method.⁷ Lactic acid (LA) was then polymerized onto this lignin analog to Chung et. al. to yield lignin-g-PLA copolymer.⁴ PLA / 30 wt. % beech wood composites were prepared using twin screw extrusion, one without compatibilizer and one with addition of 2 wt. % of lignin-g-PLA. Test specimens were prepared by injection molding. Lignin-g-PLA was characterized using Fourier transform infrared (FT-IR) spectroscopy. Cellulose, hemicellulose, lignin, ash, hydrophilic and hydrophobic extract and dry matter content were determined. Thermal and mechanical properties were determined using tensile test, flexural test, Charpy impact test, dynamic mechanical analysis (DMA), thermogravimetric analysis (TGA) and differential scanning calorimetry (DSC). FT-IR spectroscopy was

used to study the interactions of components. Addition of 30 wt. % beech wood drastically increased tensile (+ 55,6 %) modulus, flexural modulus (+ 64,5 %) and thermal stability of PLA, without major sacrifice in terms of tensile and flexural strength. Composites with added lignin-g-PLA showed further enhanced tensile modulus (+ 16,1 %) as well as enhanced flexural strength (+ 4,2 %) compared to the uncompatibilized composite. New composite is fully biobased and biodegradable and exhibits tensile and flexural properties comparable to fossil-based glass reinforced composites and may become a sustainable alternative for such materials in technical applications.

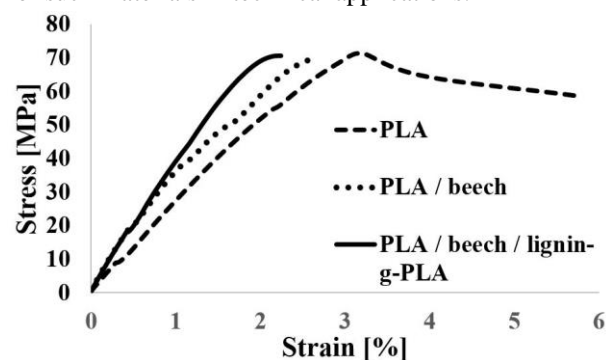


Figure 1: Tensile stress-strain curves for PLA and for compatibilized and uncompatibilized composites

References:

1. Saba, N.; Jawaid, M.; Alothman, O. Y.; Paridah, M. T. *Constr. Build. Mater.* **2016**, *106*, 149–159.
2. Mohammed, L.; Ansari, M. N. M.; Pua, G.; Jawaid, M.; Islam, M. S. **2015**, *2015*, 1–15.
3. Hassan, M. M.; Wagner, M. H. *Rev. Adhes. Adhes.* **2016**, *4* (1), 1–46.
4. Chung, Y. L.; Olsson, J. V.; Li, R. J.; Frank, C. W.; Waymouth, R. M.; Billington, S. L.; Sattely, E. S. *ACS Sustain. Chem. Eng.* **2013**, *1* (10), 1231–1238.
5. Rozman, H. D.; Tan, K. W.; Kumar, R. N.; Abubakar, A.; Mohd. Ishak, Z. A.; Ismail, H. *Eur. Polym. J.* **2000**, *36* (7), 1483–1494.
6. Thielemans, W.; Wool, R. P. *Compos. Part A Appl. Sci. Manuf.* **2004**, *35* (3), 327–338.
7. Soudham, V. P.; Rodriguez, D.; Rocha, G. J. M.; Taherzadeh, M. J.; Martin, C. *For. Stud. China* **2011**, *13* (1), 64–70.

New Developments in the Chemistry of Krypton

Matic Lozinšek^{*, 1, 2}, Hélène P. A. Mercier¹, Gary J. Schrobilgen¹

¹ Department of Chemistry, McMaster University, 1280 Main Street West, Hamilton, Ontario L8S 4M1, Canada

² Present address: Department of Physical and Organic Chemistry, Jožef Stefan Institute, Jamova cesta 39, 1000 Ljubljana, Slovenia

Krypton is the lightest member of the group 18 elements that forms compounds which can be isolated in macroscopic amounts under normal conditions¹. Its heavier congener xenon forms compounds in the oxidation states $+1/2$, $+2$, $+4$, $+6$ and $+8$, whereas krypton is present in all of its compounds in the $+2$ oxidation state. Only one compound of krypton can be synthesized from the elements, namely krypton difluoride. Therefore, KrF_2 represents a starting material for all other known compounds of this noble gas. However, the thermodynamically unstable KrF_2 is a better low-temperature F^\bullet radical source than F_2 and thus, a powerful oxidative fluorinator². The technical challenges of handling KrF_2 and its derivatives are hindering the development of krypton chemistry. Special experimental techniques need to be employed for the syntheses, crystallization, and handling of krypton compounds which can be structurally characterized by low-temperature single-crystal X-ray diffraction and low-temperature Raman spectroscopy. Krypton compounds are typically synthesized by utilization of the Lewis basicity of KrF_2 , as exemplified by the formation of $[\text{KrF}]^+$ and $[\text{Kr}_2\text{F}_3]^+$ salts upon reaction with strong Lewis acids (e.g., AsF_5 , SbF_5)³. Only recently, the ability of KrF_2 to serve as a ligand was demonstrated⁴.

In this work, complexes and co-crystals of KrF_2 were investigated in order to expand the rather limited synthetic and structural chemistry of krypton compounds.

Low-temperature crystallization of KrF_2 and $\text{Mg}(\text{AsF}_6)_2$ solutions in anhydrous HF or BrF_5 have yielded $[\text{Mg}(\text{KrF}_2)_4(\text{AsF}_6)_2]$ complex and its solvate $[\text{Mg}(\text{KrF}_2)_4(\text{AsF}_6)_2] \cdot 2\text{BrF}_5$, respectively, providing the first examples of KrF_2 coordination to a main-group metal⁵. Similarly, the reactions between $[\text{XeF}_5][\text{AsF}_6]$ and KrF_2 in anhydrous HF have resulted in adducts, $[\text{XeF}_5][\text{AsF}_6] \cdot \text{KrF}_2$ and $[\text{XeF}_5][\text{AsF}_6] \cdot 2\text{KrF}_2$, which represent the only examples of mixed noble-gas Kr/Xe compounds.

The selection of suitable compounds for co-crystallization with KrF_2 is very limited. Highly-reactive low-melting co-crystals with the composition $\text{KrF}_2 \cdot 2\text{BrF}_5$ and $4\text{KrF}_2 \cdot 3\text{BrF}_5$ were crystallized from KrF_2 solutions in BrF_5 . Their crystal structures provide insights into the KrF_2 - BrF_5 intermolecular interactions.

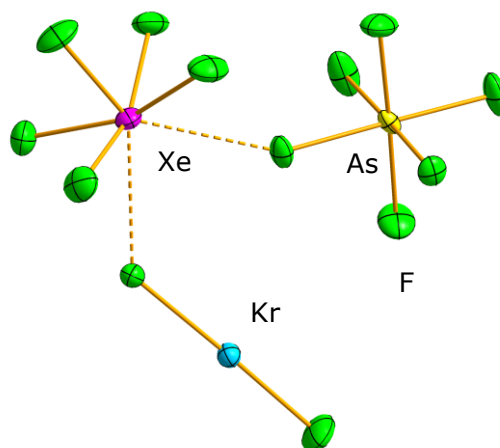


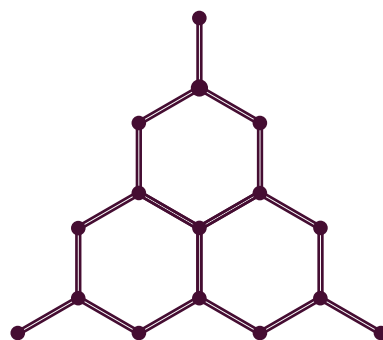
Figure 1: The asymmetric unit of the crystal structure of $[\text{XeF}_5(\text{KrF}_2)(\text{AsF}_6)]$ compound is composed of XeF_5^+ cation coordinated by KrF_2 ligand and $[\text{AsF}_6]^-$ anion. Thermal ellipsoids are shown at the 50% probability level.

References:

1. Lozinšek, M.; Schrobilgen, G. J., The world of krypton revisited. *Nat. Chem.* **2016**, 8, 732.
2. Lehmann, J. F.; Mercier, H. P. A.; Schrobilgen, G. J., The chemistry of krypton. *Coord. Chem. Rev.* **2002**, 233–234, 1–39.
3. Lehmann, J. F.; Dixon, D. A.; Schrobilgen, G. J., X-ray crystal structures of α - KrF_2 , $[\text{KrF}][\text{MF}_6]$ ($\text{M} = \text{As}, \text{Sb}, \text{Bi}$), $[\text{Kr}_2\text{F}_3][\text{SbF}_6] \cdot \text{KrF}_2$, $[\text{Kr}_2\text{F}_3]_2[\text{SbF}_6]_2 \cdot \text{KrF}_2$, and $[\text{Kr}_2\text{F}_3][\text{AsF}_6] \cdot [\text{KrF}][\text{AsF}_6]$; Synthesis and characterization of $[\text{Kr}_2\text{F}_3][\text{PF}_6] \cdot n\text{KrF}_2$; and theoretical studies of KrF_2 , KrF^+ , Kr_2F_3^+ , and the $[\text{KrF}][\text{MF}_6]$ ($\text{M} = \text{P}, \text{As}, \text{Sb}, \text{Bi}$) ion pairs. *Inorg. Chem.* **2001**, 40, 3002–3017.
4. Brock, D. S.; Casalis de Pury, J. J.; Mercier, H. P. A.; Schrobilgen, G. J.; Silvi, B., A rare example of a krypton difluoride coordination compound: $[\text{BrOF}_2][\text{AsF}_6] \cdot 2\text{KrF}_2$. *J. Am. Chem. Soc.* **2010**, 132, 3533–3542.
5. Lozinšek, M.; Mercier, H. P. A.; Brock, D. S.; Žemva, B.; Schrobilgen, G. J., Coordination of KrF_2 to a naked metal cation, Mg^{2+} . *Angew. Chem. Int. Ed.* **2017**, 56, 6251–6254.



POSTER PRESENTATIONS



CUTTING
EDGE **2017**



Phylogenomic Analysis of RNA Viruses in Invertebrates

Sabina Ott,^{1,2} Dušan Kordiš*,¹

¹ Jožef Stefan Institute, Jamova cesta 39, SI-1000 Ljubljana, Slovenia

² Jožef Stefan International Postgraduate School, Jamova cesta 39, SI-1000 Ljubljana, Slovenia

RNA viruses are the largest group of viruses representing 54/110 viral families (Figure 1). Among them are some of the most notorious human pathogens. They are excellent models for the analysis of their biodiversity and evolutionary dynamics. As viruses interact with particular host species, their mutation rates strongly depend also on the host organism. Insects epitomize biodiversity with a million documented species. Together with Entognatha (oldest hexapod lineages - Collembola, Diplura and Protura), they comprise one of two large lineages of hexapods. Some of the insect lineages, namely, Diptera, Hemiptera, Polyneoptera, Odonata, Thysanoptera along with nematods, are well known vectors of plant and insect viruses. As extremely adaptive organisms they have been set at the heart of viral evolution and acknowledged as the center of viral biodiversity¹.

However, numerous lineages of invertebrates have not been screened for RNA viruses, for example: 1) the oldest hexapod lineages (Collembola, Diplura), 2) the oldest insect lineages (Monocondylia and Zygentoma), 3) oldest metazoan lineages (Ctenophora, Cnidaria and Porifera) 4) Platyhelminthes and 5) insect lineages Lepidoptera and Hymenoptera^{1,2,3,4}. Our aim is to fill these phylogenetic gaps in terms RNA viral biodiversity.

We have screened the transcriptomic databases of the oldest hexapod, oldest metazoan, lophotrochozoan, and lepidopteran lineages for the presence of new RNA viruses and genomic databases for the presence of novel Endogenized Viral Elements (EVEs). Novel viruses and EVEs were then characterized in terms of genomic architecture and distribution and placed in the context of known viral biodiversity.

RNA viruses are grouped into 25 clades: Astro, Birna, Hepe-Virga, Hypo, Luteo-Sobemo, Narna-Levi, Bunya-Arena, Mono-Chu, Orthomyxo, Nido, Partiti-Picobirna, Permutotetra, Picorna-Calici, Reo, Toti-Chryso, Tombus-Noda, Flavi, Poty, Ophio, Cysto, Qinvirus, Weivirus, Yuevirus, Yanvirus and Zhaovirus. Altogether, in Lophotrochozoa we have found 12 of 25 clades. In basal hexapods, we have found 7/25 clades. In basal metazoans, 15/25 clades were found and in Lepidoptera, 14/25 clades were found. In basal hexapods a reovirus and an orthomyxovirus was found, but in other analysed invertebrate phyla the Mono-Chu was the prevailing clade of ss(-)RNA viruses and

Partiti-Picobirna was the prevailing clade of dsRNA viruses. The Picorna-Calici clade is the most abundant ss(+)RNA clade in all analysed invertebrate phyla. We have found that 16/25 viral clades are endogenized in at least one of the analysed invertebrate phyla. Mono-Chu was the only clade found endogenized in all analysed invertebrate phyla. Each invertebrate phylum possesses a unique collection of RNA viruses, however, five viral clades have been found in all analysed groups: Hepe-Virga, Narna-Levi, Picorna-Calici, Toti-Chryso and Tombus-Noda. Our analyses have shown that RNA viral diversity is not limited to the arthropods, but is present in all invertebrates.

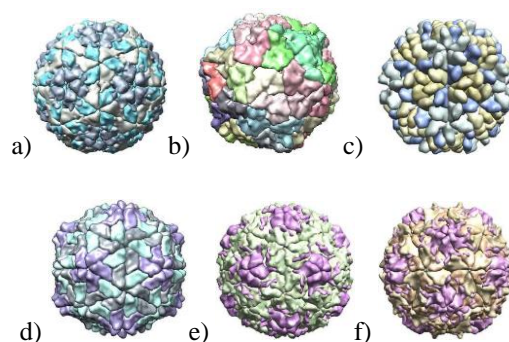


Figure 1: Example of diversity of RNA viral symmetry a) Foot and mouth disease virus (1BBT), b) Grapevine fanleaf virus (2Y26), c) Providence virus (2QQP), d) Ryegrass mottle virus (2IZW), e) Rhinovirus (1AYN), f) Poliovirus (1PO1) (Protein Data Bank; www.rcsb.org)⁴.

References:

1. Li C.X.; et al., Unprecedented genomic diversity of RNA viruses in arthropods reveals the ancestry of negative-sense RNA viruses. *eLife* **2015**, 4, 1-26. doi: 10.7554/eLife.05378
2. Shi M.; et al., Redefining the invertebrate virosphere. *Nature* **2016**, 540, 539-543.
3. Shi M.; et al., Divergent viruses discovered in arthropods and vertebrates revise the evolutionary history of the *Flaviviridae* and related viruses. *J. Virol.* **2016**, 90, 659-669.
4. Berman H.M.; et al., The Protein Data Bank. *Nucleic Acids Res.* **2000**, 28, 235-242.

Synthesis and Use of Camphor-derived Organocatalysts in Enantioselective Synthesis

Sebastijan Ričko¹, Bogdan Štefane¹, Jurij Svete¹, and Uroš Grošelj^{1,*}

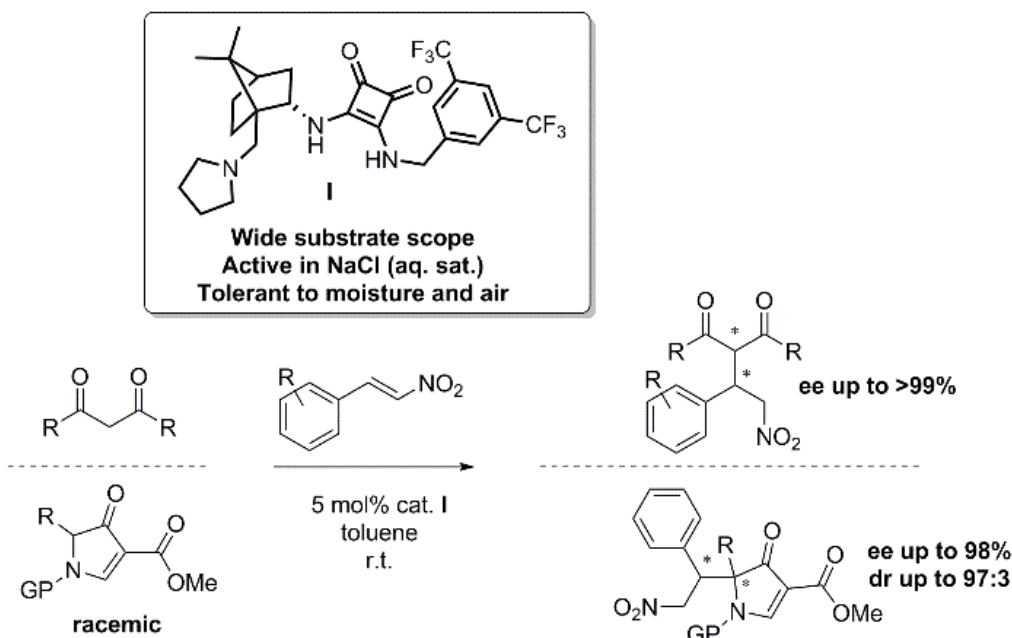
¹ Faculty of Chemistry and Chemical Technology, University of Ljubljana, Večna pot 113, SI-1000 Ljubljana, Slovenia

The search for new highly active organocatalysts with distinct reactivities is important for the further development of organic chemistry. Majority of bifunctional organocatalysts are based on diamine scaffolds derived from natural products. Camphor exists in nature as a single enantiomer and is as such a perfect starting point in the preparation of new asymmetric catalysts. Although camphor is widely employed in organic synthesis, highly active bifunctional camphor-derived organocatalysts were unknown prior to our seminal study.¹ The catalyst we developed is highly active in stereoselective additions of 1,3-dicarbonyls to *trans*- β -nitrostyrene derivatives, products were formed in excellent yields (up to 95%) with high enantioselectivities (up to >99%). It also effectively promotes stereoselective deracemisation of 4-pyrrolones by 1,4-addition to *trans*- β -nitrostyrenes.² The catalyst itself is tolerant to moisture and air. The

reactions are of broad scope with respect to reaction conditions and substrates. Reactions were also examined with DFT calculations. They suggest that the catalyst works by Takemoto's mechanism, which was presumed to be unfavorable until now.^{1,2}

References:

1. Ričko, S.; Meden, A.; Ivančič, A.; Perdih, A.; Štefane, B.; Svete, J.; Grošelj, U., Organocatalyzed Deracemisation of Δ^2 -Pyrrolin-4-ones. *Adv. Synt. Catal.*, **2017**, in press, DOI: 10.1002/adsc.201700539.
2. Ričko, S.; Svete, J.; Štefane, B.; Perdih, A.; Golobič, A.; Meden, A.; Grošelj, U., 1,3-Diamine-Derived Bifunctional Organocatalyst Prepared from Camphor, *Adv. Synt. Catal.*, **2016**, 358, 3786-3796.



Scheme 1: Organocatalysed addition of carbonyls to *trans*- β -nitrostyrene derivatives.

Trans-Activation Response Element RNA is Detectable in the Plasma of a Subset of Aviremic HIV-1–Infected Patients

Anžej Hladnik¹, Jana Ferdin¹, Katja Goričar¹, Steven G. Deeks², Boris M. Peterlin², Ana Plemenitaš¹, Vita Dolžan¹, Metka Lenassi^{*,1}

¹ Institute of Biochemistry, Faculty of Medicine, University of Ljubljana, Vrazov trg 2, SI-1000 Ljubljana, Slovenia

² Department of Medicine, University of California, San Francisco (UCSF), San Francisco, California, USA

Plasma trans-activation response element (TAR) RNA has been suggested as one of the possible biomarkers for determining the HIV-1 reservoir size in infected individuals. It is produced during non-processive transcription in HIV-1 productively infected and latent T cells (Figure 1a)¹. Our aim was to determine whether TAR RNA can be found in the blood plasma of aviremic HIV-1–infected patients and to examine whether TAR levels correlate to patient clinical characteristics.

Our study accessed 55 plasma samples from the SCOPE cohort (study approved by UCSF CHR, subjects provided informed consent): 9 uninfected, 8 viremic (non-controllers) and 38 aviremic (19 antiretroviral therapy (ART)-suppressed, 19 elite controllers) subjects. Subjects were characterized with respect to age, gender, ethnicity, HIV status (CD4+ and CD8+ counts, and HIV RNA level) and ART regimen. For TAR RNA detection, RNA extracted from plasma and plasma exosomes was reverse transcribed, amplified by PCR with TAR-specific primers (Figure 1b) and analysed by gel electrophoresis. Statistical analysis was performed using IBM SPSS Statistics (v19.0).

Our optimised PCR-based assay provided 100% specificity and 100% sensitivity for detection of TAR RNA (Figure 2)². TAR RNA was present in clinical samples of 6.3% (24/38) of aviremic HIV-1–infected patients (either treated with ART or elite controllers). Of those, TAR RNA of exosomal origin was detected only in 37.5% (9/24). Statistical analysis of the data has shown that TAR RNA levels did not correlate with patient gender, age, CD4 levels, CD8 levels and ART regime, but showed a statistically significant correlation with CD4/CD8 ratio ($P = 0.047$).

This study is the first to investigate plasma TAR RNA in a relatively large cohort of HIV-1 infected patients. Furthermore, we show that the TAR RNA molecules in the plasma of these aviremic patients are not limited to exosomes.

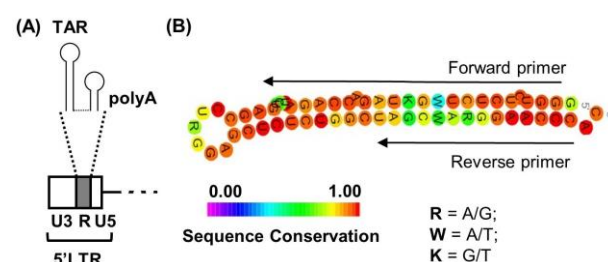


Figure 1: (A) TAR RNA as a part of 5' long terminal repeat (LTR) of the HIV-1 provirus. (B) TAR RNA sequence conservation and primer annealing sites. Modified from Harwig et al.¹

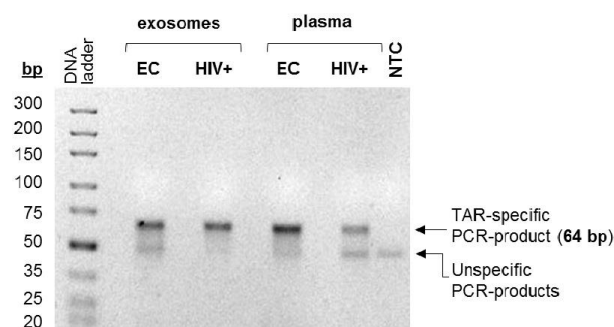


Figure 1: Detection of TAR RNA in plasma samples using amplification by PCR and separation of amplicons by gel electrophoresis. EC, elite controllers; HIV+, non-controllers; NTC, no template control. Modified from Hladnik et al.²

References:

1. Harwig, A.; Jongejan, A.; van Kampen, A. H. C.; et al., *Nucleic Acids Res* **2016**; 44 (9): 4340-4353.
2. Hladnik, A., Ferdin, J.; Goričar K.; et al., *Acta Chim. Slov.* **2017**; 64.

Photocatalytic Activity of Titanium Dioxide Thin Films Doped with Silicon or Iron

Gorazd Koderman Podboršek¹, Irena Kozjek Škofic^{*,1}

¹ Faculty of Chemistry and Chemical Technology, University of Ljubljana, Večna pot 113, SI-1000 Ljubljana, Slovenia

Titanium dioxide (TiO₂) is a commonly used material in the industry. With the development of nanotechnology, it was discovered that TiO₂ particles have photocatalytic properties. TiO₂ is today one of the most commonly used photocatalysts. The most photocatalytically active crystal modification is the anatase crystal modification. The course of the crystallization process and the crystal structure of TiO₂ can be tailored, if other elements of the periodic system are used as dopants during the synthesis. In that way the photocatalytic properties can be modified. It has been shown in previous studies that the photocatalytic activity can be improved by doping with silicon or iron¹⁻⁴.

The effect of doping on the photocatalytic properties of TiO₂ thin films has been researched. The thin films have been prepared using a simple sol-gel method, followed by the dip coating technique and thermal treatment. The sols were doped with silicon or iron and the photocatalytic activity of thin films was measured during irradiation with UV light. The surface of the thin films was analyzed with a scanning electron microscope and energy dispersion spectroscopy. The photocatalytic activity of TiO₂ thin films does not change because of doping with silicon Figure 1.

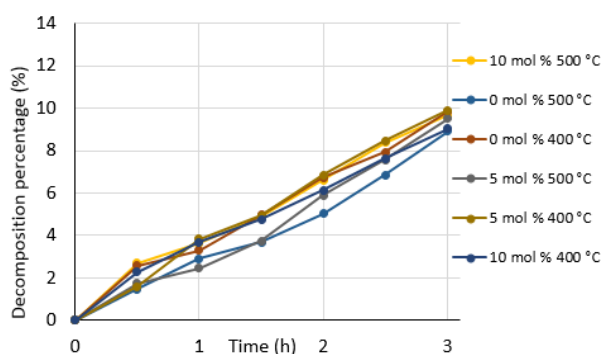


Figure 1: Dependence of decomposition percentage of the model dye on time at different temperatures of thin film baking and molar percentages of doping with silicon.

Thin films doped with iron are more photocatalytically active at lower amounts of added iron Figure 2. The photocatalytic activity is decreasing significantly by increasing the amount of added iron. Despite all that doping with iron, the photocatalytic activity of TiO₂

thin films decreases, non-doped thin films still have the highest photocatalytic activity.

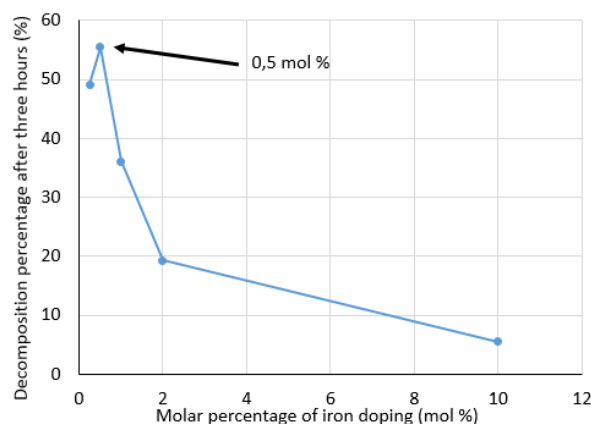


Figure 2: Dependence of decomposition percentage of the model dye on the molar percentage of doping with iron after three hours.

References:

1. Wang, C.; Bahnemann, D. W.; Dohrmann, J. K. A Novel Preparation of Iron-Doped TiO₂ Nanoparticles with Enhanced Photocatalytic Activity. *Chem. Commun.* **2000**, 16, 1539–1540.
2. Zhu, J.; Zheng, W.; He, B.; Zhang, J.; Anpo, M. Characterization of Fe-TiO₂ Photocatalysts Synthesized by Hydrothermal Method and Their Photocatalytic Reactivity for Photodegradation of XRG Dye Diluted in Water. *J. Mol. Catal. A Chem.* **2004**, 216 (1), 35–43.
3. He, C.; Tian, B.; Zhang, J. Thermally Stable SiO₂-Doped Mesoporous Anatase TiO₂ with Large Surface Area and Excellent Photocatalytic Activity. *J. Colloid Interface Sci.* **2010**, 344 (2), 382–389.
4. Bui, D. N.; Kang, S. Z.; Li, X.; Mu, J. Effect of Si Doping on the Photocatalytic Activity and Photoelectrochemical Property of TiO₂ Nanoparticles. *Catal. Commun.* **2011**, 13 (1), 14–17.

Application of German Self-Assessment Method about Management Effectiveness in Protected Areas on Slovenian Nature Parks

Eva Žunec¹

¹ Faculty of Mathematics, Natural Sciences and Information Technologies, University of Primorska, Glagoljaška 8, SI-6000 Koper, Slovenia

There is no definition of protected areas in Slovenian system of conservation. Therefore, the founder or the manager of a newly established protected area in our country is able to choose which part of the law shall be taken into consideration, under his own terms and ambitions. Management standards can significantly decrease with such actions and important restraints, crucial bans of use, vital for preservation of nature are eliminated and left out. Furthermore, they are not in compliance with minimal international standards for protected areas, constructed by the non-profit International Union for Conservation of Nature (IUCN).

German nature parks recently met a methodological approach of self-assessing their management efficiency in nature parks, where the protected area administrators as well as the general public are able to evaluate how successful the parks are in achieving their objectives in nature conservation and in the process of local development but wider region as well. Slovenia does not yet have such methodology, although the unified criteria and the great number of our nature parks, meaning regional parks and landscape parks could suggest otherwise.

The application of German self-assessment method about management effectiveness on Slovenian nature parks was composed from the following steps: translation and modifications of the German original questionnaire, for it to become suitable for Slovenian requirements, testing the obtained methodology on one of the nature parks in Slovenia - Kozjansko Regional park and the final critical analysis, whether the model is even adequate for our circumstances and future usage.

The original questionnaire was tested within three trial periods in Germany, its final version as well as mine are composed out of eighty-seven diverse questions, divided into five fields of activity: Management and Organization; Nature and Landscape; Tourism and Recreation; Communication and Education; Sustainable Regional Development. Each field is assessed with 20%, that is 100 out of total points.

The framework has been set beyond most competences, since the nature parks should become the

driving forces and coordinators of future sustainable regional development, as it was emphasized in the German campaign. By doing so, they successfully overcame the breach, formed by inconsistencies when comparing state laws and IUCN recommendations.

Similarly, Slovenia faces the problem of different levels of criteria and standards of conservation within the same category of protected areas, of non-cooperation between protected areas and a gap in communicating as well as educating the public when it comes to understanding the relevance that nature parks bear.

With such instrument the continuous improvement is possible, the quality criteria also helps to accept nature parks, their aims and provides a better support of different groups of people from social, economical and political view. Comparison between two different nature parks is practicable when looking to improve Slovenian national level of conservation.

References:

1. *German Nature Parks' Quality Campaign*. Bonn, **2008**.
2. Dudley, N.: *Guidelines for Applying Protected Area Management Categories*. Gland, Switzerland, IUCN, **2008**.
3. *Qualitätsoffensive Naturparke*. Bonn, **2010**.
4. *Zakon o ohranjanju narave; uradno prečiščeno besedilo. Uradni list Republike Slovenije, 96/2004*. Ljubljana, **2004**.

Synthesis and Bioactivity of Novel 7-(1-Aminoalkyl)pyrazolo[1,5-a]pyrimidines

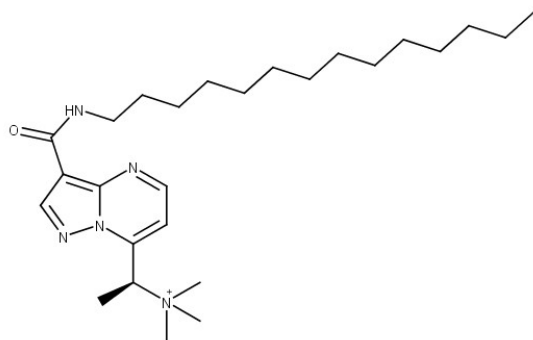
Nejc Petek, Uroš Grošelj, Franc Požgan, Bogdan Štefane, Marko Novinec, Jurij Svete *

¹ Faculty of Chemistry and Chemical Technology, University of Ljubljana, Večna pot 113, SI-1000 Ljubljana, Slovenia, jurij.svete@fkkt.uni-lj.si

Novel pyrazolo[1,5-*a*]pyrimidines were synthesized from ynones and 5-aminopyrazoles. (*S*)-Amino acids were used as starting materials and converted to 1,3-dielectrophilic ynones prepared from glycine, alanine and phenylalanine¹. 5-Aminopyrazoles were prepared from simple reagents, hydrazine hydrate and ketonitriles². Subsequent cyclization of ynones with 5-aminopyrazoles in methanol at room temperature afforded pyrazolo[1,5-*a*]pyrimidines, which were purified by column chromatography. As different ynones and 5-aminopyrazoles were used, synthesized compounds had different side chains. Pyrazolo[1,5-*a*]pyrimidine with an ester group on position 3 was of particular interest, since it was hydrolyzed under basic conditions to yield an acid, which was transformed into different carboxamides. Carboxylic group was activated with 1,1'-carbonyldiimidazole (CDI) in THF, followed by addition of amines, to give the respective amides.

In some cyclization products Boc protecting group was removed by acidolysis with HCl in ethyl acetate. The resulting free amines were treated with acetyl chloride, benzoyl chloride and benzoyl chloride to give the corresponding amides. The free amine was also quaternized with methyl iodide in methanol at room temperature.

The prepared pyrazolo[1,5-*a*]pyrimidines are useful in many fields. A compound with a lipophilic and another polar side chain was prepared by the above procedures and could act as a fluorescent marker.



Scheme 1: Potential fluorescent marker.

The synthesized compounds showed potential biological activity for inhibition of Cathepsin K. Molecular docking was carried out for all synthesized compounds and some of them were tested for inhibition of Cathepsin K. This was done by spectrophotometrically measuring the activity of Cathepsin K in the presence of different concentrations of inhibitors. The resulting data were analysed by GraphPad Prism 5.0 and inhibition constants for some compounds were calculated. The mechanism of inhibition was found to be competitive for all tested compounds.

The best inhibition was measured for a compound with a free amine group, a phenyl group at position 3 and a benzyl group on position 2 with $K_i = 77 \pm 5 \mu\text{M}$.

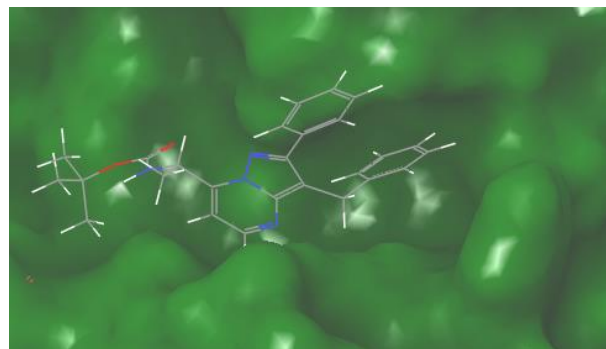


Figure 1: Pyrazolo[1,5-*a*]pyrimidine derivative docked inside the active site of Cathepsin K.

References:

1. Šenica, L., Petek, N., Grošelj, U., Svete J., A four-step synthesis of novel (*S*)-1-(heteroaryl)-1-aminoethanes from (*S*)-Boc-alanine. *Acta Chim. Slov.* **2015**, 62, 60-71.
2. Ji, N., Meredith, E., Liu, D. L., Adams, C. M., Artman, G. D., Jendza, K. C., Ma, F. P., Mainolfi, N., Powers, J. J., Zhang, C., Syntheses of 1-substituted-3-aminopyrazoles. *Tetrahedron Lett.* **2010**, 51, 6799–6801.

Mathematical Modeling of the 2014 West African Ebola Epidemic

Vita Hudi,¹ Miha Lukšič^{1*}

¹ Faculty of Chemistry and Chemical Technology, University of Ljubljana, Večna pot 113, SI-1000 Ljubljana, Slovenia

Ebola is known as one of the deadliest viral diseases today. It is caused by viruses of the genus *ebolavirus* (EBOV¹). One of the better-known species of *ebolavirus*, which was also the cause of the 2014 Ebola outbreak in west Africa, is the *Zaire ebolavirus*².

To gain better understanding of the ways how this disease spreads, two mathematical models were used³. By nonlinear least-squares regression fitting of the model functions to cumulative numbers of infected and dead people collected during the 2014 West African Ebola outbreak⁵, we calculated parameters which tell us how fast the infection is spreading and how effective are the control measures for preventing the further spread.

The first model used was the SIR (susceptible-infected-recovered) model. In this model, the population is divided into three groups: S denotes the number of individuals who are susceptible to the infection. I denotes the number of infected individuals, and R denotes the number of individuals who died of the disease or recovered from the disease and have become immune for reinfection with the same virus⁴.

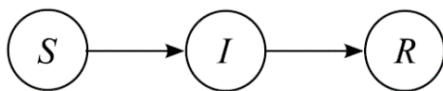


Figure 1: Flow chart for the SIR model⁴

The second model used was the SEIR (susceptible-exposed-infected-recovered) model. The difference between this model and SIR is that apart from the S , I and R groups an additional group is added: here E denotes the number of individuals who have been exposed to the virus but have not yet developed any symptoms¹.

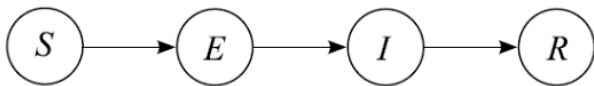


Figure 2: Flow chart for the SEIR model⁴

Solution of the differential equations and fitting was performed in GNU Octave. Both models had similar performance in describing real data. Fit functions for SIR are shown in **Error! Reference source not found..**

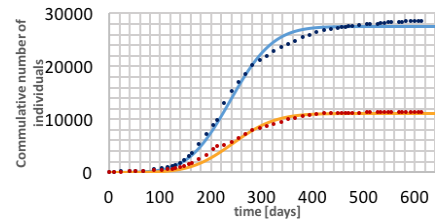


Figure 3: Dynamics of 2014 EBOV outbreak in West Africa. Data of cumulative numbers of infected cases and deaths are shown as blue circles and red circles, respectively. The lines represent the best-fit SIR model⁵.

We calculated the effective reproduction numbers (R_e) for both models, which tell us how many secondary cases are generated by an infected index case¹. The difference in reproduction numbers between SIR and SEIR models are shown in ⁵.

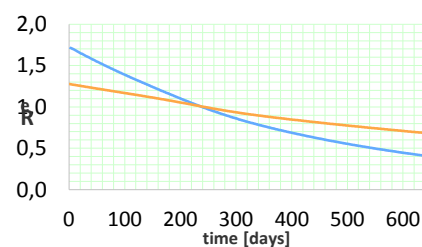


Figure 4: Effective reproduction numbers of 2014 EBOV outbreak for models SIR (orange line) and SEIR (blue line).

References:

1. Althaus, C. L., Estimating the Reproduction Number of Ebola Virus (EBOV) During the 2014 Outbreak in West Africa. *PLOS Current Outbreaks*, **2014**, 6, 1-5.
2. Feldmann, H., Ebola — A Growing Threat?. *New England Journal of Medicine*, **2014**, 371(15), 1375-1378.
3. Astacio, J.; Briere, D.; Guillen, M.; Martinez, J.; Rodriguez, F.; Valenzuela-Campos, N., *Mathematical Models To Study the Outbreaks of ebola*. Report BU-1365-M, **1996**.
4. Brauer, F., Castillo-Chavez, C., *Mathematical models in population biology and epidemiology*. 2nd ed.; Springer: New York, **2012**.
5. Wikipedia, the free encyclopedia. West African Ebola virus epidemic timeline of reported cases and deaths. https://en.wikipedia.org/wiki/West_African_Ebola_virus_epidemic_timeline_of_reported_cases_and_deaths (accessed Jun 05, 2017).

Microkinetics of Photocatalytic Partial Oxidation of Glycerol over CuO/MWCNT to Value-added Platform Chemical Building Blocks

Tomaž Pirman¹, Blaž Likozar¹, Venkata D. B. C. Dasireddy¹, Uroš Novak¹, Andrej Pohar^{1,*}

¹ Department of Catalysis and Chemical Reaction Engineering, National Institute of Chemistry, Hajdrihova 19, 1001 Ljubljana, Slovenia

A recent rapid increased demand for bio-components in fuel has caused the extensive growth of biodiesel production. This has led to vast amounts of surplus glycerol since it is the main by-product of transesterification of biomass-derived triglycerides with methanol. Therefore, there is a desire to develop a way to transform glycerol to products with higher added value, which have the potential to lower the biodiesel cost.¹

Glycerol is a versatile molecule which has three functional groups. Consequently, numerous different products can be obtained from it, such as glycolic acid, glyoxylic acid, oxalic acid, 1,3-dihydroxyacetone, glyceraldehyde, formic acid, glyceric acid and tartaric acid. All these chemicals are considered as high value added products. The method used for production of the above listed chemicals is partial oxidation.²

Oxidation is probably the most popular process for conversion of glycerol to different products, however, high selectivity for a single product is very hard to achieve. Various catalysts are utilized, while Au based-catalyst, Pt based-catalysts and Pd based-catalysts stand out as the most used. There is also a special group of catalysts, which can be applied for the conversion of glycerol. These are photocatalysts, out of which the most utilized is TiO₂. Others worth mentioning are ZnO₂, SiC and CdS. These catalysts need to be irradiated with a light intensity that has larger photon energy than the band-gap energy of the catalyst material. When this condition is fulfilled, the electron (e⁻) will be excited from the valence band, while leaving a hole (h⁺) in its place. The hole is effectively an active site in the catalyst for the oxidation of the glycerol. With photocatalytic cleavage of water we can also obtain other oxidizing agents, which are HO[•], O₂^{•-}, HOO[•] and H₂O₂.³

Our work was dedicated to photocatalytic oxidation of glycerol over Cu and Zn supported on multi-walled carbon nanotubes with added H₂O₂ as an oxidizing agent. In the present work, the glycerol oxidation was conducted on CuO/MWCNT and the effect of a basic oxide i.e. ZnO on the selectivity towards the products were examined. To compare the effect of MWCNT, a bimetallic Cu-Zn catalyst was prepared using Al₂O₃ as support. There were no reports

in the literature of using Cu-Zn/MWCNT for a base free oxidation of glycerol.

The experiments were carried out in a batch photo-reactor, where the concentration of glycerol, concentration of H₂O₂, reaction time and catalyst type were varied. The components shown in Figure 1 were detected in the sample using UHPLC, however, some of them only in very small quantities. The data obtained from the experiments were used to determine the kinetics for the partial photocatalytic glycerol oxidation process. The kinetic parameters were determined by numerically solving the mass balance equations and by conducting nonlinear regression analysis.

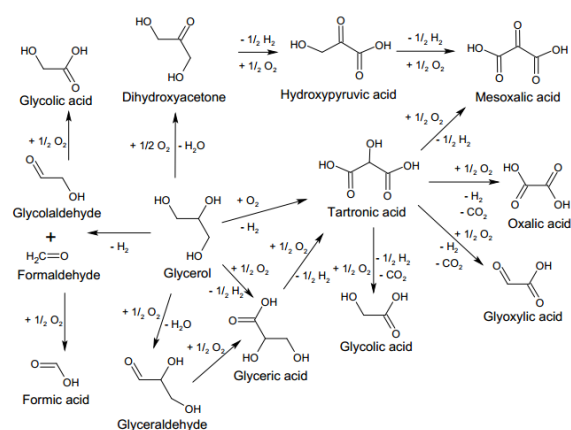


Figure 1: Scheme of expected reaction products attained by photocatalytic partial oxidation of glycerol.

References:

1. Farnetti, E., Crotti, C., Selective oxidation of glycerol to formic acid catalyzed by iron salts. *Cat. Comm.* **2016**, *84*, 1-4.
2. Augugliaro, V., Hamed El Nazer, H. A., Loddo, V., Mele, A., Palmisano, G., Palmisano, L., Yurdakal, S., Partial photocatalytic oxidation of glycerol in TiO₂ water suspensions. *Cat. Today.* **2010**, *151*, 21-28.
3. Jedsukontorn, T., Meeyoo, V., Saito, N., Hunsom, M., Route of glycerol conversion and product generation via TiO₂-induced photocatalytic oxidation in the presence of H₂O₂. *Chem. Eng. J.* **2015**, *281*, 252-264.

Hybrid Plasma Reactors for the Efficient Conversion of Methane to Liquid Chemicals

Harinarayanan Puliyalil^{1,*}, Damjan Lašič Jurković¹, Andrej Pohar¹, Blaž Likozar¹

¹ Department of Catalysis and Chemical Reaction Engineering, National Institute of Chemistry, Hajdrihova-19, 1000 Ljubljana, Slovenia, [email: hari.puliyalil@ki.si](mailto:hari.puliyalil@ki.si)

Motivated by the advantages of vast availability and lower emission of toxic gases compared to other fossil fuels, natural gas consumption has increased remarkably. Most of the natural gas deposits are in remote areas that demands long distance transportation to make it available in the market.¹ However, due to high flammability and volatile nature, oxidative upgrading of methane into liquid chemicals has achieved significant attention. Conventionally used catalytic conversion has the disadvantages of carbon deposition and associated catalyst deactivation, high temperature operation and slow switch on and off time.^{2,3} These disadvantages could be overcome by using the methodology of low temperature plasma oxidation of methane with an active catalyst in the discharge zone.

Herein, partial oxidation of methane with oxygen was achieved inside an atmospheric pressure dielectric barrier discharge incorporated with various packing materials. The experimental set up used in our laboratory is presented in Figure 1. By combining the synergy between the plasma and the embedded materials (commercially bought glass beads and zeolites), a mixture of value added chemicals including methanol, formaldehyde and C-1 and C-2 carboxylic acids were obtained.

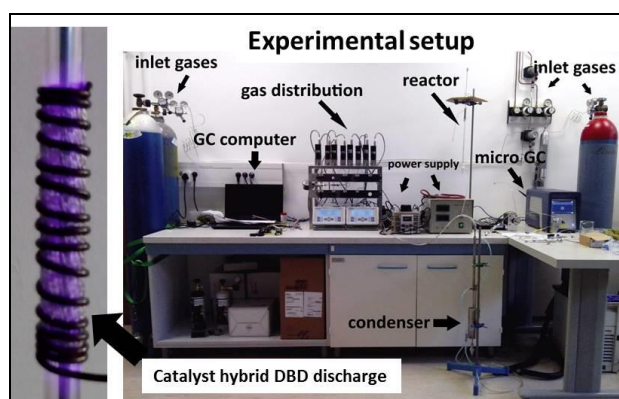


Figure 1: The experimental set up used for CH₄ conversion in the laboratory.

The results revealed that the selectivity of product formation can be varied significantly depending on the packing material embedded material (Table 1). For example, packing with zeolites increased the relative

selectivity towards formaldehyde. Nevertheless, total oxygenate selectivity was much higher in the product mixture when the reactor was packed with glass beads.

Table 1: Selectivity (%) in the obtained liquid mixture towards various oxygenates in packed bed reactors at a discharge power of 20 W and CH₄:O₂ flow rate of 80:20 (sccm)

Packing material	HCHO	CH ₃ OH	HCOOH
Glass beads	24.3	32.4	2.8
Zeolite "Large"	26	26	1.6
Zeolite "Middle A"	21.3	10.5	3.9
Zeolite "Middle B"	25.5	14.1	3.6
Zeolite "Small"	29.2	17.6	4.3

Thus to conclude, this study significantly contributes to the field of plasma driven catalysis for the conversion of methane, a highly volatile and second most abundant greenhouse gas into valuable chemicals. Upgradation of the reaction process to industrial scale process will enable the large scale utilization of natural gas and its easy and safe transportation.

Acknowledgements

This project has received funding through a Sustainable Process Industry through Resources an Energy Efficiency (SPIRE) call under the European Union's Horizon 2020 research and innovation programme (grant agreement n° 680777). The authors thank Johnson Matthey PLC for supplying the zeolites.

References:

1. Saha, D.; Grappe, H. A.; Chakraborty, A.; Orkoulas, G. *Chem. Rev.* **2016**, 116, 11436.
2. Chen, L.; Zhang, X. W.; Huang, L.; Lei, L. C. *Chem. Eng. Process. Process Intensif.* **2009**, 48, 1333.
3. Nozaki, T.; Okazaki, K. *Catal. Today* **2013**, 211, 29.

Studies on Biological Activity of Nystatin in Lipid Membranes

Daša Robič^{*1,2}, Bojan Božič³, Gregor Gomišček^{3,4}

¹ Faculty of Chemistry and Chemical Technology, University of Ljubljana, Večna pot 113, SI-1000 Ljubljana, Slovenia

² Faculty of Medicine, University of Ljubljana, Vrazov trg 2, SI-1004 Ljubljana, Slovenia

³ Institute of Biophysics, Faculty of Medicine, University of Ljubljana, Vrazov trg 2, SI-1000, Ljubljana, Slovenia

⁴ Faculty of Health Sciences, University of Ljubljana, Zdravstvena pot 5, SI-1000, Ljubljana, Slovenia

* Corresponding author: daša.robic@gmail.com

The responses of giant plasma-membrane vesicles (GPMVs), caused by different concentration of nystatin, were studied using phase-contrast and fluorescence microscopy (Figures 1 and 2). Resulting observations were compared with behavior of phospholipid vesicles and cells¹⁻³.

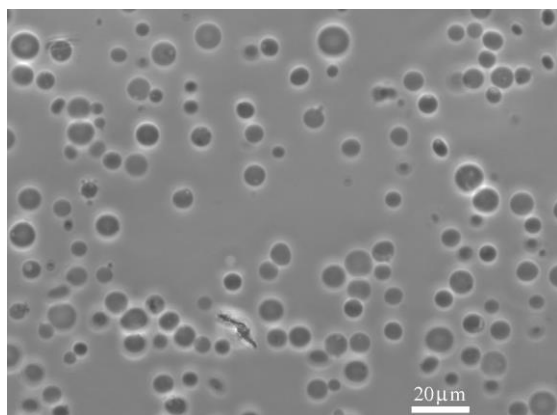


Figure 1: GPMVs at nystatin concentration of 12,5 μM.

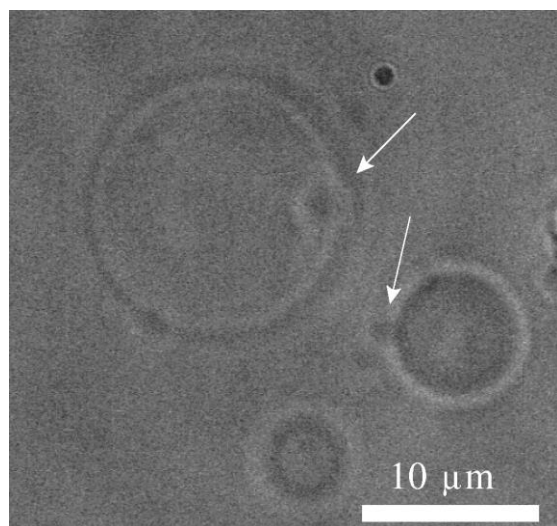


Figure 2: Spherical protrusion of GPMVs marked with white arrows.

Nystatin is a polyene antifungal pore forming agent. In the first step of pore formation, the outer surface of the membrane monolayer increases compared to the inner monolayer. The difference in surface monolayers

begins to decline with passing nystatin and lipid molecules from outer in the inner monolayer. Changes of monolayers' surfaces are reflected in changing shapes of GPMVs (small spherical protrusions, fluctuations), predicted by theory. The nystatin activity was also observed in the form of diminution of fluorescence signal.

Nystatin has a different effect on the lipid vesicles and cells than on GPMVs. The behavior is more similar to the behavior of cells than phospholipid vesicles, as the membrane composition significantly affects the action of nystatin. Spherical protrusions of GPMVs are significantly shorter compared to the ones observed in phospholipid vesicles at the same nystatin concentrations.

References:

1. Kristanc, L., Svetina, S., Gomišček, G., Effects of the pore-forming agent nystatin on giant phospholipid vesicles. *Biochim Biophys Acta* **2012**, *1818*, 636-644.
2. Kristanc, L., Božič, B., Gomišček, G., The role of sterols in the lipid vesicle response induced by the pore-forming agent nystatin. *Biochim Biophys Acta* **2014**, *1838*, 2635-2645.
3. Zemljč Jokhadar, Š., Božič, B., Kristanc, L., Gomišček, G., Osmotic Effects Induced by Pore-Forming Agent Nystatin: From Lipid Vesicles to the Cell. *PLoS ONE* **2016**, *11*, e0165098.

Modeling of Heterogeneous N-deacetylation of Chitin in Alkaline Solution

Bojana Bradić, Andrej Pohar, Uroš Novak, Blaž Likozar

National institute of chemistry, Department of Catalysis and Chemical Reaction Engineering, Hajdrihova 19,1000, Ljubljana, Slovenia

Chitin has a compact structure made from linear chain consisting β -(1, 4)-linked 2-acetamino-2-deoxy- β -D-glucopyranose with 2-amino-2-deoxy- β -D-glucopyranose.¹ Due to its poor solubility in most solvents its chemical modifications usually N-deacetylation by adding alkali solution is performed. After the degree of N-deacetylation (DDA) reaches more than 50%, it becomes soluble in acidic aqueous solutions and behaves as a cationic polyelectrolyte and it can be called chitosan¹. The nontoxic, biodegradable, and biocompatible properties of chitosan provide great potential for many applications. In near decade, chitosan has been involved practically in dietary supplements, water treatment, food, preservation, agriculture, cosmetics, pulp, paper, and medical applications.¹ Kinetics of heterogeneous deacetylation of chitin is often seen as a pseudo-first order reaction, but it has been shown that the mechanism is not simple.² The reaction follows the first order in the initial phase, and later, the process goes to an area where is limited by diffusion.³ The second phase is also limited by equilibrium and unreachable amorphous region.⁴

In this study influence of temperature, chitin particle size distribution, and NaOH concentration on the N-deacetylation kinetics were investigated. A solid to solvent ratio 1 g: 14 mL were used. Experimental conditions varied for temperature from 50 to 80 °C and mixing speed from 200 to 800 rpm. The concentration of obtained chitosan increased mainly with increasing temperature, while the mixing speed has no effect on the N-deacetylation of chitin. At the temperature of 80 °C, the highest concentration of chitosan 96% was achieved after 24 h. Furthermore, the developed mathematical model incorporated diffusion of the NaOH solution into the pores of chitin (Figure 1 left) and first order kinetics for N-deacetylation of chitin (Figure 1 right). The chitin particle size distribution has been determined using Image J and used in the model, while kinetics parameters were determined by regression analysis of the experimental data. Experimental data showed good agreement with the mathematical model for all temperatures as can be seen in Figure 2.

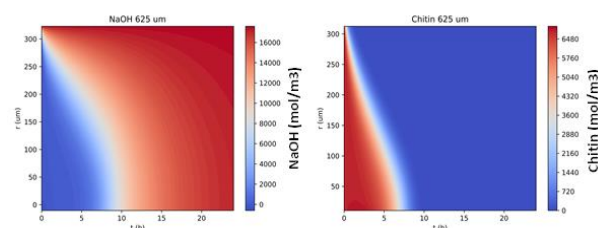


Figure 1: Simulation of NaOH diffusion (left) and chitin N-deacetylation (right) in a particle with a diameter of 625 μm .

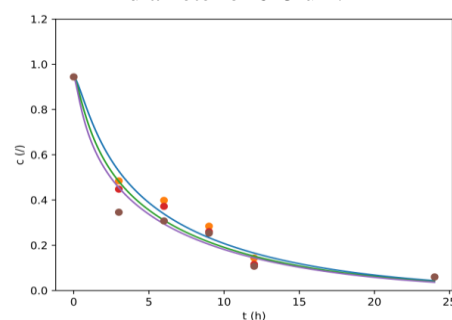


Figure 1: N-deacetylation of chitin at 50°C (yellow), 60°C (red), and 80°C (brown).

References:

1. Al Sagheer, F. A., Al-Sughayer, M. A., Muslim, S. & Elsabee, M. Z. Extraction and characterization of chitin and chitosan from marine sources in Arabian Gulf. *Carbohydrate Polymers*. 2009, 77, 410-419.
2. Liu, T.G., Li, B., Huang, W., Lv, B., J. Chen, J.X. Zhang, Zhu, L.P. Effects and kinetics of a novel temperature cycling treatment on the N-deacetylation of chitin in alkaline solution., *Carbohydrate Polymers*. 2009, 77, 110–117.
3. Liang, K., Chang, B., Tsai, G., Lee, J., Fu, W. Heterogeneous N-deacetylation of chitin in alkaline solution, *Carbohydrate Research*, 1997, 303,327-332.
4. Methacanon, P., Prasitsilp, M., Pothsree, T., Pattaraarchachai, J..Heterogeneous N-deacetylation of squid chitin in alkaline solution, *Carbohydrate Polymers*. 2003, 52 , 119–123

Adipose Triglyceride Lipase-Mediated Lipid Droplet Breakdown is Not Essential for Cell Survival During Nutrient Stress, but is Involved in Eicosanoid Production in Breast Cancer Cells

Eva Jarc^{1,2}, Ana Kump^{1,2}, Petra Malavašič¹, Anja Pucer Janež¹, Vesna Brglez¹, Thomas O. Eichmann³, Robert Zimmermann³ and Toni Petan^{1,*}.

¹ Department of Molecular and Biomedical Sciences, Jožef Stefan Institute, Jamova 39, SI-1000 Ljubljana, Slovenia

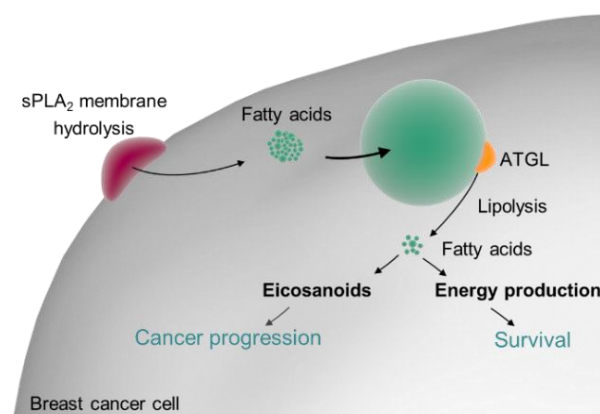
² Jožef Stefan International Postgraduate School, Jamova 39, SI-1000 Ljubljana, Slovenia

³ Institute of Molecular Biosciences, University of Graz, Humboldtstraße 50/EG, AU-8010 Graz, Austria

Lipid droplets (LDs) are dynamic organelles composed of a neutral lipid core of triacylglycerols (TAG) and cholesterol esters surrounded by a phospholipid monolayer embedded with proteins¹. LDs are involved in regulating cellular lipid metabolism and are important for the trafficking of exogenous and endogenous fatty acids (FAs)². Increased accumulation of LDs has been observed in several cancer types, including breast cancer, but whether and how LDs support cancer development and progression is not clear yet³. Secreted phospholipase A₂ (sPLA₂) enzymes release unsaturated FAs from plasma membranes of breast cancer cells and induce the formation of LDs, which are enriched with polyunsaturated FAs (PUFAs) and enable cell survival during nutrient stress⁴. LD breakdown is important for protection against cell death during nutrient restriction, but the molecular mechanisms involved are not clear. The rate limiting enzyme in the LD breakdown cascade is adipose triglyceride lipase (ATGL). Recent studies have shown that ATGL is involved in the transfer of FAs from LDs to mitochondria, but it may also mediate the synthesis of eicosanoids, lipid-derived signalling molecules involved in inflammation and cancer^{2,5}.

The aim of our study was to examine the role of ATGL in supplying LD-derived (PU)FAs for cell survival during starvation-induced nutrient stress and for the synthesis of eicosanoids in breast cancer cells. We found that ATGL depletion reduces LD breakdown and cell survival but, surprisingly, it is not necessary for sPLA₂-induced cell survival during nutrient stress. On the contrary, ATGL depletion reduced sPLA₂-induced prostaglandin E₂ synthesis in breast cancer cells. Our results suggest that ATGL-mediated LD breakdown is not essential for cell survival during starvation, but reveal a novel role for LDs and ATGL in enabling the production of pro-tumorigenic eicosanoid signalling molecules.

Thus, LDs integrate metabolic and signalling pathways in cancer cells and are potential targets for the development of new therapeutic strategies for breast cancer.



Scheme 1: Lipid droplets coordinate fatty acid trafficking with pro-tumorigenic eicosanoid signalling and cell survival mechanisms.

References:

1. Farese, R. V.; Walther, T. C., Lipid droplets finally get a little R-E-S-P-E-C-T. *Cell* **2009**, *139*, 855–860.
2. Rambold, A. S.; Cohen, S.; Lippincott-Schwartz, J., Fatty acid trafficking in starved cells: regulation by lipid droplet lipolysis, autophagy and mitochondrial fusion dynamics. *Dev. Cell* **2015**, *32*, 678–692.
3. Beloribi-Djefailia, S.; Vasseur, S.; Guillaumond, F., Lipid metabolic reprogramming in cancer cells. *Oncogenesis* **2016**, *5*, 189.
4. Pucer, A.; Brglez, V.; Payré, C.; Pungerčar, J.; Lambeau, G.; Petan, T., Group X secreted phospholipase A₂ induces lipid droplet formation and prolongs breast cancer cell survival. *Mol. Cancer* **2013**, *12*, 111.
5. Dichlberger, A.; Schlager, S.; Maaninka, K.; Schneider, W. J.; Kovanen, P. T., Adipose triglyceride lipase regulates eicosanoid production in activated human mast cells. *J. Lipid Res.* **2014**, *55*, 1–21.

Synthesis and Testing of Potential Inhibitors of the *Plasmodium falciparum* Dihydroorotate Dehydrogenase

Nika Strašek¹, Jurij Svete¹, Marko Novinec¹

¹ Faculty of Chemistry and Chemical Technology, University of Ljubljana, Večna pot 113, SI-1000 Ljubljana, Slovenia

Malaria is a third world disease that annually causes around 200 million infections and about half million deaths. The biggest issue is the rapid development of resistance to all newly approved medicines, which means that malaria is still an incurable disease. The main cause of infection is the *Plasmodium falciparum* parasite, which can be transmitted through mosquitoes of the *Anopheles* type.

Plasmodium falciparum dihydroorotate dehydrogenase (*Pf*DHODH), a fourth enzyme in the *de novo* pyrimidine biosynthesis pathway has emerged as a promising target for antimalarial drugs. *Pf*DHODH is located on the outer side of the inner mitochondrial membrane and catalyzes the conversion of dihydroorotate to orotate. The reaction requires two cofactors, a flavinmononucleotide (FMN), which is needed for the oxidation of dihydroorotate and ubiquinone, a terminal electron acceptor, necessary for the reoxidation the FMN.

In *Plasmodium falciparum* the path of *de novo* pyrimidine biosynthesis is the only source of pyrimidine production, whereas in humans this biosynthetic pathway is only one of the sources of pyrimidines, which makes a *Pf*DHODH promising target for selective inhibition. Studies have shown that *Pf*DHODH inhibition leads to parasite death.

In an effort to discover new and potent *Pf*DHODH inhibitors, a number of different compounds were virtually tested using the Schrödinger Glide molecular docking program. The best results were obtained with two types of compounds, bicyclic 3-pyrazolidinones and theophylline-7-acetamides. Bicyclic 3-pyrazolidinones were prepared by a microwave-assisted three-component reaction between a 3-pyrazolidinone, an aldehyde, and an acrylate via formation of an azomethine imine, followed by 1,3-dipolar cycloaddition. Theophylline-7-acetamides were prepared by condensation of easily available theophylline 7-acetic acid with α -amino esters, followed by hydrolysis of the ester group.

The *Pf*DHODH enzyme was prepared by transforming DH5 α *E. coli* cells with a cloning vector containing a previously inserted gene for *Pf*DHODH. The transformation was followed by the expression of protein in cells, isolation and purification of protein with nickel affinity chromatography.

The biological activity tests were performed by measuring the absorbance of the colorimetric substrate dichlorophenolindophenol (DCIP). Preliminary results show IC₅₀ values for compounds **1–3** (Figure 1) in the range of low μ M concentrations.

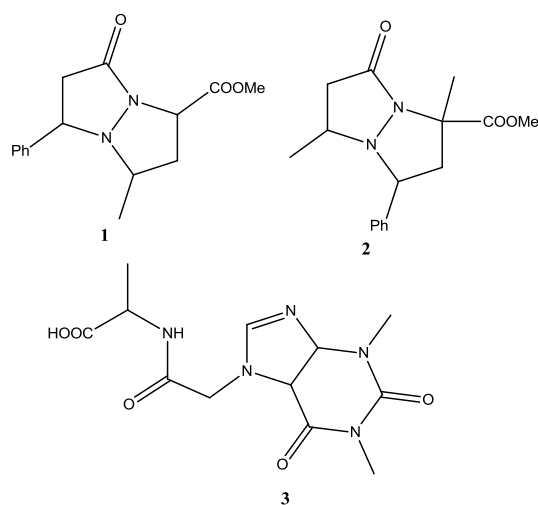


Figure 1: Structures of compounds which show most promising preliminary results.

References:

1. Baldwin, J.; Farajallah, A.M.; Malmquist, N.A. et al., Malarial Dihydroorotate Dehydrogenase. *The Journal of Biological Chemistry* **2002**, *44*, 41827–41834.
2. Grošelj, U.; Svete, J., Recent advances in the synthesis of polysubstituted 3-pyrazolidinones. *ARKIVOC* **2015**, *6*, 175–205.
3. Voynikova, Y.; Valchevab, V.; Momekova, G. et al., Theophylline-7-acetic acid derivatives with amino acids as anti-tuberculosis agents. *Bioorganic & Medicinal Chemistry Letters* **2014**, *24*, 3043–3045.

Preparation of *N*-Halo Substituted Derivatives of Bicyclo[2.2.2]octenes Obtained from Cycloadditions of Maleimides on 2*H*-Pyran-2-ones

Anja Ajdovec, Krištof Kranjc*

Faculty of Chemistry and Chemical Technology, University of Ljubljana, Večna pot 113, SI-1000 Ljubljana, Slovenia;
e-mail: kristof.kranjc@fkkt.uni-lj.si

2*H*-Pyran-2-one and its derivatives **1** are widely present in naturally occurring compounds which exhibit various biological activities. Due to their unique structural features and diverse functionality, 2*H*-pyran-2-ones serve as versatile synthons in synthetic organic chemistry.¹ They are appropriate dienes for numerous Diels–Alder reactions with a variety of dienophiles, including acetylenes (e.g. dialkyl acetylenedicarboxylates, alkyl propiolates, phenyl acetylenes, etc.), which normally form benzene rings, as well as alkenes (e.g. maleic anhydride, *N*-substituted maleimides etc.), which usually yield different bicyclo[2.2.2]octene adducts or alternatively (upon oxidation or a suitable elimination reaction) lead towards aromatic systems.²

Our goal was to prepare succinimide derivatives of bicyclo[2.2.2]octenes³ and to transform them into corresponding *N*-halo compounds (Figure, X = halogen).

We started off with the synthesis of bicyclo[2.2.2]octene framework via a double cycloaddition step. Substituted 2*H*-pyran-2-ones **1** were used as the dienes and the dienophile applied was maleimide. The reaction was carried out under conventional reflux conditions, giving products **2**.^{2,3} Our aim was to further convert the latter compounds into their *N*-halo derivatives **3**. In our primary attempts, we used trichloroisocyanuric acid as the chlorinating reagent. These reactions were carried out under green reaction conditions, at room temperature and with water as a solvent.

The final products **3** might be used as potential building blocks in crystal engineering, forming intriguing molecular architectures, including possibilities of two-dimensional linear structures with bidentate halogen bond acceptors, such as 4,4'-dipyridyl, or possibly yielding 2D networks or even 3D lattices.⁴

Our first attempts on the way towards such *N*-halo ligands based on bicyclo[2.2.2]octene skeletons and results of initial experiments on the way towards crystalline structures being connected by intra- or intermolecular hydrogen- and/or halogen bonds will be presented.

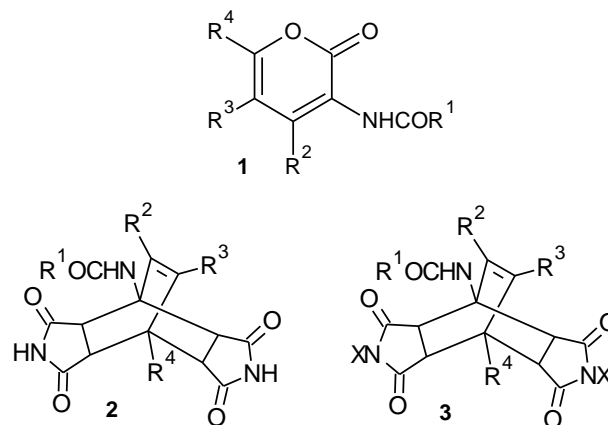


Figure 1: 2*H*-Pyran-2-one derivatives **1**, their cycloadducts with maleimide **2** and final products **3** (X = halogen)

References:

1. Ram, V. J.; Srivastava, P. Pyran-2-ones as a versatile synthon for the synthesis of diverse arenes and heteroarenes. *Curr. Org. Chem.* **2001**, *5*, 571–599.
2. For a review on Diels–Alder reactions of 2*H*-pyran-2-ones, see: Kranjc, K.; Kočevár, M., Regio- and stereoselective syntheses and cycloadditions of substituted 2*H*-pyran-2-ones and their fused derivatives. *Arkivoc.* **2013**, (i), 333–363.
3. Kranjc, K.; Kočevár, M.; Iosif, F.; Coman, S. M.; Parvulescu, V. I.; Genin, E.; Genêt, J. P.; Michelet, V. Efficient and green access to functionalized and highly constrained heteropolycyclic derivatives via a microwave-accelerated Diels–Alder cycloaddition and heterogeneous hydrogenation sequence. *Synlett.* **2006**, *7*, 1075–1079.
4. Cavallo, G.; Metrangolo, P.; Milani, R.; Pilati, T.; Primagi, A.; Resnati, G.; Terraneo, G., The halogen bond. *Chem. Rev.* **2016**, *116*, 2478–2601.

TiO₂-Mesoporous SiO₂ Films for Removal of VOCs from Indoor Air

Andraž Šuligoj^{*,1,2}, Urška Lavrenčič Štanger^{2,3}, Nataša Novak Tušar^{1,3}

¹ National Institute of Chemistry, Hajdrihova 19, SI-1000 Ljubljana, Slovenia

² Faculty of Chemistry and Chemical Technology, University of Ljubljana, Večna pot 113, SI-1000 Ljubljana, Slovenia

³ University of Nova Gorica, Vipavska 13, SI-5001 Nova Gorica, Slovenia

Titanium dioxide (TiO₂) has found its application use in many products used by humans, such as paints, solar creams, toothpaste etc. However, one area which is still lacking its application development is environmental remediation by using nano-TiO₂. Despite its remarkable properties, nano-sized titania suffers from several drawbacks; low specific surface area, relatively low adsorption and UV-light response only.

Immobilisation of the nanoparticles onto a solid support has been recognised as a promising way of addressing some of the limitations of TiO₂.¹ In this manner, hydrophilic mesoporous SiO₂ with a relatively large abundance of surface Si–OH groups is capable of both binding the TiO₂ particles via Si–O–Ti bridges and increasing the adsorption of pollutants via its high surface area.

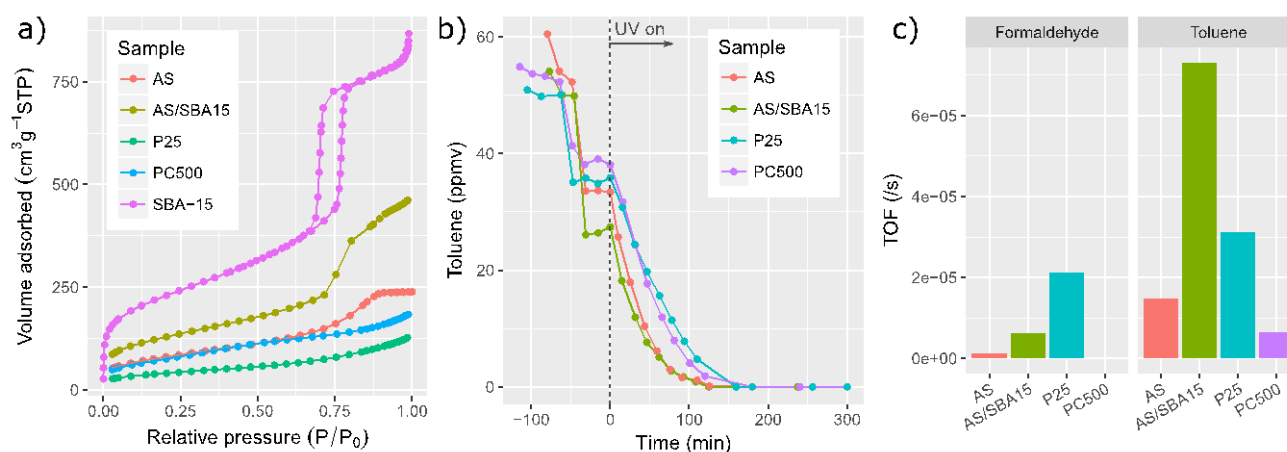


Figure 1: (a) N₂ isotherms of the samples showing the loss of ordered pore structure of SBA-15 after impregnation, (b) concentration curves for toluene degradation and (c) turnover frequencies for formaldehyde and Toluene degradation.

In this study,² ordered mesoporous silica SBA-15 was impregnated with an acidic colloidal TiO₂ suspension via a simple incipient wet impregnation method. Colloidal TiO₂ nanoparticles were produced via a green industrial process in collaboration with Cinkarna company (Celje, Slovenia). SBA-15 was synthesised via a well-known procedure described elsewhere.³ Such materials were then immobilised onto glass slides and tested for VOC (volatile organic compounds) degradation in an air-photocatalytic reactor.

It was shown that impregnation of SBA-15 silica with colloidal TiO₂ lead to decrease in uniformity of pore structure of SBA-15 (Figure 1a). Two pore sizes were observed, i.e. 6.3, 9.3 and 18.2 nm compared to 9.2 nm sized pores in pristine SBA-15. This was due to partial clogging of the pores and partial destruction of the pores upon impregnation. The air-cleaning abilities of such materials showed that in spite of the destruction of SBA-15 pores impregnation resulted in increased speed of degradation of toluene. The turnover numbers of such materials for toluene and formaldehyde

oxidation were increased ca. 6-folds compared to pure TiO₂ nanoparticles (Figure 1c). In general, these composites performed better even than the standard P-25 TiO₂ or PC500 titania, which exhibits approximately the same surface area and particle size (6 nm for both AS and PC500).

References:

- 1 Tasbihi, M.; Lavrenčič Štanger, U.; Škapin, A. S.; Ristić, A.; Kaučič, V.; Novak Tušar, N. *J. Photochem. Photobiol. A Chem.* **2010**, *216* (2–3), 167–178.
- 2 Šuligoj, A.; Lavrenčič Štanger, U.; Ristić, A.; Mazaj, M.; Verhovšek, D.; Novak Tušar, N. *Appl. Catal. B Environ.* **2016**, *184*, 119–131.
- 3 Zhao, D.; Feng, J.; Huo, Q.; Melosh, N.; Fredrickson, G.; Chmelka, B.; Stucky, G. *Science* (80). **1998**, *279* (5350), 548–552.

Basic Haematology and Cytochemical Characteristics of Blood Cells from two Freshwater Turtle Species: *Mauremys rivulata* (Valenciennes in Bory de Saint-Vincent 1833) and *Emys orbicularis* (Linnaeus 1758) in Croatia

Jan Perutka^{*,1,5}, Dean Karaica², Sandra Hodić³, Matea Cedilak⁴, Ana Štih⁵, Ana Čavčić⁶, Aleksandra Krizmanić¹, Domagoj Đikić¹

¹ Division of Animal Physiology, Department of Biology, Faculty of Science, University of Zagreb, Rooseveltov trg 6, 10000 Zagreb, Croatia

² Molecular Toxicology Unit, Institute for Medical Research and Occupational Health, 10000 Zagreb, Croatia

³ Geonatura Ltd. Consultancy in Nature Protection, Fallerovo Šetalište 22, 10000 Zagreb, Croatia

⁴ Fidelita Ltd., Prilaz Baruna Filipovića 29, 10000 Zagreb, Croatia

⁵ Association Hyla, Lipovac I. 7, 10000 Zagreb, Croatia

⁶ SÜDPACK Verpackungen GmbH & Co. KG, Jägerstraße 23, 88416 Ochsenhausen, Germany*

The Balkan Terrapin (*Mauremys rivulata*) is an endangered species that inhabits the area from Dalmatia, Albania, Greece and Cyprus all the way to Bulgaria¹.

In the Republic of Croatia, it is protected by law since only three populations remain in the Dubrovnik-Neretva County. The biggest population is located in Konavosko polje and is threatened by the degradation and disappearance of habitats (e.g. concreting of the channels and rivers). *M. rivulata* shares its habitat with the population of European Pond Turtle (*Emys orbicularis*). Using haematological and differential cytochemical techniques on the blood samples from 34 *M. rivulata* and 21 *E. orbicularis* individuals, their erythrocyte and leukocyte cells were characterised. Additional six healthy adult captive *M. rivulata* from the Zagreb ZOO were also sampled for determination of reliable erythrocyte and leukocyte reference counts.

The aim of this study was to assess physiological condition of this *M. rivulata* population. Polysaccharides and glycoconjugates were detected using the AB (Alcian Blue) and PAS (Periodic acid-Schiff) stains while ALP (Alkaline Phosphatase Enzyme) was detected using the appropriate enzyme-cytochemical method. *M. rivulata* leukocyte (5940/mm³) and erythrocyte (510000/mm³) count mean values were slightly greater than the literature mean values (leukocyte = 3500-5000/mm³; erythrocyte = 405333/mm³)². The AB stained the nuclei of all cells; eosinophils were detected in both whereas monocytes only in the blood of *M. rivulata*. Using PAS and ALP staining, lymphocytes and eosinophils were identified in both species. PAS stained heterophils of *M. rivulata* and thrombocytes of *E. orbicularis* whereas ALP stained heterophils and thrombocytes of *M. rivulata* and monocytes of *E. orbicularis*.

This study is the first report of basic haematology and blood cell cytochemical data from two Testudines species inhabiting freshwater habitats in Croatia.



Figure 1: Alkaline phosphatase staining indicating ALP enzyme activity in the *M. rivulata* eosinophil.

Table 1: Erythrocyte and leukocyte counts from healthy captive *M. rivulata* individuals (RBC: Red blood cells, WBC: White blood cells, Min: Minimum, Max: Maximum, SD: Standard Deviation).

<i>M. rivulata</i>	Post reproductive period			
Parameters	Min	Max	Mean	SD
RBC (x10 ⁶ /mm ³)	0.155	0.97	0.51	0.33
WBC (x10 ³ /mm ³)	3.40	9.30	5.94	2.37

References:

- Jelić, D.; et al., *The Red Book of Amphibians and Reptiles of Croatia*, Ministry of Environmental and Nature Protection, State institute for Nature Protection, Republic of Croatia, Zagreb, **2012**
- Yilmaz, N.; Tosunoglu, M., Hematology and some plasma biochemistry values of free-living freshwater turtles (*Emys orbicularis* and *Mauremys rivulata*) from Turkey. *N.-W. J. Zool.*, **2010**, 6(1): 109-117.

The Chiral Thiourea Organocatalyst for the Enantioselective Carbon-Carbon Bond Formation

Eva Plut¹, Sebastijan Ričko¹, Bogdan Štefane¹, Jurij Svete¹, and Uroš Grošelj^{1,*}

¹ Faculty of Chemistry and Chemical Technology, University of Ljubljana, Večna pot 113, SI-1000 Ljubljana, Slovenia

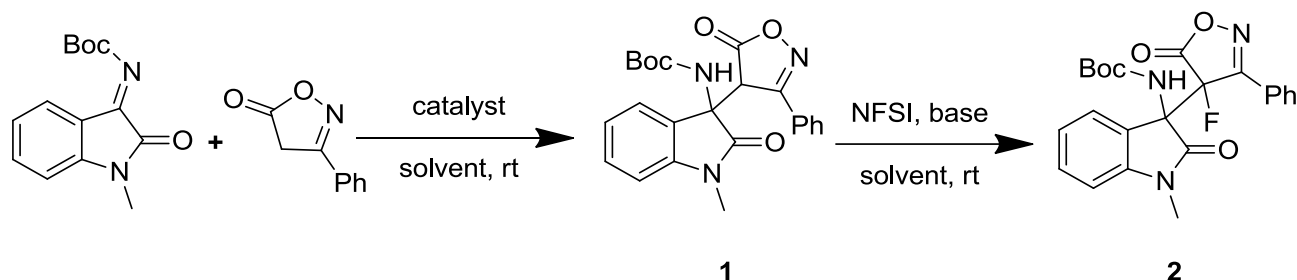


Figure 1: Reaction of *N*-methylisatin imine with 3-phenylisoxazolone.

Due to the biological activities of isatin derivatives, which scaffold can be found in a number of biologically active pharmacological agents and alkaloids, many studies of various asymmetric transformations using isatin imine as the electrophile have been made in recent years¹.

Based on our previous investigations on the organocatalytic enantioselective reaction of 4-pyrrolones and 1, 3-dicarbonyls with *trans*- β -nitrostyrenes where the highly active bifunctional camphor-derived organocatalyst was found to be the most promising one^{2,3}, we investigated the catalytic ability of various catalysts for the reaction of *N*-methylisatin imine with 3-phenylisoxazolone in toluene at room temperature. Hence, we were motivated to determine the optimal reaction condition for the reaction between isatin imine and oxazolone by screening various solvents using cinchonidine thiourea as the catalyst. We investigated the reaction of isatin intermediate **1** with *N*-fluorobenzenesulfonimide to evaluate the effect of bases on the diastereoselectivity. Reactions were performed using various organic and inorganic bases. Lowering the catalyst loading from 5 mol-% to 0.5 mol-% yielded product **2** with enantiomeric excess (ee) up to >97 % and lower diastereomer ratio (dr). Varying the catalyst, solvent, and base had a noticeable effect on the enantioselectivity and diastereoselectivity of the reaction (ee up to >98 %). The optimized conditions were used to evaluate the substrate scope of the reaction.

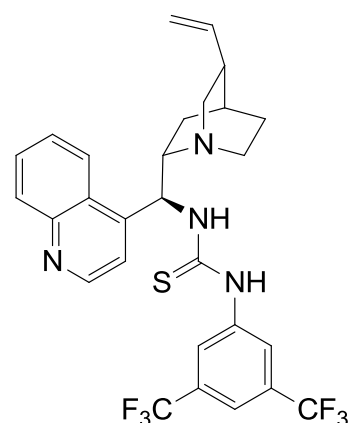


Figure 2: Cinchonidine-derived thiourea as an organocatalyst.

References:

1. Kaur, J.; Kumari, A.; Bhardwaj, V. K.; Chimni, S. S., Chiral squaramide catalyzed enantioselective decarboxylative addition of β -ketoacids to isatin imine. *Adv. Synth. Catal.* **2017**, 359, 1725-1734.
2. Ričko, S.; Meden, A.; Ivančič, A.; Perdih, A.; Štefane, B.; Svete, J.; Grošelj, U., Organocatalyzed Deracemisation of Δ^2 -Pyrrolin-4-ones. *Adv. Synth. Catal.* **2017**, in press, DOI:10.1002/adsc.201700539.
3. Ričko, S.; Svete, J.; Štefane, B.; Perdih, Grošelj, U., 1,3-Diamine-Derived Bifunctional Organocatalyst Prepared from Camphor. *Adv. Synth. Catal.* **2016**, 358, 3786-3796.

The Evolution Of Pyridine-Tethered Mesoionic Ligands And Their Palladium Complexes As Catalysts In Sustainable Cross-Coupling Reactions

Miha Virant¹, Martin Gazvoda¹, Janez Košmrlj*,¹

¹ Faculty of Chemistry and Chemical Technology, University of Ljubljana, Večna pot 113, SI-1000 Ljubljana, Slovenia

Metal-catalysed cross-coupling reactions have become inevitable protocol in the synthetic organic chemistry, enabling an expeditious access to new molecules. It is generally carried out in the presence of catalytic amounts of transition-metal complex. The central transition-metal ion is most commonly coordinated with phosphine ligands that stabilize the metal. However, the use of phosphines is accompanied by several drawbacks, such as the need for strict oxygen exclusion during manipulations, and their toxicity that makes them ecologically problematic waste^{1,2}.

A convenient alternative to phosphines was enabled with the discovery of *N*-heterocyclic carbenes (NHCs). Besides their lower toxicity compared to phosphines, NHCs also have a greater σ -donating character that contributes to enhanced stabilisation of the metal complexes. It has been discovered that electron-donating character is even greater in the abnormal NHCs, in which the carbene centre is not positioned between the nitrogen atoms of the *N*-heterocyclic framework. Furthermore, the presence of pyridine as an additional ligand proved beneficial for the stability and catalytic activity of complexes in the cross coupling reactions².

Inspired by previous discoveries, we prepared palladium complexes with 1,2,3-triazole-5-ylidene ligands tethered with pyridine. A simple laboratory procedure allowed the coordination of Py-tzNHC to palladium after deprotonation of ligand precursor. The structure of palladium complex (Figure 1) was determined by NMR spectroscopy and high-resolution mass spectrometry, and further confirmed by a single crystal X-ray diffraction analysis³.

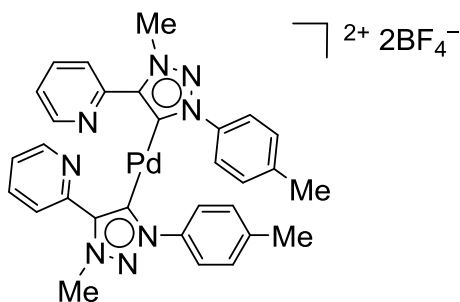
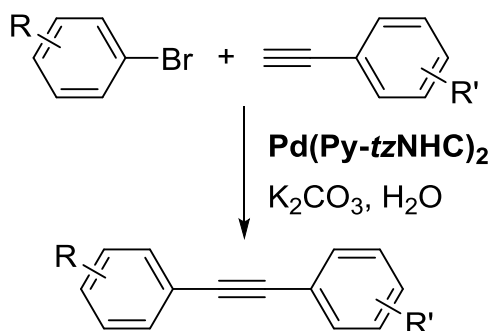


Figure 1: Palladium complex with Py-tzNHC ligands.

The catalytic activity of the palladium complex from Figure 1 has been evaluated in the Sonogashira cross-coupling of aryl bromides and acetylenes (Scheme 1). The reactions were carried out in water as the only solvent and under aerobic conditions. The catalyst was tolerated by inorganic bases, a greener alternative to the otherwise used amines. Furthermore, a broad range of (hetero)aryl bromides and acetylenes could be coupled in high yields without the necessity of copper(I) salts or other additives, rendering our procedure a “green alternative” to the classical Sonogashira protocol³.



Scheme 1: Copper-free Sonogashira reaction under green reaction conditions.

References:

- Mathew, P.; Neels, A.; Albrecht, M. 1,2,3-triazolylienes as versatile abnormal carbene ligands for late transition metals. *J. Am. Chem. Soc.* **2008**, *130*, 13534-13535.
- O'Brien, C. J.; Kantchev, E. A. B.; Valente, C.; Haddei, N.; Chass, G. A.; Lough, A.; Hopkinson, A. C.; Organ, M. G. Easily prepared air- and moisture-stable Pd-NHC (NHC=N-Heterocyclic carbene) complexes: A reliable, user-friendly, highly active palladium precatalyst for the Suzuki-Miyaura reaction. *Chem. Eur. J.* **2006**, *12*, 4743-4748.
- Gazvoda, M.; Virant, M.; Pevec, A.; Urankar, D.; Bolje, A.; Kočev, M.; Košmrlj, J. A mesoionic bis(Py-tzNHC) palladium(II) complex catalyses “green” Sonogashira reaction through an unprecedented mechanism. *Chem. Commun.* **2016**, *52*, 1571-1574.

Arylation of Selected Pyrrole-Containing Heterocycles via C–H Bond Activation

Bruno Aleksander Martek¹, Miha Virant¹, Martin Gazvoda¹, Janez Košmrlj^{*,1}

¹ Faculty of Chemistry and Chemical Technology, University of Ljubljana, Večna pot 113, SI-1000 Ljubljana, Slovenia

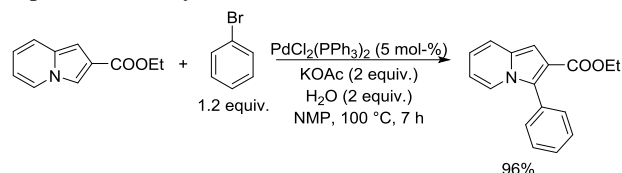
The development of processes for direct transformation of carbon–hydrogen bonds into carbo–oxygen, carbon–halogen, carbon–nitrogen, carbon–sulfur and carbon–carbon bonds remain a crucial challenge in organic chemistry. This type of selective transformations has found widespread applications across the field of chemistry, including the synthesis of natural products, polymers, agrochemicals and pharmaceuticals. Traditional approaches for the preparation of those compounds rely on pre-functionalized starting materials. However, pre-functionalization prior to the C–O, C–X, C–N, C–S or C–C bond formation adds undesired additional synthetic steps to the overall synthetic protocol. As such, avoiding this issue will improve an atom economy and increase the overall efficiency of the synthesis¹.

C–H functionalization represents a new approach in organic synthesis. Instead of focusing on selective reactions at the desired functional groups, it relies on the controlled functionalization of specific C–H bonds, even though more reactive functional groups may also be present. Owing to advancements in organometallic chemistry, new ways of site-selective C–H functionalizations have been developed. The initial approaches were focused on developing methods for the functionalization of relatively simple hydrocarbons. But nowadays, C–H functionalization has evolved into a viable strategy for the synthesis of complex targets².

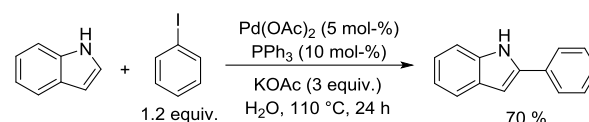
The direct C–H functionalization of heterocycles is of considerable interest for the synthesis of commercially relevant compounds². Among different types of catalytic transformations of *N*-heterocycles, direct arylation has emerged as an important alternative to traditional cross-coupling reactions in the preparation of biaryl molecules³. Between them, azoles represent important structural units frequently found in natural products, pharmaceuticals and other synthetics with biological properties^{4,5}. Direct arylation of heteroarenes, achieved via cross-coupling of (sp²) C–H bonds and aryl halides, offers an alternative to standard cross-coupling methods, which require the formation of a reactive functionality in advance of C–C coupling reactions⁴.

Herein we describe palladium-catalyzed C–H functionalization of selected pyrrole-containing heterocycles and demonstrate that by using

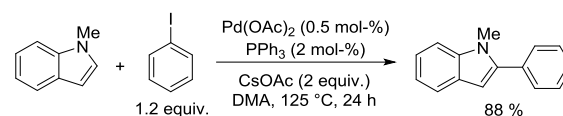
Pd/PPh₃/OAc catalytic system selected nitrogen-containing heteroarenes (**Schemes 1–3**) can be successfully arylated in high yields. This work is aimed at substantially extending the scope of the literature reported C–H arylation reactions.



Scheme 1: Synthesis of ethyl 3-phenylindolizine-2-carboxylate.



Scheme 2: Synthesis of 2-phenyl-1*H*-indole.



Scheme 3: Synthesis of 1-methyl-2-phenylindole.

References:

1. Lyons, T. W.; Sanford, M. S. Palladium-Catalyzed Ligand-Directed C–H Functionalization Reactions. *Chem. Rev.* **2010**, *110*, 1147–1169.
2. Davis, H. M.; Morton, D. Recent Advances in C–H Functionalization. *J. Org. Chem.* **2016**, *81*, 343–350.
3. Joucla, L.; Batali, N.; Djakovitch, L. "On Water" Direct and Site-Selective Pd-Catalysed C–H Arylation of (NH)-indoles. *Adv. Synth. Catal.*, **2010**, *352*, 2929–2936.
4. Lane, B. S.; Brown, M. A.; Sames, D. Direct Palladium-Catalyzed C-2 and C-3 Arylation of Indoles: A Mechanistic Rationale for Regioselectivity. *J. Am. Chem. Soc.* **2005**, *127*, 8050–8057.
5. Park, C. -H.; Ryabova, V.; Seregin, I. V.; Sromek, A. W.; Gevorgyan, V. Palladium-Catalyzed Arylation and Heteroarylation of Indolizines. *Org. Lett.*, **2004**, *6*, 1159–1162.

Oxidative Stress During Sevoflurane or Propofol Anesthesia in Dogs with Early-Stage Myxomatous Mitral Valve Degeneration

Tomsič Katerina¹, Nemec Svete Alenka¹, Nemec Ana¹, Domanjko Petrič Aleksandra¹, Vovk Tomaž², Seliškar Alenka^{*1}

¹ Veterinary faculty, University of Ljubljana, Gerbičeva ulica 60, 1000 Ljubljana, Slovenia

² Faculty of Pharmacy, University of Ljubljana, Aškerčeva 7, 1000 Ljubljana, Slovenia

Anesthesia of dogs with cardiac disease may increase oxidative stress and possibly aggravate the disease¹. We investigated whether anesthesia with propofol, which is believed to have antioxidant properties similar to vitamin E², causes less oxidative stress compared to anesthesia with propofol and sevoflurane in dogs in which oxidative stress is present due to myxomatous mitral valve disease (MMVD). Sixteen client-owned dogs with subclinical MMVD requiring periodontal treatment were included in the study. After induction with propofol, anesthesia was maintained with propofol

(8 dogs) or sevoflurane (8 dogs). Blood samples for determination of free radical scavenger vitamin E, antioxidant enzyme superoxide dismutase and lipid peroxidation product malondialdehyde were collected before premedication, 5 and 60 minutes and 6 hours after induction to anesthesia. There were no significant differences between groups in any of the parameters at each sampling time (Table 1). In conclusion, both anesthetic protocols can be used in dogs with early-stage MMVD with regard to oxidative stress.

Table 1: Values (mean \pm SD) of vitamin E, malondialdehyde and superoxide dismutase

	Group	Basal	5 minutes	60 minutes	6 hours
Vitamin E ($\mu\text{mol/L}$)	PS	67.1 \pm 27.5	62.3 \pm 26.2	60.5 \pm 26.0 *	63.5 \pm 26.6
	P	69.0 \pm 15.8	63.5 \pm 16.2 *	60.7 \pm 15.3 *	61.7 \pm 19.3 *
Malondialdehyde ($\mu\text{mol/L}$)	PS	5.26 \pm 0.90	5.55 \pm 0.73	5.58 \pm 1.09	6.33 \pm 1.34
	P	6.03 \pm 0.67	5.99 \pm 1.12	5.83 \pm 0.83	6.01 \pm 0.83
Superoxide dismutase (U/gHb)	PS	2402.5 \pm 165.1	2403.4 \pm 180.2	2418.9 \pm 191.1	2407.6 \pm 200.6
	P	2142.3 \pm 306.9	2148.0 \pm 347.9	2221.0 \pm 390.6	2219.2 \pm 411.7

PS, propofol and sevoflurane; P, propofol; *, significant difference from basal values.

References:

1. Kevin, L. G.; Novalija, E.; Stowe, D. F. Reactive oxygen species as mediators of cardiac injury and protection: the relevance to anesthesia practice. *Anesth. Analg.* 2005, 101, 1275–1287.
2. Murphy, P. G.; Myers, D. S.; Davies, M. J.; Webster, N. R.; Jones, J. G. The antioxidant potential of propofol (2,6-diisopropylphenol). *Br. J. Anaesth.* 1992, 68, 613–618.

Evaluation of Imidazolium Fluoride Based Reagents for Nucleophilic Fluorination of Organic Compounds

Jan Petrovčič¹, Blaž Alič², Gašper Tavčar², Jernej Iskra^{1,*}

¹ Faculty of Chemistry and Chemical Technology, University of Ljubljana, Večna pot 113, SI-1000 Ljubljana, Slovenia

² Jožef Stefan Institute, Department of Inorganic Chemistry and Technology, Jamova cesta 39, SI-1000 Ljubljana, Slovenia

Despite low abundance in nature, fluorinated organic compounds have numerous uses in science and medicine. Fluorinated organic compounds are irreplaceable solvents for many organic chemists. On the other hand, medicine utilizes specific isotope labelled fluorinated organic compounds in positron emission tomography (PET). Introduction of fluorine-18 in organic molecules can be achieved with nucleophilic and electrophilic fluorinating reagents. Due to the nature of technical procedure, fluorine source for preparation of nucleophilic fluorinating reagents has higher specific activity than the fluorine source for preparation of electrophilic fluorinating reagents. Nucleophilic fluorinating reagents are therefore more extensively studied.¹

The most straightforward reagents for nucleophilic fluorination are metal fluorides, but the insufficient solubility of these compounds in organic solvents limits their use. Free fluoride reagents with other counterions have been developed to overcome the solubility issues (e.g. tetraalkylammonium cations). Secondly, the inability to thoroughly dry these reagents presents another problem. Hydrogen bonding between water molecules and fluoride ions reduces the nucleophilicity of fluoride ions and thus their reactivity.² Additionally, water molecules may contribute to formation of undesired side products.

Tavčar and Alič recently utilized N-heterocyclic carbene (NHC) for preparation of imidazolium-based fluoride and two poly(hydrogen fluorides). These compounds, which show characteristics of free fluoride reagents, have been prepared by reacting 1,3-bis(2,6-diisopropylphenyl)-1,3-dihydro-2*H*-imidazol-2-ylidene with different HF sources.³

We have evaluated the use of imidazolium-based fluoride and two imidazolium-based poly(hydrogen fluorides) as reagents for fluorination of organic compounds. Using ¹H and ¹⁹F NMR analysis we investigated their nucleophilicity, basicity and substrate scope for fluorination. Special emphasis has been placed on the fluorination of different benzyl bromides (Figure 1).

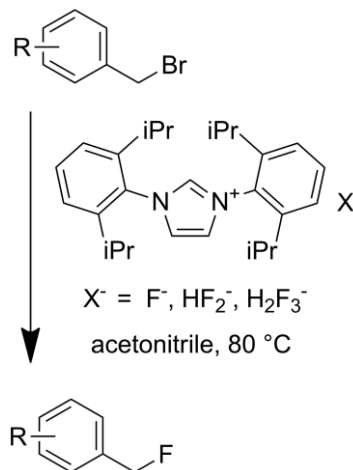


Figure 1: Nucleophilic fluorination of different benzyl bromides with imidazolium-based fluoride and two poly(hydrogen fluorides).

Imidazolium-based bifluoride proves to be a better alternative for nucleophilic fluorination of benzyl bromides than the commonly used tetrabutylammonium fluoride and tetramethyl ammonium fluoride because it is easier to handle and it is not hygroscopic.

References:

1. Kirk, K. L.: Fluorination in Medicinal Chemistry: Methods, Strategies, and Recent Developments. *Org. Process Res. Dev.*, **2008**, *12*, 305–321.
2. Clark, J. H.: Fluoride ion as a base in organic synthesis. *Chem. Rev.*, **1980**, *80*, 429–452.
3. Alič, B; Tavčar, G: Reaction of N-heterocyclic carbene (NHC) with different HF sources and ratios – A free fluoride reagent based on imidazolium fluoride. *J. Fluor. Chem.*, **2016**, *192*, 141–146.

Self-Assembly of Isotactic and Atactic Poly(Methacrylic Acid) Chains in Aqueous Solutions: Effect of Temperature

Patricija Hriberšek¹, Simona Sitar², Ema Žagar², Ksenija Kogej^{*,1}

¹ Faculty of Chemistry and Chemical Technology, University of Ljubljana, Večna pot 113, SI-1000 Ljubljana, Slovenia

² National Institute of Chemistry, Hajdrihova ulica 19, SI-1000 Ljubljana

Polymeric nanoparticles (PNs) are the subject of research because of their numerous applications. They can be used in medical diagnostics as carriers for targeted drug delivery, in paints, coatings, composite materials, ... PNs can be prepared by chemical reactions or by different types of self-assembly. Recently, a new approach was developed to induce polymer self-assembly of poly(α -alkylcarboxylic acids) into stable PNs without any assembly triggering additives, which involves heating of a homopolymer solution.^{1,2}

Our work aims at preparing stable PNs by temperature-controlled self-assembly of atactic (aPMA) and isotactic poly(methacrylic acid) (iPMA) (for a typical atactic and isotactic triad sequence see Figure 1). It was recently shown that iPMA forms nanoparticles in water at 25°C at a so-called critical degree of neutralization (α_N) of its carboxyl groups ($\alpha_N \approx 0.2$).^{3,4} This α_N corresponds to the solubility limit of this homopolymer in water. It was discussed that iPMA chains first undergo a conformational change from coil to helix, which is followed by an intermolecular association.^{3,4,5} aPMA is soluble in water at any α_N . Possible self-assembly and structural characteristics of aPMA and iPMA chains was herein studied by UV-Vis, differential scanning calorimetry (DSC), isothermal titration calorimetry (ITC), circular dichroism (CD), and static and dynamic light scattering (SLS and DLS) measurements in aqueous 0.1 M NaCl solutions in the temperature range from 0 to 95 °C. Experiments were performed with samples of aPMA and iPMA, which differ in weight average (M_w) and number average molar mass (M_n), in polydispersity, tacticity, and α_N .

Basic characterization of samples was done using asymmetrical flow field-flow fractionation (AF4) and size-exclusion chromatography (SEC). Nanoparticle formation was monitored by temperature-controlled UV-Vis experiment. The presence of helices using CD could, however, not be confirmed. Possible self-assembly was monitored by DSC and further by SLS and DLS. Using these methods we determined the radius of gyration (R_g) and the hydrodynamic radius (R_h) of iPMA associates or PNs. With ITC, the ionization enthalpies of iPMA were obtained at

different temperatures. The endothermic peak observed in ITC curves was interpreted by taking into account the conformational change and simultaneous intermolecular association between iPMA chains.

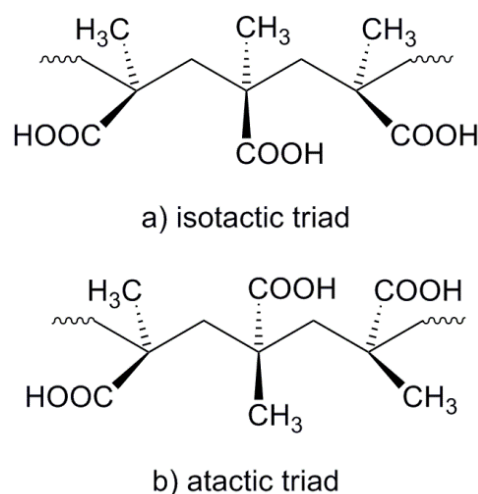


Figure 1: a) Isotactic and b) atactic triad sequence.

References:

1. Sedlák, M.; Koňák, Č., A New Approach to Polymer Self-assembly into Stable Nanoparticles: Poly(ethylacrylic acid) Homopolymers. *Macromolecules* **2009**, *42*, 7430-7438.
2. Sedlák, M.; Koňák, Č.; Dybal, J., Heat-Set Poly(ethylacrylic acid) Nanoparticles: Combined Light Scattering, Calorimetric, and FTIR Study. *Macromolecules* **2009**, *42*, 7439-7446.
3. Sitar, S.; Aseyev, V.; Kogej, K., Differences in Association Behavior of Isotactic and Atactic Poly(methacrylic acid). *Polymers* **2014**, *55*, 848- 854.
4. Sitar, S.; Aseyev, V.; Kogej, K., Microgel-like Aggregates of Isotactic and Atactic Poly(methacrylic acid) Chains in Aqueous Alkali Chloride Solutions as Evidenced by Light Scattering. *Soft Matter* **2014**, *10*, 7712-7722.
5. van den Bosch, E., Keil, Q.; Filipcsei, G.; Berghmans, H.; Reynaers, H., Structure Formation in Isotactic Poly(methacrylic acid). *Macromolecules* **2004**, *37*, 9673-9675.

Synthesis of Flower-like TiO₂ Particles

Tjaša Goltnik^{*1,2}, Lev Matoh¹, Marjan Bele², Urška Lavrenčič Štangar^{1,3}

¹ Faculty of Chemistry and Chemical Technology, University of Ljubljana, Večna pot 113, 1000 Ljubljana, Slovenia

² National Institute of Chemistry, Hajdrihova 19, SI-1001 Ljubljana, Slovenia

³ University of Nova Gorica, Vipavska 13, SI-5000 Nova Gorica, Slovenia

Titanium dioxide (TiO₂) is one of the most important transition metal oxides. It is used in self-cleaning surfaces, catalysis, photovoltaic cells, optical emission, water-splitting, paints, paper, cosmetics, etc. It is a well-researched material because of its good chemical and thermal stability, biocompatibility as well as physical, optical, and electrical properties. TiO₂ exists in three mineral forms: anatase, rutile, and brookite. In general, the anatase form is preferred due to its high photocatalytic activity and high specific surface area; additionally, it is non-toxic and relatively inexpensive. TiO₂ morphologies mainly include nanostructures such as nanotubes, nanowires, nanorods, and mesoporous structures.

The purpose of this work was to prepare TiO₂ powders that could be used to support a metal based electro-catalyst for photocatalytic water splitting with nanostructures in the form of flowers. Such structures were desirable because of their high specific surface area. Such large particles can improve the transfer of electrons between a catalyst deposited on the surface of the flowers and the conductive material on which the flowers are immobilized.

The flower-like TiO₂ nanostructures were synthesized from Ti-propoxide with a hydrothermal reaction in a highly alkaline medium. The nano morphology of the larger particles can easily be controlled by adjusting the reaction parameters. By optimizing key parameters, we were able to increase the yield of the reaction by up to ten times compared to previously reported results¹. The specific flower-like morphology is stable and remains intact even after calcination at higher temperatures.

The morphology of the prepared samples was investigated using a scanning electron microscope (SEM) – Figure 1. For further characterization, the specific surface area of different samples was measured and the photocatalytic activity of the prepared powders was tested under UV illumination.

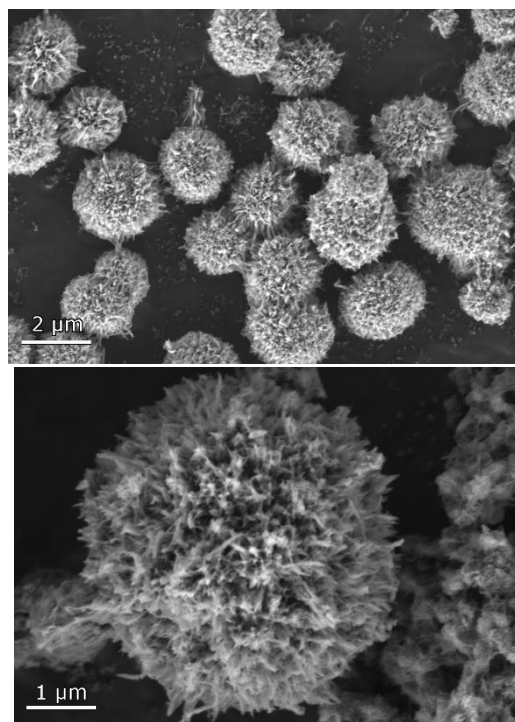


Figure 1: SEM images of flower-like TiO₂ nanostructures.

References:

1. M. Liu, W. Lu, L. Zhao, C. Zhou, H. Li, W. Wang: Fabrication and photocatalytic properties of flower-like TiO₂ nanostructures. *Trans. Nonferrous Met. Soc. China*, **2010**, *20*, 2299–2302
2. M. Malekshahi Byranvanda, A. Nemati Kharata, L. Fatholahib, Z. Malekshahi Beiranvandc: A Review on Synthesis of Nano-TiO₂ via Different Methods. *Journal of nanostructures*, **2013**, *3*, 1-9
3. H. Song, T. Chen, Y. Sun, X. Zhang, X. Jia: Controlled synthesis of porous flower-like TiO₂ nanostructure with enhanced photocatalytic activity. *Ceramics International*, **2014**, *40*, 11015–11022

Oxidation of Guanine Nucleos(t)ides with Peroxynitrite

Jernej Ekar^{*,1,2}, Peter Podbevšek^{1,3}, Janez Plavec^{1,2,3}

¹ Slovenian NMR centre, National Institute of Chemistry, Hajdrihova 19, SI-1001 Ljubljana, Slovenia

² Faculty of Chemistry and Chemical Technology, University of Ljubljana, Večna pot 113, SI-1000 Ljubljana, Slovenia

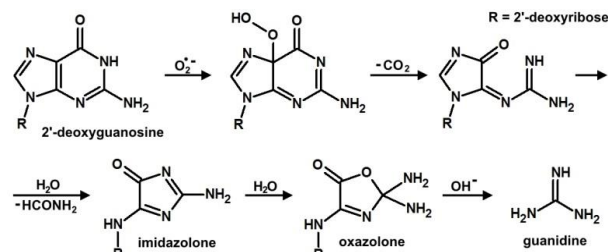
³ EN-FIST Centre of Excellence, Trg OF 13, SI-1000 Ljubljana, Slovenia

Guanine residue is the most easily oxidizable nucleotide of all four that form DNA¹. Being also the building block of guanine quadruplexes which predominantly form on protective chromosomes ends, it exhibits an important role in oxidative stress reactions. When exposed to oxidizing agents such as peroxynitrite, it undergoes transformation first into 8-oxo-7, 8-dihydroguanine, following imidazolone and oxazolone², but also into some other products¹. Peroxynitrite is an interesting oxidizer, formed in our cells by reaction of superoxide anion radical and nitrogen oxide (NO)³. This highly reactive species can undergo isomerization into nitrate (V) or decomposition into various products such as hydroxyl radical, nitrite, different nitrogen oxides and singlet oxygen^{3, 4, 5}. Oxidation properties of peroxynitrite are furthermore highly dependent on pH and temperature of media in which reaction takes place³. We confirmed this to be true while observing that time needed for the oxidation completion varies with temperature in the form of faster reaction when sample is heated.

Our work was centered around 2'-deoxyguanosine 5'-monophosphate (dGMP) and 2'-deoxyguanosine (dG). While using ¹³C and ¹⁵N fully labeled samples for NMR analysis, we managed to indirectly confirm oxidation route shown in Scheme 1 by identification of side products formate and CO₂¹. Formate is the actual proof of formamide being reaction intermediate as is formed by its hydrolysis. We also determined presence of guanidine which arises from oxazolone in alkali media and elevated temperature² and additionally its hydrolysis product, urea. Both, guanidine and urea were detected in much smaller quantities than carbonate and formate. Reasons can be found in potential further oxidation of guanidine/urea into carbonate. In ¹³C NMR spectra we can observe a new set of signals for a dG/dGMP oxidation product. The new set exhibits comparable linewidths and couplings constants as dG/dGMP signals, only at slightly shifted chemical shifts. Mass spectra suggest the new set of NMR signals can be attributed to either guanine (glycoside bond cleavage) or some isomer of dG/dGMP.

Additionally, comparison of oxidation products formed while reacting dG/dGMP with ONOO⁻ and with H₂O₂ in the presence of CuCl₂ shows that many of

the same species have formed. This supports the peroxynitrite decomposition mechanism where peroxide anion and/or hydroxyl radical are formed. Another interesting observation arises from universality of peroxynitrite action as formate is not formed only when reacting ONOO⁻ with dG/dGMP but also whenever it is mixed with any organic compound with at least one C–H moiety. Universal reaction mechanism of formate formation is still to be proposed.



Scheme 1: dG oxidation route and products

References:

1. Neeley, W. L.; Essigmann, J. M., Mechanisms of Formation, Genotoxicity, and Mutation of Guanine Oxidation Products. *Chem. Res. Toxicol.* **2006**, *19* (4), 491-505.
2. Cadet, J.; Berger, M.; Buchko, G. W.; Joshi, P. C.; Raoul, S.; Ravanat, J.-L., 2,2-Diamino-4-[(3,5-di-O-acetyl-2-deoxy-β-D-erythro-pentofuranosyl)amino]-5-(2H)-oxazolone: A Novel and Predominant Radical Oxidation Product of 3',5'-Di-O-acetyl-2'-deoxyguanosine. *J. Am. Chem. Soc.* **1994**, *116* (16), 7403-7404.
3. Kissner, R.; Koppenol, W. H., Product Distribution of Peroxynitrite Decay as a Function of pH, Temperature, and Concentration. *J. Am. Chem. Soc.* **2002**, *124* (2), 234-239.
4. Richeson, C. E.; Mulder, P.; Bowry, V. W.; Ingold, K. U., The Complex Chemistry of Peroxynitrite Decomposition: New Insights. *J. Am. Chem. Soc.* **1998**, *120* (29), 7211-7219.
5. Molina, C.; Kissner, R.; Koppenol, W. H., Decomposition kinetics of peroxynitrite: influence of pH and buffer. *Dalton Trans.* **2013**, *42*, 9898-9905

Wildfire Propagation Modeling

Marko Radak¹, Simon Schnabl¹

¹ Faculty of Chemistry and Chemical Technology, University of Ljubljana, Večna pot 113, 1000 Ljubljana, Slovenia

Depending on the fire location and nature of the fuel source, different kinds of fire can occur and one of them is wildfire, which is one of the major natural disasters affecting population, vegetation and wildlife around the world. They represent a self-sustaining combustion of vegetation-derived fuel spreading across a certain portion of landscape. What will the behavior and spreading formation of a fire front be, is strongly in dependence of wind direction and intensity, slope characteristics, air temperature, humidity, fuel type and density, day time and season. They cause socio-economical consequences affecting all generally involved factors. On behalf of that, the knowledge of fire and wildfires is necessary, when analyzing its spreading and behavior processes. To prevent greater damages to certain areas, wildfires can be studied through modeling, on behalf of which preventive action can be taken to minimize the potential environmental risks.

Possible method for wildfire propagation modeling is cellular automata (CA). CA is a discrete dynamical system, which models complex behavior based on certain local transition rules. It consists of a lattice of cells ($1 \leq d < \infty$; d = dimension of lattice, e.g. $d = 1$ is 1D lattice), which can be in different states ($2 \leq k$; k = number of cell states, e.g. in binary state, $k = 2$, (0, 1)). The behavior of dynamics of observed cells is based on local transition rules (φ) together with the cells neighborhood (r = radius of neighborhood), which determines the cells state in the next time step or so called generation (t = time step, e.g. $t = n$, n^{th} generation). In the simplest case the basic principle for 1D CA determines the observed cells outcome in the next generation ($t + 1$) in dependence of its neighborhood state in the previous generation (t).^{1,2} The process of a 1D CA can be described with Equation 1.

$$C_{i+1,j}(t+1) = \varphi[C_{i,j-1}(t), C_{i,j}(t), C_{i,j+1}(t)] \quad (1)$$

Complexity that CA can achieve can be seen on a simple binary principle 1D CA, $r = 1$, $k = 2$. The 3-cell unit ($2r + 1$) generates 8 combinations of neighborhood states, where each combination generates an outcome of a cell in two possible states (0, 1). Possible local transition rules that we gain from the 8 combination outcomes is 256. One of the 256 local transition rules is visualized in Figure 1.

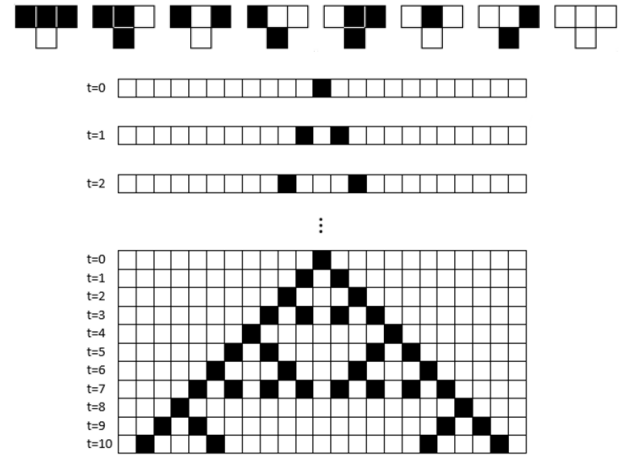


Figure 1: Local transition rules (10 generations)

Expanding the radius to 2, generates 32 neighborhood state combinations with associated 4.294,967,296 local transition rules. In a 2D CA Moore neighborhood, $r = 1$, $k = 2$, generates 512 neighborhood state combinations and 1.341×10^{154} local transition rules.

How a wildfire spread simulation looks like is visualized in Figure 2. The simulation represents a 2D CA where the fire front spreads through landscape vegetation (brown-grass, green-forest, gray-population area, blue-river) under the influence of wind from the east.

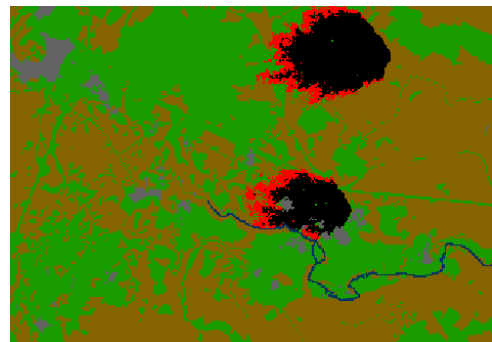


Figure 2: Wildfire spread (wind influence)

References:

1. Maeda, K-I, Sakama, C: Identifying cellular automata rules. *J. Cell. Autom.* **2007**, 2, 1-20.
2. Shiffman, D., *The Nature of Code: Simulating Natural Systems with Processing*. <http://natureofcode.com/book/chapter-7-cellular-automata/> (accessed July 7, 2017)

Hydrothermal Synthesis of Nanostructured TiO₂ Particles with High Surface Area

Lev Matoh^{1,*}, Urška Lavrenčič Štanger¹

¹ Faculty of Chemistry and Chemical Technology, University of Ljubljana, Večna pot 113, 1000 Ljubljana, Slovenia

TiO₂ is a versatile material that has been extensively researched for over a decade. It is widely used in a variety of applications and products in the energy storage/conversion and environmental purification including self-cleaning surfaces, air and water purification systems, sterilization, water splitting and photoelectrochemical conversion. Because of its chemical stability, easy synthesis and good efficiency nanostructured TiO₂ is of special interest as a photocatalyst or catalytic support.

When used as support for electro catalysts or in photovoltaics, good interparticle connectivity is crucial as structural defects that occur in the connections between particles can trap electrons due to the difference in conduction band energies. This can be somewhat mitigated by producing larger particles with morphologies that retain a high surface area. Since the particles are larger, fewer connections between them are necessary to allow electron transfer.

In this work we present a simple method to prepare nanostructured TiO₂ particles in powder form that could be of potential interest as catalytic support. The morphology and larger particle size can promote the transfer of electrons while the nanostructures that make up the particles ensure a large specific surface area necessary for catalytic reactions or the dispersion of a surface deposited catalyst.

The powders were prepared from different Titanium precursors using a hydrothermal method in a highly alkaline solution. Different morphologies can be prepared by adjusting the reaction parameters ranging from flower-like to highly compacted nanowires. The morphology of the prepared samples is stable and does not change after calcination at higher temperatures. The short reaction times, scalability and high concentrations of titanium in the reaction solution also allow for production of larger quantities of the powders.

The surface morphology of the prepared TiO₂ powders was examined using scanning electron microscopy (SEM) - Figure 1. To further characterize the samples, specific surface area for different morphologies was measured and the photocatalytic activity of the prepared powders was tested by degrading a model azo-dye pollutant under UV irradiation.

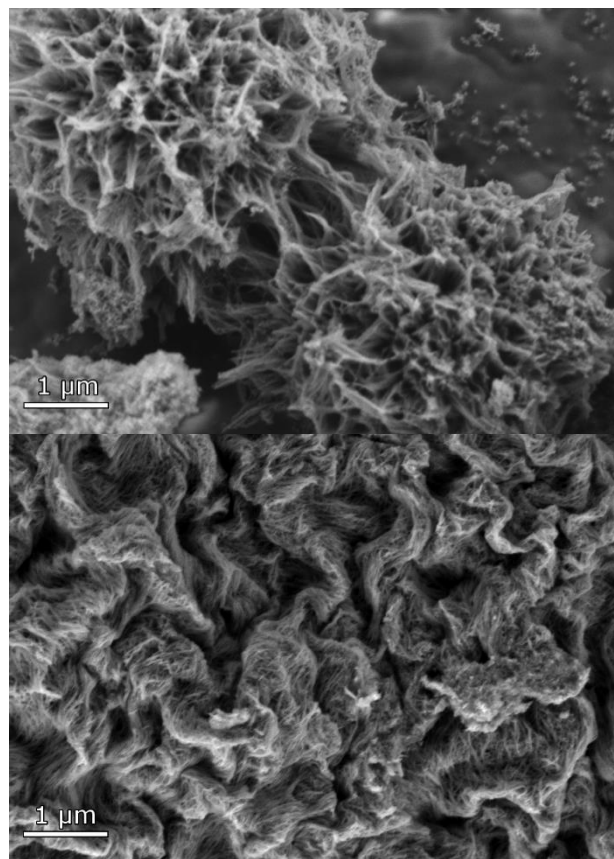


Figure 1: SEM images of the prepared TiO₂ nanostructured flower-like particles (top) and highly compacted nanowires (bottom).

References:

1. L. Min, L. Wei-ming, Z. Lei, Z. Chun-lan, L. Hai-ling, W. Wen-jing: Fabrication and photocatalytic properties of flower-like TiO₂ nanostructures. *Trans. Nonferrous Met. Soc. China*, **2010**, 20, 2299–2302.
2. M. Malekshahi Byranvanda, A. Nemati Kharata, L. Fatholahib, Z. Malekshahi Beiranvande: A Review on Synthesis of Nano-TiO₂ via Different Methods. *Journal of nanostructures*, **2013**, 3, 1-9.

Phytotoxicity of Guaiacol and its Nitrated Derivatives

Maksimiljan Adamek^{1,2}, Marta Debeljak¹, Katarina Vogel-Mikuš,^{3,4} Marija Bešter-Rogač², Ana Kroflič*,¹

¹ Department of Analytical Chemistry, National Institute of Chemistry, Hajdrihova 19, SI-1000 Ljubljana, Slovenia

² Faculty of Chemistry and Chemical Technology, University of Ljubljana, Večna pot 113, SI-1000 Ljubljana, Slovenia

³ Biotechnical Faculty, University of Ljubljana, Jamnikarjeva ulica 101, SI-1000 Ljubljana, Slovenia

⁴ Jožef Stefan Institute, Jamova cesta 39, SI-1000 Ljubljana, Slovenia

Nitroaromatic compounds are known for their detrimental effects on the environment¹. However, little is known about exact toxicity mechanisms of these types of compounds in plants. This also applies to nitrated derivatives of guaiacol (GUA). GUA is present in wood smoke due to pyrolysis of lignin, which is a natural polymer notably found in the secondary plant cell wall. Due to toxic effects of nitrated derivatives of guaiacol (NG), which are mostly secondarily formed in the atmosphere from GUA, biomass burning could be an important source of phytotoxic pollutants.

Phytotoxicity of GUA and its nitrated derivatives (4-nitroguaiacol (4NG), 5-nitroguaiacol (5NG), 6-nitroguaiacol (6NG), and dinitroguaiacol (DNG)) was investigated in maize and sunflower plants. Plants were grown in Hoagland nutrient solutions containing one of the investigated compounds. Compound uptake from nutrient solutions was tracked by high-performance liquid chromatography (HPLC). After the treatment, roots and green plant parts were freeze dried and stored. Plant extracts were analysed by liquid chromatography tandem mass spectrometry (LC-MS) and results will be used to discuss possible mechanisms of phytotoxicity.

Visual examination revealed that all compounds inhibited plant growth when compared to the control plants, with DNG inhibiting growth the most. Analysis of nutrient solutions showed that GUA uptake was the most rapid, followed by the uptake of mono-NG and DNG. Analysis of plant extracts revealed that the amount of aromatic compounds was larger in root samples than in green parts. Amounts of GUA and mono-NG were larger in sunflower extracts when compared to maize extracts. NG compounds were not detected in the above-ground plant parts of maize and we conclude that they are only adsorbed on the roots or retained in root cell walls.

GUA and NG exhibit phytotoxic effects. Correlation between the number of nitro groups and phytotoxicity was found. However, the rate of compound uptake and the number of nitro groups are anticorrelated (Figure 1). Similar data were obtained in biodegradation studies of nitroaromatic compounds¹.

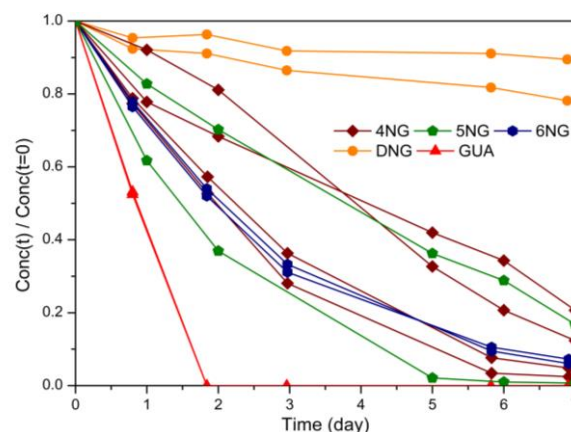


Figure 1: Decrease of concentration of investigated compounds in nutrient solutions during the treatment.

We hypothesize that plants use GUA and NG in lignin biosynthesis, due to structural similarities between these compounds and lignin monomers. The presence of nitro groups and the absence of a hydroxypropene side chain allow formation of fewer bonds between lignin monomers, which results in cell wall loosening. This could trigger a cell wall damage response, which can inhibit plant growth². However, we cannot exclude the possibility of phytotoxicity resulting from oxidative stress or that phytotoxic compounds originate from biotransformation of GUA and NG. Further research is needed to fully understand the mechanisms of phytotoxicity of nitroaromatic compounds.

This work was supported by the Slovenian Research Agency (Contract No. P1-0034).

References:

1. Spain, J. C. (Ed.); Hughes, J. B. (Ed.); Knackmuss, H. J. (Ed.), *Biodegradation of Nitroaromatic Compounds and Explosives*. CRC Press LLC, **2000**.
2. Raggi, S.; *et al.*, The Arabidopsis Class III Peroxidase AtPRX71 Negatively Regulates Growth under Physiological Conditions and in Response to Cell Wall Damage. *Plant Physiology*, **2015**, 169, 2513–2525.

G-quadruplex Structure of DNA Oligonucleotides with GC Ends

Daša Pavc^{1,2}, Baifan Wang¹, Primož Šket^{*,1,3}, Janez Plavec^{*,1,2,3}

¹ Slovenian NMR Center, National Institute of Chemistry, Hajdrihova 19, SI-1000 Ljubljana, Slovenia

² Faculty of Chemistry and Chemical Technology, University of Ljubljana, Večna pot 113, SI-1000 Ljubljana, Slovenia

³ EN-FIST Center of Excellence, Trg OF 13, SI-1000 Ljubljana, Slovenia

G-quadruplexes are non-canonical secondary structures formed by G-rich DNA sequences. Main building blocks of G-quadruplexes are stacked G-quartets, which are formed by four guanine residues in planar arrangement connected with Hoogsteen type of hydrogen bonds. Monovalent cations which are localized between stacked G-quartets reduce the repulsion of carbonyl oxygen atoms and promote stacking of G-quartets¹.

In the present study we structurally characterized two G-rich DNA oligonucleotides S3 d(GCG₂AG₄AG₂) and S4 d(GCG₂AG₄AG₂CG) which both have the 5'-GC end. Such short G-rich oligonucleotides with GC ends are expected to form long G-wires on the basis of inter-quadruplex GCGC linkages². Both sequences also contain three G-tracts of different lengths and two adenine residues separating the G-tracts, with oligonucleotide S4 having additional CG at 3'- end. Oligonucleotides S3 and S4 fold into single,

well-defined G-quadruplex structure in the presence of sodium cations and sodium phosphate buffer (pH 6.8) at 25°C. Main tool in our study was NMR spectroscopy with CD and UV spectroscopy as complementary techniques. We unambiguously assigned imino and aromatic proton resonances and with that we were able to determine the folding topologies of G-quadruplexes formed by both oligonucleotides with analysis of different regions of 2D NOESY spectra Figure 1. The high resolution structures of S3 and S4 were calculated by simulated annealing protocol based on NOE-derived distance restraints. Based on intensity of intra-nucleotide H8-H1' 2D NOESY cross-peaks glycosidic bond torsion angles were restrained to the *syn* χ 30° - 90° and *anti*-region χ 200° - 80°. From 2D DQF-COSY spectra we obtained restraints for pseudorotation phase angles of sugar rings, corresponding to the North and South-type conformation.

We discovered that G-quadruplex structures of S3 and S4 are symmetric dimers comprised of two G-quartets, A(GGGG)A hexad, GCGC-quartet and N1-carbonyl G-G base pair. G-quadruplex of S4 has two GC overhangs at 3'- end, which are stacked in G-quartet formed by G9 and G12 residues. GCGC-quartet and A(GGGG)A hexad are rare structural features that

were to the best of our knowledge for the first time observed in the same G-quadruplex structure. Another interesting structural feature is that the G1 residue at 5'- end is located in the middle of the G-quadruplex structure. All residues are in the *anti* conformation with respect to glycosidic bond except G1 residue which is in the *syn* conformation. Sugar rings of most residues correspond to the South-type conformation except the sugar ring of the A10 residue, which corresponds to the North-type conformation.

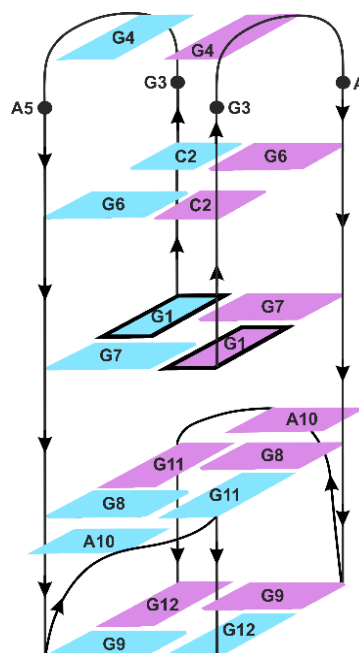


Figure 1: Folding topology of dimeric G-quadruplex formed by oligonucleotide S3.

References:

1. Šket, P.; Plavec, J., Diversity of DNA and RNA G-quadruplex structures. In *Biological Relevance & Therapeutic Applications of DNA- & RNA-Quadruplexes*, Monchaud, D., Ed. Future Science Ltd: London, UK, **2015**; pp 22-36.
2. Ilc, T.; Šket, P.; Plavec, J.; Webba da Silva, M.; Drevenšek-Olenik, I.; Spindler, L., Formation of G-Wires: The Role of G:C-Base Pairing and G-Quartet Stacking. *J. Phys. Chem. C* **2013**, *117* (44), 23208-23215.

Impact of the Vent-Shape on the Efficiency of the Natural Smoke Ventilation and Heat Transfer from a Small Compartment

Marjan Lukežič¹, Simon Schnabl^{1,*}

¹ Faculty of Chemistry and Chemical Technology, University of Ljubljana, Večna pot 113, 1000 Ljubljana, Slovenia

A natural smoke and heat transfer ventilation is simulated and analysed through various ceiling vent-shapes (Figure 1). Horizontal vent-shapes are positioned at the centre of the ceiling. Fire source is placed in the centre and corner of the floor. The area of vent-shapes is 1 m². Fire Dynamics Simulator (FDS) and Pyrosim are used in the analysis.

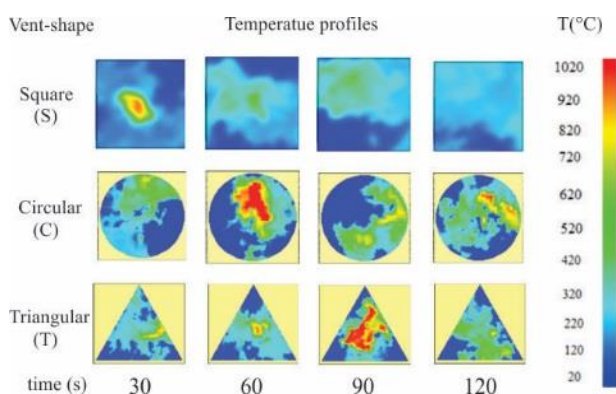
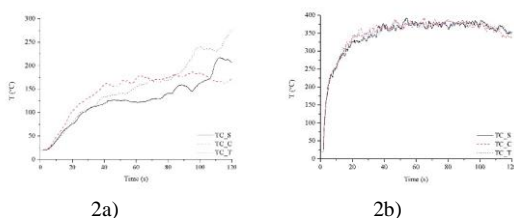


Figure 1: The temperature profiles for different horizontal vent shapes; fire source is placed in the centre

Figure 1 showed the impact of different vent shapes on temperature profiles distribution. Different temperature profiles were compared with each other. It is impossible concluded, which vent shape is the best in time interval between 0 s and 120 s.

Figures 3a and 3b showed temperature response vs. time for all three vent shapes.



Figures 2a and 2b: The average temperatures in the layer of thermocouples

Figure 2a helps us understand that square vent had the lowest averaged temperatures from the start of the simulation to 110 s. The time interval between 110 s and 120 s indicate that, circular vent was more favourable than other two vents.

Since the beginning of the simulation to 35 s, triangular vent was more effective than a square vent. Above 90 s and further triangular vent was the least favourable. Figure 2b showed the corner case scenario. If fire source is placed in the corner square, circular and triangular vent shape had no influence on efficiently ventilation.

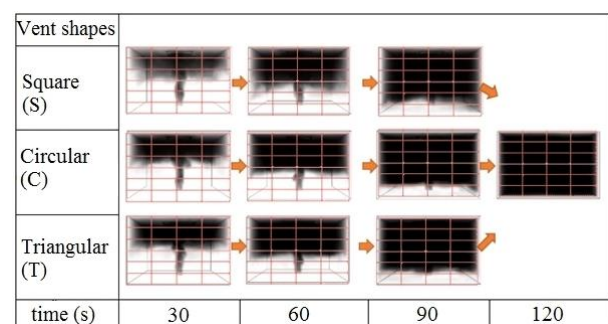


Figure 3: The smoke layer generation for different horizontal vent shapes (side view)

Figure 3 shows the process of formation of a layer of smoke. The time delay between each stage is 30 seconds. The smoke layer is shown from the side view. Fig. 3 showed position the formation of a smoke layer up to 60 s; probably the best were square and circular vent shape.

The layout of the initial and boundary conditions allowed us to focus only on type of vent shape. The shape of the opening had a direct impact on the efficiency of the natural smoke ventilation and heat transfer. However, we cannot generally emphasize one of the vent shapes (square, circular or triangular) as the most effective throughout all time interval.

Reference:

1. R.M. Doheim, Y.G. Yohanis, A. Nadjai, H. Elkadi, The impact of atrium shape on natural smoke ventilation, *Fire Safety Journal* **2014**, 63, 9-16.

Removal of Artificial Sweeteners from Aquatic Solutions by Ozonation

Barbara Debevec*, Martin Lubej, Gabriela Kalčíkova, Andreja Žgajnar Gotvajn

Faculty of Chemistry and Chemical Technology, University of Ljubljana, Večna pot 113, SI-1000 Ljubljana, Slovenia

Artificial sweeteners are synthetic food additives with intense sweet taste much sweeter than natural sugar. Because of their advantages, they are massively produced for food industry and also for other products (e.g. for dental care)¹. But for their high stability – the ability to stay mostly unchanged while travelling through human bodies, wastewater treatment plants and environment – they are becoming class of pollutants that needs to be researched for their impact on environment.

One of problematic artificial sweeteners is saccharin (SAC). We have evaluated the ability of removing SAC from aquatic solutions with one of the advanced oxidation processes (AOPs), ozonation.

For this purpose we performed experiments under different conditions: the concentration of ozone in gas phase (4.86 g h^{-1} and 3 g h^{-1}), concentration of hydrogen peroxide (0.2 ; 1 ; 2 ; 10 g L^{-1}) and time of experiment (2 , 3 , 8 hours). The initial concentration of SAC in aquatic solutions remained the same for all experiments and the degradation of saccharin in aquatic samples was monitored during ozonation with measuring of total organic carbon (TOC).

First, we focused on ozonation of SAC without H_2O_2 and performing two experiments for two hours, changing only one parameter – dose of O_3 (calibrating concentration of O_3 in gas phase and gas flow). At dose 4.86 g h^{-1} of O_3 there was no noticeable trend in the decline of concentration of SAC (Figure 1). At dose 3 g h^{-1} the degradation was partially successful (removal reached 60%). The experiment was run under maximal concentration of O_3 in gas phase and minimal flow that can be achieved with generator of ozone that we used.

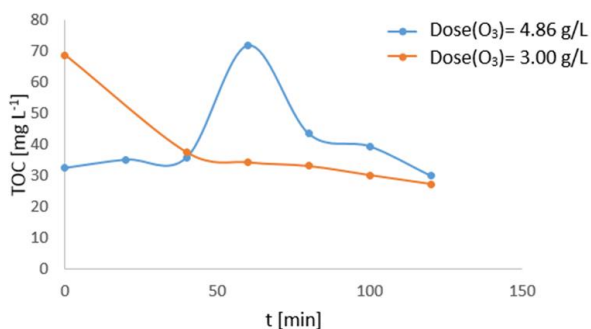


Figure 1: Changing of concentration of SAC expressed as TOC vs. time for experiments without hydrogen peroxide

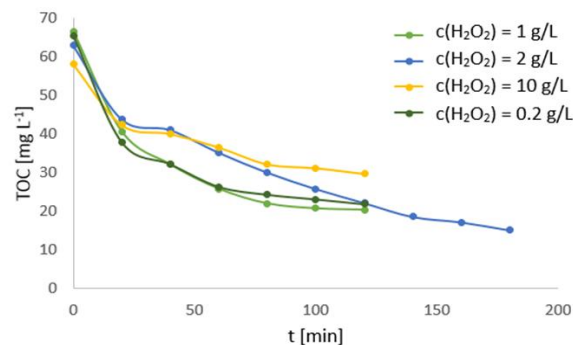


Figure 2: Changing of concentration of SAC expressed as TOC vs. time for experiments with hydrogen peroxide

To increase the oxidation efficiency we maintained the concentration of O_3 in gas phase at the highest level and added H_2O_2 at different concentrations (0.2 ; 1 ; 2 ; 10 g L^{-1}) (Figure 2). Addition of H_2O_2 accelerated and improved degradation of SAC. But at the same time this effectiveness was not proportional with the amount of H_2O_2 – we concluded that higher concentration does not necessarily mean more effective decomposition. The highest degradation in two-hour experiment was achieved at concentration 1 g L^{-1} of H_2O_2 : 69% . The experiment with 2 g L^{-1} of H_2O_2 was monitored longer, for three hours. On the basis of collected results we determined the order of reaction ($n = 2$) and the rate constant ($k = 0.0002527 \text{ L s}^{-1} \text{ mg}^{-1}$). In the last two experiments (10 g L^{-1} and 0.2 g L^{-1} of H_2O_2) after two-hour sampling ozonation was extended for additional six hours until equilibrium concentration of saccharin was attained. Degradation in both experiments reached 81% with a minimal difference.

Despite the harsh experimental conditions we did not manage to remove the SAC from water solution completely. But with this research we explored the possibilities of using ozonation for degradation SAC in aquatic solutions and narrowed the research area and set of suitable AOPs for this case.

References:

1. R. L. Myers: The 100 Most Important Chemical Compounds: a Reference Guide. Westport: Greenwood Publishing Group **2007**, 33-35, 241-243.

Comparison of Oxidation Techniques for Removal of Antibiotic Tiamulin

Igor Bosevski^{1,*}, Damjan Koder¹, Nastja Smolnikar¹, Polona Starašinič¹, Gabriela Kalčíkova¹
Andreja Žgajnar Gotvajn¹

¹ Faculty of Chemistry and Chemical Technology, University of Ljubljana, Večna pot 113, 1000 Ljubljana, Slovenia

Use of antibiotics in modern society is an important source of environmental contamination, especially in case of environmentally persistent molecules. Even low concentrations of antibiotics in the environment promotes the selection of antibiotic resistance genes and antibiotic resistant bacteria^{1,2}. In scope of our research we were comparing oxidative techniques; semi-batch and continuous ozonation, as well as Fenton oxidation in terms of their ability to mineralize veterinary antibiotic (tiamulin) in aquatic medium. Tiamulin was selected as a model substance with high environmental persistence.

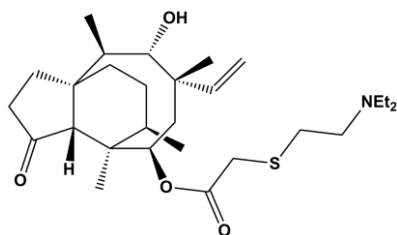


Figure 1. The structural formula of tiamulin³.

In the experiments ozone generator by a Xylem Water Solutions GmbH Herford, type OCS Modular 8 HC was used. Operating pressure 0.5 bar, gas flow 0.08 m³ h⁻¹. Nominal concentration of ozone in the gas was 100 g m⁻³. In a semi-batch mode, ozone was bubbled through a glass laboratory reactor (250 mL), containing 200 mL of tiamulin solution (Figure 2). In a continuous mode, ozone was bubbled through a glass column (3500 mL) (Figure 2). Liquid was circulated in a counter-current with respect to ozone bubble path, in a closed loop including a reservoir. Fenton oxidation was done using ordinary laboratory glassware, with FeSO₄ as a catalyst and hydrogen peroxide as oxidation reagent.

Degradation rate of tiamulin was monitored indirectly by measurement of COD, according to ISO 6060, 1989 and TOC according to ISO 8245, 1999. As an additional insight into the degree of oxidation of antibiotic, also an average oxidation state of carbon in the solution was calculated. The concentration of ozone in the solution was determined by using colorimetric method 118755, Merck Ozone Test.

Results of our study indicated that ozonation is a feasible technology for removal of tiamulin. When

using ozonation in a semi-batch mode, already small doses of ozone (in a molar ratio ozone:COD = 0.1) reduce TOC and COD to 15 and 25 % respectively.

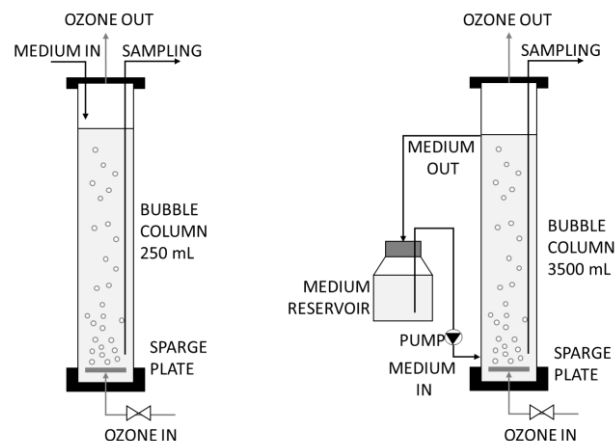


Figure 2. Set-up for semi-batch and continuous ozonation.

In terms of average oxidation state of carbon, 18 % of complete mineralization is achieved under same conditions. Comparable reductions of TOC and COD (12 and 23 % respectively) in a continuous processing mode were achieved with an order of magnitude larger doses of ozone (in a molar ratio ozone/COD between 1.1 and 2.2). Fenton reagent at molar ratio peroxide/COD 0.8 provides 22 % reduction on TOC and 30 % on COD, while at a molar ratio peroxide/COD of 4, the reduction to both TOC and COD is about 60 %.

References:

1. Boxall, A. B. A.; Kolpin, D. W.; Halling-Sorensen, B.; Tolls, J., Are veterinary medicines causing environmental risks? *Environmental science & technology*. **2003**, 37(15), 286A-294A
2. John Jensen, P. H., Effects of the antibacterial agents tiamulin, olanquinox and on the soil invertebrate species *Folsomia fimetaria* (Collembola) and *Enchytraeus crypticus* (Enchytraeidae). *Chemosphere*. **2003**, 50(3), 437–443.
3. Fazakerley, N. J.; Procter, D. J., Synthesis and synthetic chemistry of pleuromutilin. *Tetrahedron*. **2014**, 70(39), 6911-6930.

In vitro Assessment of Potential Papillary Urothelial Neoplasm Treatment with Functionalized Polyethyleneimine Coated Magnetic Nanoparticles

Klemen Strojan¹, Jasna Lojk^{1, 2}, Vladimir B. Bregar¹, Mateja Erdani Kreft², Jurij Svete³, Peter Veranič^{*, 2}, Mojca Pavlin^{*, 1, 4}

¹ Group for Nano and Biotechnological Applications, Faculty of Electrical Engineering, University of Ljubljana, Tržaška cesta 25, SI-1000 Ljubljana, Slovenia

² Institute of Cell Biology, Faculty of Medicine, University of Ljubljana, Vrazov trg 2, SI-1000 Ljubljana, Slovenia

³ Faculty of Chemistry and Chemical Technology, University of Ljubljana, Večna pot 113, SI-1000 Ljubljana, Slovenia

⁴ Institute of Biophysics, Faculty of Medicine, University of Ljubljana, Vrazov trg 2, SI-1000 Ljubljana, Slovenia

Papillary urothelial neoplasia is a group of non-invasive urinary bladder cancers that have a high recurrence rate and can progress to an invasive form of bladder cancer. This treatment typically involves transurethral resection followed by intravesical therapy, where chemotherapeutic agents are administered directly into the bladder. Despite obvious advantage of local delivery, intravesical therapy has its limitations and it is an important area for further development, in which nanoparticles (NPs) proved to be a promising strategy for improvement¹.

Normal porcine urothelial cells (NPU) have been shown to have a much lower rate of endocytosis than papillary urothelial neoplasm cells (RT4), which could be used as a mechanism for selective delivery of toxic compounds, such as polyethyleneimine coated nanoparticles (PEI NPs). In order to reduce their non-

selective membrane toxicity, we had successfully functionalized PEI NPs with L-glutathione reduced (PEI_GSH NPs)² or bovine serum albumin (PEI_BSA NPs), as confirmed with Fourier Transform Infrared Spectroscopy (FTIR), Dynamic Light Scattering (DLS) and Zeta potential measurements³.

However, 24h after exposure, PEI_BSA NPs had similar effect on viability of both RT4 and NPU cells. PEI_BSA NPs showed some selective toxicity towards papillary urothelial neoplasm cells compared to normal cells after 3h, but this was not confirmed after 24h. In order to achieve selective toxicity, further optimization of the NP formulation and exposure protocols are necessary¹.

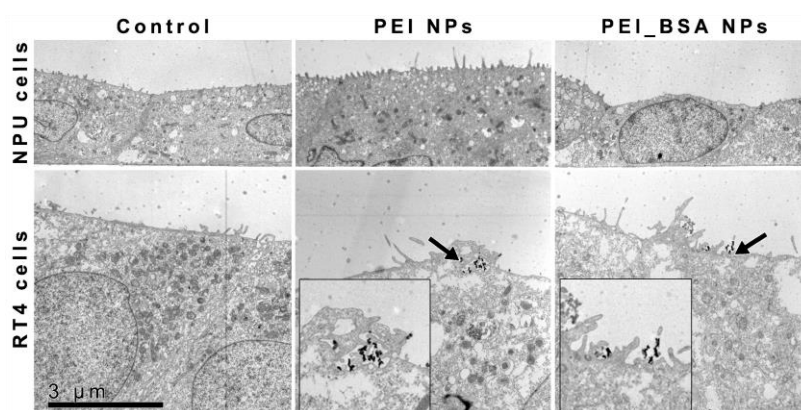


Figure 1: TEM micrographs of NPU and RT4 cells without NPs (control), with 50 $\mu\text{g/ml}$ PEI NPs or 50 $\mu\text{g/ml}$ PEI_BSA NPs after 3 h incubation. Arrows denote NPs. Viability assay showed that BSA coating reduced NPs toxicity immediately after exposure and that PEI_BSA NPs were more toxic to RT4 cells compared to NPU cells at 50 $\mu\text{g/ml}$ NPs concentration.

References:

1. Neusch, L.; Wambacher, M.; Wirth, E.-M.; Spijker, S.; Kählig, H.; Wirth M.; Gabor, F.; *Int. J. Pharm.* **2013**, *450*, 163–176.
2. Strojan, K.; Lojk, J.; Bregar, V.B.; Veranič, P.; Pavlin, M. *Toxicol. In Vitro*, **2017**, *41*, 12–20.
3. Strojan, K.; Lojk, J.; Bregar, V.B.; Erdani Kreft, M.; Svete, J.; Veranič, P.; Pavlin, M. *Acta Chim. Slov.* **2017**.

Microwave Assisted C–H Bond Functionalization of Phenylpyrimidines in Water

Miha Drev*, Uroš Grošelj, Bogdan Štefane, Jurij Svete, Franc Požgan

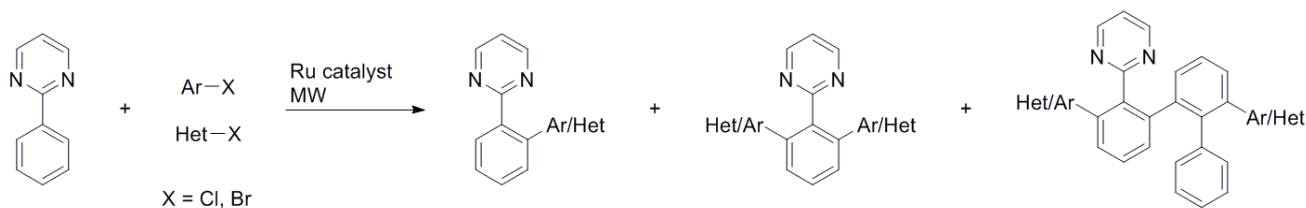
Faculty of Chemistry and Chemical Technology, University of Ljubljana, Večna pot 113, SI-1000 Ljubljana, Slovenia

The biaryl and *N*-heteroaromatic moieties are important synthetic motifs for a wide range of application in pharmaceutical and natural products,¹ agrochemicals and functional materials,² and ligands for selective catalysis.³ These structures can be obtained by direct C–H bond activation and subsequent functionalization of easily accessible starting materials in the presence of transition metals as catalysts. This method contributes to considerably shortening synthetic sequence compared to traditional metal-catalyzed cross-coupling reactions. In this way, the reactions are more attractive from the economically and ecologically point of view.

In our previous work we have shown that a ruthenium-carboxylate is an efficient catalytic system for direct arylation of 4-phenylpyrimidine in 1,4-dioxane at 150 °C.⁴ In contrast with this methodology,

herein we report a greener and faster method for preparation of arylated or heteroarylated phenylpyrimidines.

The reaction performed in water as preference solvent in the presence of an appropriate ruthenium catalyst shows the superior transformation unlike other organic solvents such as NMP, ethanol, toluene, and 1,4-dioxane. Due to the high temperatures and long reaction times which are needed under conventional heating for a successful C–H bond functionalization, the reaction was performed under microwave irradiation. Thus the reaction time for complete conversion could be dramatically shortened.



Scheme 1: Synthesis of mono- and di(hetero)arylated phenylpyrimidines.

References:

1. Nicolaou, K. C.; Bulger, P. G.; Sarlah D., Palladium-Catalyzed Cross-Coupling Reactions in Total Synthesis. *Angew. Chem. Int. Ed.*, **2005**, *44*, 4442-4489.
2. Hassan, J.; Sévignon, M.; Gozzi, C.; Schulz, E.; Lemaire, M., Aryl–Aryl Bond Formation One Century after the Discovery of the Ullmann Reaction. *Chem. Rev.*, **2002**, *102*, 1359-1470.
3. Schuster O.; Yang, L.; Raubenheimer, H. G.; Albrecht, M., Beyond Conventional *N*-Heterocyclic Carbenes: Abnormal, Remote, and Other Classes of NHC Ligands with Reduced Heteroatom Stabilization. *Chem. Rev.*, **2009**, *109*, 3445-3478.
4. Štefane, B.; Fabris, J.; Požgan, F., C–H Bond Functionalization of Arylpyrimidines Catalyzed by an in situ Generated Ruthenium(II) Carboxylate System and the Construction of Tris(heteroaryl)-Substituted Benzenes. *Eur. J. Org. Chem.*, **2011**, *19*, 3474-3481.

Electric Conductivity of Gel Electrolytes

Ana Oberlintner,¹ Tjaša Rijavec,¹ Gregor Marolt,¹ Saša Skale,² Janez Cerar*,¹

¹ Faculty of Chemistry and Chemical Technology, University of Ljubljana, Večna pot 113, SI-1000 Ljubljana, Slovenia

² SKALA, Ekološko-tehnično svetovanje, sanacije, površinske zaštite kovinskih in betonskih površin Saša Skale s.p., Lušečka vas 30, Lušečka vas, SI-2319 Poljčane, Slovenia

Aqueous gel electrolytes surprisingly show enhanced conductivity as compared to their corresponding solutions. Therefore, in order to improve performance of batteries, dye-sensitized solar cells, and electrochromic devices gel electrolytes are intensively studied¹. On the contrary, the number of basic studies of electric conductivity of gel electrolytes is very limited². Upon reviewing the literature on the topic, a variety of explanations for enhanced conductivity in gels can be found. One of these is the phenomenon of the hopping mechanism, which postulates that mobility of iodide ions can remarkably increase in gels when compared to mobility of other anions.

We conducted a study, where electric conductivity of different aqueous electrolyte solutions and their corresponding 1 wt% agar gels were measured. Four different 0.1 M solutions were prepared: sodium iodide (NaI), lithium chloride (LiCl), sodium chloride (NaCl) and potassium iodide (KI). The prepared solutions were gelated with agar. It was confirmed that in the whole temperature range (15 °C – 55 °C) studied gels are electrically more conductive than corresponding solutions and that this increase in conductivity is far

larger than the conductivity of pure gel (Figure 1). While the difference between the aqueous solution and its gel remained observable, we detected no specific enhancement of conductivity of gelated iodide solutions. These experiments were further expanded to “gel capacitor” study to confirm our previous observations.

In addition, the solutions and their gels were analysed with electrochemical impedance spectroscopy. The gathered spectra are complex and cannot be undoubtedly interpreted. Further studies should be conducted.

References:

1. Stojadinović, J.; Dushina, A.; Trócoli, R.; La Mantia, F. Electrochemical Characterization of Gel Electrolytes for Aqueous Lithium-Ion Batteries. *Chempluschem* **2014**, 79, 1507–1511.
2. Bielejewski, M.; Puszkarska, A.; Tritt-Goc, J. Thermal Properties, Conductivity, and Spin-Lattice Relaxation of Gel Electrolyte Based on Low Molecular Weight Gelator and Solution of High Temperature Ionic Liquid. *Electrochim. Acta* **2015**, 165, 122–129.

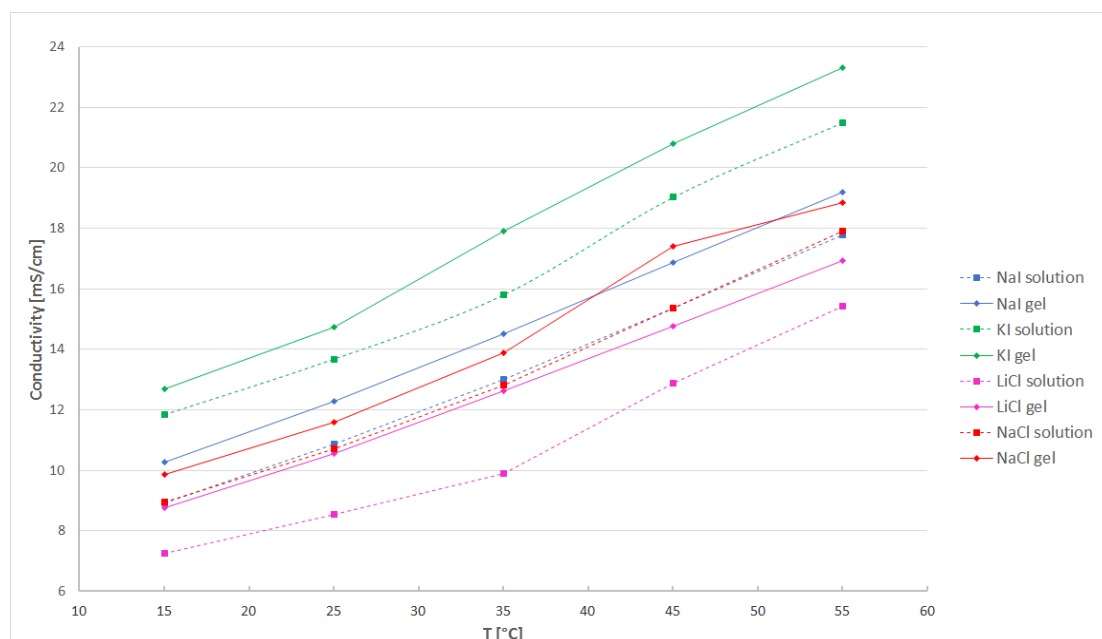


Figure 1: Conductivities of 0.1 M aqueous solutions and their corresponding 1% agar gels as a function of temperature.

Theoretical Study of 'Graphene-Like' Monomer Structures

Matjaz Dlouhy¹, Tomaž Urbic^{1,*}

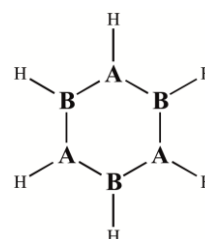
¹ Faculty of Chemistry and Chemical Technology, University of Ljubljana, Večna pot 113, SI-1000 Ljubljana, Slovenia, tomaz.urbic@fkkt.uni-lj.si

Graphene is a two-dimensional (2D) atomic crystal which consists of carbon atoms that form an ordered honeycomb lattice. It is a rudimental building block for a range of carbon materials such as three-dimensional (3D) graphite, one-dimensional (1D) carbon nanotubes and zero-dimensional (0D) fullerene. Due to its many unique properties an intensive research of graphene has begun in 2004 after a relatively simple micromechanical exfoliation technique proposed by the Nobel prize laureate K. S. Novoselov and A. K. Geim.¹

Graphene's most interesting feature is its crystal structure. With 0.4 to 1.7 nm in thickness, this material is the thinnest crystal known to date.² Graphene is extremely electrically and thermally conductive, very elastic and impermeable to any molecules. It is also the strongest material ever measured and has a current density that is a million times greater than in typical metals. Because of these and many other enviable properties such as large surface area of about 2675 m² g⁻¹ and 2.3 % absorption in the white light spectrum, graphene, since its discovery, represents a golden mine in terms of developing new applications or refining current ones in different fields of science and technology.³ But graphene is not 'the end of the road' in academic circles. Since 2011 many new studies have been conducted and reports published about the existence of so called 'graphene-like materials' which are being developed intensively among physical chemists and material scientists. The term 'graphene-like materials' is often used in the literature as a common name to two groups of quasi-2D systems with significantly different composition and properties.⁴

Previous theoretical predictions have shown promising silicon- or germanium-based counterparts of graphene and exhibit similar electronic characteristics.⁴ In our study we theoretically examined hexagonal structures which could represent 'graphene-like' hexagonal network. In some cases planar structures similar to graphene were found, some exhibiting a structure similar to cyclohexane chair conformation or other known forms (twist boat form, boat form, half-chair form). Considering the appropriate stoichiometry we constructed A₃B₃H₆ cyclic rings shown in Scheme 1 using elements of the alkaline earth metals (A¹) and chalcogens (B²) (Be₃O₃H₆, Mg₃O₃H₆, etc.) and elements from the third (A²) and

fifth (B²) group of elements of the periodic table. Elements were chosen according to the Table 1 to form a stable A₃B₃H₆ molecule.



Scheme 1: Graphical representation of input molecule, all molecules consist of 12 elements and are positioned accordingly to *D*_{3h} point group symmetry.

Table 1: Atoms used to form a stable A₃B₃H₆ molecule.

A ¹	A ²	B ²	B ¹
Be	B	N	O
Mg	Al	P	S
Ca	Ga	As	Se

Due to the importance of C↔C bonds in organic and organometallic chemistry we also carried out calculations on heavier tetrels with equivalent electron atoms such as silicon, germanium and tin in form of stable X₆H₆ molecule. Considering theoretical study, we compared results of six different calculation methods and two different basis sets using the Gaussian 09 program suite.⁵

References:

1. Novoselov, K. S., Geim, A. K., Morozov, S. V., Zhang, Y., Dubonos, S. V., Grigorieva, I. V. and Firsov A. A., Electric Field Effect in Atomically Thin Carbon Films. *Science* **2004**, *306*, 666-669.
2. Shearer, C. J., Slattery, A. D., Stapleton, J. G., Shapter, J. G., and Gibson, C. T., Accurate Thickness Measurement of Graphene. *Nanotechnology* **2016**, *27*, 125704.
3. Ivanovskii, A. L., Graphene-based and Graphene-like materials. *Russian Chemical Reviews* **2012**, *81*, 571-605.
4. Mingsheng, X., Liang, T., Shi, M. and Chen, H., Graphene-Like Two-Dimensional Materials. *Chemical Reviews* **2013**, *113*, 3766-3798.
5. Frisch, M. J., Trucks, G. W., Schlegel, H. B. et al., Gaussian 09, Revision A.1 2009, *Gaussian Inc.* Wallingford, CT.

Impact of the Electrolytes in the Li-S Battery System on the Process of Electrocrystallization of Lithium Sulfide

Tina Paljk¹, Sara Drvarič Talian², Miran Gaberšček^{1,2}, Robert Dominko^{*,2}

¹ Faculty of Chemistry and Chemical Technology, University of Ljubljana, Večna pot 113, SI-1000 Ljubljana, Slovenia

² National Institute of Chemistry, Hajdrihova 19, SI-1000 Ljubljana, Slovenia

Lithium-sulfur batteries represent a perspective technology for low-cost and high-density electrochemical energy storage. Due to the low mass of sulfur and the exchange of two electrons, this system has a higher energy density and a specific capacity of more widespread lithium-ion batteries.

A typical Li-S battery cell consists of a lithium anode and a sulfur-containing carbon cathode, with a liquid electrolyte. Li-S batteries are based on the following reaction:



The typical Li-S battery discharge curve consists of two plateaus. During the high voltage plateau, the molecules of sulfur S_8 are first reduced to long chain polysulfides, Li_2S_6 , which dissolve into the electrolyte and are subsequently reduced to lower order polysulfides Li_2S_4 and Li_2S_2 ^{1,2}. The further reduction to Li_2S takes place at a lower voltage plateau. This step is the most important because the larger part of the theoretical capacity comes from the reduction of Li_2S_4 to Li_2S ¹.

As stated, the last level in discharging the battery is the formation of lithium sulfide. This compound is insoluble in the electrolyte and is precipitated as a non-conducting precipitate on the electrode surface^{1,2}. Once solid Li_2S precipitates from the electrolyte and begins to form on the sulfur cathode, it grows and covers the conductive surface. The deposit forms an insulating film over the sulfur-carbon cathode, potentially stopping any ionic and electronic access to the active material^{1,2}.

Understanding the kinetics and morphology of electrodeposited Li_2S is paramount to goal oriented development of better performance and high energy Li-S batteries.

With the right analysis of the experimental potentiostatic discharge curves and the observation of the discharge product^{1,3} we were able to investigate the mechanism of electrocrystallization of lithium sulfide in different electrolytes. The experiments were done by applying a constant potential to a partially discharged

battery cell, through which, voltage and current curves as shown in Figure 1 were obtained. Different cell setups, electrolytes and potential settings were employed.

The decline in current value during the initial stages of the potentiostatic part of the experiment is due to the remaining polysulfides reduction reaction. The peak shape in the discharge current shown corresponds to nucleation and growth of Li_2S . This peak is subsequently isolated from the gathered data and fitted with equations for different nucleation and crystal growth mechanisms, through which knowledge about morphology and electrocrystallization of Li_2S is acquired.

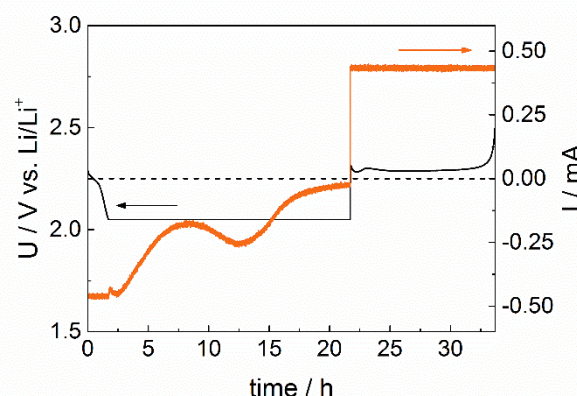


Figure 1: Voltage (black) and current (orange) profile during an experiment for determination of electrocrystallization parameters for Li_2S in Li-S batteries.

References:

1. Fan, F.Y.; Carter, W.C.; Yet-Ming Chiang, Mechanism and Kinetics of Li_2S Precipitation in Lithium-Sulfur Batteries. *Advanced Materials*, **2015**, 27, 5093–5247.
2. Ren, Y.X.; Zhao, T.S.; Liu, M.; Tan, P.; Zeng, Y.K., Modeling of lithium-sulfur batteries incorporating the effect of Li_2S precipitation. *Journal of Power Sources*, **2016**, 336, 115–125.
3. Fan, F.Y.; Yet-Ming Chiang, Electrodeposition Kinetics in Li-S Batteries: Effects of Low Electrolyte/Sulfur Ratios and Deposition Surface Composition. *J. Electrochem. Soc.*, **2017**, 146, A917–A922.

Non-thermal Plasma Assisted Removal of Proteins from Shrimp Shell Waste Material

Milka Borić^{1,2,*}, Harinarayanan Puliyalil², Uroš Novak², Blaž Likozar²

¹ Faculty of Technology and Metallurgy, Karnegijeva 4, 11000 Belgrade, Serbia

² National Institute of Chemistry, Department of Catalysis and Chemical Reaction engineering, Hajdrihova 19, SI-1000 Ljubljana, Slovenia

Utilization of natural resources and other waste materials is essential for promoting material efficiency¹. Crustacean shells has been recycled and utilized as a source of chitin, the second abundant natural polymer. Chitin and its derivative chitosan have been found to be very useful materials for many purposes in food industry or biomedical applications².

The most common method for chitin isolation from crustacean shells involves demineralization and deproteinization². In order to reduce negative environmental impact, our research provided chitin isolation from shrimp shell waste, by excluding deproteinization step by alkali treatment. The surface protein removal step using various alkalis takes at least a few hours.

Plasma is a surface modification technique that enables the removal of the superficial layer from organic or inorganic substrates as presented in numerous examples³. Herein, we have explored non-thermal plasma processing for the efficient removal of the surface protein that is wrapped around the chitin fibers. The process has been optimized in an atmospheric pressure dielectric barrier discharge reactor (DBD) with different N₂/O₂ gas mixtures for the removal of the superficial protein layer that enables the release of the chitin from the matrix without any alkali treatment. The major attraction for the non-thermal plasma processing is that it completely avoids the wet chemical alkali treatments and removes the surface protein as smaller molecules such as CO, CO₂, H₂ or CH₄.

Furthermore, the surface of materials was analyzed using ATR-FTIR, before and after non-thermal plasma treatment. Protein, chitin and CaCO₃ concentration were calculated based on calibration curve obtained using FTIR Spectrum Quant software. Total nitrogen content was determined by Kjeldahl method.

These techniques further revealed the selective removal of the surface protein in all samples. Figure 1 demonstrates removal of protein which is confirmed by loss of amino group around 1520 cm⁻¹, and amide I around 1640 cm⁻¹ originated from protein-chitin matrix located on the surface of the material⁴. Also, all samples showed decrease in total protein content from

47.9 % to 26.4 % in raw shrimp shells, and from 43.6 % to 34.4 % in demineralized shrimp shells. Chitin, protein and CaCO₃ concentration were determined using FTIR spectrum Quant. Calibration curves were obtained from peak area of components using Beers low module. Protein content on the surface of both, whole shrimp shells and demineralized shrimp shells decreased from 27.18 % and 24.54 % respectively, to zero in all samples after non-thermal plasma treatment. Chitin concentration also increased in all samples, while CaCO₃ concentration remain almost the same before and after non-thermal plasma treatment.

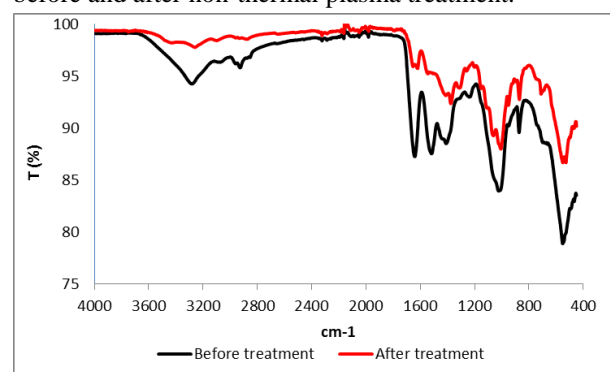


Figure 1: FTIR spectra (450-2000 cm⁻¹ spectral range) of shrimp shells (*Pandalus borealis*) before and after non-thermal plasma treatment

Non-thermal plasma treatment improved chitin isolation from shrimp shell waste, by excluding deproteinization.

References:

1. Ning, J.; Xi, C., Sustainability: Don't waste seafood waste. *Nature*, **2015**, 524, 155–157
2. Younes, I., & Rinaudo, M. Chitin and chitosan preparation from marine sources. Structure, properties and applications. *Marine Drugs*, **2015** 13(3), 1133–1174
3. Puliyalil, H.; Cvelbar, U. Selective Plasma Etching of Polymeric Substrates for Advanced Applications. *Nanomaterials*, **2016**, 6, 108
4. Stankiewicz, B. A.; Mastalerz, M.; Hof, C. H. J.; Evershed, R. P. m Biodegradation of the chitin-protein complex in crustacean cuticle. *Org. Geochem*, **1998**, 28, 67–76.

Additional Applications of Enaminones

Urša Tomažin¹, Uroš Grošelj¹, Marta Počkaj¹, Franc Požgan¹, Bogdan Štefane¹, Jurij Svete^{*,1}

¹ Faculty of Chemistry and Chemical Technology, University of Ljubljana, Večna pot 113, SI-1000 Ljubljana, Slovenia

In the world of organic chemistry enaminones are known as synthetic intermediates for preparation of various heterocyclic compounds. In the flood of all the new reactions, their chemical properties were overlooked. Structural similarity with well-known tetradentate ONNO, salen/salphen and acacen/acacphen ligands hints the possibility of forming coordination bonds with oxygen and nitrogen atoms. By linking two enaminones together a tetradentate ligand is formed. Structure and therefore the size and affinity of the bonding site could be altered with changing the structure of the starting compounds.

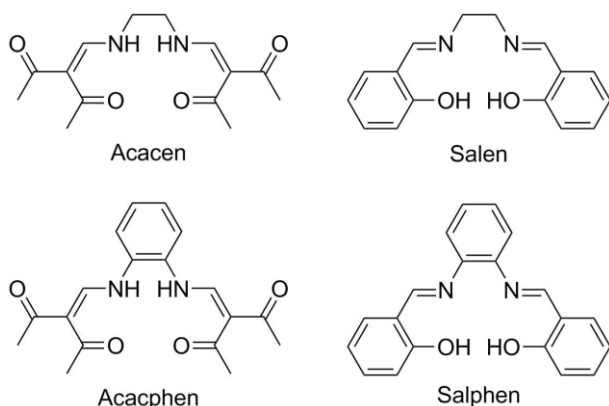
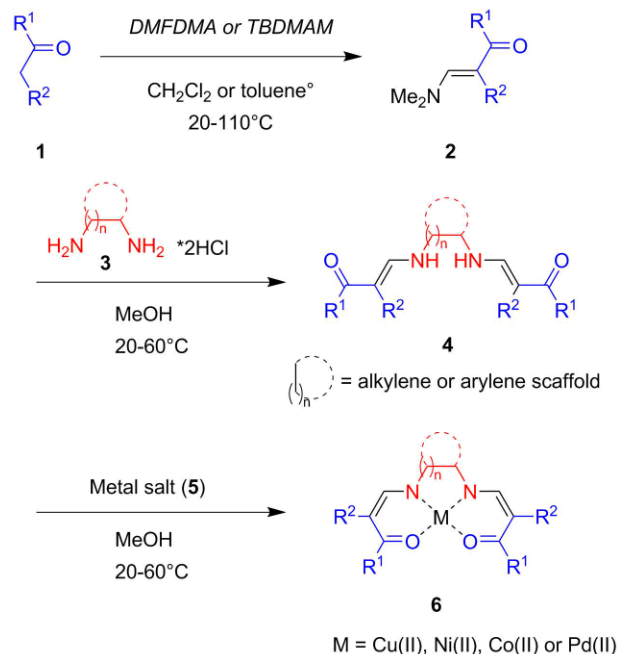


Figure 1: Acacen/acacphen and salen/salphen ligands

By combinatorial acid-catalyzed transamination between six primary diamines **3** and eight enaminones **2** 46 acacen-type ligands **4** were prepared. Products were used as tetradentate ligands for coordination of copper(II), nickel(II), cobalt(II), and palladium(II)¹. However, the complexes **6** were only formed with 1,2-diamine-based enamino ketones and an unprotected enamino lactam. A general three-step synthesis is outlined in the **Scheme 1**. The isolated Cu(II)-complexes **6** were tested as catalysts in copper catalyzed azomethine imine-alkyne cycloaddition (CuAIAC) reaction² of 1-(4-chlorobenzylidene)-5,5-dimethyl-3-pyrazolidinone-1-azomethine imine to methyl propiolate; two out of six isolated Cu(II)-complexes **6** showed good catalytic activities.



Scheme 1: Reaction mechanism

As it is shown enaminone ligands **4** can be used as ligands in coordination chemistry and as catalysts; however, due to their structural variability and easy introduction of various functionalities they may also be useful in biological applications and material science.

References:

1. Tomažin, U.; Grošelj, U.; Počkaj, M.; Požgan, F.; Štefane, B.; Svete, J.; Combinatorial Synthesis of Acacen-Type Ligands and Their Coordination Compounds. *ACS Comb. Sci.* **2017**, in print, doi: 10.1021/acscombsci.7b00027.
2. (a) Pušavec Kirar, E.; Grošelj, U.; Mirri, G.; Požgan, F.; Strle, G.; Štefane, B.; Jovanovski, V.; Svete, J.; "Click" Chemistry: Application of Copper Metal in Cu-Catalyzed Azomethine Imine-Alkyne Cycloadditions. *J. Org. Chem.* **2016**, *81*, 5988-5997. (b) Hori, M.; Sakakura, A.; Ishihara, K.; Enantioselective 1,3-Dipolar Cycloaddition of Azomethine Imines with Propioloylpyrazoles Induced by Chiral π -Cation Catalysts. *J. Am. Chem. Soc.*, **2014**, *136*, 13198–13201.

Ruthenium(II) Coordination Compounds as Inhibitors of 15-lipoxygenase-1

Katja Traven¹, Nikolaos Eleftheriadis², Sara Seršen¹, Jakob Kljun¹, Jure Bezenšek¹, Branko Stanovnik¹, Frank J. Dekker², and Iztok Turel^{*,1}

¹ Faculty of Chemistry and Chemical Technology, University of Ljubljana, Večna pot 113, SI-1000 Ljubljana, Slovenia

² Department of Pharmaceutical Gene Modulation, Groningen Research Institute of Pharmacy, University of Groningen, Antonius Deusinglaan 1, 9713 AV Groningen, The Netherlands

Lipoxygenases metabolize polyunsaturated fatty acids into signalling molecules such as leukotrienes and lipoxins, which play a regulatory role in several inflammatory lung diseases such as asthma, chronic obstructive pulmonary disease and chronic bronchitis. Human 15-lipoxygenase-1 (15-LOX-1) is an important mammalian lipoxygenase and plays a crucial role in the biosynthesis of these inflammatory signalling molecules. New classes of inhibitors are needed to explore the lipoxygenases as therapeutic targets. In this study we present several types of ruthenium(II) (Ru(II)) complexes as novel inhibitors of 15-LOX-1. Our study includes two novel Ru(II) complexes (**C1a** and **C1b**, Figure 1), bearing the sulphur macrocycle 1,4,7-trithiacyclononane, *S*-bonded dimethylsulphoxide, and chelate *N,N*- or *N,O*-donor ligands and three previously published Ru(II) complexes with the general formula $[(\eta^6\text{-}p\text{-cymene})\text{RuCl}(\text{O},\text{O-ligand})]\text{Cl}$.¹

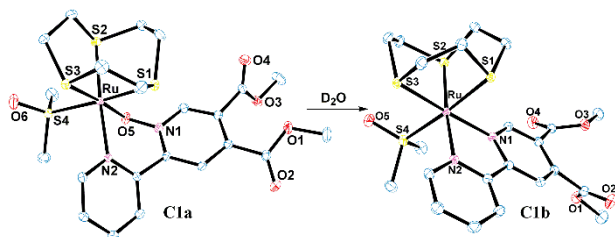


Figure 1: Crystal structures of novel Ru(II) complexes **C1a** and **C1b** with heteroatom labelling. Hydrogen atoms and hexafluorophosphate anions are omitted for clarity. The thermal ellipsoids are shown at the 20% probability level.

In order to estimate the stability of these complexes the behaviour of novel Ru(II) complexes in aqueous solution was investigated by means of ¹H NMR spectroscopy at room temperature. Interestingly, complex **C1a** and **C1b** show a completely different behaviour in aqueous solution. Complex **C1b** is relatively stable, since no changes were observed in ¹H NMR spectra after dissolution in D₂O in the timeframe of the experiment. On the other hand, for complex **C1a** additional peaks were observed already after 30 minutes and after one day the presence of an

intermediate compound is observed, which is later on converted further into complex **C1b** (Figure 2). After a month, complex **C1a** is fully converted to complex **C1b**, which is overall a reduction reaction.

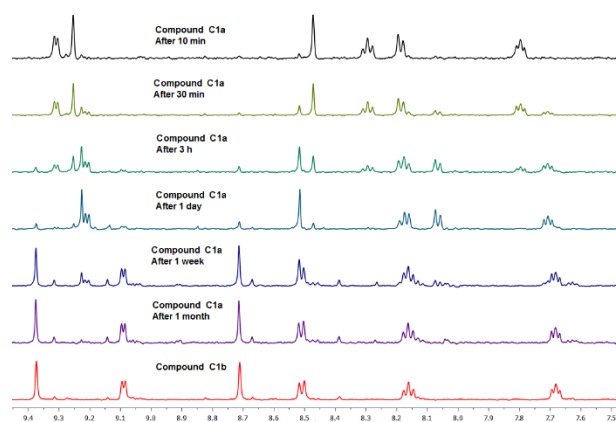


Figure 2: Time-dependent ¹H NMR spectra of complex **C1a** in aqueous solution (first six spectra) in comparison to **C1b** complex (spectrum at the bottom).

All five Ru(II) complexes together with free ligands and ruthenium precursors were screened for inhibition at concentrations of 50 μM . The data reveal four Ru(II) complexes as inhibitors of 15-LOX-1 with a potency in low micromolar range, whereas the respective free ligands showed no inhibition of the enzyme. Noteworthy is that between the newly synthesized complexes, only the complex **C1a** showed inhibition while structurally similar complex **C1b** showed no inhibition of the enzyme. More comprehensive results will be discussed in poster session.

References:

1. Traven, K.; Eleftheriadis, N.; Seršen, S.; Kljun, J.; Bezenšek, J.; Stanovnik, B.; Turel, I.; Dekker, F. J., Ruthenium complexes as inhibitors of 15-lipoxygenase-1. *Polyhedron* **2015**, *101*, 306-313.

Characterization of Allosteric Mechanism of Cathepsin K Using a Novel Allosteric Effector

Tjaša Goričan¹, Nejc Petek¹, Jurij Svete¹, Marko Novinec^{*,1}

¹ Faculty of Chemistry and Chemical Technology, University of Ljubljana, Večna pot 113, SI-1000 Ljubljana, Slovenia

Cathepsin K belongs to the family of papain-like proteases, enzymes that have a fundamental role in degradation of protein substrates in (endo)lysosomes¹. Apart from that it has additional functions among which the most important is its involvement in degradation of bone tissue². In the human body, cathepsin K must be carefully regulated since its elevated activity is associated with numerous diseases. Allosteric regulation is one of the processes by which cathepsin K can be regulated. In this mode the binding of an effector to the allosteric site causes the transmission of allosteric signaling via amino acid residues in the allosteric pathway to the active site³. It is already known that glycosaminoglycans are natural effectors of cathepsin K⁴. Furthermore, it has also been shown that two synthetic compounds NSC13345 and NSC94914 bind to its allosteric site and inhibit its enzyme activity^{5,6}.

On the basis of the crystal structure of an allosteric effector bound to cathepsin K we synthesized a new compound Su-Gly-O-Me which binds to the same allosteric site with higher affinity and in a novel binding mode, as seen by the determined structure of the newly developed compound bound to cathepsin K (Figure 1). We characterized Su-Gly-O-Me using different synthetic substrates and determined the kinetic mechanism of the compound, which was the same partial inhibition/ activation mechanism previously determined for the effectors NSC13345 and NSC94914^{5,6}. The newly developed compound partially inhibited the degradation of FITC-labelled collagen. In the presence of glycosaminoglycans, its inhibitory activity was reduced, which is consistent with its binding mode and differs from the behavior of known effectors. We also tested the specificity of this compound and showed that it binds not only to cathepsin K but also to cathepsin S. However, it does not bind to cathepsins B, L or V.

Based on crystallographic and molecular dynamics data, we predicted which residues are important for the binding of the compound Su-Gly-O-Me and for signal propagation from the allosteric site to the active site of cathepsin K (Figure 1). We verified these predictions by alanine mutagenesis and identified residues critical for binding of Su-Gly-O-Me to the allosteric site and

several residues critical for transmission of allosteric signaling.

The obtained results will be used to develop new compounds with higher affinities and specificities for potential research and medical applications. Furthermore, by identifying all residues critical for transmission of allosteric signaling we will be able to characterize the whole allosteric mechanism of cathepsin K.

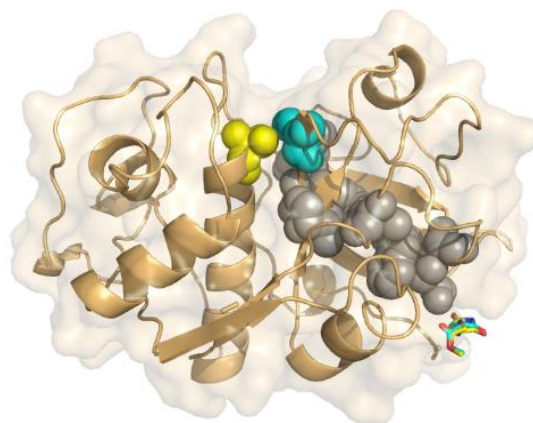


Figure 1: Predicted allosteric pathway (grey spheres) from the allosteric site where Su-Gly-O-Me binds (yellow and blue sticks) to active site residues Cys25 (yellow spheres) and His162 (blue spheres).

1. Novinec, M.; Lenarčič, B., Papain-like peptidases: structure, function, and evolution. *Biomol Concepts*, **2013**. 4(3). 287-308.
2. Novinec, M.; Lenarčič, B., Cathepsin K: a unique collagenolytic cysteine peptidase. *Biol Chem*, **2013**. 394(9). 1163-1179.
3. Tsai, C.J.; Nussinov, R., A unified view of "how allostery works". *PLoS Comput Biol*, **2014**. 10(2). e1003394.
4. Li, Z.; Kienetz, M.; Cherney, M.M.; James, M.N.; Bromme, D., The crystal and molecular structures of a cathepsin K:chondroitin sulfate complex. *J Mol Biol*, **2008**. 383(1). 78-91.
5. Novinec, M.; Korenč, M.; Caflisch, A.; Ranganathan, R.; Lenarčič, B.; in Baici, A., A novel allosteric mechanism in the cysteine peptidase cathepsin K discovered by computational methods. *Nat Commun*, **2014**. 5. 3287.
6. Novinec, M., Rebernik, M. in Lenarčič, B., An allosteric site enables fine-tuning of cathepsin K by diverse effectors. *FEBS Lett*, **2016**. 590 (24), 4507-4518.

Modelling of Liquid Glycols: Molecular Dynamics and SWAXS Studies

Jure Cerar,^a Andrej Jamnik,^a Matija Tomšič^{*,a}

^a Faculty of Chemistry and Chemical Technology, University of Ljubljana, Večna pot 113, SI-1000 Ljubljana, Slovenia

* Matija.Tomsic@fkkt.uni-lj.si

In scope of wider structural study of simple organic liquids, we performed a detailed structural investigation of simple liquid terminal glycols ranging from ethane-1,2-diol to pentane-1,5-diol at 25 °C. For this purpose, the experimental *small- and wide-angle x-ray scattering* (SWAXS) technique and the theoretical model based *molecular dynamics* (MD) computer simulations were combined. The simulations were performed utilizing the *transferable potential for phase equilibria – united atom* (TraPPE-UA) force field model¹ and provided a direct insight into the structure of the model systems. The validity of the model was checked by comparison of the calculated scattering intensities obtained from the simulation following the *complemented system approach*² and the experimental scattering data. We found satisfactory performance of all model glycols except of propane-1,3-diol. To investigate the origins of the characteristic scattering peak and the shoulder in the low-*q* regime in the scattering curves the partial scattering contributions arising from the correlation among different groups of the alcohol molecules were also calculated. The results showed that molecular organization is in large extent governed by the H-bonding between the hydroxyl groups. The polar –OH groups namely interconnect and form long branched skeletons, whereas the nonpolar alkyl parts of the molecules occupy the intermediate space between them. The inhomogeneities in the spatial electron density distribution caused by such molecular organization lead to the observed characteristic scattering curves, where the distinctive peak seems to origin mainly from the correlations within the hydrophobic regions of the alkyl chains, while the shoulder in low-*q* regime arise from the correlations between the –OH skeletons. To gain better insight into the structuring of the model system the radial and spatial pair distribution functions were calculated and visualized. Interesting information on molecular conformations was obtained from the intramolecular spatial distribution functions and the end-to-end distance distribution functions. These results showed that in all studied glycols the more or less stretched molecular conformations are preferred. The statistical analysis of the H-bonded –OH aggregates showed that the probability of occurrence for a certain aggregate size decreased with increasing the size, even though also large aggregates with 300

and more –OH groups could be found. In addition, some cyclic –OH aggregates were found in these systems – among those the 4- and 5-membered rings were obviously preferred in all cases. We can conclude, that the obtained results for the structure of glycols nicely complement the ones of the previously studied simple alcohols, aldehydes and organic acids.³⁻⁶

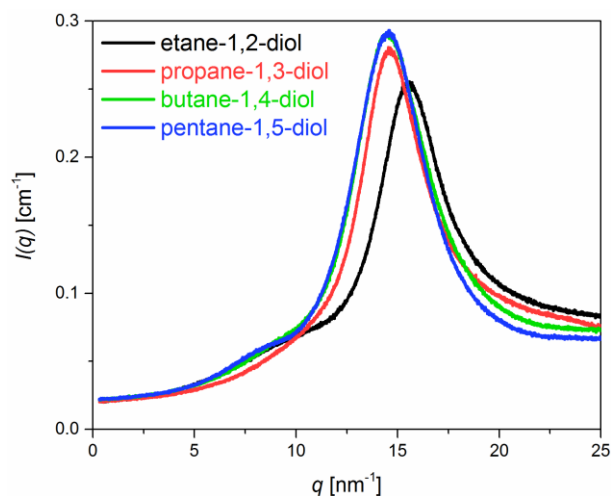


Figure 1: Experimental SWAXS scattering curves of simple terminal glycols ranging from ethane-1,2-diol to pentane-1,5-diol.

References:

1. B. Chen, J. J. Potoff, J. I. Siepmann, *J. Phys. Chem. B* **2001**, *105* (15), 3093-3104.
2. A. Lajovic, M. Tomšič, A. Jamnik, *J. Chem. Phys.* **2010**, *133* (17), 174123.
3. M. Tomšič, A. Jamnik, G. Fritz-Popovski, L. Vlček, *J. Phys. Chem. B* **2007**, *111*(7), 1738-1751.
4. A. Lajovic, M. Tomšič, G. Fritz-Popovski, L. Vlček, A. Jamnik, *J. Phys. Chem. B* **2009**, *113*(28), 9429-9435.
5. Lajovic, M. Tomšič, A. Jamnik, *Acta Chimica Slovenica* **2012**, *59*(3), 520-527.
6. J. Cerar, A. Lajovic, A. Jamnik, M. Tomšič, *Journal of Molecular Liquids* **2017**, *229*, 346.

Stereoselective Organocatalyzed Michael Addition of Hydroxy-Pyrroles to *trans*- β -Nitrostyrenes

Anže Ivančič¹, Sebastijan Ričko¹, Anže Meden¹, Bogdan Štefane¹, Andrej Perdih², Jurij Svete¹, Uroš Grošelj^{1,*}

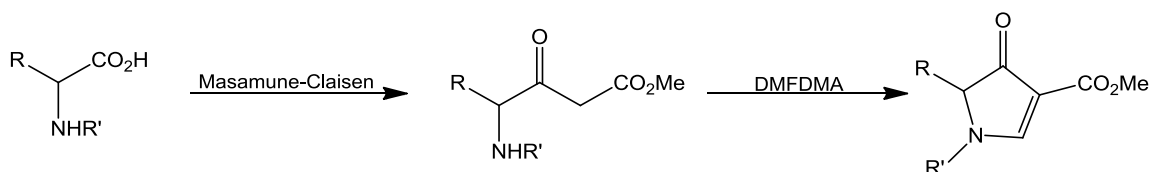
¹ Faculty of Chemistry and Chemical Technology, University of Ljubljana, Večna pot 113, 1000 Ljubljana, Slovenia

² National Institute of Chemistry, Hajdrihova 19, Ljubljana, Slovenia

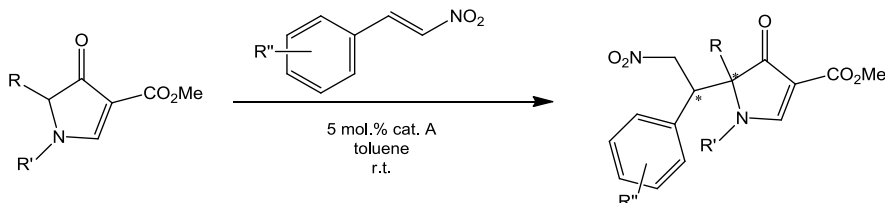
In spite of constant development in asymmetric organic synthesis, the stereoselective formation of tetrasubstituted carbon stereogenic center still remains a great challenge in modern organic synthesis.¹ Along with transition metal catalysis, asymmetric organocatalysis has turned out to be a reliable tool for functionalization of enolizable carbonyl compounds for its operative simplicity, easily available organocatalysts and benign reaction conditions.² In the family of 5-membered planar heterocycles there are numerous compounds that have potential as intermediates for synthesis of natural products and/or their synthetic analogues. Functionalizations of thiazolones, oxazolones and imidazolones are well

known,^{3,4,5} however there was little known about functionalizations of pyrrolones *i.e.* hydroxy-pyrroles despite the fact of their being the building blocks of many bioactive molecules.⁶ This motivated us to research the organocatalyzed reactions of pyrrolones with different electrophiles.

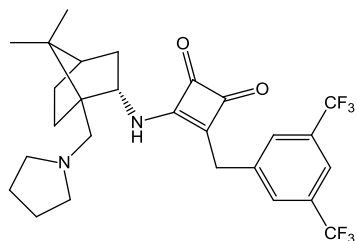
5-monosubstituted 4-oxo-1*H*,5*H*-pyrrole-3-carboxylates were prepared from α -aminoacids in two steps and were later functionalized with Michael addition to *trans*- β -nitrostyrenes in the presence of organocatalyst at room temperature. Reactions proceeded with high enantioselectivity (ee up to 98 %) and diastereoselectivity (dr up to 97:3).



Scheme 1: Two step pyrrolone synthesis.



Scheme 2: Michael addition of pyrrolones to *trans*- β -nitrostyrenes.



Scheme 3: Camphor organocatalyst used in the process.

References:

1. Volume 3: Carbon-Carbon Bond Formation (Ed.: I. Marek) in Comprehensive Organic Synthesis, 2nd Edition (Eds.: P. Knochel, G. A. Molander), Elsevier, Amsterdam, **2014**.
2. Ričko S.; Meden A.; Ivančič, A.; Perdih, A.; Štefane, B.; Svete, J.; Grošelj, U., Organocatalyzed Deracemisation of Δ^2 -Pyrrolin-4-ones. *Adv. Synt. Catal.*, 2017, *in press*, doi: 10.1002/adsc.201700539
3. Diosdado, S.; Etxabe, J. et al., *Angew. Chem.* **2013**, *125*, 12062-12067
4. Qiao, B.; An, Y. et al., *Org. Lett.* **2013**, *15*, 2358-2361
5. Etxabe, J.; Izquierdo, J. et al., *Angew. Chem.*, **2015**, *127*, 6987-6990
6. McNab, H.; Monahan, L. C., 3-Hydroxypyrroles In Pyrroles, Part 2: The Synthesis, Reactivity, and Physical Properties of Substituted Pyrroles; Jones, R. A., Ed.; Chemistry of Heterocyclic Compounds; John Wiley & Sons: New York, NY, **1992**; 48, 525-616.

The Impact of Copper Nanoparticles on the Composting Process

Sabina Kolšek¹, Andreja Žgajnar Gotvajn^{*1}, Anita Jemec², Gabriela Kalčíkova¹

¹ Faculty of Chemistry and Chemical Technology, University of Ljubljana, Večna pot 113, 1000 Ljubljana, Slovenia

² Biotechnical Faculty, University of Ljubljana, Večna pot 111, SI-1000 Ljubljana, Slovenia

An increasing use of products containing nanoparticles (NPs) leads to higher concentrations of NPs in the environment. Nowadays more and more NPs are introduced into the soil. They get there either for remediation purposes, with mineral/ organic fertilizers or pesticides and may have potential impact on composting microorganisms and other animals.^{1,2} Because of possible leaching of NPs from soil to aquatic environment, such contaminated soils pose a risk to groundwater quality and aquatic organisms as well.³

As Cu NPs are often found in soils as a result of pesticide application (in vineyards, orchards and on fields), we examined their impact on the composting process (where biodegradable organic matter is converted to a stable form). The real concentrations of CuO NP and Cu salts were applied to the plant material which was then composted.



Figure 1: Composting of plant material.

The impact of CuO NPs on soil enzymes (dehydrogenase and urease) was studied and the leaching test was made to simulate possible transitions of CuO NPs from the soil into the groundwater. The accumulation of CuO NPs and their effect on *Porcelino scaber*, terrestrial organisms involved in the

composting process, were also studied. As evident from the literature reviews, copper nanoparticles often have negative effects on bacteria in the soil, as well as on aquatic and terrestrial organisms. Our results did not show any harmful effects of CuO NPs. As real as possible concentrations of Cu, appearing in agriculture, have been used and such concentrations showed no effect on the studied organisms. The obtained results indicate that the pesticides, containing CuO NPs and being used throughout the year in rural areas, are not toxic to tested organisms and do not affect the composting process. Further long-term studies are needed in order to obtain a better understanding how Cu NPs affect composting process.

References:

1. Joško, I., Oleszczuk, P., Futa, B.: The effect of inorganic nanoparticles (ZnO, Cr₂O₃, CuO and Ni) and their bulk counterparts on enzyme activities in different soils. *Geoderma* **2014**, 232-234, 528-537.
2. Dinesh, R., Anandaraj, M., Srinivasan, V., Hamza S.: Engineered nanoparticles in the soil and their potential implications to microbial activity. *Geoderma* **2012**, 173-174, 19-27.
3. Tegenaw, A., Tolaymat, T., Al-Abed, S., El Badawy, A., Luxton, T., Sorial, G., Genaidy, A.: Characterization and Potential Environmental Implications of Select Cu-Based Fungicides and Bactericides Employed in U.S. Markets, *Environmental Science and technology* **2015**, 49, 1294–1302.

Chemometric Characterization of Slovenian Red Wines

Milena Ivanović,¹ Anja Petek,¹ Maša Islamčević Razboršek,¹ Mitja Kolar*,²

¹ Faculty of Chemistry and Chemical Engineering, University of Maribor, Smetanova ulica 17, 2000 Maribor, Slovenia

² Faculty of Chemistry and Chemical Technology, University of Ljubljana, Večna pot 113, 1000 Ljubljana, Slovenia

Wine is a complex matrix and its major components are water (81 %), ethanol (between 11 % and 15 %) and sugars. Additionally, it contains a wide range of organic and inorganic compounds, including phenolic compounds, different organic acids and nitrogenous compounds.¹ The concentration levels of these compounds are influenced by several oenological factors such as origin, vine variety, winemaking practices, ageing and vintage.

Slovenia is a small European country with a long history of wine production in three key wine growing regions, Podravje in the east, Primorska in the west and Posavje just south of the center. In Slovenia there are more than 28,000 wineries, producing between 80 and 90 million litres annually, of which 25 % is red wine. Most of the red wine is produced in Primorska from two well-known vine varieties, Refošk and Merlot.

Wine classification is a very important topic in order to detect possible frauds and to establish wine authenticity, which is an important consideration in international markets.² Slovenian wine legislation prescribes that all wines should be submitted to chemical and sensoric-organoleptic analysis before being released to the market. After wines pass the tests, they are assigned a quality level according to the Zaščiteno geografsko poreklo (ZGP), which is similar to the European Union's QWPSR system (Quality Wines Produced in Specified Regions.)

In this study, total phenolic (TPC), flavonoid (TFC) and tannin (TTC) contents, total SO₂, total acids, pH, and reducing sugars were measured in twenty five Slovenian red wines from three key wine producing regions. The results were chemometrically analysed and the wines were classified according to wine growing region and vine variety. Principal component analysis (PCA) proved that TPC, TFC and TTC contents were primarily responsible for variation in the wines. PC1 is well discriminated between Primorska (group 1) and Podravje (group 2) wines (Figure 1). The wines from the Posavje region (group 3) were positioned in the middle; some samples were dispersed into group 2. The highest percentage of phenolic compounds (TPC, TFC and TTC) was found in wine samples from the Primorska region. Additionally, linear discriminant analysis (LDA) was performed and resulted in the satisfactory classification of samples by

both vine variety and region. This study demonstrates the usefulness of variable selection and also suggests the application of a developed model which could be used for wine classification according to several other parameters such as vintage, winemaking practices and alcohol content.

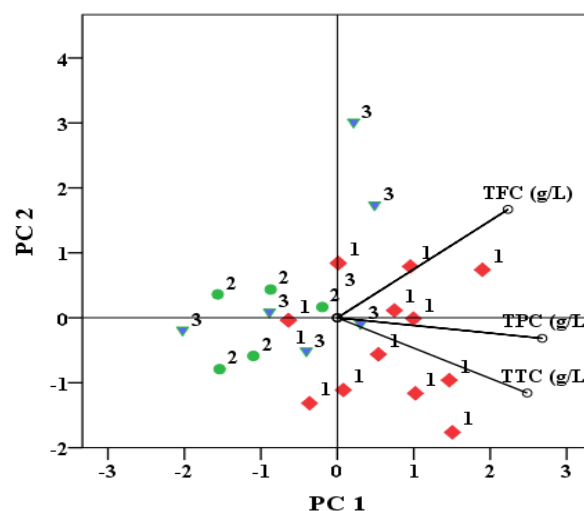


Figure 1: PCA bi-plot in the plane PC2 vs. PC1. The objects are labelled by Slovenian wine growing regions. The first principal component (PC1) explained 78 % of the variation between the samples, and the second (PC2) explained 18 % of the variation. PC1 and PC2 values separate samples according to TPC and TFC, respectively (\diamond Primorska wine growing region; Δ Podravje wine growing region and \circ Posavje wine growing region).

References:

1. S. Moncayo, J. D. Rosales, R. Izquierdo-Hornillos, J. Anzano, J. O. Caceres, Classification of Red Wine Based on Its Protected Designation of Origin (PDO) Using Laser-Induced Breakdown Spectroscopy (LIBS). *Talanta* **2016**, 158, 185–191.
2. R. Garrido-Delgado, L. Arce, A.V. Guamán, A. Pardo, S. Marco, M. Valcárcel, Direct coupling of a gas–liquid separator to an ion mobility spectrometer for the classification of different white wines using chemometrics tools. *Talanta*. **2011**, 84, 471–479.

Evaluation of *Trametes Versicolor*'s Capability for Nanoparticle Synthesis and Bioremediation

Urban Gartner¹, Gabriela Kalčíková¹, Andreja Žgajnar Gotvajn*¹

¹ Faculty of Chemistry and Chemical Technology, University of Ljubljana, Večna pot 113, 1000 Ljubljana, Slovenia

Trametes versicolor is a fungus of many capabilities. It produces different substances, many of which, like polysaccharidopeptides have medicinal properties. Fungi naturally grow on solid surfaces so submersive cultivation has to be properly adapted.¹ Therefore, cultivating of the fungus in submersive cultures can be challenging. According to literature, *Trametes versicolor* was shown to be capable of synthesizing nanoparticles² and degrading organic substances that can't be degraded by other microorganisms.^{3,4} They produce substances (enzymes, polysaccharides, terpenoids) that have reducing capabilities which make metallic and other ions in solutions to precipitate in the form of nanoparticles². Enzymes of these fungi are supposedly responsible for degradation of persistent organic substances. Enzymes (laccase, manganese peroxidase, lignin peroxidase) of *Trametes versicolor* produced extracellularly degrade lignin in different ways. These enzymes are nonspecific and are capable of degrading a whole range of substances like antibiotics, dyes, nitrophenoles, persistent pollutants in wastewaters and other.^{3,4}

Objective of this work was to carry out preliminary experiments to evaluate if *Tremetes versicolor* can be applied for silver nanoparticles synthesis or used in other environmental technologies, such as removal of persistent pollutants from mature landfill leachates and degradation of pharmaceuticals. As model substance antibiotic tiamulin was studied.

First analysis of nanoparticle synthesis experiments pointed to nanoparticle formation inside the mixture of liquid growth medium, fungi and dissolved AgNO₃. Transmission electron microscopy analysis showed the nanoparticles weren't formed only because of the fungi, but also because of the effect of the growth medium. Nanoparticles that were present weren't only silver nanoparticles but probably also silver chloride and silver oxide nanoparticles. Degradation experiments showed that strains of *Trametes versicolor* Tv6 and Tv11 were not able to degrade mature landfill leachate or tiamulin. Degradation was followed by measurements of total organic carbon (TOC). Figure 1 shows average changes of TOC in samples containing tiamulin in different concentrations after addition of fungi (T1: 1 g/L tiamulin, T2: 0.5 g/L tiamulin and T3: 0.25 g/L

tiamulin). TIA1, TIA2 and TIA3 represent total organic carbon values of fresh tiamulin solutions at the beginning of the experiment. Average TOC values of parallels with different tiamulin concentrations and fungi never fell far under TIA values. That indicates that fungi aren't capable of extensive degradation of tiamulin. TOC data from experiments with leachate gave us similar results. Visual analysis, dry mass measurements and enzyme activity analysis showed, that landfill leachate inhibits growth of fungus and enzyme activity. Same analyses also showed that tiamulin seems to slightly enhance fungal growth.

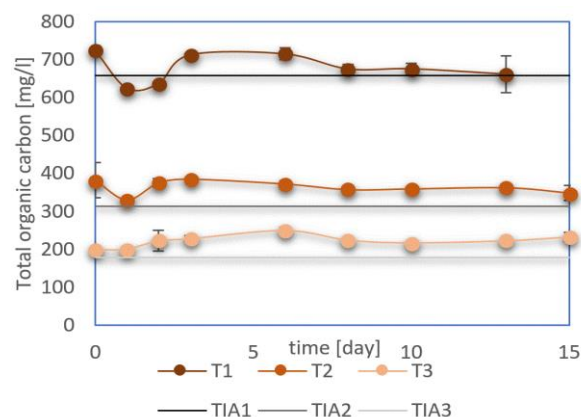


Figure 1: Total organic carbon concentrations at different times during the experiments with tiamulin.

References:

1. Smole J., *Submerzna kultura glive Trametes versicolor v mešalnem bioreaktorju*. Ljubljana: Biotehniška fakulteta 2015, diplomsko delo.
2. Narayanan K. B., Sakthivel N.; Biological synthesis of metal nanoparticles by microbes. *Adv. Colloid Interface Sci.* **2010**, 156, 1–13.
3. Cruz-Morató C., Ferrando-Climent L., Rodriguez-Mozaz S., Barceló D., Marco-Urrea E., Vincent T., Sarrà M.; Degradation of pharmaceuticals in non-sterile urban wastewater by *Trametes versicolor* in a fluidized bed bioreactor. *Water Res.* **2013**, 47, 5200–5210.
4. Saetang J., Babel S.; Fungi immobilization for landfill leachate treatment. *Water Sci. Technol. J. Int. Assoc. Water Pollut. Res.* **2010**, 62, 1240–1247.

Development of a SPME-GC-MS/MS Method for the Determination of Some Contaminants from Food Contact Material

Luka Žnideršič^{*,1,2}, Helena Prosen¹, Anita Mlakar²

¹ Faculty of Chemistry and Chemical Technology, University of Ljubljana, Večna pot 113, 1000 Ljubljana, Slovenia

² Krka, d.d., Novo mesto, Šmarješka cesta 6, SI-8501 Novo mesto, Slovenia

The synthesis and processing of basic polymer compounds which results in safer, cleaner and more resistant plastic materials intended for food contact packaging materials requires the implementation of various additives such as plasticizers, process aids, antioxidants, slipping agents, flame retardants and many other types of compounds. The latter have been found to be mostly low molecular weight substances that can easily migrate into the containing food and beverages.¹

Based on controlled extraction studies and the probability of their occurrence in food samples, nine compounds with different chemical properties and different roles as additives were selected. These include the preservatives methylparaben, ethylparaben, propylparaben and butylparaben, the antioxidants butylated hydroxyanisole, butylated hydroxytoluene and *tert*-butylhydroquinone, the plasticizer *N*-butylbenzenesulfonamide (NBBS) and the flame retardant tris(2-butoxyethyl) phosphate (TBEP). The listed compounds have been subject to many controversies in recent studies or were already proven to have negative health effects.² The most commonly employed methods for the determination of parabens and antioxidants include solid phase extraction³ (SPE) and solid phase microextraction⁴ (SPME), coupled to chromatographic techniques such as liquid or gas chromatography. The chromatographic determination of NBBS and TBEP is poorly researched.

The aim of this work is the development of a cheap, fast, simple, sensitive and environmentally friendly method for simultaneous determination of all nine compounds. SPME sampling coupled with gas chromatography-tandem mass spectrometry (GC-MS/MS) was chosen as the best approach. Firstly, the chromatographic conditions were optimized in order to ensure good separation between the analytes. HP-5MS UI column was employed to ensure proper peak shapes as especially parabens tend to show significant tailing on regular GC columns (Figure 1). Helium as the carrier gas at a constant flow rate was employed. Once good separation and a fast temperature program was achieved, the parameters of the mass spectrometer were optimized. Appropriate quantification and qualification ion transitions at optimal collision energies were

selected in order to assure the best sensitivity and identification confirmation for each compound. A polyacrylate (PA) fiber with 85 µm phase thickness was chosen as the best option for extraction of all 9 analytes. Parameters such as extraction time and temperature, sample volume and sodium chloride concentration were optimized to ensure the best possible extraction efficiency.

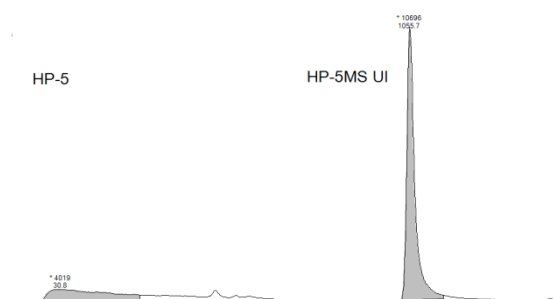


Figure 1: Comparison of methylparaben peak shape, peak area and signal-to-noise ratio using a regular HP-5 column vs. using an inert HP-5MS UI column.

References :

1. Vera P.; Canellas E.; Nerin C.; Migration of odorous compounds from adhesives used in market samples of food packaging materials by chromatography olfactometry and mass spectrometry (GC-O-MS), *Food Chem.* **2014**, *145*, 237-244.
2. Byford, J.R.; Shaw, L.E.; Drew, M.G.B.; Pope, G.S.; Sauer, M.J.; Darbre, P.D.; Oestrogenic activity of parabens in MCF7 human breast cancer cells, *J. Steroid Biochem. Mol. Biol.* **2002**, *80*, 49-60.
3. Gonzalez-Marino, I.; Quintana, J. B.; Rodriguez, I.; Cela, R., Simultaneous determination of parabens, triclosan and triclocarban in water by liquid chromatography/electrospray ionisation tandem mass spectrometry., *Rapid Commun. Mass Spectrom.* **2009**, *23*, 1756.
4. Canosa, P.; Rodriguez, I.; Rubi, E.; Bollain, M. H.; Cela, R., Optimisation of a solid-phase microextraction method for the determination of parabens in water samples at the low ng per litre level, *J. Chromatogr. A.* **2006**, *1124*, 1-2.

Fesoterodine Fumarate Batch Crystallization Modelling: Mass Transfer Resistances, Kinetics, Equilibrium and Particle-size Distribution Prediction

Marko Trampuž^{*.1}, Dušan Teslić², Blaž Likozar¹

¹ Department of Catalysis and Chemical React. Eng., National Institute of Chemistry, Hajdrihova 19, 1001 Ljubljana

² Sandoz Development Centre Slovenia, Lek d.d., Kolodvorska 27, 1234 Mengeš

Crystallization is the most important technological operation in the chemical production of active pharmaceutical ingredients (APIs). Due to a large number of process parameters that influence crystalline product quality, in-depth understanding of elementary mechanisms (nucleation, crystal growth, agglomeration, breakage, dissolution etc.) is necessary for development, optimization and control of a robust crystallization process.¹ Mathematical modelling has recently been acknowledged as a valuable tool for such purpose and a number of successful examples of crystallization modelling may already be found in the literature.²

A mathematical model for batch cooling crystallization of fesoterodine fumarate, an API used in the treatment of overactive bladder syndrome,³ in 2-butanone was developed in order to understand the impact of different process conditions on crystal size distribution. The model was developed in MATLAB and is based on population balance, mass balance and energy balance, thermodynamic equilibrium and kinetics of nucleation, crystal growth and crystal agglomeration. Population balance equation was solved numerically by method of classes.⁴

Equilibrium concentration (solubility curve) of fesoterodine fumarate in 2-butanone in the studied temperature range was measured by in-line FTIR spectroscopy, that was calibrated with samples of known concentration at different temperatures. A calibration model was developed using partial least squares (PLS) regression. Crystallization experiments were performed in a 2 L RC1 batch reactor. Five different process conditions were varied: cooling rate, stirring rate, amount of seed crystals, size distribution of seed crystals and seeding temperature. Experiments were monitored by in-line FTIR spectroscopy (concentration measurement) and Focused Beam Reflectance Measurement (FBRM) to measure the number and size distribution of crystals. FBRM was calibrated with samples of crystal slurries that were analyzed by optical microscopy. Final products were analyzed by laser diffraction and optical microscopy. Kinetic parameters were determined with the simultaneous regression of the concentration curves and crystal size distributions. The model was validated by a comparison of the simulated results with

experimental results performed under different process conditions.

The developed model allows the simulation of temperature and concentration profile of the crystallization mixture, as well as time-dependent number and size distribution of the formed crystals (Figure 1). The impact of the studied process conditions on the kinetics of nucleation, crystal growth and crystal agglomeration and consequently on crystal size distribution may thus be evaluated.

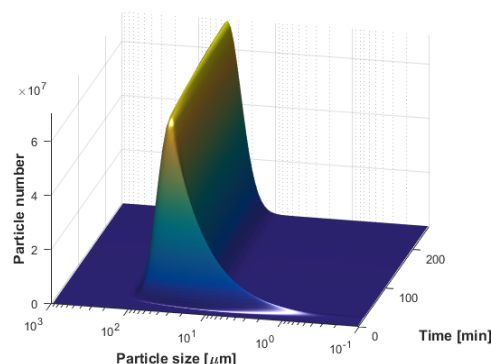


Figure 1: Time-dependent modelling simulation of crystal-size distribution evolution

In the future, the model will be further validated by a comparison with the experiments under different process conditions at various operation scales.

References:

1. a) Myerson, A. S., *Handbook of Industrial Crystallization*. 2nd ed.; Butterworth-Heinemann, **2001**, b) Tung, H. H. et. al., *Crystallization of Organic Compounds: An Industrial Perspective*. 1st ed.; Wiley, **2009**.
2. Pohar, A.; Likozar, B., Dissolution, Nucleation, Crystal Growth, Crystal Aggregation, and Particle Breakage of Amlodipine Salts: Modeling Crystallization Kinetics and Thermodynamic Equilibrium, Scale-up, and Optimization. *Ind. Eng. Chem. Res.* **2014**, 53, 10762-10774.
3. Ciambecchini U. et. al., US8049031 B2: Solid Forms of Fesoterodine Fumarate. **2011**.
4. Abbas, A., Romagnoli, J. A., Multiscale modeling, simulation and validation of batch cooling crystallization. *Sep. Purif. Technol.* **2007**, 53, 153-163.

Highly Efficient Titania Thin Films, Co-doped with Nitrogen and Platinum

Boštjan Žener^{1,*}, Romana Cerc Korošec¹

¹ Faculty of Chemistry and Chemical Technology, University of Ljubljana, Večna pot 113, 1000 Ljubljana, Slovenia

Semiconductor photocatalysis has attracted much interest in recent years as an alternative for treating water, polluted with hazardous materials. Titanium dioxide has emerged as the most widely investigated photocatalyst because of its chemical stability, non-toxicity and inexpensive price.¹ Titanium dioxide can exist in three polymorphic modifications: anatase, rutile and brookite. In all three modifications, titanium ion is surrounded by 6 oxygen ions in an octahedral coordination, but the distortion of the octahedron varies from one modification to another. Photocatalysis is used to describe a process during which a semiconductor (titanium dioxide) interacts with light to produce reactive oxidizing species, which then oxidizes adsorbed pollutants, forming CO₂ and H₂O. The main drawback of using titanium dioxide as a photocatalyst is the width of its band gap. Electrons can only be excited onto the conduction band by UV light ($\lambda < 380$ nm). In order to increase the photocatalytic activity of titanium dioxide under visible light illumination, materials have been doped with metals and nonmetals.²

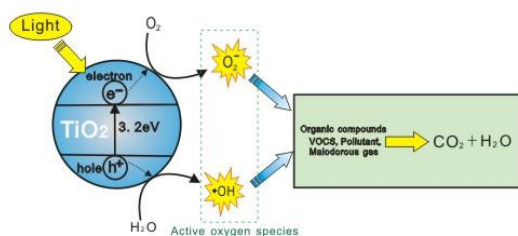


Figure 1: Process of photocatalysis.

Titania thin films and powders were prepared by a particulate sol-gel synthesis, using titanium tetrachloride as a precursor. During the synthesis, different quantities of various acids were added. After the first step of the synthesis, different chemicals, which acted as sources of metal and nonmetal dopants and hydroxypropyl cellulose (HPC, organic polymer, which increases the thickness and the porosity of materials) were added. These sols were then deposited onto object glasses by dip-coating technique and then thermally treated in a muffle furnace. The immobilization of TiO₂ in the form of a thin film significantly reduces some of the drawbacks of practical application of heterogeneous photocatalysis; for instance the need to separate the powder from the

suspension after photocatalytic reaction, or the tendency of the particles to agglomerate in aqueous dispersions.³

Photocatalytic activity of the prepared thin films was then determined by measuring the degradation rate of Plasmocorinth B (PB), an organic azo dye, which is widely used in textile industry as a textile colourant. The degradation rates were calculated from UV-Vis absorption spectra. Thin films were analysed with thermal analysis (TG), X-ray diffraction (XRD) and scanning electron microscopy (SEM). Changes in conductivity and pH values of the PB solution were also measured during its degradation.

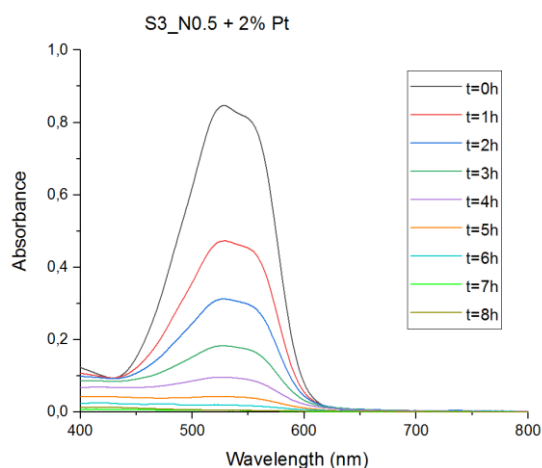


Figure 2: Absorption spectra of Plasmocorinth B, degraded with titania thin films, during visible light illumination.

References:

1. Songkhum, P., Tantirungrotechai, J., Synthesis, characterization and catalytic activity of nitrogen and iron (III) co-doped TiO₂, *Res. Chem. Intermed.* **2013**, 39, 1555-1561.
2. Peng, T., Zhao, D., Dai, K., Shi, W., Hirao, K., Synthesis of Titanium Dioxide Nanoparticles with Mesoporous Anatase Wall and High Photocatalytic Activity, *J. Phys. Chem. B* **2005**, 109, 4947-4952.
3. Addamo, M., Bellardita, M., Di Paola, A., Palmisano, L., Preparation and photoactivity of nanostructured anatase, rutile and brookite TiO₂ thin films, *Chem. Commun.* **2006**, 47, 4943-4945.

Toxicity of Veterinary Antibiotic Tiamulin to Freshwater Organisms

Ula Rozman^{*,1}, Andreja Žgajnar Gotvajn¹, Gabriela Kalčíkova¹

¹ Faculty of Chemistry and Chemical Technology, University of Ljubljana, Večna pot 113, SI-1000 Ljubljana, Slovenia

Antibiotics can enter the environment from various sources. There are a lot of evidences suggesting that the main problem regarding antibiotics is a development of antibiotic resistance genes and impact on bacterial community in soil and water. Nowadays, the problem of veterinary antibiotics has been widely recognized: for decades they have been extensively used prevent livestock's diseases. Most veterinary antibiotics enter the environment by animal manure, which is used as fertilizer¹. The global consumption of veterinary antibiotics in 2010 was 63.000 tons and was projected to rise to 106.600 tons in 2030².

Antibiotic tiamulin is used only in veterinary medicine for treatment and prophylaxis of dysentery, pneumonia and mycoplasmal infections on pig and poultry.³ Therefore tiamulin is often present in manure and if such manure is used as fertilizer persistent tiamulin can stay for a long time in a field. Due to runoff tiamulin easily enters an aquatic ecosystem⁴. The aim of this study was to investigate impact of tiamulin on well-known tests organisms in ecotoxicology waterflea *Daphnia magna*, duckweed *Lemna minor* and bacterium *Vibrio fischeri*.

24 h old nauplii of *Daphnia magna* were exposed to concentrations of tiamulin from 25 mg/l to 85 mg/l for 24 h and 48 h. Results showed that 24h EC₅₀ was 43,6 ± 0,5 mg/l. Nauplii were exposed for another 24 hours and results showed significant increase of toxic impact expressed as decrease of EC₅₀ value to 48 sh EC₅₀ 14,2 ± 4,8 mg/l. Test organism *Lemna minor* was also exposed to different concentrations of tiamulin (from 10 mg/l to 100 mg/l) for 7 days and effective concentration, EC₅₀, was 22,6 ± 0,8 mg/l. At higher concentrations of tiamulin we observed also lack of photosynthetic pigments called chloroses (**Fig. 1**). Bacterium *Vibrio fischeri* were exposed to different concentrations of tiamulin (from 125 mg/l to 1000 mg/l) for 30 minutes and the results showed, that tiamulin do not significantly influence *Vibrio fischeri* because the EC₅₀ value was quite high (492,9 ± 21,1 mg/l).

Tiamulin is a very persistent antibiotic and thus it is expected that organisms in the environment can easily come into the contact with it and long term effects can be expected. Our results showed, that *Daphnia magna* and *Lemna minor* are the most sensitive to tiamulin, while *Vibrio fischeri* is not.

Tiamulin also negatively affect photosynthetic pigments of plant. This is in agreement with previous results⁵ where tiamulin significantly inhibit growth of freshwater algae (EC₅₀ = 0,165 mg/l) and cyanobacteria (EC₅₀ = 0,003 mg/l). Therefore we expect that tiamulin could present potential threat for plants and algae – important producers in the aquatic ecosystems.



Figure 1: *Lemna minor* exposed to different concentrations of tiamulin for 7 days (first line from left to right: 0 mg/l, 10 mg/l, 20 mg/l, 40 mg/l, second line from left to right: 0 mg/l, 60 mg/l, 80 mg/l, 100 mg/l).

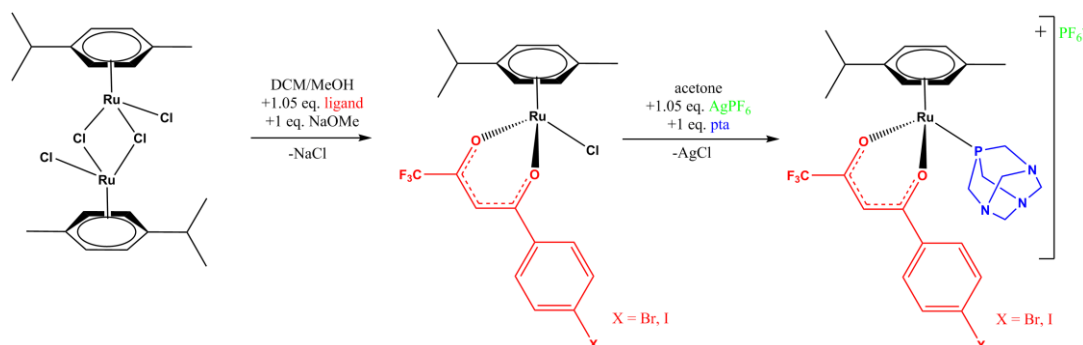
References:

1. Kümmerer, K. *Pharmaceuticals in the Environment: Sources, Fate, Effects and Risks*, 1st ed.; Springer-Verlag: Berlin-Heidelberg, 2001.
2. Pan, M.; Chu, L.M. Leaching behavior of veterinary antibiotics in animal manure-applied soils. *Science of the Total Environment*. **2017**, 579, 466-473.
3. Committee for veterinary medicinal products. Tiamulin, summary report (1). The European Agency for the Evaluation of Medicinal Products. [Online] August 1999 http://www.ema.europa.eu/docs/en_GB/document_library/Maximum_Residue_Limits_-_Report/2009/11/WC500015563.pdf (accessed May 15, 2017).
4. Schlüsener, M.P.; Bester, K. Persistence of antibiotics such as macrolides, tiamulin and salinomycin in soil. *Environmental Pollution*. **2006**, 143, 565-571.
5. Halling-Sørensen, B. Algal toxicity of antibacterial agents used in intensive farming. *Chemosphere*. **2000**, 40, 731-739.

Structural Investigation of Novel Ruthenium-Diketonate Complexes

Matija Uršič¹, Tanja Lipec¹, Anton Meden¹ and Iztok Turel*,¹

¹ Faculty of Chemistry and Chemical Technology, University of Ljubljana, Večna pot 113, 1000 Ljubljana, Slovenia



Scheme 1: Synthesis scheme for the newly prepared ruthenium-diketonate complexes.

Chemotherapy is an extensively used cancer treatment therapy, with cisplatin and other platinum-based drugs being one of the most frequently used drugs. Nevertheless, the severity of their side effects has spurred research into metal-based drugs with improved properties. First about three decades ago, and again roughly fifteen years later, ruthenium-based complexes have emerged as promising agents with anti-tumor and anti-metastatic properties.¹ Quite different from biological activity, catalytical properties of ruthenium complexes have been firmly established and broadly implemented in organic chemistry, especially in olefin metathesis.² Our group has previously published various papers on catalytically and biologically active complexes with novel diketonates. They have exhibited their potential for use as catalysts for ortho arylation via C-H activation,³ as well as anticancer activity on CH1 ovarian cancer line in the low micromolar range.⁴

In relation to our previous work, four novel ruthenium diketonate complexes were synthesized and fully characterized (Scheme 1). Their crystal structures and spectroscopic data were compared to two previously published complexes in an effort to identify the impact of a relatively minor substitution of the ligand-bound halogen atom on the physico-chemical properties of the complex and possible emergent structural elements or trends that might help to predict and explain possible structure-activity relationship in future biological and catalytical testing. One of the more significant finds was a halogen bond mediated dynamic disorder in two diketonate-pta complexes (Figure 1).⁵

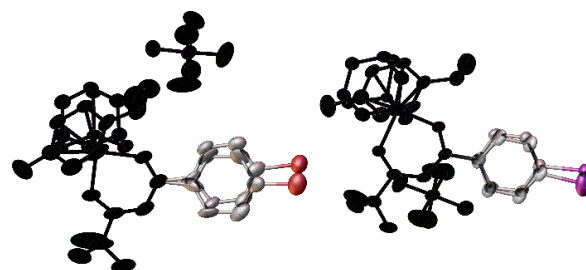


Figure 1: Halogen bond mediated dynamic disorder in two ruthenium-diketonate-pta complexes. Darkness shows the degree of overlap between the two possible extremes in the structure.

References:

- Ang, W. H.; Dyson, P. J., Classical and non-classical ruthenium-based anticancer drugs: Towards targeted chemotherapy. *Eur. J. Inorg. Chem.* **2006**, (20), 4003-4018.
- Naota, T.; Takaya, H.; Murahashi, S. I., Ruthenium-catalyzed reactions for organic synthesis. *Chem. Rev.* **1998**, 98 (7), 2599-2660.
- Seršen, S.; Kljun, J.; Požgan, F.; Štefane, B.; I., T., Novel organoruthenium(II) β -diketonates as catalysts for ortho-arylation via C-H activation. *Organometallics* **2013**, 32 (2), 609-616.
- Seršen, S.; Kljun, J.; Kryeziu, K.; Panchuk, R.; Alte, B.; Körner, W.; Heffeter, P.; Berger, W.; Turel, I., Structure-Related Mode-of-Action Differences of Anticancer Organoruthenium Complexes with β -Diketonates. *J. Med. Chem.* **2015**, 58 (9), 3984-3996.
- Uršič, M.; Lipec, T.; Meden, A.; Turel, I., Synthesis and Structural Evaluation of Organo-Ruthenium Complexes with β -Diketonates. *Molecules* **2017**, 22 (2), 326.

Non-symmetric Phenyl Substituted 1,2,4,5-tetraoxanes; Synthesis and Optimization

Griša Grigorij Prinčič¹, Jernej Iskra^{1,*}

¹ Faculty of Chemistry and Chemical Technology, University of Ljubljana, Večna pot 113, SI-1000 Ljubljana, Slovenia

Hydrogen peroxide is an unstable molecule mostly used in redox reactions. Side products of oxidative processes involving hydrogen peroxide is usually water and is therefore often used as a reagent of choice in the field of »green chemistry«, area of chemistry focused on design of processes that minimize use of chemicals or production of waste¹. Reactions of hydrogen peroxide are, however, not limited only to oxidations. Its direct incorporation into organic scaffold leads to formation of organic peroxide molecules with interesting properties and functionality.

1,2,4,5-tetraoxanes are a group of compounds with 2 O-O bonds and proven antimalarial activity. They can be produced by condensing a carbonyl and *gem*-dihydroperoxide with acid catalyst in fluorinated alcohol (template catalysis). In their structure they bear two peroxide functionalities bridged with two carbon atoms (Figure 1). The latter configuration gives these compounds their biological activity. Interestingly, though, the type of structure on opposite sides of tetraoxane ring strongly determines biological activity; antimalarial activity was observed only on *dispiro* molecules, whereas *spiro* derivatives exhibited much lower, in some cases even negligible activity².

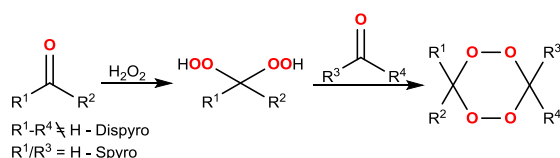


Figure 1: Basic synthetic procedure pathway for tetraoxane preparation from carbonyl compounds and hydrogen peroxide.

Our research has focused mainly on synthesis of non-symmetric phenyl substituted, therefore *spiro* 1,2,4,5-tetraoxanes by condensation of an appropriate substituted aldehyde and *gem*-dihydroperoxide with an acid catalyst in fluorinated alcohol as a solvent. Further optimization of the reaction conditions such as temperature, concentration of acid and reaction time was however attempted. Moreover, effort was made to not only increase the overall yield of the reaction but to also improve selectivity over non-symmetric rather than symmetric tetraoxane formation and minimize unwanted side product formation (Figure 2).

Detailed NMR analysis of synthesized molecules was conducted in order to evaluate the role of substituent in the 2' position of the aromatic part on conformational preference of molecules.

Substituted thioureas have also proven to be effective catalysts in both, peroxidation of aldehyde substrates to *gem*-dihydroperoxides and condensation of the latter to 1,2,4,5-tetraoxanes, respectively. Their selectivity towards production of non-symmetric tetraoxanes and efficacy as a catalyst will have been further examined through the course of this work.

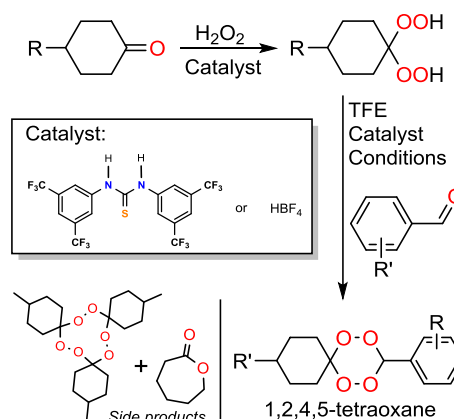


Figure 2: Preparation of phenyl substituted non-symmetric 1,2,4,5-tetraoxanes. Catalyst selection in the bracket and possible side products.

References:

1. Rao A. S.; Mohan H. R.; Iskra J., Hydrogen Peroxide. *e-EROS Encyclopedia of Reagents for Organic Synthesis*. John Wiley & Sons. **2013**.
2. Iskra, J., One-pot synthesis of non-symmetric tetraoxanes with the H_2O_2 /MTO/fluorous alcohol system. *Tetrahedron L.* **2003**, 44, 6309-6312.
3. Terent'ev, A. O., Synthesis of five and six membered cyclic organic peroxides: Key transformations into peroxide ring-retaining products. *Beilstein J.* **2014**, 20, 34-114.

Oxidation of Trifluoromethylthiolated Aromatic Compounds with Hydrogen Peroxide

Monika Horvat¹, Gregor Kodrič¹, Marjan Jereb¹, Jernej Iskra^{*,1}

¹ Faculty of Chemistry and Chemical Technology, University of Ljubljana, Večna pot 113, SI-1000 Ljubljana, Slovenia

Many fluorinated organic molecules are biologically active and can have great importance in different fields of medicine, pharmacology, agricultural chemistry and material science¹. Moreover, compounds containing several fluorine atoms present an important role in drug design. Trifluoromethyl group (CF₃-) is one of the most important fluorinated substituents. A very attractive modulation of this group has gained by the introduction of the trifluoromethylthio group (CF₃S-), which is considered to be the key fragment in many types of biologically active compounds, because of its strong electronegativity and high lipophilicity^{2,3}. Classical reagents for the introduction of CF₃S- groups are toxic, therefore the development of new and easy-to-handle electrophilic, nucleophilic, and radical reagents for the insertion of this stable group, has been intensely studied². The introduction of these groups could be carried out indirectly with the interconversion of functional groups or directly with CF₃SCl³. Molecules with the CF₃S- group are key intermediates for the synthesis of biologically active trifluoromethyl sulfones and sulfoxides. The main reagent for such reactions is *meta*-chloroperoxybenzoic acid, though yields of the products are often low. Therefore, the development of effective and environmentally friendly oxidation methods are becoming more desired^{2,4}.

Hydrogen peroxide is a very powerful oxidizing agent, which forms only water as a by-product, and it has in recent years, been used in numerous reactions.⁵

Since oxidation of CF₃S- substituted organic molecules to their respective sulfoxides or sulfones is hard to achieve using mild and selective reagents, we studied the use of hydrogen peroxide as an oxidizing agent. Our research is based on a selective conversion of the CF₃S- functional group in organic molecules into their respective sulfoxide or sulfone. On a selected phenol the sulfoxide CF₃S- group was first introduced using an electrophilic reagent (*N*-trifluoromethylsulfany)aniline (PhNHSCF₃). In the second part, the CF₃S- group was converted to the corresponding sulfoxide using hydrogen peroxide, respectively. Moreover, our future goal is to merge both procedures as a one-pot synthesis.

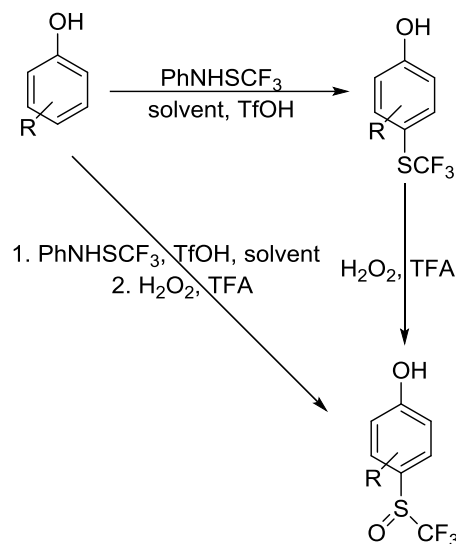


Figure 1: The synthesis of sulfoxide.

References:

1. Braun T.; Hughes R. P., *Organometallic Fluorine Chemistry*. Topics in Organometallic Chemistry 52; Springer: Switzerland **2015**.
2. Zeng Y.; Hu J., Silver-Mediated Trifluoromethylthiolation-Iodination of Arenes. *Org. Lett.* **2016**, *18*, 856-859.
3. Jereb M.; Gosak K., Acid-promoted direct electrophilic trifluoromethylthiolation of phenols. *Org. Biomol. Chem.* **2015**, *13*, 3103-3115.
4. Karmakar R.; Mamidipalli P.; Hong S., Benzannulation of trienes Initiated by an Alder-Ene Reaction and Subsequent Trifluoromethylthiolate Addition. *Org. Lett.* **2016**, *18*, 3530-3533.
5. Rao A. S.; Mohan H. R.; Iskra J., Hydrogen Peroxide. *e-EROS Encyclopedia of Reagents for Organic Synthesis*. John Wiley & Sons. **2013**.

Copper Catalyzed Synthesis of 6,7-dihydro-1*H*,5*H*-pyrazolo[1,2-*a*]pyrazolones, Followed by Ring Opening

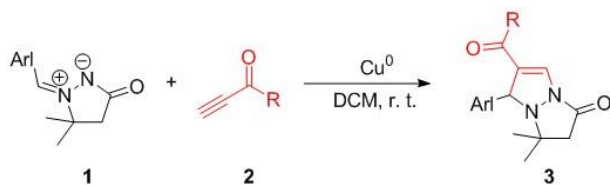
Eva Pušavec Kirar,¹ Uroš Grošelj,¹ Franc Požgan,^{1,2} Bogdan Štefane,^{1,2} Jurij Svete*,^{1,2}

¹ Faculty of Chemistry and Chemical Technology, University of Ljubljana, Večna pot 113, SI-1000 Ljubljana, Slovenia

² EN-FIST Centre of Excellence, Trg osvobodilne fronte 13, SI-1000 Ljubljana, Slovenia

3-Pyrazolidinone-1-azomethine imines and ynones give 6,7-dihydro-1*H*,5*H*-pyrazolo[1,2-*a*]pyrazolones in 1,3-dipolar cycloaddition reactions. These reactions usually proceed at high temperatures, for example at the boiling point of anisole¹. In contrast, when a catalyst is added, reactions can proceed at room temperature². We were the first to use elemental copper as a catalyst for reactions between azomethine imines and ynones³.

Reactions catalyzed by copper(0) were regioselective and gave fluorescent products in high yields at room temperature in dichloromethane.



Scheme 1: 1,3-Dipolar cycloaddition, catalyzed by elemental copper.

Table 1: Results of 1,3-dipolar cycloaddition, catalyzed by elemental copper.

	Arl	R	Yield (%)
3a	4-NO ₂ C ₆ H ₄	CH ₂ NHBoc	89
3b	4-ClC ₆ H ₄	CH ₂ NHBoc	95
3c	3,4,5-(MeO) ₃ C ₆ H ₂	CH ₂ NHBoc	96
3d	Ph	CH ₂ NHBoc	92
3e	1-pyrenyl	OMe	88

Reaction time depended on the surface of the catalyst. A larger surface meant a faster reaction. However, the reactions do not proceed on the surface of the catalyst. With a series of experiments, the reaction mechanism was determined.

We noticed that some of the products lost their fluorescence over time. The reason for that is the ring opening reaction of 6,7-dihydro-1*H*,5*H*-pyrazolo[1,2-*a*]pyrazolones followed by oxidation which gives pyrazoles.

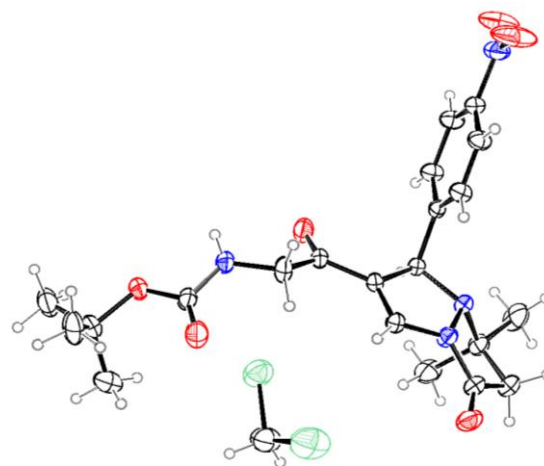
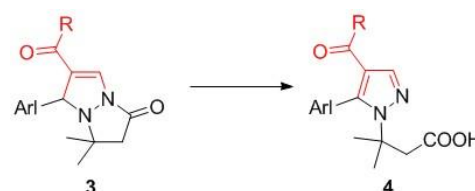


Figure 1: X-ray structure of **3a**.



Scheme 2: Ring opening reaction.

Reaction rate on the structure of cycloadducts, solvents used for the reaction and on the presence of an acid or base. When trifluoroacetic acid was added, the ring opening process was faster and by adding trimethylamine the reaction rate was slowed down.

References:

1. Pezdirc, L.; Stanovnik, B.; Svete, J., *Aust. J. Chem.* **2009**, 62 (12), 1661–1666.
2. Shintani, R.; Fu, G. C., *J. Am. Chem. Soc.* **2003**, 125 (36), 10778–10779.
3. Pušavec Kirar, E.; Grošelj, U.; Mirri, G.; Požgan, F.; Strle, G.; Štefane, B.; Jovanovski, V.; Svete, J., *J. Org. Chem.* **2016**, 81 (14), 5988–5997.

Development of DNA Barcoding Approach Based on rRNA Genomic Sequences for Detection of Cyanobacteria in Environmental Samples

Mojca Juteršek¹, Marina Klemenčič¹, Marko Dolinar^{*,1}

¹ Faculty of Chemistry and Chemical Technology, University of Ljubljana, Večna pot 113, SI-1000 Ljubljana, Slovenia

Cyanobacteria are photoautotrophic prokaryotes with very long evolutionary history, through which they have diversified into a variety of species with different morphologies¹. Despite their morphological diversity, it is difficult to identify and discriminate cyanobacteria based on their phenotype. Moreover, use of morphology-based methods often results in erroneous identification. Consequently, DNA-based methods have been used instead.

We aimed to develop a DNA barcoding-based method for identification of cyanobacteria that could potentially be used for analysis of environmental samples. DNA barcoding is a method based on determining nucleotide sequence of a suitable short genomic region from an organism of interest and its comparison to a database of sequences, where each sequence has an assigned organism of origin. Since rRNA genomic regions have already been widely used for phylogenetic studies of cyanobacteria, we decided to base our method on 16S rRNA and 16S-23S ITS genomic regions.

Firstly we tested our approach on cultured members of *Synechocystis* genus in order to determine discrimination power of the selected regions. It is known that 16S is less diverse among closely related species or strains and therefore it might not be able to provide the desired discerning power². We successfully amplified 16S and ITS regions from 9 different *Synechocystis* strains and determined their nucleotide sequences. Our results clearly showed that ITS region is highly diverse and could be used to identify different species as well as strains of *Synechocystis* genus, while 16S showed high sequence identities and proved to be less useful.

Next, we wanted to use our approach on an environmental sample for which we could predict species of cyanobacteria present. We collected samples of a cyanobacterial bloom from Lake Bled that is known to be caused by *Planktothrix rubescens* and amplified 16S and ITS regions. As expected, by comparing 16S sequences to nucleotide sequences in databases we were not able to identify the species, while the ITS region clearly showed that the sample contained *Planktothrix rubescens*.

Our final step was to test our approach on environmental samples from waters without visible

cyanobacterial presence and with unknown species composition. We collected samples in Dolenjska region and determined nucleotide sequences of 16S regions from some of the samples. However, we were unable to determine cyanobacterial species present in samples, because databases lacked assigned 16S nucleotide sequences that would match our results.

In conclusion, DNA barcoding based on rRNA sequences shows considerable potential for identification of cyanobacteria. Currently, this method is more applicable for analysis of cultured species or cyanobacterial blooms, whereas for other environmental samples sequence databases still need to expand.



Figure 1: Microscopic photograph of *Planktothrix rubescens* in a sample from Lake Bled.

Acknowledgement

This project was a part of research assignment made in collaboration with high school students from Gimnazija Novo mesto: Evgenija Burger, Lucija Marzel Djuranovič and Luka Petravič.

References:

1. Mazard, S.; Penesyan, A.; Ostrowski, M.; Paulsen, I. T.; Egan, S., Tiny microbes with a big impact: The role of cyanobacteria and their metabolites in shaping our future. *Mar. Drugs* **2016**, *14*, E97.
2. Boyer, S. L.; Flechtner, V. R.; Johansen, J. R., Is the 16S-23S rRNA internal transcribed spacer region a good tool for use in molecular systematics and population genetics? A case study in cyanobacteria. *Mol. Biol. Evol.* **2001**, *18*, 1057-1069.

Protein Expression and Characterization of Three *M. aeruginosa* NIES843 Orthocaspases

Jure Zabret¹, Marina Klemenčič¹, Marko Dolinar^{*, 1}

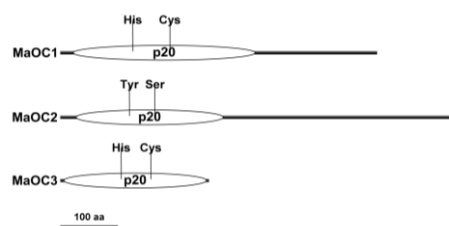
¹ Faculty of Chemistry and Chemical Technology, University of Ljubljana, Večna pot 113, SI-1000 Ljubljana, Slovenia

Harmful cyanobacterial blooms exhibit a controlled dying that mirrors metazoan, plant and protozoan programmed cell death (PCS)¹, a process that is carried out by caspases and metacaspases respectively². Orthocaspases, equally to metazoan caspases, and plant, fungal or protozoan metacaspases belong to the C14 peptidase family. These proteins all contain a so-called p20 domain with a characteristic fold and a catalytic dyad, formed by histidine and cysteine residues. Until now, only one orthocaspase has been biochemically characterized: MaOC1 from the cyanobacterium *Microcystis aeruginosa* PC 7806². To further investigate this group of enzymes we characterized orthocaspases from a different *M. aeruginosa* strain, NIES-843, which contains three orthocaspases. We termed them MaOC1, MaOC2 and MaOC3 (Scheme 1). Only MaOC1 and MaOC3 contain the conserved catalytic dyad, while in MaOC2 His is replaced by Tyr and Cys is replaced by Gly residue.

We expressed all three orthocaspases as recombinant proteins with C-terminal His-tags in *E. coli*. MaOC1 and MaOC2 formed insoluble protein aggregates (inclusion bodies)³ during heterologous expression, which demanded (i.) adaptation of the standard solubilisation and refolding method³ for MaOC1 and (ii.) lowering the growth temperature and halving the expression time for MaOC2, thereby exploiting protein aggregating dynamics³ to obtain the soluble enzyme. MaOC3 was obtained from the soluble fraction. After refolding, MaOC1 was shown to be an active protease with cleavage after positively charged amino acid residues. On the other hand, MaOC2, lacking the catalytic dyad, exhibited no catalytic activity towards the synthetic substrates. However, we observed that MaOC2 forms structured soluble oligomers, corresponding to formations of heptamers or octamers *in vitro*, which have also been observed for other catalytically inactive orthocaspases (unpublished data). Contrary to expectations, no enzymatic activity was observed for MaOC3. Alignment of its amino acid sequence with the homologous metacaspase MCA2⁴ from *Trypanosoma brucei* revealed that in MaOC3, Cys92 residue, conserved in MCA2 and *M. aeruginosa* PCC 7806

MaOC1, is replaced by a proline residue. Cys92 has been shown to be important for substrate orientation and active site formation⁴. Inactivity of MaOC3 therefore presents evidence for structural similarities between meta- and orthocaspases.

For now, the role of orthocaspases in PCD remains elusive, but it presents potential for further research. Insights into this process could present novel strategies for counteracting harmful cyanobacterial blooms and for crucial understanding of the industrially interesting and ecologically important group of organisms – cyanobacteria.



Scheme 1: Schematic representation of the domain architecture of orthocaspases MaOC1, MaOC2 and MaOC3

References:

1. Ross, C.; Santiago-Vázquez, L.; Paul, V. Toxin release in response to oxidative stress and programmed cell death in the cyanobacterium *Microcystis aeruginosa*. *Aquat. Toxicol.* **2006**, *78* (1), 66–73.
2. Klemenčič, M.; Novinec, M.; Dolinar, M. Orthocaspases are proteolytically active prokaryotic caspase homologues: the case of *Microcystis Aeruginosa*. *Mol. Microbiol.* **2015**, *98* (1), 142–150.
3. Fink, A. L. Protein aggregation: folding aggregates, inclusion bodies and amyloid. *Folding and Design.* **1998**, *3* (1), R9-23.
4. McLuskey, K.; Rudolf, J.; Proto, W. R.; Isaacs, N. W.; Coombs, G. H.; Moss, C. X.; Mottram, J. C. Crystal structure of a *Trypanosoma brucei* metacaspase. *Proc. Natl. Acad. Sci. U. S. A.* **2012**, *109* (19), 7469–7474.

Targeting Cathepsins B, S and L with DARPin/stefinA-conjugated Liposomes in Cancer

Andreja Bratovš^{1,2}, Lovro Kramer¹, Olga Vasiljeva^{1,2}, Boris Turk^{*,1,2,3}

¹ Department of Biochemistry and Molecular and Structural Biology, Jožef Stefan Institute, Jamova 39, SI-1000 Ljubljana, Slovenia

² Jožef Stefan International Postgraduate School, Jamova 39, SI-1000 Ljubljana, Slovenia

³ Faculty of Chemistry and Chemical Technology, University of Ljubljana, Večna pot 113, SI-1000 Ljubljana, Slovenia

Cysteine cathepsins are papain-like lysosomal proteases, synthesized as proenzymes and activated in the lysosome. In healthy cells, they are localized in the endolysosomal vesicles. They have been shown to play a role in different stages of cancer progression.

Among the cathepsins, increased levels of cathepsin B have been demonstrated in many different types of cancer, including breast cancer and melanoma. Similarly, upregulation of cathepsins S and L in various cancers was reported. Cathepsins B, S and L can also be secreted into the tumor microenvironment, which, together with their overexpression in different cancer types, makes them promising targets for targeted drug delivery and diagnostics^{1,2}.

To target cathepsin B on the surface of cancer cells and in the tumor microenvironment we prepared DARPin-conjugated liposomes, while stefin A-conjugated liposomes were used for cathepsin L/S targeting. Liposomes are a widely used drug delivery system for small molecules as well as proteins. An advantage of the liposomal delivery system is the possibility of functionalizing the surface and thus enabling active targeting³. DARPins (designed ankyrin repeat proteins) are recombinant antibody mimetics with high stability and specificity for their targets⁴. In our work, we used DARPin 8h6, which specifically binds to cathepsin B⁵. Stefin A is an endogenous inhibitor of cysteine cathepsins, including cathepsins S and L. Its small size, high stability and absence of disulfide bonds make it appropriate for active targeting.

We successfully prepared liposomes and subsequently conjugated DARPin 8h6 or stefin A to their surface. Both DARPin 8h6 and stefin A conjugated liposomes bound to recombinant cathepsin B or L and S respectively *in vitro*. DARPin 8h6 conjugated liposomes also exhibited greater binding to cancer cells compared to control non-conjugated liposomes, thus confirming their efficiency as a targeting system.

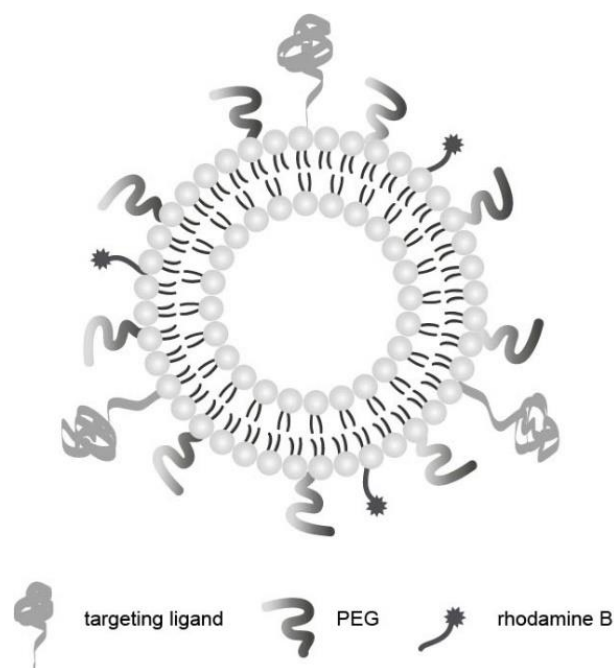


Figure 1: Illustration of a surface-functionalized liposome.

References:

1. Olson, O. C.; Joyce, J. A., Cysteine cathepsin proteases: regulators of cancer progression and therapeutic response. *Nature reviews. Cancer* **2015**, *15* (12), 712.
2. Kramer, L.; Turk, D.; Turk, B., The Future of Cysteine Cathepsins in Disease Management. *Trends in Pharmacological Sciences* **2017**.
3. Allen, T. M.; Cullis, P. R., Liposomal drug delivery systems: from concept to clinical applications. *Advanced drug delivery reviews* **2013**, *65* (1), 36-48.
4. Binz, H. K.; Stumpp, M. T.; Forrer, P.; Amstutz, P.; Plückthun, A., Designing repeat proteins: well-expressed, soluble and stable proteins from combinatorial libraries of consensus ankyrin repeat proteins. *Journal of molecular biology* **2003**, *332* (2), 489-503.
5. Kramer, L. *et al.*, Non-invasive in vivo imaging of tumour-associated cathepsin B by a highly selective inhibitory DARPin. *Theranostics* **2017**, *7* (11), 2806-2821.

Timelapse-Microscopy Analysis of Stochastic Cell Fate Decisions in the Nematode *Caenorhabditis Elegans*

Simone Kienle¹, Nicola Gritti¹, Ana Kriselj^{1,2}, Yvonne Goos¹, Jeroen van Zon^{*,1}

¹Quantitative Developmental Biology, AMOLF, Science Park 104, 1098 XG Amsterdam, Netherlands

²Faculty of Chemistry and Chemical Technology, University of Ljubljana, Večna pot 113, SI-1000 Ljubljana, Slovenia

During gonad development in *C. elegans*, two cells obtain their fate stochastically in a process called AC/VU decision. Wild-type hermaphrodites have only one anchor cell (AC), while in worms where LIN-12 or LAG-2 are absent two AC's can be observed. To study the process of AC/VU decision in live animals we follow *lag-2* gene expression using time-lapse microscopy.

During the development of an organism, cells frequently obtain their fate stochastically. This means that the same cells can obtain different cell fates by randomly choosing one cell fate out of several possible ones. Stochastic cell fate decisions can occur either in a cell autonomous manner or involve communication between neighboring cells with direct contact¹.

As an example of a simple stochastic cell fate decision we chose to study the AC/VU decision in the nematode worm *C. elegans*. During gonad development two cells, Z1.ppp and Z4.aaa, are formed which can become either a so-called anchor cell (AC) or a ventral uterine cell (VU). The genes responsible for the AC/VU decision are already known. Z1.ppp and Z4.aaa interact with each other via Notch signaling with the ligand LAG-2 binding to the Notch receptor LIN-12. So far it was thought that both cells are born with equal amounts of LIN-12 and LAG-2 and that over time a small difference in *lin-12* activity gets amplified into an all-or-nothing decision with *lin-12* being expressed only in the VU cell and *lag-2* only in the AC as shown in Figure 1.

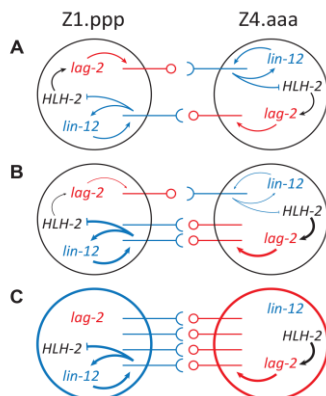


Figure 1: Current model of the AC/VU decision².

To follow the cells and gene expression dynamics over time in live animals we are using a new technique,

which combines microfabrication, fluorescence microscopy and time-lapse microscopy. For this we used polyacrylamide microchambers to capture single animals and image them during their development³.

We imaged animals with *lag-2::YFP* transcriptional reporter and found that mother cells divide around the L2 ecdysis. Most importantly, birth order plays a crucial role in the decision process, with the second born cell being most likely to obtain the AC fate (Figure 2, A). Our most recent studies are focusing on the effect of reduced expression of *lin-12*, to test if Notch signaling defines the birth order factor in the AC/VU decision (Figure 2, B).

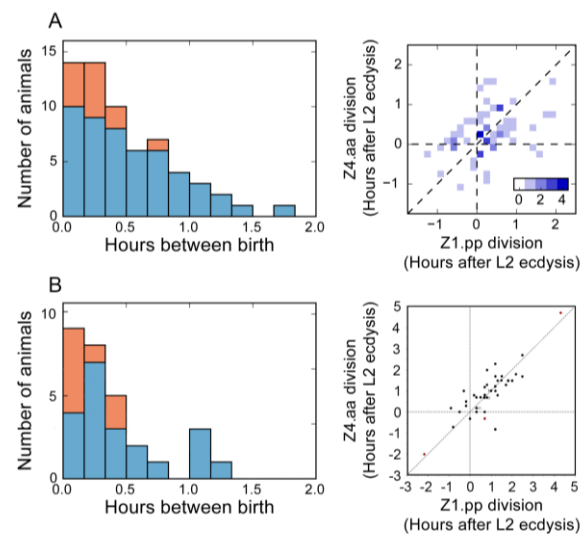


Figure 2: Comparison of the AC/VU decision in *lag-2::YFP* (A) and *lin12(0)* strains (B). The second born cells (blue) are more prone to the AC fate than the first born cells (orange).

References:

1. Losick, R.; Desplan, C., Stochasticity and Cell Fate. *Science* **2008**, *320*, 65-68.
2. Seydoux, G., Greenwald, I.; Cell Autonomy of *lin-12* Function in a Cell Fate Decision in *C. elegans*. *Cell* **1989**, *57*, 1237-1245
3. Gritti, N. *et al*, Long-term time-lapse microscopy of *C. elegans* post-embryonic development. *Nat. Commun.* **2016**, *7*:12500 doi: 10.1038/ncomms12500

Effect of Bacterial Growth Rate on Phage Growth Parameters and Bacteriophage Fitness

Dominik Nabergoj¹, Petra Modić², Aleš Podgornik*,^{1,2}

¹ Center of Excellence for Biosensors, Instrumentation and Process Control - COBIK, Tovarniška cesta 26, SI-5270 Ajdovščina, Slovenia.

² Faculty of Chemistry and Chemical Technology, University of Ljubljana, Večna pot 113, SI-1000 Ljubljana, Slovenia

Bacteriophage therapy is nowadays becoming again a very interesting alternative in fighting against bacterial infections¹. Advantages of bacteriophage therapy in comparison with classical chemical antibiotics are present due to special properties of phages. Main advantages are low inherent toxicity, minimal disruption of normal flora, narrower potential for inducing resistance, rapid discovery and biofilm clearance².

Although, there still exist the problem of robust and efficient production of bacteriophages for purpose of bacteriophage therapy³. In addition, pharmaceutical manufacturing is nowadays changing the trend from a batch to continuous production. Thus, we can speculate that phage production for bacteriophage therapy will follow the same path in the future and new knowledge in this field is required⁴. Due to potential higher phage production needs in the future, it is important to understand how physiological state of the host influence propagation of phages.

In our case, we have performed several experiments in chemostat to better understand how bacterial growth rate influence phage growth parameters (adsorption rate (δ), latent period (L) and burst size (b), respectively) and bacteriophage fitness (λ). Later is defined as an increase of phages in medium over time and can be for a constant bacterial concentration (C) described by following equation⁵:

$$\lambda = \delta \cdot C (b \cdot e^{-L \cdot \lambda} - 1)$$

As a model system, a well-studied phage T4 and *Escherichia coli* K-12 as a host was used. Bacteria was grown in chemostat operating at dilution rates (exactly defines bacterial growth rate) in the range between 0.06 to 0.98 h⁻¹ and when steady state was reached, experiments for determination of phage growth parameters were performed. Table 1 includes the results of phage growth parameters as a function of dilution rate. Bacteriophage fitness was calculated for each dilution rate by inserting experimentally determined phage growth parameters in before mentioned equation. Obtained results are shown in Table 2. Further detailed study is currently underway to confirm obtained trends.

Table 1: Phage growth parameters as a function of dilution rate.

Dilution rate (h ⁻¹)	Adsorption constant (10 ⁻⁹ mL min ⁻¹)	Latent period (min)	Burst size (PFU cell ⁻¹)
0.06	2.6 ± 0.24	80 ± 4	8 ± 2
0.26	1.1 ± 0.19	41 ± 1	20 ± 5
0.50	0.81 ± 0.04	36 ± 4	33 ± 6
0.73	0.42 ± 0.07	29 ± 3	66 ± 7
0.98	0.52 ± 0.04	27 ± 1	89 ± 4

Table 2: Bacteriophage fitness vs. dilution rate.

Dilution rate (h ⁻¹)	Bacteriophage fitness (h ⁻¹)
0.06	2.86
0.26	4.91
0.50	5.73
0.73	6.80
0.98	8.06

References:

1. Reardon, S., Phage therapy gets revitalized. *Nature*. **2014**, *510*, 7503, 15-16.
2. Loc-Carrillo, C.; Abedon, S.T., Pros and cons of phage therapy. *Bacteriophage*. **2011**, *1*, 2, 111-114.
3. Merabishvili, M.; Pirnay, J.P.; Verbeken G., Chanishvili, N.; Tediashvili, M., Quality-Controlled Small-Scale Production of a Well-Defined Bacteriophage Cocktail for Use in Human Clinical Trials. *PLoS ONE*. **2009**, *4*, 3: e4944.
4. Podgornik, A.; Janež, N., Smrekar, F.; Peterka, M., Continuous Production of Bacteriophages, in *Continuous Processing in Pharmaceutical Manufacturing*. Wiley-VCH Verlag GmbH & Co. KGaA, Weinheim, Germany, **2014**.
5. Bull, J.J., Optimality models of phage life history and parallels in disease evolution. *J Theor Biol*. **2006**, *241*, 928-938.

Effect of Dilution Rate on Productivity of Continuous Production of Bacteriophages

Dominik Nabergoj¹, Nina Kuzmič², Aleš Podgornik^{*,1,2}

¹ Center of Excellence for Biosensors, Instrumentation and Process Control - COBIK, Tovarniška cesta 26, 5270 Ajdovščina, Slovenia.

² Faculty of Chemistry and Chemical Technology, University of Ljubljana, Večna pot 113, 1000 Ljubljana, Slovenia

Bacteriophages (phages) are bacterial viruses which are amplified during the process of infection and final lysis of bacteria. As a natural killers of bacteria, phages are nowadays regaining attention due to alarming widespread emergence of bacteria resistant to majority of antimicrobial agents.¹ The advantages of antibacterial effect of phages have already been recognized and bacteriophage therapy was used in various fields such as veterinary medicine,² agriculture,³ food industry,⁴ and also in human medicine.⁵

Amplification of phages on laboratory scale in shaking culture flasks is a routine procedure but for the purpose of bacteriophage therapy higher concentrations and amount of phages are needed. To solve that problem and keeping in mind the increasing interest for continuous production in pharmaceutical industry,⁶ we have decided to elucidate the effect of dilution rate on productivity of continuous production of phages.

For the purpose of this study, previously developed miniature system for continuous cultivation of phages which consists of two connected glass bioreactors (working volume of 25 mL and 5 mL, respectively) and single pump was used. Fresh LB medium was continuously pumped in the first bioreactor where bacteria was growing and continuously introduced into second bioreactor where multiplication of phages occurred. As a model system, a well-studied phage T4 and *Escherichia coli* K-12 as a host was used. The flow rate was set between 0.1 and 0.35 mL min⁻¹ and when the steady state was reached, concentration of phages (P) at the outflow from the second bioreactor was evaluated by standard plaque assay and average values were obtained. Productivity (P_r) of continuous production of phages was calculated from average phage titers (P) and dilution rate (D) in second bioreactor by Equation 1. Table 1 includes the results of our experiments.

$$P_r = P \cdot D \quad (\text{Equation 1})$$

The results from Table 1 indicate that there should exist an optimal value of dilution rate (D_{opt}) at which the productivity of continuous production of phages

should reach maximum value. Further detailed study is currently underway to confirm that hypothesis.

Table 1: Productivity of continuous production of phages as a function of dilution rate.

Flow rate (mL min ⁻¹)	Dilution rate (h ⁻¹)	Average phage concentration (PFU mL ⁻¹)	Average productivity (PFU mL ⁻¹ h ⁻¹)
0.1	1.2	6.24E+07	7.49E+07
0.15	1.8	1.13E+08	2.03E+08
0.2	2.4	2.65E+08	6.35E+08
0.3	3.6	4.80E+08	1.73E+09
0.35	4.2	4.44E+07	1.87E+08

References:

1. Spellberg, B.; Guidos, R.; Gilbert, D.; Bradley, J.; Boucher, H.W.; Scheld, W.M.; Bartlett, J.G.; Edwards, J. Jr., Infectious Diseases Society of America. The epidemic of antibiotic-resistant infections: a call to action for the medical community from the Infectious Diseases Society of America. *Clin. Infect. Dis. Off. Publ. Infect. Dis. Soc. Am.* **2008**, *46*, 155–164.
2. Atterbury, R.J., Bacteriophage biocontrol in animals and meat products. *Microb. Biotechnol.* **2009**, *2*, 601–612.
3. Jones, J.B.; Vallad, G.E.; Iriarte, F.B.; Obradović, A.; Wernsing, M.H.; Jackson, L.E.; Balogh B.; Hong J.C.; Momol, M. T., Considerations for using bacteriophages for plant disease control. *Bacteriophage* **2012**, *2*, 208–214.
4. García, P.; Martínez, B.; Obeso, J.M., Rodríguez A. Bacteriophages and their application in food safety. *Lett. Appl. Microbiol.* **2008**, *47*, 479–485.
5. Abedon S.T., Kuhl S.J., Blasdel B.G., Kutter E.M. Phage treatment of human infections. *Bacteriophage*. **2011**, *1*, 66–85.
6. Lee, S.L.; O'Connor, T.F., Yang, X.; Cruz, C.N.; Chatterjee, S.; Madurawe, R.D.; Moore, C.M.V.; Yu, L.X.; Woodcock J., Modernizing pharmaceutical manufacturing: from batch to continuous production. *J. Pharm. Innov.* **2015**, *10*, 191.

Influence of Waste Prevention on Greenhouse Gases Emissions of Waste Management in Croatia

Predrag Korica^{1,*}, Andreja Cirman², Andreja Žgajnar Gotvajn³

¹ Croatian Agency for the Environment and Nature, Radnička cesta 80, Zagreb, Croatia

² University of Ljubljana, Faculty of Economics, Kardeljeva ploščad 17, SI-1000, Ljubljana, Slovenia

³ University of Ljubljana, Faculty of Chemistry and Chemical Technology, Večna pot 113, 1000, Ljubljana, Slovenia

The reduction, reuse, and recycling of materials and energy are often regarded as three possible approaches of circular economy¹, however, those three approaches can have different influence on the environment regarding the levels of pressures which they create. In this work, the IPCC methodology² was used to determine the differences between 3 scenarios: the Baseline scenario (state as it is), the Scenario of waste recycling increase by 50 % (WRI) and the Scenario of waste generation decrease by 50 % (WGD); regarding their Greenhouse Gas Emissions (GHGE). In order to calculate the scenarios the calculation model was build based on the Life-cycle assessment approach which covers the downstream processes (processes after the product becomes waste – the waste management system)³. The IPCC methodology calculates the GHGE from biological treatment of waste (biogas production from waste and composting of waste); from incineration of waste and from landfilling of waste. For the purpose of this study under the incineration both the incineration with and without energy recovery were considered; and the biological treatments of waste are regarded as recycling operations.

As the case study the data on the waste generation and management of the 638 waste streams in the Republic of Croatia were used. The data were collected from Croatian Agency for the Environment and Nature. As the Baseline scenario the yearly averages for the period 2009-2015 were used. The results show that the dominant source of GHGE from waste management in Croatia is landfilling causing 92 % of total GHGE. In the case of the biological treatment of waste, results show the increase of 50 % in GHGE in WRI, as expected; while in the case of WGD results show the decrease of 52 %. In the case of the incineration of waste the results show the decrease of 34% in the case of WRI and the decrease of 54 % in the favour of WGD. In the case of the landfilling, WRI decreases GHGE only by 2.7 % while the WGD causes decrease of 22 %. In the case of Croatia, the results show that the decrease in waste generation would significantly more decrease the GHGE than the increase in waste recycling in regard to the period observed (Table 1).

Table 1: The Greenhouse emissions of waste management by different scenarios (Gg of CO₂ equivalents)

	Baseline	50% increased recycling	50% decreased generation
Biogas production (NO ₂)	7.32	10.98	3.49
Composting (CH ₄)	63.17	94.76	30.20
Composting (NO ₂)	45.18	67.77	21.60
Total Biological treatment	115.68	173.52 (50%*)	55.28 (-52%*)
Incineration (CH ₄)	0.03	0.02	0.01
Incineration (NO ₂)	0.00	0.00	0.00
Incineration (CO ₂)	85.30	56.28	39.59
Total Incineration	85.33	56.29 (-34%*)	39.61 (-54%*)
Landfilling (CH ₄)	2188.02	2128.48 (-2.72%*)	1711.53 (-21.78%*)
Grand total	2389.03	2358.29 (-1.3%*)	1806.41 (-24%*)

* % of change in regard to Baseline scenario

References:

1. Feng, Z. Circular economy overview. Beijing, China: People's Publishing, **2004**.
2. The Intergovernmental Panel on Climate Change (IPCC) **2017**. [Cited: 25.03.2017] <http://www.ipcc-nggip.iges.or.jp/public/2006gl/>.
3. Cleary, J., The incorporation of waste prevention activities into LCA of municipal solid waste management systems: methodological issues. *Int. J. Life Cycle Assess.* **2010**, 6(15), 579 – 589.

Impact of Antibiotic Tiamulin Fumarate on Extracellular Ligninolytic Enzymes of Fungus *Dichomitus Squalens*

Sanja Popovič*,¹, Gabriela Kalčíková¹, Andreja Žgajnar Gotvajn¹

¹ Faculty of Chemistry and Chemical Technology, University of Ljubljana, Večna pot 113, SI-1000 Ljubljana, Slovenia

In recent years, more and more pharmaceuticals are emerging in the environment. They are used for the treatment and prevention of microbial infections in veterinary medicines and growth promoters in aquaculture in livestock production. They can reach the environment in different ways, for example through animal faeces that are contaminated with antibiotics or by application of manure used for fertilization of fields. Thus the antibiotics located in the fertilizer come into contact with the soil. Heavy rains can wash antibiotics out of the soil and they enter the aquatic ecosystem^{1,2}. For removal of different pollutants such as antibiotics bioremediation is increasingly used. This is a process in which microorganisms are used to transform or decompose pollutants into non-hazardous or less hazardous substances. Bioremediation targets the use of microorganisms that attack pollutants with their enzymes and convert them into harmless compounds³.

The aim of this thesis was to evaluate the efficiency of the extracellular enzymes (laccase and manganese peroxidase (MnP)) of the selected white-rot fungi *Dichomitus squalens* for decomposition of the antibiotic tiamulin. First we assess the impact of inducer to obtain a high enzymatic activity of fungus. We used three different inducers: beech dust of dimensions 0.125-0.300 mm, straw powder of dimensions 0.125-0.300 mm and straw pieces of approximate size 1 cm. The cultures were cultivated on shakers at a temperature of 28 °C and a mixing speed of 150 rpm. In addition, the cultures with straw pieces were also grown without shaking, only in an incubator at a temperature of 28 °C. The pellet form of growth appeared in shaken samples, indicating that the fungus adapted well to submerged cultivation, although the natural tendency of the fungus was to grow on the surface of the substrate rather than in the aqueous medium. In samples that weren't shaken, a filamentous form of growth appeared on the surface of the substrate. As we can see, mixing plays an important role in the pellet formation.

Beech wood stimulates the production of laccase so the highest activities of laccase were with beech wood as an inducer. Although straw stimulates production of MnP, their activities were higher with beech wood.

The other part of experiment was to determinate if these enzymes have ability to degrade tiamulin. In the blank sample, the enzyme filtrate and deionized water were used, while in the other samples tiamulin (400, 800 and 1600 mg/L) was added. In all of the samples the enzymatic activities were increasing vs. time and, if compared to the blank sample, the activities were higher. The activity in the sample with 400 mg/L, 800 mg/L and 1600 mg/L were 50, 61 and 56 %, higher in comparison to control, respectively. Based on the results obtained, we can conclude that the enzymes used tiamulin for their processes and did not pose a problem to their functioning, otherwise the activity would constantly drop.

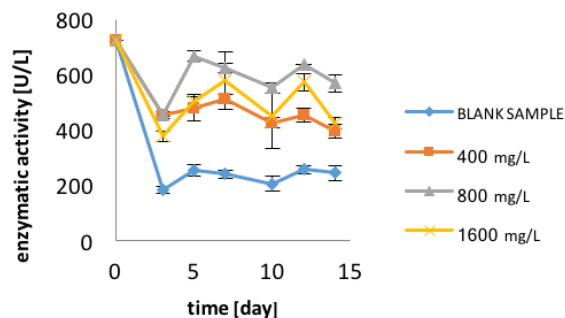


Figure 1: Enzymatic activity of laccase for samples with different concentrations

References:

1. Gulkowska, A., Removal of antibiotics from wastewater by sewage treatment facilities in Hong Kong and Shenzhen, China. *Water research* **2008**, 42, 395 – 403.
2. Schlüsener, M., Fate, pathways and methods for the determination of selected antibiotics and steroid hormones in the environment, Doctoral disertation, The Department of Chemistry of the University of Duisburg-Essen, 2005, str. 1-2.
3. Karigar, C.; Rao, S., Role of Microbial Enzymes in the Bioremediation of Pollutants: A Review. *Enzyme Research* **2011**, 11 p.

Synthesis of Bimetal Fenton-like Catalyst for Wastewater Treatment

Ines Kulašić¹, Anton Meden¹, Alenka Ristić², Nataša Zabukovec Logar^{2,3},
Nataša Novak Tušar^{*,2,3}

¹ Faculty for Chemistry and Chemical Technology, University of Ljubljana, Večna pot 113, 1000 Ljubljana, Slovenia

² National Institute of Chemistry, Hajdrihova 19, 1000 Ljubljana, Slovenia, e-mail: natasa.novak.tusar@ki.si

³ University of Nova Gorica, Vipavska 13, 5000 Nova Gorica, Slovenia

Discharge of wastewater, contaminated with organic pollutants, represents a serious environmental problem. One of the most efficient ways to degrade such pollutants are the so-called advanced oxidation processes (AOP). Their efficiency is based on the generation of strongly oxidizing species (e.g. HO•), which completely decompose organic pollutants and convert them into non-toxic products such as CO₂, H₂O and inorganic species. Among all of the AOPs, traditional Fenton processes have been widely applied for wastewater treatment. The usage of iron as the catalyst in traditional Fenton process is quite common for its high abundance, environmental compatibility, low commercial cost and high reactivity.¹ Although traditional Fenton catalysts represent an efficient way to waste-water treatment, it shows some major drawbacks. Since iron forms ferric hydroxide sludge at pH > 4, acidic conditions (pH ~ 3) are required for practical applications.

A promising alternative of iron as the Fenton-like catalyst is manganese, which has been proven as an effective catalyst working under neutral pH, when incorporated into porous silica support.^{1,2} The major advantage of using manganese instead of iron is the neutral pH of the effluents during the treatment, which means that effluents no longer need to be neutralized before discharge.

However, during a time period, leaching of manganese ions occurs when catalyst is used multiple times. Therefore it is essential to stabilize the latter into the silicate support in order to ensure its recycling. It is possible to do that using another metal and prepare bimetal catalyst.^{3,4} For our project we synthesized bimetal Fenton-like catalyst, incorporating manganese and copper into microporous crystalline (S-1) and mesoporous amorphous silica (KIL-2) supports. Various manganese concentrations (Mn/Si ratio from 0.005 to 0.05) have been used. Copper was incorporated with amount of 6 weight % using incipient wetness impregnation. Copper, added via incipient wetness impregnation, usually incorporates in the form of copper oxide. We wanted to observe, if this happens also with our manganese-functionalized porous silicates. Moreover, we wished to discover

whether or not the concentration of manganese would influence the formation of copper oxide on the surface. XRD, SEM and nitrogen physisorption characterization techniques were used for this purpose. The XRD results suggested that CuO is not formed in the presence of manganese at selected experimental conditions (Figure 1). To get more insight, further study using AR TEM is in progress.

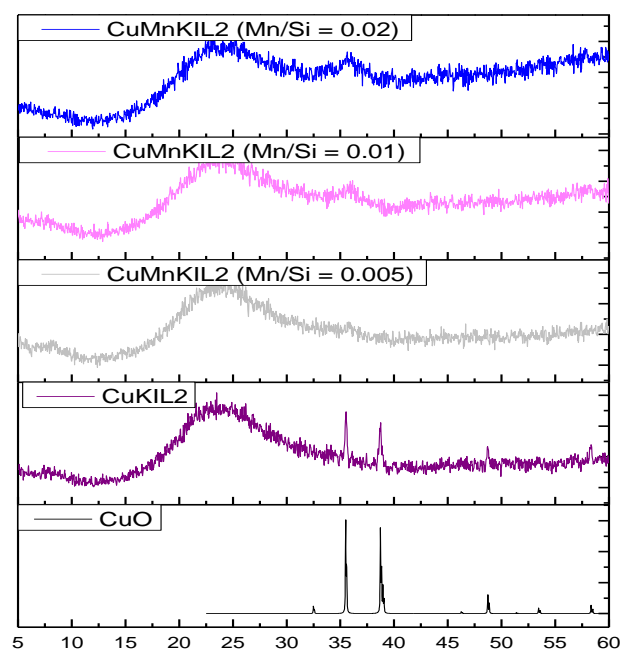


Figure 1: XRD diffractograms of CuMnKIL-2 (Mn/Si molar ratio from 0.02 to 0.005), CuKIL-2 and CuO reference samples.

References:

1. Bokare, A. D., Choi, W., *J. of Hazardous Mater.* **2014**, 275, 121-135.
2. Novak Tušar, N., Maučec, D., Rangus, M., Arčon, I., Mazaj, M., Cotman, M., Pintar, A., Kaučič, V., *Adv. Funct. Mater.* **2012**, 22, 820–826.
3. Gu, J., Zhang, Y.-W., Franklin, T.F., *Chem.Soc.Rev.*, **2012**, 41, 8050-8065.
4. Popova, M., Ristić, A., Mazaj, M., Maučec, D., Dimitrov, M., Novak Tušar, N., *ChemCatChem* **2014**, 6, 271-277.

Numerical Simulation of Ethene Molecular Motion in a Small Chamber

Marian Lukežič¹, Marko Radak¹, Simon Schnabl^{1,*}

¹ Faculty of Chemistry and Chemical Technology, University of Ljubljana, Večna pot 113, 1000 Ljubljana, Slovenia

Ethene ($\text{H}_2\text{C}=\text{CH}_2$) gas is simulated in a chamber as motion of molecules with molecular mass 28 g/mol.

Simulations often use molecules for tracking flows in the observed volume. Several different types of molecules can be monitored simultaneously. The analysis is performed using Fire Dynamics Simulator (FDS) and Pyrosim.

Procedure for defining molecular motion in a observed volume is as follows:

- define the individual gas (appropriate name or gas selection in a predefined database). If the database does not include the wanted gas, then it must be defined with parameters: M , \bar{C} and ε/k .
- define the location and size of the surface through which the gas will enter the observed volume, defining the mass or volume flow of gas,
- define a function that describes how the mass or volume fraction of gas changes with time.

Figures 1, 2, 3, 4 show molecular motion ($\psi_{\text{CO}} = 150$ ppm and $\phi = 10$ mL/min). The three flaps are located on the opposite side according to the source of the molecule inflow. Bottom flap is opened.

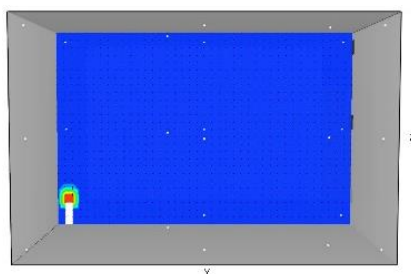


Figure 1: Molecular motion simulation, $t = 1,0$ s.

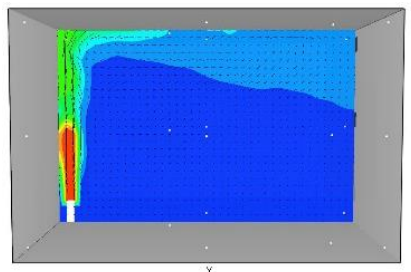


Figure 2: Molecular motion simulation, $t = 60,0$ s.

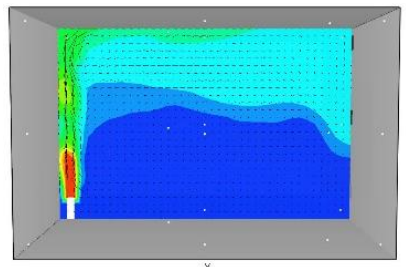


Figure 3: Molecular motion simulation, $t = 120,0$ s.

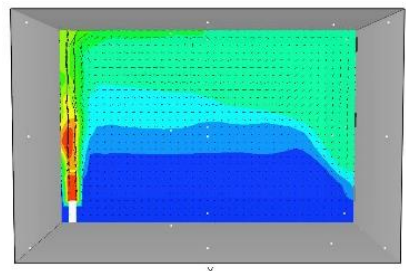


Figure 4: Molecular motion simulation, $t = 180,0$ s.

Due to numerical analysis of molecular motion we can conclude the following:

- Molecule movement of hot or warm molecules in the chamber depends on buoyancy of warm air. Molecules above the source point move vertically to the ceiling, where they incline and move towards the chamber walls and then down to the bottom, from where they move back to the source point.
- With exception to nearby locations of the flap opening, the influence of the bottom flap opening on molecule distribution can be neglected.
- Influence of molecule quantity on concentration is as expected high, but does not influence on molecule movement. After a certain time period the concentration of molecules in all measurement points is proportional to the injected share of molecules.

References:

1. A. J. Chorin, J. E. A. Marsden. *Mathematical Introduction to Fluid Mechanics*. Springer-Verlag New York, **1993**, 3th ed., Vol. 4, 172.
2. R.C. Reid, J. M. Prausnitz, and B. E. Poling. *Properties of Gases and Liquids*. McGraw-Hill, New York, **1987** 4th ed., 116.

Correlation Between Surface Roughness and Wetting Properties of Stainless Steel Surfaces

Domen Žalec*, Matic Može, Mark Lakić, Mihael Turkovic, Matevž Zupančič

Faculty of Mechanical Engineering, University of Ljubljana, Aškerčeva 6, 1000 Ljubljana, Slovenia,
domen.zalec@gmail.com

Surface roughness and its wettability and wickability are important factors in many applications including boiling heat transfer engineering^{1,2}. Most methods that modify the wetting properties of a surface e.g. laser texturing, application of coatings, etching etc. also change the structure and roughness of the surface. In our research, we focused on finding possible correlations between the surface roughness of a stainless steel surface and its wetting properties. In order to establish whether such correlation(s) exist, multiple stainless steel samples were either polished or sanded by hand using sandpaper with grit sizes ranging from P100 to P1000 (according to ISO 6344 standard). Multiple tests including static contact angle measurement and measurement of 1D roughness parameters experiments were performed and repeated multiple times on every surface.

Samples measuring 17x50 mm² with a thickness of 0,635 mm were made from a sheet of SAE 304 steel. Eighteen samples were prepared in total including two untreated controls. Seven different treatments were used and each of them was applied to a pair of samples by a different experimenter. All samples were rigorously cleaned using tap water and 96 % ethanol prior to any treatment and after it. Sanding was performed in only one direction (parallel to the longer edge of the sample) using 200 strokes and a new sandpaper every 20 strokes.

Surface wettability was tested through static contact angle measurements using double-distilled water at room temperature. A small droplet was deposited on each surface multiple times, photographed and wiped off. The images were then processed using appropriate software to determine the contact angles on both sides of each droplet (see Figure 1). Since the surface structure was directional on sanded samples, different angles were recorded depending on the orientation of the camera in regards to the sample; uneven spreading of water droplets was both expected and observed. Overall, the wettability of samples treated with finer sandpaper was lower than that of the samples that were sanded using lower grit sandpaper.

Roughness parameters R_a , R_z , R_y and R_q were measured using a portable surface roughness tester (Mitutoyo) to determine the arithmetic mean deviation

of the profile, the maximum height of the profile etc. As expected, recorded roughness parameters were the highest on the surfaces treated using sandpaper with low grit sizes. There were also significant differences between both directions of measurement (perpendicular and parallel to sanding direction).

The summarized results indicate that a rather complex correlation between surface roughness and its wetting properties certainly exists. Lower roughness resulted in higher static contact angles and subsequently inferior wetting properties of surfaces. Our results mostly concur with the results of other studies in the field³ but show some discrepancies that should be addressed in a follow-up study.

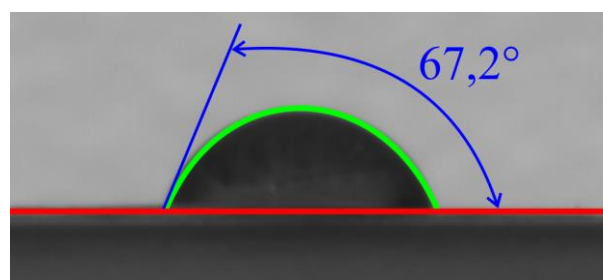


Figure 1: An example of static contact angle measurement using a deposited water droplet.

References:

1. Kim, B. S.; Lee, H.; Shin, S.; Cho, H. H. Interfacial wicking dynamics and its impact on critical heat flux of boiling heat transfer. *Appl. Phys. Lett.* **2014**, 105 (19), 191601.
2. Ahn, H. S.; Park, G.; Kim, J. M.; Kim, J.; Kim, M.H. The effect of water absorption on critical heat flux enhancement during pool boiling. *Exp. Therm. Fluid Sci.* **2012**, 42, 187–195.
3. Kubiak, K. J.; Wilson, M. C. T.; Mathia, T. G.; Charval, Ph. Wettability versus roughness of engineering surfaces. *Wear* **2011**, 271 (3–4), 523–528.

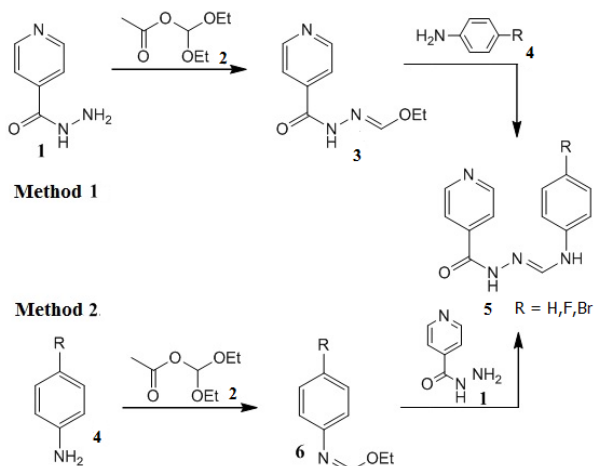
Reactions of Ethoxymethylene Hydrazones with Anilines

Eva Žos¹, Marko Krivec¹, Janez Košmrlj^{*,1}

¹ Faculty of Chemistry and Chemical Technology, University of Ljubljana, Večna pot 113, SI-1000 Ljubljana, Slovenia

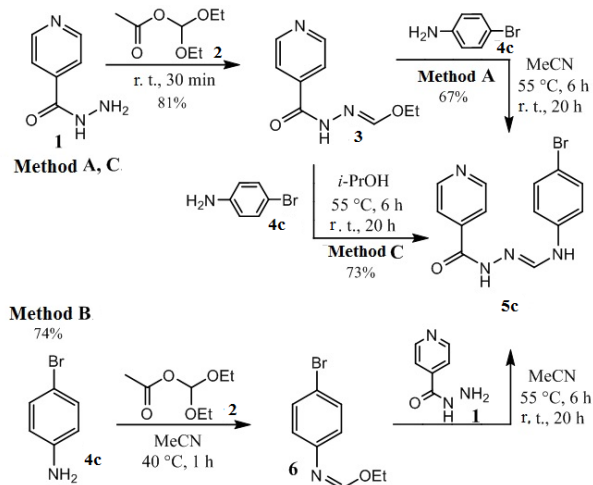
Heterocyclic hydrazones constitute an important class of biologically active compounds, which have attracted attention of medicinal chemists due to their activities¹. Isonicotinic acid hydrazide (isoniazid) belongs to the group of the first line anti-tuberculous drugs being in clinical practice over 50 years. Chemical modifications of isoniazid have been performed at all parts of the molecule, and its combination with other active molecules is frequently applied². Hydrazones are also known as a good source of a C₁ fragment that can participate in the formation of either C-N or C-C bond. Thus, upon treatment of ethoxymethylene hydrazones with primary or secondary amines, affords corresponding formamidrazones³.

In this research, the synthesis of selected formamidrazones **5** was performed through the conversion of isoniazid (**1**) into ethoxymethylene hydrazine **3** and subsequent reactions with anilines **4** (Scheme 1, Method 1).⁴ An alternative approach involved the reaction of the aniline **4** with diethoxymethyl acetate (**2**), which upon substitution with isoniazid provided the desired compounds **5** (Scheme 1, Method 2).



Scheme 1: The synthetic pathways of selected formamidrazones

p-Bromo substituted product **5c** was prepared by three different approaches, which gave different yields (Scheme 2).



Scheme 2: Three different approaches for the preparation of product **5c**.

All synthesized compounds have been characterized by melting point, ¹H NMR spectroscopy, IR spectroscopy, and HRMS. As evident from the ¹H NMR spectra, the compounds were present in multiple isomeric forms.

References:

- Özdemir A.; Kaplancıklı Z.A.; Turan-Zitouni G.; Revial G., Synthesis of some novel hydrazone derivatives and evaluation of their antituberculosis activity. *Marmara Pharm. J.* **2010**, *14*, 79–83.
- Vavříková E.; Polanc S.; Kočevár M.; Košmrlj J.; Horváti K.; Bősze S.; Stolaříková J.; Imramovský A.; Vinšová J., New series of isoniazid hydrazones linked with electron-withdrawing substituents. *Eur. J. Med. Chem.* **2011**, *46*, 5902–5909.
- Imramovský A.; Polanc S.; Vinšová J.; Kočevár M.; Jampílek J.; Rečková Z.; Kaustová J., A new modification of anti-tubercular active molecules. *Bioorg. Med. Chem.* **2007**, *15*, 2551–2559.
- Košmrlj B.; Koklič B.; Polanc S.: Transformations of hydrazine derivatives. Ethoxymethylene hydrazones as powerful reagents in organic synthesis. *Acta Chim. Slov.* **1996**, *43*, 153–162.

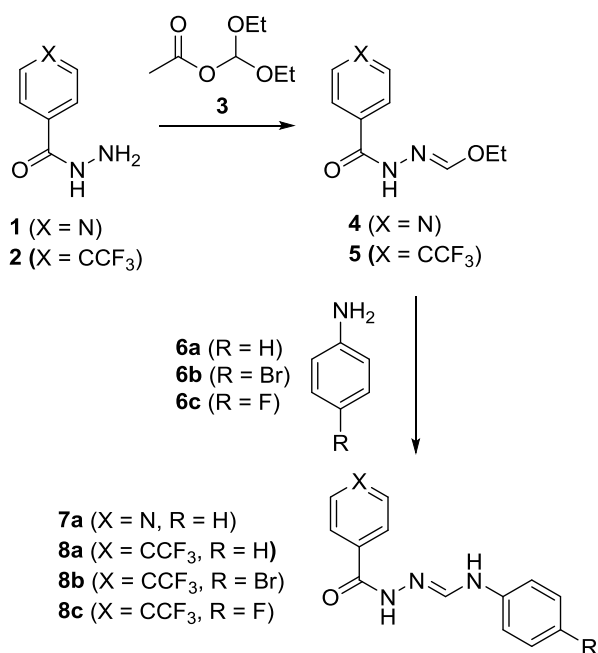
The Synthesis of Selected Hydrazoneformamides

Anže Pavlin¹, Marko Krivec¹, Janez Košmrlj^{*,1}

¹ Faculty of Chemistry and Chemical Technology, University of Ljubljana, Večna pot 113, SI-1000 Ljubljana, Slovenia; e-mail: janez.kosmrlj@fkkt.uni-lj.si

This research project is aimed at finding new hydrazoneformamide derivatives of anti-tubercular activity.

For a drug to be efficient, it is important to possess appropriate hydrophilic/hydrophobic properties, certain physicochemical characteristics, and that the adducts potentially formed produce an observable biological response¹. It has been previously suggested that the methine linker in the hydrazoneformamide structure enables hydrolysis under the physiological conditions and release of the hydrazine and the aniline parts. The combined molecule of hydrazoneformamide thus serves as a prodrug. Involvement of fluoroquinolones as second line antituberculars to the potential active molecule seems to be promising².

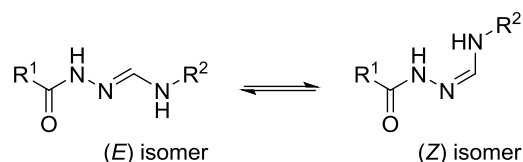


Scheme 1: Synthesis of hydrazoneformamides **7** and **8**.

The synthetic pathway was based on the preparation and subsequent conversion of ethoxymethylene hydrazones **4** and **5** with nitrogen nucleophiles **6**. We have thus prepared several hydrazoneformamides **7a** and **8a-c** (Scheme 1).

We have observed that the synthesized derivatives **4**, **5**, **7**, **8** with C=N double bond exist in solution in two

isomeric forms, *E* and *Z* (Scheme 2). This phenomenon was already previously detected and described³.



Scheme 2: *E* and *Z* isomers.

Additionally, we determined the ratio between *E* and *Z* isomers of intermediate **3** in two different deuterated solvents with ¹H NMR spectroscopy (Table 1).

Table 1: Ratio between *E* and *Z* isomers of intermediate **3** in different deuterated solvents.

Ratio <i>E</i> : <i>Z</i>	
DMSO- <i>d</i> ₆	1 : 0.5
CDCl ₃	1 : 0.2

References:

- Ventura, C.; Martins, F., Application of Quantitative Structure–Activity Relationships to the Modeling of Antitubercular Compounds. 1. the Hydrazide Family. *J. Med. Chem.* **2008**, *51*, 612-624.
- Vavříková, E.; Polanc, S.; Kočever, M.; Horváti, K.; Bösze, S.; Stolaříková, J.; Vávřova, K.; Vinšová, J., New fluorine-containing hydrazones active against MDR-tuberculosis. *Eur. J. Med. Chem.* **2011**, *46*, 4937-4945.
- Košmrlj, B.; Koklič, B.; Polanc, S., Transformations of hydrazine derivatives. Ethoxymethylene hydrazones as powerful reagents in organic synthesis, *Acta Chim. Slov.* **1996**, *43*, 153-162.
- Vavříková, E.; Polanc, S.; Kočever, M.; Košmrlj, J.; Horváti, K.; Bösze, S.; Stolaříková, J.; Imramovský, A.; Vinšová, J., New series of isoniazid hydrazones with electron-withdrawing substituents. *Eur. J. Med. Chem.* **2011**, *46*, 5902-5909.

Organoruthenium-Clioquinol Complex Impairs Tumour Cell Invasion by Inhibiting Cathepsin B Activity

Jakob Kljun^{1,*}, Ana Mitrović², Izidor Sosič², Stanislav Gobec², Iztok Turel¹, Janko Kos^{2,3}

¹ Faculty of Chemistry and Chemical Technology, University of Ljubljana, Večna pot 113, 1000 Ljubljana

² Faculty of Pharmacy, University of Ljubljana, Aškerčeva 7, 1000 Ljubljana, Slovenia, Slovenia

³ Department of Biotechnology, Jožef Stefan Institute, 1000 Ljubljana, Slovenia

Over the past years, organometallic compounds, including organoruthenium compounds, gained a lot of attention as anticancer agents. The flagship compound of the Turel group [Ru(η^6 -*p*-cymene)Cl(cq)] (**1**; Figure 1); cqH = clioquinol was first investigated as potential anticancer agent and it was demonstrated that induces caspase-dependent cell death in leukaemia cells. This activity is copper independent and is improved compared to the parent compound, clioquinol. The study of the mode of action reveals that this clioquinol–ruthenium complex does not intercalate between DNA base pairs. Additionally, this clioquinol–ruthenium complex shows proteasome-independent inhibition of the NF κ B signalling pathway, with no effects on cell-cycle distribution. These data suggest a mechanism of action that involves a target profile that is different from that for clioquinol alone.¹

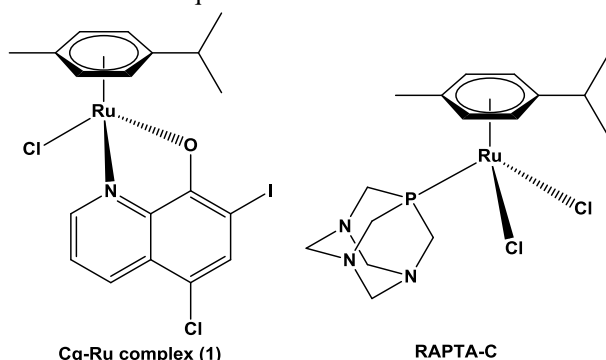


Figure 1: Structures of ruthenium-clioquinol complex (**1**) and established ruthenium antimetastatic agent RAPTA-C

Encouraged by the preliminary results we decided to perform an in-depth study of the mode of action of this compound. We discovered that complex **1** is a potent inhibitor of cathepsin B, a lysosomal cysteine peptidase, involved in tumour cell invasion and metastasis. In the low micromolar concentration range, the clioquinol-ruthenium complex did not exhibit cytotoxic effects on MCF-10A neoT and U-87 MG cells; it did, however, significantly reduce their ability for extracellular matrix degradation and invasiveness in two independent cell-based models, measuring either electrical impedance in real time or the growth of multicellular tumour spheroids implanted in Matrigel, a

model representing the extracellular matrix. These results confirm the clioquinol-ruthenium complex (**1**) as being an effective inhibitor of tumour invasion with potency similar to that established for the ruthenium complex RAPTA-C.²

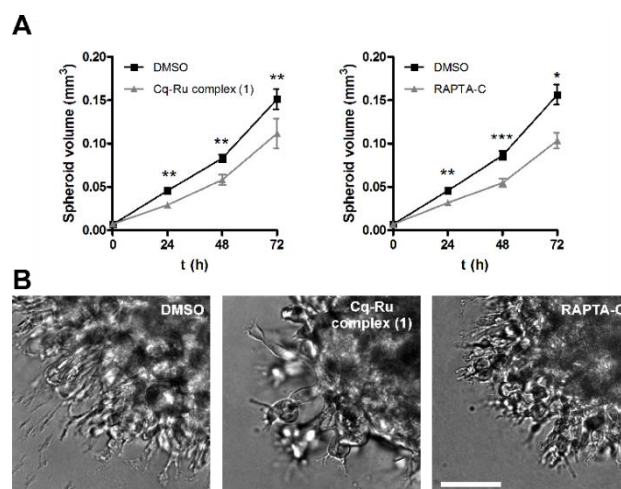


Figure 2: Clioquinol-ruthenium complex (**1**) and RAPTA-C impair invasion of U-87 MG cells in a 3D in vitro model of tumour invasion. **(A)** U-87 MG MCTS were implanted in Matrigel (5 mg/mL) and covered with growth medium, both containing DMSO (0.05%) or the respective compound (1.25 μ M). The MCTS volume was monitored for up to three days by measuring the spheroid dimensions. Data are presented as means \pm SEM ($n = 2$). **(B)** Representative images of U-87 MG MCTS were obtained at day three after implantation. Scale bar, 100 μ m. * $P < 0.05$, ** $P < 0.01$, *** $P < 0.001$.

References:

- Gobec, M.; Kljun, J.; Sosič, I.; Mlinarič-Raščan, I.; Uršič, M.; Gobec, S.; Turel, I., Structural characterization and biological evaluation of a clioquinol-ruthenium complex with copper-independent antileukaemic activity. *Dalton Trans.* **2014**, 43, 9045-9051.
- Mitrović, A.; Kljun, J.; Sosič, I.; Gobec, S.; Turel, I.; Kos, J., Clioquinol-ruthenium complex impairs tumour cell invasion by inhibiting cathepsin B activity. *Dalton Trans.* **2016**, 45, 16913-16921.

Lipid Droplets Protect Cancer Cells From Lipotoxicity And Oxidative Stress

Ana Kump^{1,2}, Eva Jarc^{1,2}, Petra Malavašič¹, Ema Guštin¹, Toni Nagode¹, Anja Pucer Janež¹, Thomas O. Eichmann³, Robert Zimmermann³ and Toni Petan^{*,1}

¹ Department of Molecular and Biomedical Sciences, Jožef Stefan Institute, Ljubljana, Slovenia

² Jožef Stefan International Postgraduate School, Ljubljana, Slovenia

³ Institute of Molecular Biosciences, University of Graz, Graz, Austria

One of the hallmarks of cancer is the ability of cancer cells to adapt and survive in stressful, nutrient and oxygen-deprived conditions. Recent studies have revealed that scavenging fatty acids from the tumour microenvironment enables cancer cell survival during stress, but excessive amounts of free fatty acids can also be toxic to cells (lipotoxicity). Breast cancer cells are often exposed to high amounts of extracellular fatty acids derived from neighboring adipose tissue. Thus, their ability to regulate the pro-survival and lipotoxic activities of fatty acids is critical for tumour progression. Clarifying these regulatory mechanisms may provide new therapeutic opportunities in breast cancer¹.

Elevated accumulation of lipid droplets has been observed in different cancers and cells exposed to nutrient or oxidative stress². Lipid droplets are organelles that regulate the uptake, storage and use of lipids according to cellular needs³. They store triglycerides (TAGs) and cholesterol esters and accumulate in cells exposed to excess free fatty acids to reduce their lipotoxicity. However, the role of lipid droplets in the regulation of lipotoxicity and the protection of cancer cells from stress is still not understood. The main aim of this study was to examine whether we can affect the lipotoxicity of extracellularly-derived polyunsaturated fatty acids (PUFAs) in highly invasive breast cancer cells by altering the fatty acid composition of lipid droplets or by interfering with lipid droplet synthesis or breakdown. We found that high micromolar concentrations of PUFAs, but not oleic acid, induce lipid droplet accumulation, oxidative stress and cell death in breast cancer cells. Inhibiting TAG synthesis by targeting the diacylglycerol acyltransferase 1 (DGAT-1) enzyme led to a decrease in lipid droplet amount and an increase PUFA lipotoxicity. On the contrary, we found that reducing fatty acid release from PUFA-rich lipid droplets by suppressing TAG lipolysis via depletion of adipose triglyceride lipase (ATGL) leads to a reduction in lipotoxicity. Finally, we show that the secreted phospholipase A2 (sPLA2) enzyme hydrolyses plasma membrane phospholipids, induces

lipid droplet accumulation and reduces PUFA-induced cell damage. Remarkably, our lipidomic analyses revealed that sPLA2 increases the proportion of fatty acids with low unsaturation levels stored in lipid droplets, thus effectively segregating and protecting the oxidation-prone PUFAs within lipid droplets. In summary, lipid droplets are antioxidant and pro-survival organelles that protect cancer cells against oxidative stress and PUFA lipotoxicity. Therefore, inhibiting lipid droplet formation or stimulating lipolysis may provide new therapeutic opportunities for targeting invasive breast cancer.

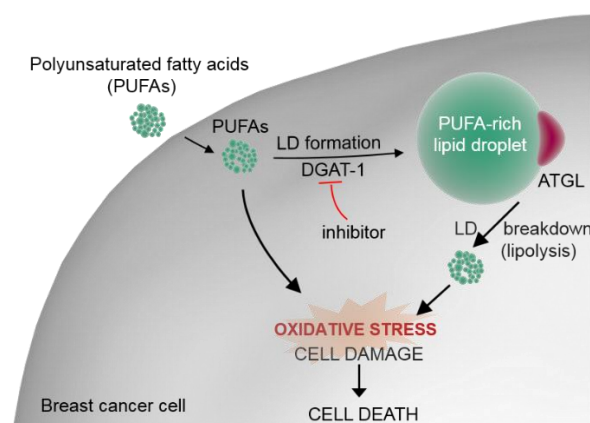


Figure 1: Lipid droplets protect from lipotoxicity by storing PUFAs.

References :

1. N.N. Pavlova, C.B. Thompson, The Emerging Hallmarks of Cancer Metabolism, *Cell Metab.*, 23 (2016) 27–47.
2. Schumacker, P., Reactive Oxygen Species in Cancer: A Dance with the Devil. *Cancer Cell* 2015, 27, 156-157.
3. Pucer, A., Group X secreted phospholipase A2 induces lipid droplet formation and prolongs breast cancer. *Mol. Cancer* 2013, 12:111.

Corrosion Monitoring by Utilizing Electrochemical Impedance Spectroscopy and Visual Inspection Evaluation

Klemen Berlec¹, Anja Ajdovec¹, Rok Narobe¹, Nika Prosen¹, Martin Rozman¹, Barbara Vrečer¹, Gregor Marolt¹, Saša Skale², Janez Cerar^{*,1}

¹ Faculty of Chemistry and Chemical Technology, University of Ljubljana, Večna pot 113, 1000 Ljubljana, Slovenia

² SKALA, Ekološko-tehnično svetovanje, sanacije, površinske zaščite kovinskih in betonskih površin Saša Skale s.p., Lušečka vas 30, SI-2319 Poljčane, Slovenia

Corrosion is the gradual deterioration of materials, typically metals. It is a costly worldwide problem and expenses appear in many different sectors, such as infrastructure, utilities, transportation, production, manufacturing, etc. In addition to the huge cost in economic terms, corrosion is also the source of many of the disasters that cause loss of lives and devastating pollution to the environment. Our society would therefore greatly benefit from innovative solutions in this area and to be able to provide such solutions, even more systematic studies are necessary.

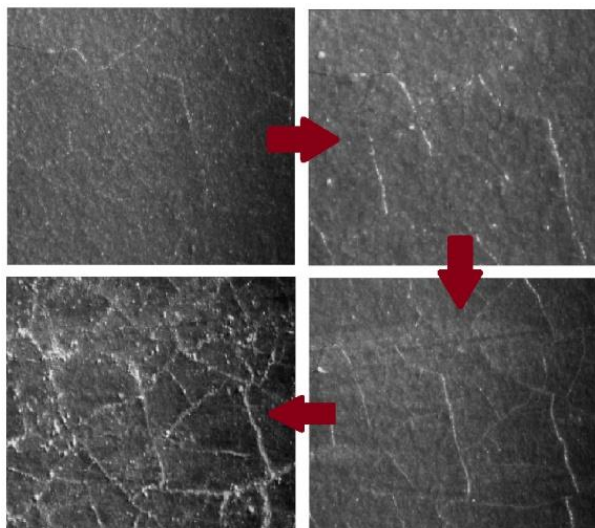


Figure 1: Optical photomicrography of a cracking anti-corrosion coating (40× magnification).

In our study, degradation and consequent corrosion of various coatings on steel plates were monitored. Three different types of coatings were investigated (one of them was applied in several thicknesses). The coated plates were exposed in different environments (according to ISO standards) and degradation was monitored using well-established visual inspection¹ and electrochemical impedance spectroscopy (EIS)^{2,3}. Our objective was to examine and compare results of the two methods.

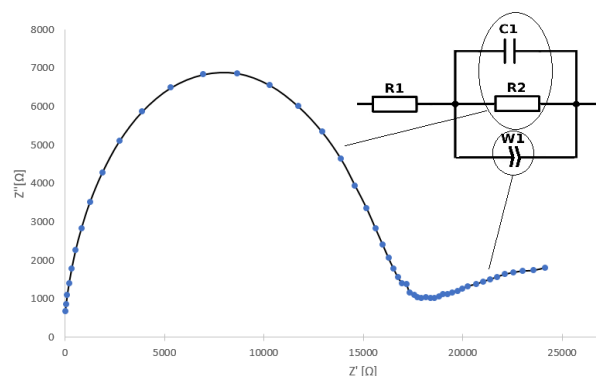


Figure 2: Projected electric circuit fitted to the measured EIS spectrum.

The development of corrosion on a very fundamental level was interpreted by fitting various electrical circuits to the EIS experimental data. Our interpretations were compared with visually observing specific traits characteristic to every stage of corrosion.

Moreover, the amount of leached lead from the coating was measured by using polarography. These observations are of interest because of heavy metal ions' environment pollution.

The presented work will be a minor contribution towards the understanding of the differences between the two important corrosion evaluation methods.

References:

1. Leidheiser, H. Jr. Corrosion of Painted Metals—A Review. *Corrosion*. **1982**, 38, 374-383.
2. Skale, S. Vrednotenje protikorozijske zaščite z epoksi premazi s pomočjo elektrokemijske impedančne spektroskopije. Ph. D. Dissertation, Faculty of Chemistry and Chemical Technology, Maribor, **2009**.
3. Rammelt, U.; Reinhard G. Application of electrochemical impedance spectroscopy (EIS) for characterizing the corrosion-protective performance of organic coatings on metals. *Prog. Org. Coat.* **1992**, 21, 205-226.

Structural Features of α -Hydrazino Peptidomimetics as Potential Modulators of p53-MDM2 Interaction

Luka Kavčič¹, Gregor Ilc^{2,4}, Kristina Vlahoviček-Kahlina³, Ivanka Jerić³, Janez Plavec^{*,1,2,4}

¹ Faculty of Chemistry and Chemical Technology, University of Ljubljana, Večna pot 113, SI-1000 Ljubljana, Slovenia

² Slovenian NMR Centre, National Institute of Chemistry, Hajdrihova ulica 19, SI-1000 Ljubljana, Slovenia

³ Division of Organic Chemistry and Biochemistry, Ruđer Bošković Institute, Bijenička cesta 54, 10000 Zagreb, Croatia

⁴ EN-FIST Centre of excellence, Trg Osvobodilne fronte 13, SI-1000, Ljubljana, Slovenia

Life at the molecular level exists as a complex interplay of cellular biomolecules. Many physiological as well as pathological processes require highly specific protein-protein interactions and their modulation is an attractive route in the field of drug design. However, targeting these interactions is usually a very challenging task compared to receptor or enzyme inhibition because of the vast variety of proteins' binding interfaces. In order to tackle this problem, peptidomimetics that imitate protein-like secondary structures were introduced, which can adapt and bind competently to large surfaces. Hydrazino peptides possess substitutions of natural amino acids with α -hydrazino counterparts and can be perceived as derivatives of β -peptides with nitrogen replacing the additional C β atom in the main chain. Because of backbone extension with NH group acting as hydrogen bond donor as well as acceptor, they can form non-canonical secondary structures because of rearrangement of intramolecular hydrogen bond pattern¹.

p53 is the central tumour suppressor protein, which is known to be overly repressed by upregulated MDM2 protein in cancer cells. Based on the minimal octapeptide p53-derived sequence, required to bind MDM2 with μ M affinity, a series of hydrazino peptides were synthesized in order to finely modulate this interaction by altering the number and the position of α -hydrazino acid substitutions².

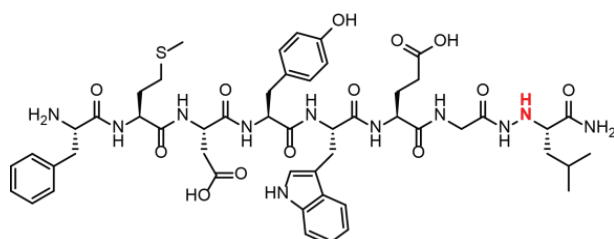


Figure 1: Structure of α -hydrazino peptidomimetic with the additional amino group in the peptide backbone marked in red.

Comparison of chemical shifts for HN, H α and C α resonances of the α -hydrazino peptide (Figure 1) with parent sequence peptide in DMSO- d_6 indicates that the hydrazino group affects mainly the local chemical environment. Detailed analysis of NMR spectra revealed two resolved sets of signals for HN and H α protons of flanking residues, which could be attributed based on previous work on α -hydrazino oligomers³ to E/Z isomerism of the hydrazide link (Figure 2).

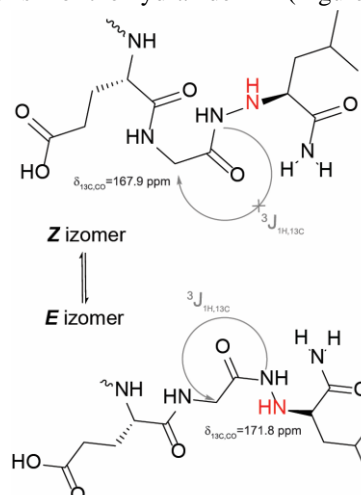


Figure 2: Conformational equilibrium between E and Z isomer of α -hydrazino peptidomimetic. Only three C-terminal residues are shown for clarity.

1. Avan, I.; Hall, C. D.; Katritzky, A. R. Peptidomimetics via modifications of amino acids and peptide bonds. *Chem. Soc. Rev.* **2014**, 43, 3575-3594.
2. Suć, J.; Tumir, L.-M.; Glavaš-Obrovac, L.; Jukić, M.; Piantanida, I.; Jerić, I. The impact of α -hydrazino acids embedded in short fluorescent peptides on peptide interactions with DNA and RNA. *Org. Biomol. Chem.*, **2016**, 14, 4865–4874.
3. Le Grel, P.; Salaün, A.; Mocquet, C.; Le Grel, B.; Roisnel, T.; Potel, M. Z/E Isomerism in N $^{\alpha}$ -N $^{\alpha}$ -Disubstituted Hydrazides and the Amidoxo Bond: Application to the Conformational Analysis of Pseudopeptides Built of Hydrazinoacids and α -Aminooxyacids. *J. Org. Chem.*, **2011**, 76, 8756–8767.

Use of Carbohydrate-binding Proteins for Affinity Separation of Glycoproteins

Rok Miklavčič¹, Katja Hrovat Arnež¹, Gregor Gunčar^{*, 1}

¹ Faculty of Chemistry and Chemical Technology, University of Ljubljana, Večna pot 113, SI-1000 Ljubljana, Slovenia

Carbohydrate-binding proteins are proteins that bind free or bound sugars but do not modify them. The main group of carbohydrate-binding proteins are lectins that are present in a diversity of organisms. Many other proteins, like viral hemagglutinins, are also capable of binding sugar moieties but are not classified as lectins. Carbohydrate binding proteins exhibit a wide variety of specificity for monosaccharides or oligosaccharides displayed on glycoproteins and cell surfaces¹. Interactions of carbohydrate-binding proteins with saccharides are usually relatively weak, which ensures specificity, but still permits dissociation.

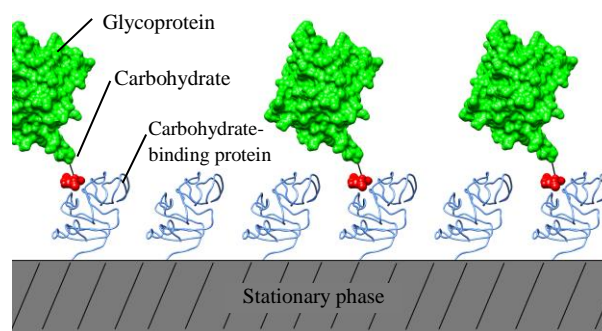
Protein glycosylation is one of the most important post-translational modifications of proteins, contributing to stability, function, recognition and folding of proteins. Abnormal glycosylation state of cellular components was found to be correlated with cancer progression and malignancy². Additionally, many biological drugs are glycoproteins and require correct glycans for their biological activity. Since lectins exhibit high glycospecificity, they present suitable analytical tools for distinguishing protein glycoforms by means of affinity chromatography, blotting or enzyme-linked assays^{1,2}. However, lectins used for these methods are frequently isolated from plants, having the downside of complicated protein purification with low yields. On the other hand, recombinant techniques and large scale fermentation with simple organisms (such as *E. coli*) offer a chance for production of large quantities of proteins³.

In this work we selected two carbohydrate-binding proteins for high yield production in *E. coli* BL21[DE3]pLysS. First protein was the rhesus rotavirus hemagglutinin, which exhibits binding specificity for glycans with terminal N-acetylneuraminic acid, a frequent feature of human glycoproteins. The second protein was rPA-ILNmE6, a mutated form of *Pseudomonas aeruginosa* lectin PA-IL, which binds disaccharide Gal β 1-4GlcNAc³. Synthetic genes optimized for *E. coli* codon usage were cloned in bacterial expression plasmid pMCSG7 under the T7 promoter. Soluble His-tagged proteins were produced utilizing optimized autoinduction protocol and ZYM-5052 media with yields of approximately 30 mg of protein per litre of culture. Proteins were isolated with immobilized metal affinity chromatography in

high purity. We also designed an affinity chromatography based assay using isolated proteins to determine their ability to bind sialoprotein fetuin (Fig. 1). For affinity chromatography, fetuin was injected on Ni Sepharose columns, packed with VP8 or rPA-ILNmE6. SDS-PAGE analysis of fractions confirmed different interactions of fetuin with VP8-packed column compared to rPA-ILNmE6-packed column.

This work highlights the possibility for plentiful production of carbohydrate-binding proteins in *E. coli* and their use to distinguish protein glycoforms with a simple chromatography-based assay.

Figure 1: Scheme of affinity chromatography assay with carbohydrate-binding proteins for separation of glycoproteins.



References:

1. Lam, S. K.; Ng, T. B. Appl. Microbiol. Biotechnol. 2011, 89 (1), 45–55.
2. Yang, Z.; Hancock, W. S. J. Chromatogr. A 2004, 1053 (1–2), 79–88.
3. Keogh, D.; Thompson, R.; Larragy, R.; McMahon, K.; O'Connell, M.; O'Connor, B.; Clarke, P. Biochim. Biophys. Acta 2014, 1840 (6), 2091–2104.
4. Dormitzer, P. R.; Sun, Z.-Y. J.; Blixt, O.; Paulson, J. C.; Wagner, G.; Harrison, S. C. J. Virol. 2002, 76 (20), 10512–10517.

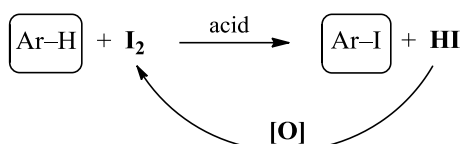
Exploiting Hydrogen Peroxide's Potential in Oxidative Iodination of Arenes

Rok Narobe¹, Jernej Iskra^{*,1}

¹ Faculty of Chemistry and Chemical Technology, University of Ljubljana, Večna pot 113, SI-1000 Ljubljana, Slovenia

Iodinated aromatic compounds are important intermediates in a synthesis of various pharmaceutical and bioactive substances. There are a lot of classical methods for synthesis of those intermediates, but they are often concerning in terms of sustainable development. These methods often require the use of heavy metals reagents and strong oxidizing agents. Therefore, the development of new “green” iodination methods is still an open research topic.

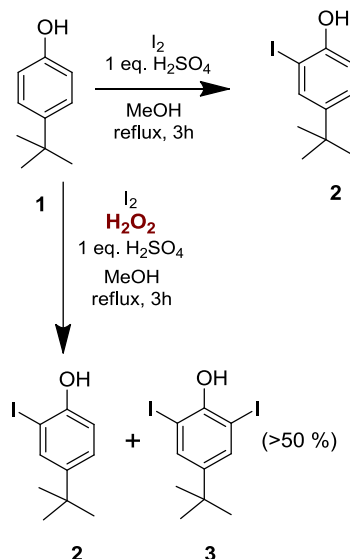
Iodine itself is quite an unreactive electrophile, therefore it requires some form of activation. To overcome the problem of low reactivity of iodine, iodination is often performed under oxidative conditions in strongly acidic media¹ (Scheme 1).



Scheme 1: Oxidative iodination of an arene

The oxidative media enables the use of additional 50 mol% of iodine for electrophilic iodination by converting HI to I₂. By using hydrogen peroxide as a “green” oxidant, it is possible to create a “green” oxidative iodination process.

In course of our research of oxidative iodination of arenes, we observed unexpected iodination rate acceleration and selectivity while using hydrogen peroxide as an oxidant (Scheme 2). This is an intriguing observation because iodine is known to form many species varying from polyiodide species (I₃⁻, I₅⁻) to various “I⁺” species (e.g. ICl)² and even more oxidized iodine species. Our observation suggests that hydrogen peroxide plays an important role in converting some less reactive iodine species to another more reactive. Moreover, some of the iodine oxidation reactions are autocatalytic (e.g. formation of IO₃⁻)³. The latter might carry some yet unexploited potential.



Scheme 2: Hydrogen peroxide's effect on the selectivity of iodination

Our focus will be on clarifying which iodine species causes the observed reaction rate difference while using hydrogen peroxide in the iodination process. We will also present our attempts of exploiting autocatalytic reactions in iodinating process. Furthermore, we investigated if the same applies also to other halogenation reactions.

References:

1. Podgoršek, A.; Zupan, M.; Iskra, J., Oxidative Halogenation with “Green” Oxidants: Oxygen and Hydrogen Peroxide. *Angew. Chem. Int. Edit.* **2009**, *48*, 8424-8450.
2. Bedrač, L.; Iskra, J., Iodine(I) reagents in hydrochloric acid-catalyzed oxidative iodination of aromatic compounds by hydrogen peroxide and iodine. *Adv. Synth. Catal.* **2013**, *355*, 1243-1248.
3. Schmitz, L. G., The oxidation of iodine to iodate by hydrogen peroxide. *Phys. Chem. Chem. Phys.* **2001**, *3*, 4741-4746.

Problems Related to Laboratory Breeding of Water Flea Daphnia magna

Mojca Zalokar¹, Andreja Žgajnar Gotvajn¹, Gabriela Kalčikova¹

¹ Faculty of Chemistry and Chemical Technology, University of Ljubljana, Večna pot 113, SI-1000 Ljubljana, Slovenia

Water flea (*Daphnia magna*) is one of the most commonly bred species of aquatic fleas. It belongs to *Brachiopoda* group. Water fleas are indicators of a clean water, therefore they are used for testing acute and/or chronic toxicity. They grow up to a few millimeters (1). The optimum temperature for them is from 18 to 22 °C (2). They reproduce sexually and incompletely with parthenogenesis, where the female wears unbleached diploid eggs on her back in the area between the hive and the hull. Latter occurs only in favorable conditions. Therefore, we must provide optimal conditions for their survival and reproduction. Medium has to contain optimal nutrients, suitable pH, sufficient amount of dissolved oxygen, appropriate light, temperature etc. On the other hand, sexual reproduction occurs and female exits the haploid eggs, from which male develop.

Daphnia magna are very sensitive organisms strongly reacting to changes in their environment including different types of pollution. This can be reflected in a number of fertilities, number of haploid eggs and even in a number of deaths. Therefore, we have to be very careful during daphnids breeding. It is also very important that we have appropriate basic reagents for the preparation of the medium, otherwise the poisoning of the entire population can occur. Moreover, it is crucial to test the suitability of medium on their nauplii, before they are used for breeding of adult water fleas. The test of the medium is done by leaving the nauplii in a new medium for a few days and observing their response.

Water fleas should be fed daily or at least 3 times per week and the medium should contain 0,1 – 0,2 mg C/water flea (2).

During the week they were fed daily with *Spirulina* 6mg/20 water fleas and 2 times per week with *Vitakraft fish food; Premium VITA (flake-mix)* 20 mg/20 water fleas. During the cultivation, the daily amount of *Spirulina* food was increased to 8 mg/20 water fleas and at end of the week to 10 mg/20 water fleas. By increasing the amount of food we consequently increased the daily ratio of nauplii per flea.

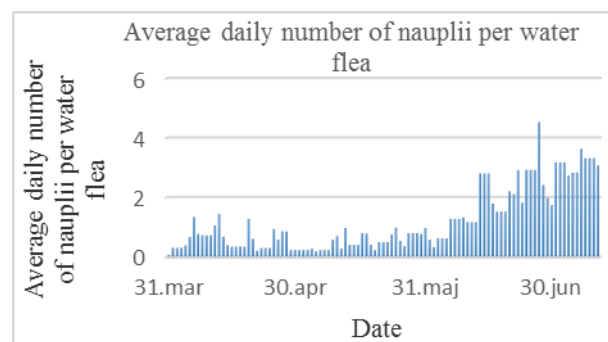
At the begging of breeding black, haploid eggs were observed on the back of the water flea. It was

suspected that this was due to inadequate light, so an additional light source was added to prevent the formation of haploid eggs.

During a few weeks of breeding, it was noticed that water fleas need some time to get used to a new medium. This is reflected in a number of nauplii per flea. Through my experiment I noticed that older water fleas have the capability to adapt faster and easier to a new medium than the younger ones. The information about how much time has passed since the medium was made, plays an important role as well.

Throughout my research I observed that the response of water fleas that were put in a several days old medium, was better, than in a freshly prepared medium.

Graph 1 shows an average daily number of nauplii increasing with the days of cultivation. The cause of the increase can be attributed to the good laboratory practice of the grower, faster adaptation of water fleas, their age and optimum conditions.



Graph 1: Average daily number of nauplii per water flea.

References:

1. Žgajnar Gotvajn, A.; Kalčikova, G.; Zagorc-Končan, J., *Ekotoksikološki praktikum*. UL FKKT: Ljubljana, **2014**.
2. OECD (2012), Test No. 211: *Daphnia magna* Reproduction Test, OECD Publishing, Paris.
3. Ten Berge, W.F., Breeding *Daphnia magna*, *Hydrobiologia* **1978**, vol. 59, 2,pag. 121-123.

Novel HPLC-UV Method for Simultaneous Determination of Fat-soluble Vitamins and Coenzyme Q10 in Medicines and Supplements

Žane Temova Rakuša,¹ Eva Srečnik,¹ Robert Roškar*,¹

¹ Faculty of Pharmacy, University of Ljubljana, Aškerčeva cesta 7, SI-1000 Ljubljana, Slovenia

Fat-soluble vitamins (FSVs) are essential for a variety of biochemical and physiological functions in the human body. However, quality control of vitamin preparations (in form of medicines and nutritional supplements) is extremely important, because of their widespread use and the possible risk of toxicity from excessive intake of vitamins A and D¹. To our knowledge none of the published HPLC methods offer simultaneous determination of FSVs and β -carotene and coenzyme Q10, which are often found along in pharmaceuticals. Therefore, we aimed to develop rapid, accurate and precise and selective HPLC-UV method for simultaneous quantification of FSVs (in most commonly used forms: A-palmitate, D3, E-acetate, K1 and β -carotene) and coenzyme Q10, using simple extraction procedures.

Optimization of chromatographic conditions - Various C18 reversed phase columns in temperature range 25-40°C, various mixtures of acetonitrile, tetrahydrofuran and water at flow rates 0.5-2.0 mL/min and detection wavelengths 210-325 nm were tested to optimize the chromatographic separation of all tested vitamins as well as both reduced and oxidized form of CoQ10. Optimal chromatographic separation of the analytes in minimal analysis time (8 min) was achieved on a Luna C18 150×4.6 mm column at 25°C using acetonitrile-tetrahydrofuran-water (50:45:5, v/v/v) as a mobile phase at flow-rate of 1 mL/min with detection wavelength 270 nm. The developed method resulted in symmetric and separated peaks and shorter retention time of the analytes (**Fig.1**) compared to other similar published HPLC-UV methods.

Optimization of sample preparation - Sample preparation is a crucial step in the analysis of commercially available multivitamin pharmaceuticals. We developed simple and fast extraction procedures, which provided suitable recoveries and sample stability of all analytes.

Method validation - The method was successfully validated according to ICH guidelines Q2(R1)² in terms of selectivity, linearity, limit of quantification, precision, accuracy, recovery, sample stability and robustness.

Assay in nutritional supplements and medicines - The method was further applied for quantification of

the analytes in selected liquid and solid dosage forms (tablets and capsules), registered as nutritional supplements and prescription medicines. High recoveries and low standard error values confirmed the suitability of the established HPLC method for routine quantification of the target analytes in commercial multi-vitamin preparations without any pre-treatment (some liquid preparations) or after a simple and rapid pre-treatment. Considering that most of the tested preparations had considerably higher contents than labelled (up to 150%), quality control of these preparations is of extreme importance.

The developed reversed phase HPLC method is the first published for quantification of these five fat-soluble vitamins and coenzyme Q10 within a single chromatographic run. Analysis time of only 8 min is favorable in comparison to other published HPLC-UV methods for determination of fewer fat-soluble vitamins.

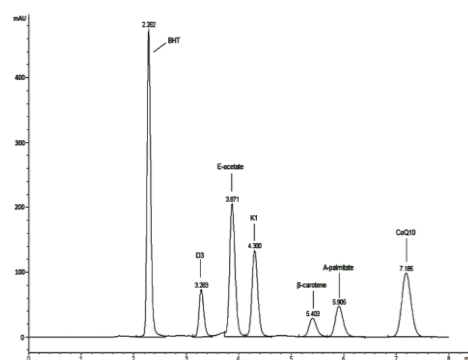


Figure 1: A chromatogram of standard analytes mixture

References:

1. Granado-Lorencio, F., Rubio, E., Blanco-Navarro, I., Pérez-Sacristán, B., Rodríguez-Pena, R., García López, F.J. Hypercalcemia, hypervitaminosis A and 3-epi-25-OH-D3 levels after consumption of an "over the counter" vitamin D remedy. a case report. Food Chem. Toxicol. **2012**, 50, 2106-8.
2. International Conference on Harmonization (ICH). Validation of analytical procedures: Text and methodology Q2(R1), Geneva, Switzerland, **2005**.

Correlation between Binding Surfaces and the Thermodynamics of Camelid Antibody Fragments Binding to Antigens

Uroš Zavrtanik¹, San Hadži¹, Jurij Lah¹

¹ Faculty of Chemistry and Chemical Technology, University of Ljubljana, Večna pot 113, SI-1000 Ljubljana, Slovenia

Thermodynamic properties of Nanobodies (Nb) binding to different antigens were investigated using crystal structures of Nb-antigen complexes from The Protein Data Bank (PDB) to obtain solvent accessible surface area and to characterize their properties. Parametrized equations (Baker and Murphy) were used to calculate thermodynamic quantities (ΔH , ΔS , ΔC_p , ΔG) from structural (solvent accessible surface areas) data. To see how well thermodynamics of binding is predicted by this structure-based approach, we searched for experimental measurements of thermodynamic parameters of binding in the literature and compared them to the calculated ones. An attempt was made to establish new relations between the calculated and experimental values. These new relations were then used in an attempt to improve thermodynamic description of Nb-antigen binding. Furthermore we also managed to obtain new structural descriptor of Nb-antigen complexes – number of intermolecular (Nb-antigen) hydrogen bonds. We found that new structure-based descriptor, number of intermolecular hydrogen bonds, is well correlated with measured changes of enthalpy (ΔH) (Figure 1). We found out that solvent accessible surface area is not reliable structural descriptor of binding thermodynamic and other more detailed structural descriptors, e.g. hydrogen bond, should be used in addition to get more accurate description of binding thermodynamics.

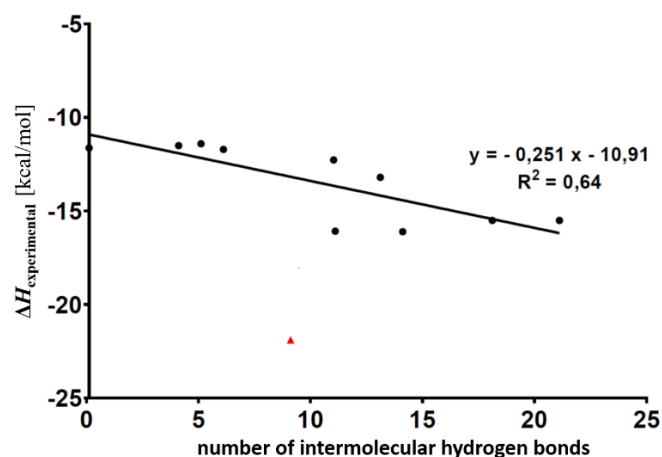


Figure 1: Correlation between number of intermolecular (Nb – antigen) hydrogen bonds and experimental ΔH (obtained from literature).

References:

1. Robertson, A. D.; Murphy, K. P., Protein Structure and the Energetics of Protein Stability. *Chem. Rev.* **1997**, 97, 1251–1268.
2. Baker, B. M.; Murphy, K. P., Prediction of binding energetics from structure using empirical parameterization. *Methods Enzymol.* **1998**, 295, 294–315.
3. Lee, B.; Richards, F. M., The interpretation of protein structures: estimation of static accessibility. *J. Mol. Biol.* **1971**, 55, 379–400.

The Effect of Clinical *Escherichia coli* Strains on Recipient Ability in Conjugative Transfer

Gaja Špes¹, Jaka Zupanič¹, Marjanca Starčič Erjavec^{*1}

¹ Department of Biology, Biotechnical Faculty, University of Ljubljana, Jamnikarjeva 101, SI-1000 Ljubljana, Slovenia

In the microbial world, the genetic transmissions are widely used and have great importance for forming new genomic features. Plasmids are genetic structures in a cell that can replicate independently of the chromosome. By the transmission, the donor cell hands over its plasmid to the recipient cell during their direct contact. This is called conjugation. With this form of a genetic transport, the recipient gains new features, which provide it with a better chance of survival¹. It is believed that recipient cell cannot avoid being used as a recipient in conjugative transfer². *Escherichia coli*, a gram-negative bacteria, lives in the intestinal system and acts as an intestinal commensal. Pathogenic *E.coli* strains cause various diseases³. Features, which are needed for successful pathogenesis, are often gained with conjugation. Until now, it was believed that the frequency of conjugation depends only on the plasmid and not on the bacterial strain. The main goal of our work was to carry out experiments which can prove or disprove the previous statement.

In the present study, we have used two different conjugative plasmids. Plasmid RK2: Ap,Kn,Tc is conjugative plasmid, which encodes antibiotics tetracycline (Tc), ampicillin (Ap) and kanamycin (Kn). Plasmid R6K: Ap,Sm is conjugative plasmid, which encodes antibiotics Ap and streptomycin (Sm). For donor strain we have used *E.coli* HB101 strain. With HB101 strain, we transferred plasmid DNA to recipient other strains DL4, DL30, DL52, DL54, DL55, DL63, DL80, DL82 and DL94, which were isolated from patients with symptomatic urinary tract infections. We added antibiotics with the following concentrations (Ap, 100 µg/ml; Sm, 150 µg/ml; Kn, 30 µg/ml).

Conjugation assays were performed on solid medium. We took single colonies of donor and recipient strains and inoculated them in 5 ml of liquid LB with the appropriate antibiotics. Liquid LB was incubated with aeration at 37 °C overnight. The volume of 50 µl of overnight cultures were transferred to 5 ml liquid LB without antibiotics and incubated with aeration at 37 °C for 2 h. Later on, we centrifuged 1 ml of the recipient strain at 5000 g for 10 min. The supernatant was discarded and cells were resuspended in 400 µl of the donor strain culture. 1 ml of combined cultures were added to solid LB plate and incubated at 37 °C for 24 h. Subsequently, we resuspended

conjugation mixture with 1 ml of 1 × dPBS (Phosphate buffered saline) 0.01 M (pH 7.2 ± 0.2). With conjugation mixture and 1 × dPBS, we prepared tenfold dilutions and plated on selective plates for CFU counts of the transconjugants and the recipient strain.

Our results showed variability in recipient ability among the studied DL strains. Conjugation frequencies for pR6K ranged from $6.84 \times 10^{-7} \pm 1.14 \times 10^{-7}$ to $7.04 \times 10^{-10} \pm 1.33 \times 10^{-10}$. By DL82 strain conjugation assay was not successful. Conjugation frequencies for pRK2 ranged from $3.93 \times 10^{-1} \pm 6.64 \times 10^{-1}$ to $2.30 \times 10^{-7} \pm 1.50 \times 10^{-7}$. In this study we showed, that different *E.coli* strains have different recipient abilities in conjugative transfers.

Table 1: Results of conjugation essays which show important differences

Recipient strains	Conjugation frequency (Average ± standard deviation)	
	With pRK2	With pR6K
DL30	3.9E-01 ± 6.6E-01	3.0E-09 ± 8.9E-10
DL57	2.3E-07 ± 1.5E-07	8.1E-10 ± 1.4E-10
DL80	3.6E-04 ± 3.3E-04	6.8E-07 ± 1.1E-07
DL82	4.2E-04 ± 4.8E-04	0
DL94	7.8E-04 ± 4.0E-04	7.0E-10 ± 1.3E-10

References:

- de la Cruz F.; Davies J. Horizontal gene transfer and the origin of species: lessons from bacteria. *Trends Microbiol* **2000**, 8, 128–133.
- Pérez-Mendoza D.; de la Cruz F. *Escherichia coli* genes affecting recipient ability in plasmid conjugation: are there any? *BMC Genomics* **2009**, 10, 71.
- Dale AP.; Woodford N. Extra-intestinal pathogenic *Escherichia coli* (ExPEC): Disease, carriage and clones. *J Infect* **2015**, 71, 615–626.

Separation of Amino Acids by Various Chromatography Columns

Blaž Kozjan¹, Matevž Pompe¹

¹ Faculty of Chemistry and Chemical Technology, University of Ljubljana, Večna pot 113, SI-1000 Ljubljana, Slovenia

Amino acids are important and basic compounds in pharmaceutical applications and are used as precursors for synthesizing further pharmaceutical substances. Generally, separation of amino acids by chromatography is mostly carried out with previous derivatization, preventing that any charge may be present. Successfully synthesized derivate is then analysed on reversed phase column. The purpose of our research was to separate a mixture of three amino acids (proline (Pro), leucine (Leu), isoleucine (Ile)) without previous derivatization. Furthermore, we try to separate isoleucine and leucine, two isomeric forms successfully within one chromatographic analysis.

Use of reversed – phase columns does not work well, therefore we tried to separate mixture with various columns appropriated for determining polar analytes. We tested many columns with modified silica particles, mixed – mode columns and columns with BEH technology. Mixed – mode columns combine long hydrophobic alkyl chain with ion – exchange group, providing hydrophobic and electrostatic interactions at the same time. So it is possible to separate polar and charged analytes which show little or no retention on reversed phase columns¹.

Columns with BEH technology provide new series of reversed phase columns which exhibit higher pressure and wider pH range than usual reversed – phase column. Reason for that are modified silica particles forming an ethylene bridge. Ethylene Bridged Hybrid (BEH) technology synthesis offers many advantages over conventional silica – based particles, including the ability to control surface silanol activity for better reproducibility, peak shape and retention time².

Residual silanol groups form additional interactions which are often detrimental for an analysis of basic analytes. Problematic are silanol groups (Si-OH) as well as dissociated silanol groups (Si-O⁻). Latter at pH above 7 often serve as an ion – exchanger whereas protonated silanol groups can perform as donor or acceptor of hydrogen bond. The BEH particle is prepared from two high purity monomers: tetraethoxysilane (TEOS) and bis(triethoxysilyl) ethane (BTEE), which results in a highly stable, pH resistant, and mechanically strong particle allowing seamless transfer from UPLC, UHPLC, HPLC and preparative separations^{2,3}. X – Bridge C₁₈ is a good example of

column which has a stationary phase based on BEH particles. Chromatogram is shown on Figure 1.

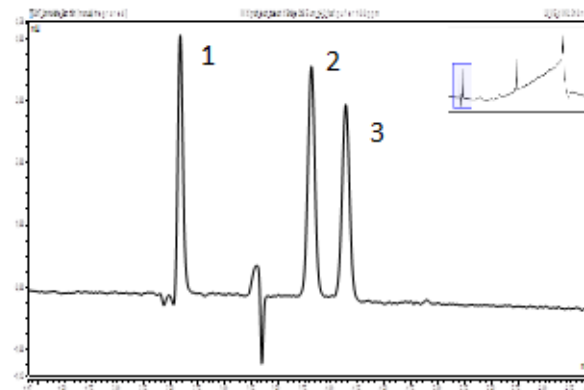


Figure 1: Zoomed chromatogram of separation of three amino acids on X – Bridge C₁₈ column (1-proline, 2-isoleucine, 3-leucine)

References:

1. Zhang, K.; Liu, X., Mixed – mode chromatography in pharmaceutical and biopharmaceutical applications. *Journal of Pharmaceutical and Biomedical Analysis* **2016**, 130, 19–34
2. <http://www.waters.com/webassets/cms/library/docs/720001159en.pdf> (accessed 26. 6. 2017)
3. Swartz, M. E., UPLCTM - An introduction and Review. *Journal of Liquid Chromatography & Related Technologies* **2007**, 28, 1253–1263

Structural Studies of ALS-Associated Proteins

Jakob Rupert¹, Boris Rogelj^{*,1,2,3}, Vera Župunski¹

¹ Faculty of Chemistry and Chemical Technology, University of Ljubljana, Večna pot 113, SI-1000 Ljubljana, Slovenia

² Department of Biotechnology, Jožef Stefan Institute, Jamova 39, Ljubljana SI-1000, Slovenia

³ Biomedical Research Institute, Puhova 10, Ljubljana SI-1000, Slovenia

Amyotrophic lateral sclerosis is a fatal progressive neurodegenerative disease¹. As of today, an increasing number of genetic factors have been linked to the progression, age-of-onset and susceptibility of the disease, with RNA metabolism and RNA-protein substructure being a particularly fast evolving focus of research². On the opposite, the structural analysis of protein products of various ALS-associated genes, such as *TARDBP*³, *FUS*⁴, *C9ORF72*⁵ and the recently associated *ANXA11*⁶, has yet to achieve a major breakthrough as of determining the complete 3D structure of the protein.

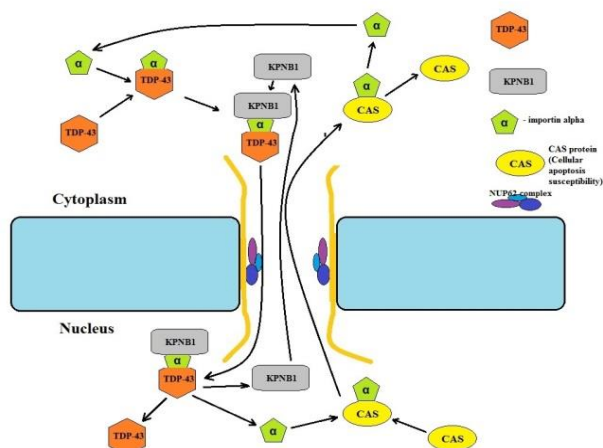


Figure 1: A schematic representation of TDP-43 nuclear transport mechanism with interacting proteins.⁷

We have expressed, isolated and purified products of genes involved in ALS pathogenesis, with the final aim of producing protein crystals, suitable for structure-determining experiments with X-ray diffraction. The major obstacle is the solubility and stability of the proteins, obtained in bacterial and mammalian expression system, as they are predominantly sequestered in inclusion bodies and tend to aggregate in protein droplets at sudden temperature changes. The stability and solubility were increased by mean of adding reducing agents, glycerol, EDTA and calcium. Further stability was achieved by truncating the wild-type AnxA11, while co-expression with interacting partners (Figure 1) was attempted to increase the yield of soluble TDP-43. Determination of crystal structures of ALS proteins will provide additional insight into understanding the protein

aggregation, interaction partners and the role of calcium signalling in the pathogenesis.

References:

1. Rowland, L. P.; Shneider, N. A., Amyotrophic lateral sclerosis. *N. Engl. J. Med.* **2001**, *344*, 1688–1700.
2. Taylor, J. P.; Brown, R. H.; Cleveland, D. W., Decoding ALS: from genes to mechanism. *Nature* **2016**, *539*, 197–206.
3. Neumann, M.; et al., Ubiquitinated TDP-43 in frontotemporal lobar degeneration and amyotrophic lateral sclerosis. *Science* **2006**, *130*, 130–133.
4. Vance, C.; et al., Mutations in FUS, an RNA processing protein, cause familial amyotrophic lateral sclerosis type 6. *Science* **2009**, *323*, 1208–1211.
5. Renton, A.E.; et al., A Hexanucleotide Repeat Expansion in C9ORF72 Is the Cause of Chromosome 9p21-Linked ALS-FTD. *Neuron* **2011**, *72*, 257–268.
6. Smith, B.N.; et al., Mutations in the vesicular trafficking protein annexin A11 are associated with amyotrophic lateral sclerosis. *Sci Transl Med.* **2017**, *9*, 1–16.
7. Nishimura, A.L.; et al., Nuclear import impairment causes cytoplasmic trans-activation response DNA-binding protein accumulation and is associated with frontotemporal lobar degeneration. *Brain* **2010**, *133*, 1763–1771

Synthesis and Characterization of Cd(II) Complexes with the Condensation Product of 2-quinolinecarboxaldehyde and Girard's T Reagent

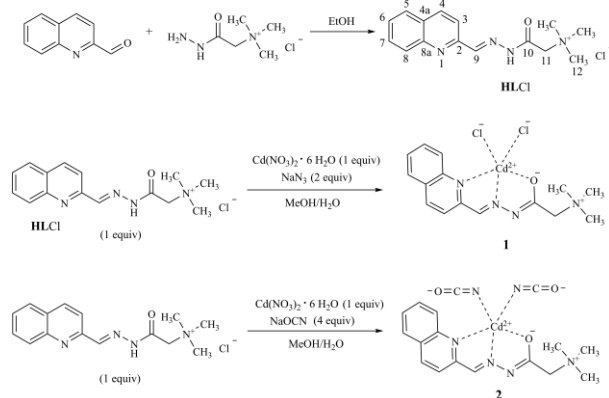
Andrej Pevec¹, Iztok Turel¹, Mima Č. Romanović², Katarina Anđelković², Milica Milenković², Božidar Čobeljić^{*, 2}

¹ Faculty of Chemistry and Chemical Technology, University of Ljubljana, Večna pot 113, SI-1000 Ljubljana, Slovenia

² Faculty of Chemistry, University of Belgrade, Studentski trg 12-16, 11000 Belgrade, Serbia

A tridentate NNO condensation product of 2-quinolinecarboxaldehyde and Girard's T reagent (**HLCl**) in the presence of N_3^- and OCN^- ions coordinates with cadmium(II) giving mononuclear Cd(II) complex $[\text{CdLCl}_2]$ (**1**) and $[\text{CdL}(\text{NCO})_2]$ (**2**). Crystal structure of complex **1** was determined using X-ray analysis, while the structure of complex **2** was determined using IR, NMR spectroscopy and elemental analysis.

The reaction of 2-quinolinecarboxaldehyde and Girard's T reagent performed according to the previously reported method¹ yielded the ligand (*E*)-*N,N,N*-trimethyl-2-oxo-2-(2-(quinolin-2-ylmethylene)hydrazinyl)ethan-1-ammonium chloride (**HLCl**), which was used for the synthesis of complexes **1** and **2** (Scheme 1).



Scheme 1. Synthesis of complexes **1** and **2**.

In complexes **1** and **2** hydrazone ligand is coordinated in deprotonated formally neutral zwitter-ionic form. The presence of basic OCN^- and N_3^- anions in the reaction solution caused deprotonation of hydrazone ligand. In both complexes Cd(II) is pentacoordinated with quinoline nitrogen, azomethine nitrogen and carbonyl oxygen atoms from hydrazone ligands and two monodentates (Cl^- in complex **1**, and OCN^- in complex **2**).

On the basis of IR spectroscopy results for complexes **1** and **2** coordination of **HLCl** ligand in deprotonated α -oxyazine form was confirmed. The new band at 1535 cm^{-1} in the spectrum of complex **1** and at

1524 cm^{-1} in the spectrum of complex **2** corresponding to $\nu(-\text{O}-\text{C}=\text{N})$ vibration of deprotonated hydrazone moiety, appeared instead of the band of carbonyl group of non-coordinated hydrazonic form of **HLCl** at 1699 cm^{-1} . In the IR spectrum of complex **2** two strong bands appeared at 2197 cm^{-1} and 2160 cm^{-1} which can be attributed to the vibration of coordinated cyanate ions.

The molecular structure (ORTEP) of **1** is depicted in Figure 1. In complex **1**, Cd1 has fivefold coordination with tridentate ligand **L** and two Cl^- ligands (Cl1 and Cl2). The ligand **L** is coordinated to Cd1 in the zwitterionic form through NNO set of donor atoms forming two fused five-membered chelation rings.

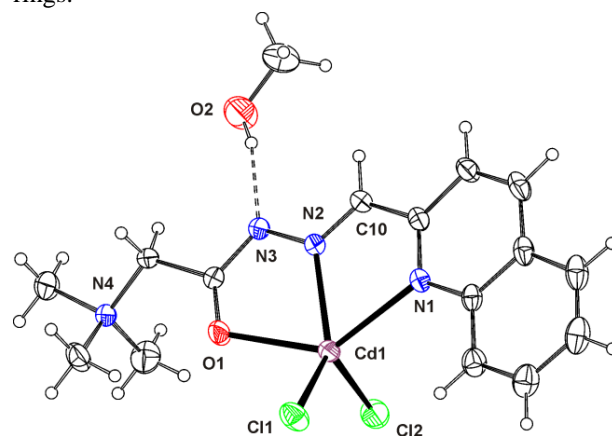


Figure 1. ORTEP view of **1** (thermal ellipsoids are at 30% probability)

References:

1. Romanović, M. Č.; Čobeljić, B. R.; Pevec, A.; Turel, I.; Spasojević, V.; Tsaturyan, A. A.; Shcherbakov, I. N.; Anđelković, K. K.; Milenković, M.; Radanović, D.; Milenković, M. R., Synthesis, crystal structure, magnetic properties and DFT study of dinuclear Ni(II) complex with the condensation product of 2-quinolinecarboxaldehyde and Girard's T reagent. *Polyhedron* **2017**, *128*, 30–37.

Fluoridooxidovanadates(V) with Small Nitrogen-Containing Cations

Andraž Oštrek^{1,2}, Matic Lozinšek*,¹

¹ Department of Inorganic Chemistry and Technology, Jožef Stefan Institute, Jamova 39, 1000 Ljubljana, Slovenia

² Faculty of Chemistry and Chemical Technology, University of Ljubljana, Večna pot 113, 1000 Ljubljana, Slovenia

Fluoridooxidovanadates or anionic vanadium oxyfluorides exhibit a rich structural chemistry^{1,2}. These compounds are typically synthesized via solvothermal methods. Hence, the vanadium(V) starting material is usually reduced yielding products containing vanadium(IV) (or vanadium(III)). Anionic vanadium(V) oxyfluorides are therefore less explored than the respective +4 analogs.

Alternatively, fluoridomonooxidovanadates(V) can be prepared in anhydrous hydrogen fluoride (aHF) by Lewis acid-base reactions of vanadium trifluoride oxide, VOF_3 , with fluoride-ion donors³. These encompass reactions of VOF_3 with metal or non-metal fluorides, reactions with salts (e.g., chlorides)^{4,5} that upon solvolysis in aHF yield the corresponding fluoride salts *in situ*, and reactions with Brønsted-Lowry bases which also form the corresponding fluoride salts with HF *in situ*.

In the present work, novel fluoridomonooxidovanadate(V) salts containing small nitrogen-base derived cations were synthesized in aHF and structurally characterized, namely ammonium, methylammonium, hydrazinedium, and uronium (O-protonated). Three different anions were observed in the studied compounds: an edge-sharing dimer in $\text{N}_2\text{H}_6[\text{V}_2\text{O}_2\text{F}_8]\cdot\text{HF}$, a *cis*-fluoride-bridged (corner-sharing) zigzag chain anion in $\text{CH}_3\text{NH}_3[\text{VOF}_4]$ and $(\text{NH}_2)_2\text{COH}[\text{VOF}_4]$, and an edge-sharing and corner-sharing polymeric chain in $\text{NH}_4[\text{V}_2\text{O}_2\text{F}_7]$ (**Fig.**). All of the aforementioned anions are composed of $[\text{VOF}_5]$ octahedral units which possess a short terminal $\text{V}=\text{O}$ and a long bridging $\text{V}-\text{F}$ axial bonds and display an intrinsic primary C_4 [001] out-of-center distortion⁶. The axial oxido ligand also exerts repulsion on the equatorial fluorido ligands and this “roof effect” is demonstrated by the more open *cis*- $\text{O}-\text{V}-\text{F}$ angles ($>90^\circ$). In the crystal structures of these compounds cations and anions are interconnected by complex networks of $\text{N}-\text{H}\cdots\text{F}$ hydrogen bonds.

The described products were characterized in the solid state by low-temperature single-crystal X-ray diffraction and Raman spectroscopy. In addition, the crystal structure of $\text{N}_2\text{H}_6\text{F}_2\cdot 2\text{HF}$ was also determined.

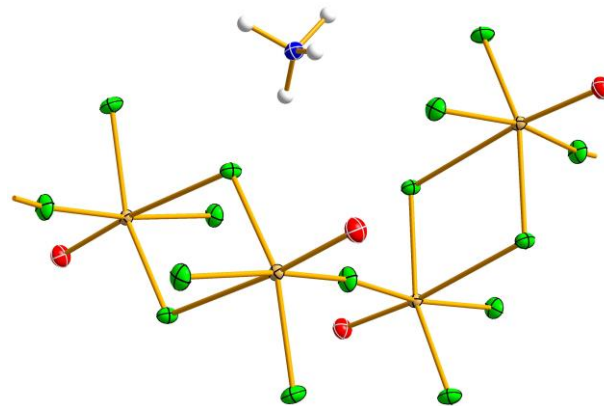


Figure 1: A polymeric chain anion is observed in the crystal structure of $\text{NH}_4[\text{V}_2\text{O}_2\text{F}_7]$. Thermal ellipsoids are drawn at the 50% probability level, whereas the hydrogen atoms are depicted as small spheres of arbitrary radius.

References:

1. Aidoudi, F. H.; Black, C.; Arachchige, K. S. A.; Slawin, A. M. Z.; Morris, R. E.; Lightfoot, P., Structural diversity in hybrid vanadium(IV) oxyfluorides based on a common building block. *Dalton Trans.* **2014**, 43, 568–575.
2. Yeon, J.; Felder, J. B.; Smith, M. D.; Morrison, G.; zur Loye, H.-C., Synthetic strategies for new vanadium oxyfluorides containing novel building blocks: structures of V(IV) and V(V) containing $\text{Sr}_4\text{V}_3\text{O}_5\text{F}_{13}$, $\text{Pb}_7\text{V}_4\text{O}_8\text{F}_{18}$, $\text{Pb}_2\text{VO}_2\text{F}_5$, and Pb_2VOF_6 . *CrystEngComm* **2015**, 17, 8428–8440.
3. Lozinšek, M.; Goreshnik, E.; Žemva, B., Lead fluoridooxidovanadates(V), $\text{Pb}(\text{V}_2\text{O}_2\text{F}_8)$, $\text{Pb}(\text{VOF}_5)$, and mixed valent fluoridooxidovanadate(IV,V), $\text{Pb}_3\text{F}(\text{V}_4\text{O}_3\text{F}_{18})$. *Z. Anorg. Allg. Chem.* **2012**, 638, 2123–2128.
4. Lozinšek, M.; Goreshnik, E.; Žemva, B., Silver(I) tetrafluoridooxidovanadate(V) – $\text{Ag}[\text{VOF}_4]$. *Acta Chim. Slov.* **2014**, 61, 542–547.
5. Lozinšek, M., Hydroxylammonium tetrafluoridooxidovanadate(V) – $(\text{NH}_3\text{OH})[\text{VOF}_4]$. *Acta Chim. Slov.* **2015**, 62, 378–384.
6. Halasyamani, P. S., Asymmetric cation coordination in oxide materials: Influence of lone-pair cations on the intra-octahedral distortion in d^0 transition metals. *Chem. Mater.* **2004**, 16, 3586–3592.

Compost Water Extract (Compost Tea) as an Alternative Nutrient Solution for Vegetables Grown on Hydroponic System

Gregor Šilc¹, Matjaž Rejec¹, Jan Zupančič, Črt Železnik¹, Rok Mihelič*¹

¹ University of Ljubljana, Biotechnical Faculty, Department of Agronomy, Jamnikarjeva 101, SI-1000 Ljubljana, Slovenia; rok.mihelic@bf.uni-lj.si

Agriculture is facing land loss and scarcity of mined plant nutrients, especially phosphorus¹. In EU 45 million metric tons of municipal waste is composted yearly². Nutrients within compost could partly replace mined minerals. The present hydroponic systems use exclusively highly soluble mineral salts. These data encouraged our team to research use of compost water extract as an 'organic' alternative in hydroponic system, for growing vegetables.

We first try to optimize compost water extract characteristics and subsequently compare growing vegetables on coconut fibres fertilized either with mineral salts or with compost water extract. Before usage, compost was tested for heavy metals: the concentrations were within the limits of the legislation.⁵ Split plot scheme with three repetitions was used in the design of the experiment. The control group was fertilized with standard 'Hoagland' solution of soluble mineral salts³. Phytotoxicity of compost extract and the control was tested *in vitro* by measuring number of germinated seeds and root growth of garden cress (*Lepidium sativum* L.)⁴. The phytotoxicity tests were showed the mixing ratio between compost and water should be between 5 % and 10 % (compost mass in water; w/V). The compost was extracted and aerated by shaking the solution with a horizontal shaker for 212 hours. During this, the EC remained consistent, while the average pH was rising inconsistently from 7.32 to 8.33. This was probably caused by the liveness of the extract. Upon these measurements we concluded that 3 hours of compost extraction time was long enough for practical application in hydroponics. In the second part of experiment, the filtered (coarse, 'tea-bag' filter; 0,25 mm mesh) compost water extract was used in comparison to the Hoagland solution for growing tomatoes (*Solanum lycopersicum* L.) and lettuce (*Lactuca sativa* L.). Experiment was conducted in greenhouse at Biotechnical Faculty in Ljubljana, between march and august in 2015. Each of the compost extract batches was filtered, aerated and used for vegetable fertigation within 7 days. The vegetable plants were observed weekly. In the first five weeks for tomato and the two weeks for lettuce, there were no distinct differences between the control and the experiment groups. After five weeks, the tomato control group started to show signs of fungi leaf infections. No crop protections were used during the

experiments. In time, some of the control group tomatoes withered and even died, due to diseases. While both experiment groups have shown mild disease symptoms, the group fertigated with compost extract produced higher biomass as the control group. The experiment was repeated with lettuce yielding similar results with higher biomass production, after two weeks and higher root mass, at the end of 30 days growing time. All plants in experiment group had higher root growth. Lettuce in the control group had lower contents of nitrate in fresh biomass by 9 % and 78 % less biomass production.

This paper describes the properties of compost water extract for usage in hydroponic systems. With a preliminary experiment we showed the promising possibility of the recycled composted organic waste use on non-arable land replacing mineral fertilizers for hydroponics, which is a good example towards circular economy. For production on a bigger scale, more research would have to be done. It was noticed that the main challenge for crop production lie in livingness of the extract, which changes the properties of the compost extract in time⁶.

References:

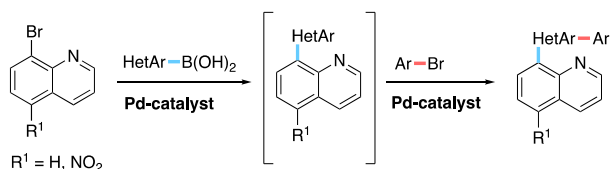
1. Taddeo, R.; Kolppo, K.; Lepisto R., Sustainable nutrients recovery and recycling by optimizing the chemical addition sequence for struvite precipitation from raw swine slurries, **2016**, *180*, 52-58.
2. Blumenthal, K., Generation and treatment of municipal waste, Eurostat Statistics in focus 31/2011, **2011**
3. Hoagland, D. R.; Arnon, D. I., the water-culture method for growing plants without soil, University of California, College of Agriculture, Agricultural Experiment Station, **1938**.
4. Mitelut, A. C.; Popa, M. E., Seed germination bioassay for toxicity evaluation of different composting biodegradable materials, Rom. Biotech. Lett., **2011**, *16*, 1.
5. Uradni list Republike Slovenije, 3646. Uredba o mejnih vrednostih vnosa nevarnih snovi in gnojil v tla, **2005**, *85*, 8709.
6. Ingham, E. R., The compost tea brewing manual 5th edition, Soil Foodweb Incorporated, **2005**, 12-22

Synthesis of 8-Heteroarylquinolines via Sequential One-Pot Palladium-catalyzed reaction

Helena Brodnik Žugelj¹, Uroš Grošelj¹, Franc Požgan¹, Jurij Svete¹, Bogdan Štefane^{*,1}

¹ Faculty of Chemistry and Chemical Technology, University of Ljubljana, Večna pot 113, SI-1000 Ljubljana, Slovenia

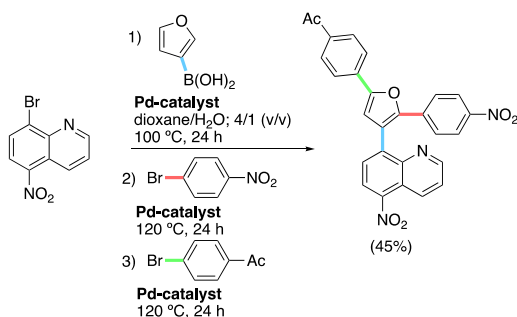
8-Heteroarylquinolines present an important group of heterocyclic compounds, which are often found in various natural compounds with interesting biological activity.¹ Furthermore, the quinoline motif is often found in many important pharmaceutical compounds. For example, nitroxoline (8-hydroxy-5-nitroquinoline) and a few of its derivatives have shown promising results as potential inhibitors for Cathepsin B.² To further explore the structure-activity relationship, we envisioned to develop an efficient synthetic methodology which would allow access to a variety of structurally diverse 8-heteroarylquinoline derivatives.³



Scheme 1: Sequential one-pot Pd-catalyzed synthesis of 8-heteroarylquinolines.

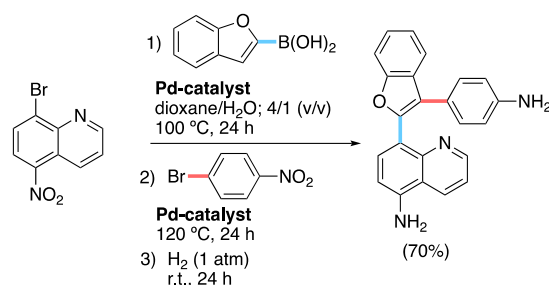
By employing a two-step one-pot Pd-catalyzed Suzuki–Miyaura cross-coupling reaction followed by a direct C–H functionalization reaction, we managed to synthesize a number of polyarylated systems without the isolation of intermediates in good yields (Scheme 1).

Given the possibility of combining several reaction steps within a single vessel we managed to accomplish a sequential three-step one-pot transformation including the initial Suzuki–Miyaura cross-coupling reaction between 8-bromo-5-nitroquinoline and furan-3-ylboronic acid followed by two direct C–H arylation steps. The corresponding trisubstituted furan derivative was isolated in an overall 45% yield (Scheme 2).



Scheme 2: One-pot synthesis of polyarylated furan.

Furthermore, we managed to carry out a Suzuki reaction between 8-bromo-5-nitroquinoline and benzofuran-2-ylboronic acid and further react the Suzuki coupling product with 4-bromonitrobenzene giving rise to a C2-arylated product. After completion of the C–H functionalization step, the crude reaction mixture was exposed to 1 atm of hydrogen at room temperature for 24 h, after which the final product was isolated in a good (70%) yield (Scheme 3).



Scheme 3: One-pot Suzuki–Miyaura cross-coupling/arylation/hydrogenation reaction sequence.

References:

- (a) Huang, C. Q.; Wilcoxon, K.; McCarthy, J. R.; Haddach, M.; Grigoriadis, D.; Chen, C., Synthesis and SAR of 8-Arylquinolines as potent corticotropin-Releasing factor₁ (CRF₁) receptor antagonists. *Bioorg. Med. Chem. Lett.*, **2003**, *13*, 3375–3379. (b) Michael, J. P., Quinoline, quinazoline and acridone alkaloids, *Nat. Prod. Rep.*, **2008**, *25*, 166–187.
- Sosić, I.; Mirković, B.; Arenz, K.; Štefane, B.; Kos, J.; Gobec, S., Development of New Cathepsin B Inhibitors: Combining Bioisosteric Replacements and Structure-Based Design To Explore the Structure-Activity Relationships of Nitroxoline Derivatives, *J. Med. Chem.*, **2013**, *56*, 521–533.
- Brodnik, H.; Požgan, F.; Štefane, B., Synthesis of 8-heteroaryl nitroxoline analogues via one-pot sequential Pd-catalyzed coupling reactions, *Org. Biomol. Chem.*, **2016**, *14*, 1969–1981.

Density and Viscosity of Aqueous Solutions of Functionalized Quaternary Ammonium Surfactants

Agnieszka Hamera^{1,2}, Žiga Medoš², Marija Bešter-Rogač²

¹Faculty of Chemistry, Maria Curie-Skłodowska University Lublin, Poland

²Faculty of Chemistry and Chemical Technology, University of Ljubljana, Ljubljana, Slovenia

Surfactants are widely used compounds in industry and everyday life where commonly mixtures of non-ionic, cationic and anionic surfactants are used. Especially quaternary ammonium salts such as alkyltrimethylammonium chlorides and bromides, have been widely studied [1-3]. No information can be found in the literature, how functionalization of a side alkyl chain on the quaternary nitrogen affects their surfactant properties, among which the value of critical micelle concentration, cmc, is regarded as one of the main characteristics at characterization of surfactants.

In this contribution four quaternary ammonium surfactants were investigated (Figure 1): a) N-decyl-N,N,N-trimethylammonium chloride, C₁₀TMACl, b) N-(2-methoxyethyl)-N,N-dimethyl-N-decylammonium chloride, (C₂OMe)C₁₀DMACl, c) N-(2-hydroxyethyl)-N,N-dimethyl-N-decylammonium chloride, (C₂OH)C₁₀DMACl, and d) N-(2-ethoxy-2-oxoethyl)-N,N-dimethyl-N-decylammonium chloride, (C₂OOEt)C₁₀DMACl.

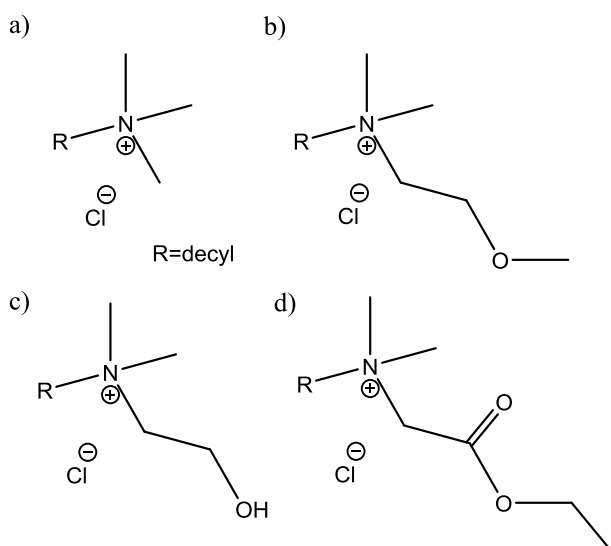


Figure 1 Studied quaternary ammonium surfactants.

Densities and viscosities of aqueous solution for all studied systems were measured before and after cmc in the temperature range from 5 °C to 55 °C (in steps of 10 °C). From the temperature and concentration dependence estimated properties the interaction in the systems will be discussed.

A. H. is grateful the Traineeship program under project “Visa on the labour market” enabling her stay at Faculty of Chemistry and Chemical Technology, University of Ljubljana. This work was supported by the Slovenian Research Agency (Contract No. P1-0034).

References:

1. Kroflič, A.; Šarac, B.; Bešter-Rogač, M. Influence of the alkyl chain length, temperature, and added salt on the thermodynamics of micellization: Alkyltrimethylammonium chlorides in NaCl aqueous solutions. *J. Chem. Thermodyn.* **2011**, *43*, 1557–1563.
2. Šarac, B.; Bešter-Rogač, M. Temperature and salt-induced micellization of dodecyltrimethylammoniumchloride in aqueous solution: A thermodynamic study. *J. Colloid Interface Sci.* **2009**, *338*, 216–221.
3. del Ria, J. M.; Prieto, G.; Sarmiento, F.; Mosquerat V. Thermodynamics of Micellization of N-Octyltrimethylammonium Bromide in Different Media. *Langmuir* **1995**, *11*, 1511–1514.

Syntheses of Substituted 2H-Pyran-2-ones with a Special Emphasis on Attempted Synthesis of Derivatives that Contain 2-fluoro-4-methoxyphenyl Group

Nik Rus,¹ Krištof Kranjc*,¹

¹ Faculty of Chemistry and Chemical Technology, University of Ljubljana, Večna pot 113, SI-1000 Ljubljana, Slovenia; e-mail: kristof.kranjc@fkkt.uni-lj.si

2H-Pyran-2-ones form a very diverse group of organic molecules which vary greatly in their use and functions. Their occurrence in nature ranges from signal molecules in bacteria, toxins used for defense by frogs, anti-mould agents, to fragrances in some plants and fruits.¹ By combining this versatile building block with a fluorine-containing functional group² we aimed to show that it is possible to synthesize this kind of molecule which could potentially lead to combining the best of both worlds.

The synthesis of two different 2-fluoro-4-methoxyphenyl-group containing 2H-pyran-2-ones³ from their starting precursors was achieved (i.e. 5-acetyl-3-benzoylamino-6-methyl-2H-pyran-2-one and 3-benzoylamino-6-(2-fluoro-4-methoxyphenyl)-2H-pyran-2-one). When synthesizing the former, the starting reagents have been acetylacetone, DMFDMA and hippuric acid. For the synthesis of the latter, we have used 2-fluoro-4-methoxyacetophenone, DMFDMA and hippuric acid (Figure 1).

A further transformation via the Diels–Alder reaction with maleic anhydride forming a bicyclo[2.2.2]octene derivative⁴ was successfully accomplished. A scale-up of the synthesis of one of the 2-fluoro-4-methoxyphenyl-substituted 2H-pyran-2-one worked well. Additionally, we also showed that the Diels–Alder reaction of the 2-fluoro-4-methoxyphenyl derivatives of 2H-pyran-2-ones can take place with similar results as in other cases, regardless of the conditions used: conventional heating under reflux (open-vessel approach) or application of closed vessels (ACE thick-walled glass tubes) at higher temperatures

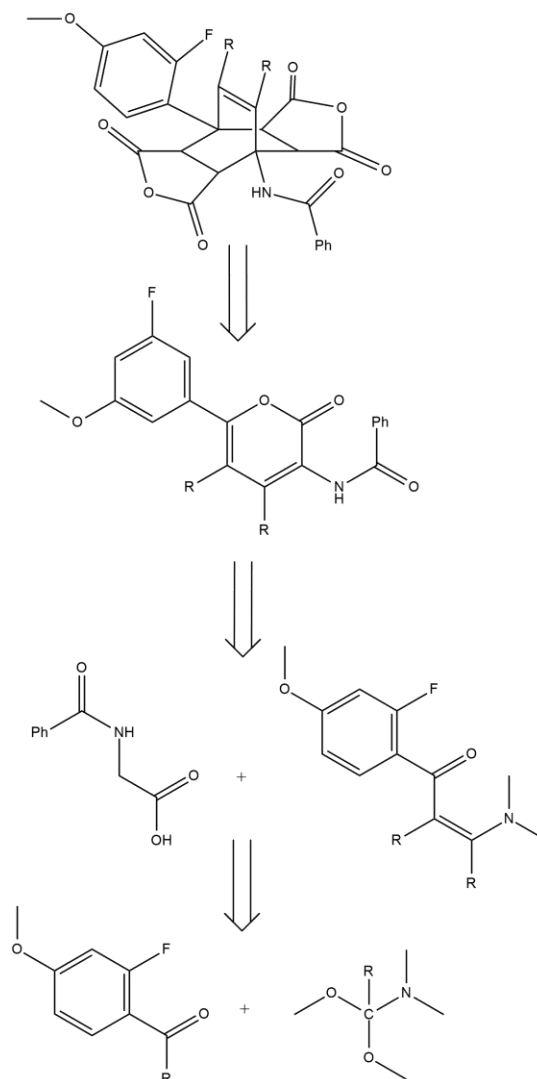


Figure 1: Retrosynthesis approach to the bicyclo[2.2.2]octene adducts.

References:

- Goel, A; Ram, VJ: Natural and synthetic 2H-pyran-2-ones and their versatility in organic synthesis. *Tetrahedron*, **2009**, 65, 7865–7913.
- Hagmann, WK: The Many Roles for Fluorine in Medicinal Chemistry. *J. Med. Chem.*, **2008**, 51, 4359–4368.
- Kranjc, K; Kočevár, M: Regio- and stereoselective syntheses and cycloadditions of substituted 2H-pyran-2-ones and their fused derivatives. *Arkivoc*, **2013**, (i), 333–363.
- Kranjc, K; Perdih, F; Kočevár, M: Effect of ring size on the *exo/endo* selectivity of a thermal double cycloaddition of fused pyran-2-ones. *J. Org. Chem.*, **2009**, 74, 6303–6306.

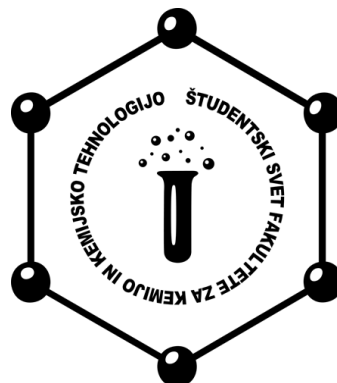
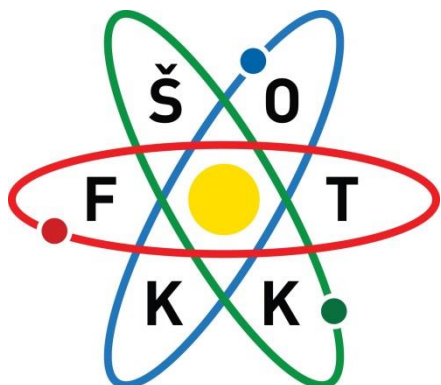


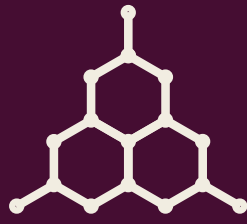
METTLER TOLEDO

MERCK



KEMOMED
BRINGING SOLUTIONS





CUTTING
EDGE **2017**